

Alma Mater Studiorum – Università di Bologna

DOTTORATO DI RICERCA IN  
INGEGNERIA CIVILE, CHIMICA, AMBIENTALE E DEI MATERIALI

Ciclo XXIX

Settore Concorsuale di afferenza: 08/A4

Settore Scientifico disciplinare: ICAR/06

**SURVEYING AND THREE-DIMENSIONAL MODELING  
FOR PRESERVATION AND STRUCTURAL ANALYSIS  
OF CULTURAL HERITAGE**

**Presentata da: ILENIA SELVAGGI**

**Coordinatore Dottorato  
Prof. Luca Vittuari**

**Relatore  
Prof. Gabriele Bitelli**

**Correlatori  
Prof. Luca Vittuari  
Prof. Andreas Wieser**

**Esame finale anno 2017**



# Table of contents

Introduction .....	9
1.1 Research context .....	9
1.2 Thesis outline.....	11
Geomatics in the field of cultural heritage .....	13
2.1 Introduction.....	13
2.2 Surveying throughout the history .....	13
2.3 Geomatics.....	14
2.4 Preservation of cultural heritage.....	14
2.4.1 Historical outline.....	15
2.5 The integration of Geomatics techniques for the survey of cultural heritage .....	20
2.5.1 Terrestrial Laser Scanner TLS.....	21
2.5.2 Close Range Photogrammetry CRP.....	24
Three dimensional modeling for structural analysis.....	26
3.1 Introduction.....	26
3.2 Finite Element approach .....	26
3.2.1 Description.....	27
3.2.2 Linear static stress analysis.....	31
3.2.3 Dynamic analysis .....	32
3.3 FE modeling .....	34
3.4 FEM in cultural heritage .....	36
3.5 Legislative framework in the field of structural analysis for cultural heritage.....	47
3.5.1 Regulations and decree laws in Italy .....	48
3.6 Considerations.....	51
From point cloud to FE model .....	52
4.1 Introduction.....	52
4.2 The transformation of dense point cloud datasets.....	53
4.2.1 Restrictions .....	56
4.3 The transformation of point cloud dataset into FE model: procedures.....	59
4.3.1 Semi-automatic approach: Cloud2FEM procedure .....	60
4.3.2 Semi-automatic approach: HPC procedure .....	65
4.3.3 Automatic approach: From raw point cloud to FE model .....	70
4.3.4 Automatic approach: Discretization of the three-dimensional space.....	71
4.4 Considerations.....	73

<b>The San Felice sul Panaro Fortress case of study.....</b>	<b>74</b>
5.1 Introduction.....	74
5.2 Historical description.....	74
5.3 Seismic vulnerability of the Fortress .....	76
5.4 Measurements.....	77
5.5 Fortress: numerical model and structural analysis .....	79
5.5.1 Cloud2FEM procedure.....	80
5.6 Mastio tower .....	84
5.6.1 Cloud2FEM procedure.....	85
5.7 North tower .....	92
5.8 Considerations.....	97
<b>The Baptistery of Aquileia case of study.....</b>	<b>99</b>
6.1 Introduction.....	99
6.2 Historical description.....	100
6.3 Data acquisition.....	106
6.3.1 Terrestrial Laser Scanner .....	107
6.3.2 Close Range Photogrammetry.....	112
6.4 Three-Dimensional complete model.....	116
6.4.1 Numerical modeling .....	116
6.4.2 Comparison with old data .....	119
6.5 Three-dimensional model of the Baptistery.....	120
6.5.1 Geometrical modeling from old data .....	126
6.5.2 Comparison of results.....	129
6.6 Geometrical evaluation of baptismal font .....	134
6.6.1 Photogrammetric data: acquisition, processing and results.....	134
6.6.2 Comparison with old data .....	138
6.6.3 Columns: geometrical analysis and static considerations.....	142
6.7 Structural analysis with different procedures .....	145
6.7.1 CLOUD2FEM procedure.....	147
6.7.2 HCP procedure.....	149
6.7.3 Automatic methods.....	153
6.8 Results .....	155
6.8.1 Comparison between semi-automatic procedures.....	155
6.8.2 Comparison between three-dimensional geometrical models.....	158

6.8.3	Comparison between geometrical reconstruction and HPC model.....	162
6.8.4	Comparison between HPC procedure and automatic methods .....	164
6.9	Considerations.....	166
<b>The San Luzi Bell Tower case of study .....</b>		<b>169</b>
7.1	Introduction.....	169
7.2	Description.....	169
7.3	Measurement .....	171
7.4	Bell tower: numerical model .....	174
7.5	Finite Element Model .....	177
7.5.1	Cloud2FEM procedure.....	178
7.5.2	HPC Procedure.....	179
7.6	Considerations.....	185
<b>Conclusions and further outlook .....</b>		<b>187</b>
<b>Acknowledgements.....</b>		<b>190</b>
<b>References .....</b>		<b>192</b>



## Abstract

*Dense point clouds can be used for three important steps in structural analysis, in the field of cultural heritage, regardless of which instrument it was used for acquisition data.*

*Firstly, they allow deriving the geometric part of a finite element (FE) model automatically or semi-automatically. User input is mainly required to complement invisible parts and boundaries of the structure, and to assign meaningful approximate physical parameters.*

*Secondly, FE model obtained from point clouds can be used to estimate better and more precise parameters of the structural analysis, i.e., to train the FE model.*

*Finally, the definition of a correct Level of Detail about the three-dimensional model, deriving from the initial point cloud, can be used to define the limit beyond which the structural analysis is compromised, or anyway less precise.*

*In this work of research, this will be demonstrated using three different case studies of buildings, consisting mainly of masonry, measured through terrestrial laser scanning and photogrammetric acquisitions.*

*This approach is not a typical study for geomatics analysis, but its challenges allow studying benefits and limitations. The results and the proposed approaches could represent a step towards a multidisciplinary approach where Geomatics can play a critical role in the monitoring and civil engineering field.*

*Furthermore, through a geometrical reconstruction, different analyses and comparisons are possible, in order to evaluate how the numerical model is accurate. In fact, the discrepancies between the different results allow to evaluate how, from a geometric and simplified modeling, important details can be lost. This causes, for example, modifications in terms of mass and volume of the structure.*

## Keyword

Terrestrial Laser Scanning; Close Range Photogrammetry; historical buildings; cultural heritage; geometric modeling; numerical modeling; comparison data; finite element analysis; structural analysis.



## FOREWORD

The present research concerns mainly the Geomatics applied to the cultural heritage; afterwards, a structural analysis has been carried out on the case studies examined. This has been possible thanks to my background studies and to the freelance activities as civil engineering.

The research was focused on preservation of cultural heritage, and the transformation from point cloud data into models suitable for the structural analysis.

The research was started by Prof. Gabriele Bitelli and Prof. Luca Vittuari. All the work here presented, was conducted under their supervision and thanks to their advices.

The San Felice sul Panaro Fortress (MO) was faced, due to the numerous damages that has suffered, by the Emilia earthquake, in 2012. The Fortress was measured by ABACUS s.a.s, using a Terrestrial Laser Scanner, and it is object of several studies that aim to preserve its integrity. The research presented derives from a collaboration with the structural area of DICAM Department.

The Baptistery of Aquileia (UD) was chosen as case study because it is suitable for different analysis, and for the integration of different techniques of data acquisition. Some issues are furthermore related to the analysis of a structural situation which no longer exists, reconstructed as a 3D model using historical documentation. The research was carried out by means of a multidisciplinary approach, with the involvement of University of Udine, in particular with Prof. D. Visintini and PhD A. Spangher

Finally, the research included a period abroad, financed by the Marco Polo program issued by DICAM; it was spent in the Institute of Geodesy and Photogrammetry IGP ETH, Zurich, Switzerland.

During these months the research work was carried out under the supervision of Prof. Andreas Wieser, and was mainly focused on the programming codes, and transformation from initial point cloud dataset into FE model. In this period, different procedures and objects were analysed.

### 1.1 Research context

Cultural heritage preservation should be seen as an integrated process of inter-related and dependent steps, in order to obtain as the final aim of each heritage intervention, the protection of the object.

There are many challenges in digital preservation and documentation projects related to the technology implemented, data management, data archiving, public delivery, and educational resources. In this way, a complete process for heritage recording and preservation can become appropriate (Kacyra, 2009).

The historical study and the knowledge that an architectural building has been subjected to the time, is very important not only in order to understand the vicissitudes and the transformations, but also for analysing critically the elements of which it is characterized. In particular, the analyses and the models carried out for the case studies, are not random, but they reflect precise reasons that ranging in different areas: from the purely architectural characters, to the geometric executive elements, to the structural analysis and deformations that the analysed structures show.

An architectural building survey is defined as inventory-taking and recording the current state of a three-dimensional object and its graphic presentation in mostly two-dimensional scaled plans. Thus, it represents one of the basic methods for acquiring information on existing structures, in order to supply base data for building-related research and planning in various applications such as historical building research, cultural heritage preservation, building redevelopment.

However, in the Geomatics field, the geometrical three-dimensional recording of complex objects has to be accomplished today with a high level of accuracy, through a combination of photogrammetric multi-image procedures and terrestrial laser scanners as computer-assisted data recording systems. Due to their ability to scan a very large number of three-dimensional points without control point signalisation within a short time, laser scanners offer a range of potential applications, especially in the documentation of architectural objects. Images acquired with the photogrammetric approach, offer additional in high resolution information, which can be used both for the construction of the object and for texture mapping. Of course, if accurate documentation is not required, geometrical abstractions, such as parallelisms, right angles and geometrical primitives, are often used for the simplification of the scaled adaptation of the geometrical map/image in the CAD modeling process (Kersten, et al., 2014).

In particular, close-range photogrammetry and terrestrial laser scanning (TLS) are two typical techniques to reconstruct three-dimensional objects (Fritsch, Khosravani, Cefalu, & Wenzel, 2011). Both techniques enable the collection of precise and dense three-dimensional point clouds. Terrestrial Laser Scanner is a polar measurement system, which directly generates three-dimensional object points and provide color information as well. The accuracy of the final point cloud is defined by the angular resolution of the instrument, while the precision of the points is mainly defined by the distance precision. This leads to a rather consistent precision behavior over a medium range. However, the resolution of TLS point clouds at the object is limited, due to the minimum acquisition distance and the limited distance precision. A higher point density on the object can be reached using photogrammetry. By using imagery acquired at short distance in combination with photogrammetric surface reconstruction methods, point clouds with high resolution at the object and high precision are obtained.

Reality-based spatial data from advanced geomatics techniques can provide an accurate reproduction of objects. The creation of realistic 3D models and their visualization is becoming more and more popular. They are a part of the modern digital age: see virtual realities, cultural heritage documentation, geospatial

applications, 3D games, TV/movie post-production and special effects (Quan, 2010). In particular, three-dimensional point clouds models, with their spatial and radiometric data (also temporal information, in case of progressive survey) help to obtain the two-dimensional and three-dimensional generation geometry, which guarantee appropriateness of geometrical accuracy, and to obtain all correlate information, to complete the semantic definition (Quattrini, Malinverni, Clini, Nespeca, & Orlietti, 2015). Some issues regarding interoperability of data and geometric approximation of architecture, however, are still open. In fact, for the parametric modelling of cultural heritage, the control of LoD (Level of Detail), the structural elements complexity level and the pre-determined discretization of the model is fundamental (Barazzetti, et al., 2015 a)), (Chiabrandò, Sammartano, & Spanò, 2016)).

With the improvement and the efficiency of technology, point cloud data derived from TLS and CRP, are characterized by a very high precision. As final output, in fact, a point cloud dataset with a millimetric precision will be obtained. The usual techniques for three-dimensional surveys and three-dimensional measurements with these different techniques are used in several and different fields, as for example for monitoring of landslides (Bitelli, Dubbini, & Zanutta, 2004) and rockfalls (Strunden, Ehlers, Brehm, & Nettesheim, 2015), for verifying the load-dependent deformations of a viaduct (Zogg & Ingensand, 2008), for monitoring the behavior of dams, or quantitatively documenting the deformation of hydraulic structures (Tschirschwitz, Mechelke, Jansch, & Kersten, 2016).

Nevertheless, the dense and accurate point cloud data cannot only be used for descriptive modeling of deformations, or in order to obtain directly results about structural analysis, like for example values in terms of frequency and displacements. It may also be the starting point for structural modeling using finite elements (FE) provided that some prior knowledge about the material and about the boundary conditions such as constraints and loading is available.

In addition to the mechanical and constitutive characteristics, the geometric definition of a structure is a fundamental data, to not neglect any important data in the structural analysis.

Most of three-dimensional models, however, especially in the structural field, are very simplified because they are realized starting from the most traditional procedures, actually starting from the measurements of plans, fronts and sections made by direct survey. These three-dimensional models are very useful and corresponding to reality in modern constructions, for example in concrete and steel element or building, but they are not so accurate for objects in the field of cultural heritage, composing by very complex geometries. As input, Geomatics data are very complex and detailed, on the contrary the structural engineer tends to obtain a simplified and defined data, in order to have models suitable for common software. In fact, most of geometric models used for structural analysis are really simple and this simplification could be acceptable for modern constructions, but is not indicated for buildings and objects belonging to cultural heritage, which present much more complex geometries.

For this reason, the goal of this research is to place as connection between the Geomatics and the structural analysis field, defining and evaluating different ways for the elaboration of the data starting from the initial point cloud dataset, in order to be suitable for the structural analyses. The studies developed on three different building belonging to the cultural heritage, have allowed the achievement of an adequate level of knowledge with a versatile and multidisciplinary approach, very important for carrying out analyses in different settings (geometrics, architectural, structural etc...).

Furthermore, once identified the procedures for transforming the initial point cloud dataset in output data suitable for structural analysis, it will be necessary to find the most appropriate method for a correct definition of the output. In order to define this, three case studies with different geometric characteristics and acquired with different techniques have been examined. Furthermore, another goal is to define the Level of Detail (LoD) of the three-dimensional models, in order to have a correct representation of the

geometry of the examined objects, without losing important details nor compromise the result deriving from the structural analyses.

## 1.2 Thesis outline

The work presented in this thesis, is ideally divided into four parts.

The first part (chapters 2 and 3) concerns a theoretical and general part, in which the contribution of geomatics for cultural heritage, and FE approach for structural analysis are analysed.

The second part (chapter 4) faces new procedures and different approaches in order to connect geomatics data with structural analysis.

In the third part (chapters 5-6-7) the procedures, discussed in the second part, will be applied with three different case study and the results will be compared and disputed.

The conclusions and recommendations for further works are given in the final part, the fourth.

In detail, the structure of the thesis is the following:

### *Geomatics in the field of cultural heritage and FE modeling*

Chapter 2: The second chapter focused on the cultural heritage. At first, a brief introduction on how the survey field has been evolved over time, until the identification of a new discipline: Geomatics. Through an historical outline, the concept of “heritage” applied for architectural building and, in general, for the conservation of monument, has been analysed. The concept of the preservation of cultural heritage is changed and has evolved over the centuries, and with this, also the documents and laws, not only in Italy but from a European point of view, by mentioning the most important Charters and Articles. Finally, the importance of the integration about Geomatics techniques has been explained, with a brief description of the used techniques of measurements in this work of research.

Chapter 3: A study about the existing modeling for cultural heritage has been carried out, with a particular attention for the Finite Element approach, that is the method used for structural analyses of cultural heritage. Different studies on contributions existing in literature, have been analysed, in order to evaluate what are the issues and how the structures belonging to the cultural heritage field are faced. Furthermore, the legislative framework in the field of structural analysis for cultural heritage is outlined, with a comparison between Italian Normative and European decrees and standards (Eurocode).

### *Procedures and approaches for connecting geomatic disciplines to Finite Element models*

Chapter 4: In this chapter, after a brief analysis on the existing contributed concerning the automatic transformation of the point cloud dataset, in different ways and fields, the procedures identified in this work of research have been explained. They are distinguished in two different approach, semi-automatic and automatic. The distinction has been made, depending on whether the contribution of the operator is or minimal or necessary.

### *Application of the methods identified for three different case studies*

- Chapter 5: The first case study analysed has been San Felice sul Panaro Fortress (MO), an important building damaged by the earthquake of Emilia, in 2012. The analyses have been focused on the transformation from initial complex point cloud, into a polygonal model with continuous surfaces. Hence, a structural analysis with a semi-automatic approach has been carried out. From the structural analysis of the entire building, it has been emerged that the most stressed elements of the Fortress are the Mastio tower and the North tower, for this reason they have been studied also as isolated buildings.
- Chapter 6: The structure composing the Basilica of Aquileia (UD) have been analysed with a particular attention for the Baptistery. After an accurate study concerning the historical analysis, through several historical old data and documents, and a data acquisition of its external part and internal one, several and different analyses have been carried out as, for example, geometric and numerical modeling and comparison data, or overlap between old (historical) data and point cloud. At last, the four different procedures have been applied, with a comparison between different output models in terms of displacements and frequency.
- Chapter 7: The last case study is the Bell tower of San Luzi church (CH). With a high of 60 metres, the input data (measured using TLS) was very noisy. After some problems faced in order to obtain a correct polygonal model, the two semi-automatic procedures have been applied, in order to obtain a final FE model. Furthermore, with a hypotheses concerning the loads and the sections of the beams inside the Tower, also a structural analysis has been carried out, in particular a static analysis, and a dynamic analysis with the natural frequencies of the main model of shape.

## Geomatics in the field of cultural heritage

### 2.1 Introduction

The preservation of cultural heritage buildings requires an interdisciplinary approach with specialists of different areas of knowledge, traditional and innovative techniques of intervention, compatibility, ethics of the conservation, etc. Recording and documentation are also important because they promote the economic value of the cultural heritage, such as cultural tourism and regional development; increase and strengthen the cultural and social identity at different levels (local, regional, international); contribute to prevent theft and illicit traffic of cultural heritage goods. The importance of documenting and, subsequently, recording data, referred to cultural and natural heritage, is well internationally recognized and has been argument of discussions and researches since the theory of restoration and conservation has begun to take hold. It is the task of heritage managers and decision makers to establish policies and programs for the correct recording and effective management of conservation-related information.

In this first chapter, first of all, a quick view of the changes of the surveying and the geomatics techniques throughout the history has been carried out, in order to understand the evolution of the discipline over time. Then, specifically the preservation of cultural heritage has been addressed, also through the documents, and the conventions related to this field. Hence, the integration of geomatics techniques with a hint to the geomatic surveying techniques used for the case studies of this research have been analysed.

### 2.2 Surveying throughout the history

In order to better comprise the topic, it cannot be separated by the historical evolution it has underwent. Each historical period has considered Geomatics and survey with different approaches: the actual way to conceive and propose this topic, is the result of previous studies with sequences of different epochs. Several documents give testimony of this discipline since ancient times, when the human being was to the continue investigation of a dialogue with the architectural, urban and territorial reality where he lived. The most authentic evidences are represented on engraving, painting, sculptures and stones: elements of representation of the time.

Several ancient communities, and in particular the Greek one, have obtained such high levels that still now they are the base for further studies in many areas of this discipline. The knowledge about architectural survey from the Greek community are pretty poor. The Greeks knew and used a system of measurement because they gave great importance to geometric analysis and to optical corrections. The survey in Roman architecture differs from the Greek because it is characterized by own peculiarities. The real innovation compared to the past, is that they founded a real professional category in the architectural field, recognized by the government. Romans, with their Forma Urbis, realized that urban space could be represented only if public and private spaces are surveyed, for underlining not only individual buildings, but also the relationships between them. In the Renaissance, the main goal was to identify the rules concerning the ancient construction of the building and the drawing was considered an instrument of knowledge and investigation unknown before. Teamwork, to the detriment of individual production for surveying elaboration, allows a higher range of research field for surveying elaboration. The result is the survey of the buildings with the construction of perspective views.

Therefore, the survey has always existed, with operations of measurement and drawing; nevertheless, it is only in XIX° century that there were graphics restitutions with rigorous measures, that introduce to the new and current scientific discipline: Geomatics.

## 2.3 Geomatics

The term “Geomatics” is a neologism: it derives from the hybridization of a Greek word  $\gamma\epsilon\omicron\omicron$ , with the suffix *-matics* deriving from Informatics. The use of this term includes all the disciplines of environmental and territorial survey, pointing out the decisive aspect that the informatics has got.

In particular, this word was born in Laval University, in Canada, at the beginning of this century, with the increase of knowledge for the potentialities offered by electronic computing, which they are revolutionizing surveying and representation sciences. The use of computerized drawing, therefore, was compatible with processing data, until then unknown. In the last decades, the development of surveying disciplines has been intense: from geodesy to topography of precision, from photogrammetry to remote sensing, from numerical cartography to Geographic Information System (GIS). Therefore, Geomatics involves techniques and technology from topography, analytic and digital photogrammetry, remote sensing from satellites, airborne systems and UAV, three-dimensional scanning and modelling, numerical cartography, geographic information systems, etc. In the last years, this discipline has grown also because it includes, in interdisciplinary way, lots of digital data and information, surveyed with very different procedures and sensors, that have to be organised, developed and processed. For these reasons, it represents a systemic, integrated and multidisciplinary approach that, at the same time, is characterized by not synthesizable standard elements. In fact, every case study has own characteristic, not absolute but relative to the object or element that has to be analysed.

## 2.4 Preservation of cultural heritage

Historical structures and monuments are symbols of the cultural identity and they constitute the most important part of the cultural heritage ( (Grussenmeyer, et al., 2012); (Vatan , Selbesoğlu, & Bayram , 2009)). Three-dimensional modeling and continuously monitoring of historical objects is a crucial issue (Fritsch D. , Khosravani, Cefalu, & Wenzel, 2011). According to UNESCO (UNESCO, 1972), the geometric documentation can be defined as the action of acquiring, processing, presenting and registering the data necessary for the determination of the position, shape and size of a monument within a three-dimensional space and at a given moment in time. That is, such documentation records the present state of a heritage element, providing the basis for the study of its past (Martínez, Santiago, & Gil, 2015).

The importance of cultural and natural heritage documentation is well recognized at international level, and there is an increasing pressure to document and preserve heritage by digital means. The continuous development of new sensors, data capture methodologies, the multi-resolution three-dimensional representations and the improvement of existing ones can contribute significantly to the 3D documentation, conservation, and digital presentation of heritages and to the growth of the research in this field.

The increasing request, in order to obtain very detailed surveys in the field of cultural heritage, has been one of the most important elements in the recent development of terrestrial laser scanning and photogrammetry. In fact, measuring millions of points, these techniques allow to achieve complete and detailed three-dimensional models, with a millimeter accuracy. For this reason, the field of cultural heritage produces a more frequent interest from scientific community, regarding Geomatics and surveying fields. The versatility

of the survey for cultural heritage is very ample; for this reason, it doesn't have to be considered only as a correct measurement of an object, with its graphic representation. On the contrary, Geomatics and surveying belong to a more complex context, characterized by scientific strictness, which need appropriate instruments and knowledge in order to acquire and analyse any case study.

The recording of position, dimensions and/or shape is a necessary part of almost every project related to the conservation of cultural heritage, consisting of an important element of the documentation and analysis process. For example, knowing the size and shape of a topographic feature located in a historic landscape, can help archaeologists to identify its significance; knowing how quickly a stone carving is eroding helps a conservator to determine the appropriate action for its protection; while simply having access to a clear and accurate record of a building façade, is a help to schedule the work for its restoration. It is common to present such measurements as plans, sections and/or profiles plotted on hardcopy for direct use on site. However, with the evolution of new methods of three-dimensional measurement, and through computer software, there is a growing demand for three-dimensional digital information. There is a variety of techniques available to generate three-dimensional survey information.

#### 2.4.1 Historical outline

Traditionally 'heritage' was defined as architecture or archaeology or movable objects. Now 'heritage' includes buildings, monuments, landscapes, urban areas, countryside, maritime sites, buried remains and objects. 'Historic environment' or 'place' are now common terms. These trends can be traced in the European Conventions and Charters as well as in thinking about World Heritage which is moving from defining specific categories towards integrated conservation and cultural landscapes.

To start with the historical evolution in the time, however, it is important a reference to the concept of 'culture' which has been studied by anthropologists. It may be useful to begin, for example, the definition of 'culture' by Edward Burnett Tylor in his *Primitive Culture* (1871):

*Culture [...] is that complex whole which includes knowledge, belief, art, morals, law, custom, and any other capabilities and habits acquired by man as a member of society.*

With the progress of time, the definition has gradually become more complex. The legal framework for the protection of heritage sites began to develop at national and international level in the nineteenth century. In particular, the International Museums Office (IMO) was established in 1926 by the League of Nations; its aim was to promote the activities of the museums and every country by organizing joint work and research to be undertaken in common. During its existence, IMO organised a number of events for setting the scene for the development of an international movement for cultural heritage conservation. Among these, the Athens Conference of 1931 on the protection and conservation of monuments of art and history was included.

Over the recent decades, all the international bodies and agencies have passed resolutions concerning the obligation for protection, conservation and restoration of monuments. The Athens Convention (1931), The Hague Agreement (1954), the Chart of Venice (1964) and the Granada Agreement (1985) are only a few of these resolutions in which the need for geometric documentation of the monuments is also stressed, as part of their protection, study and conservation.

UNESCO (1945) and the Council of Europe have formed specialized organizations for this goal. In particular, UNESCO is part of ONU (Organization of United Nations for Education, Science and Culture). It was created on 4<sup>th</sup> November 1946 in Paris, and still now its headquarters is there. ICOMOS (International Council for Monuments and Sites) is the most important one, but also CIPA (International Committee for Architectural

Photogrammetry), ISPRS (International Society for Photogrammetry & Remote Sensing), ICOM (International Council for Museums), ICCROM (International Centre for the Conservation and Restoration of Monuments) and UIA (International Union of Architects) are all involved in this task.

The Convention for the Protection of Cultural Property in the Event of Armed Conflict adopted at The Hague (Netherlands) in 1954, as a consequence to the massive destruction of the cultural heritage in the Second World War, is the first international treaty of a world, dedicated exclusively to the protection of cultural heritage in the event of armed conflict. The Convention was adopted together with a Protocol in order to prevent the export of cultural property from occupied territory, requiring the return of such property to the territory of the State from which it was removed.

The International Charter for the Conservation and Restoration of Monuments and Sites, better known as the Venice Charter, has provided a set of guiding principles for the protection of historical monuments and sites since its editing, in 1964. It also had an instrumental role in the establishment of international organizations for the conservation of natural and cultural heritage.

This document composes of 16 articles, distinct in eight parts, including aim, conservation and restoration; among these, most important are the following:

- Article 2: The conservation and restoration of monuments must have recourse to all the sciences and techniques which can contribute to the study and safeguarding of the architectural heritage.
- Article 7: A monument is inseparable from the history to which it bears witness and from the setting in which it occurs. The moving of all or part of a monument cannot be allowed except where the safeguarding of that monument demands it or where it is justified by national or international interest of paramount importance.
- Article 16: In all works of preservation, restoration or excavation, there should always be precise documentation in the form of analytical and critical reports, illustrated with drawings and photographs. Every stage of the work of clearing, consolidation, rearrangement and integration, as well as technical and formal features identified during the course of the work, should be included. This record should be placed in the archives of a public institution and made available to research workers. It is recommended that the report should be published.

The Convention concerning the Protection of the World Cultural and Natural Heritage, adopted by the General Conference at its seventeenth session in Paris, in 1972, is a unique legal instrument, based on the idea that some cultural and natural heritage sites are of universal and exceptional importance and need to be protected as part of the common heritage of humanity. One of the most original aspects of the World Heritage Convention is the explicit link between natural and cultural heritage, traditionally considered as separate. During the general Conference, definition of the cultural it is given in the first article:

- Article 1. For the purposes of this Convention, the following shall be considered as “cultural heritage”:
  - monuments: architectural works, works of monumental sculpture and painting, elements or structures of an archaeological nature, inscriptions, cave dwelling and combinations of features, which are of outstanding universal value from the point of view of history, art or science;
  - groups of buildings: groups of separate or connected buildings which, because of their architecture, their homogeneity or their place in the landscape, are of outstanding universal value from the point of view of history, art or science;
  - sites: works of man or the combined works of nature and man, and areas including archaeological sites which are of outstanding universal value from the historical, aesthetic, ethnological or anthropological point of view.

The concept of national cultural heritage has become well-known thanks, in part, to the mediation of UNESCO, which obtained the consensus of the member states regarding the notion of universal cultural heritage, which also recognises environmental, as well as cultural assets, as constitutional. This extension of the concept of heritage has also been acknowledged by the Italian State, thanks to UNESCO membership and the establishment of the Ministry of Cultural and Environmental Wealth in 1975.

In 1975, in the European Charter of the Architectural Heritage, adopted by the Council of Europe in Amsterdam, we can read:

“[...] Recognizing that the architectural heritage, an irreplaceable expression of the wealth and diversity of European culture, is shared by all people and that all the European States must show real solidarity in preserving that heritage; Considering that the future of the architectural heritage depends largely upon its integration into the context of people's lives and upon the weight given to it in regional and town planning and development schemes... [...]”;

- Art. 1 -The European architectural heritage consists not only of our most important monuments: it also includes the groups of lesser buildings in our old towns and characteristic villages in their natural or manmade settings. For many years, only major monuments were protected and restored and then without reference to their surroundings. More recently it was realized that, if the surroundings are impaired, even those monuments can lose much of their character. Today it is recognized that entire groups of buildings, even if they do not include any example of outstanding merit, may have an atmosphere that gives them the quality of works of art, welding different periods and styles into a harmonious whole. Such groups should also be preserved. The architectural heritage is an expression of history and helps us to understand the relevance of the past to contemporary life.
- Art. 2 -The past as embodied in the architectural heritage provides the sort of environment indispensable to a balanced and complete life. In the face of a rapidly changing civilization, in which brilliant successes are accompanied by grave perils, people today have an instinctive feeling for the value of this heritage. This heritage should be passed on to future generations in its authentic state and in all its variety as an essential part of the memory of the human race. Otherwise, part of man's awareness of his own continuity will be destroyed
- Art. 3 - The architectural heritage is a capital of irreplaceable spiritual, cultural, social and economic value. Each generation places a different interpretation on the past and derives new inspiration from it. This capital has been built up over the centuries; the destruction of any part of it leaves us poorer since nothing new that we create, however fine, will make good the loss. Our society now has to husband its resources. Far from being a luxury this heritage is an economic asset which can be used to save community resources. The structure of historic centres and sites is conducive to a harmonious social balance. By offering the right conditions for the development of a wide range of activities our old towns and villages favoured social integration. They can once again lend themselves to a beneficial spread of activities and to a more satisfactory social mix.

ICOMOS (1996) stresses the need of recording information in order to make easier the decisions to be taken and the safety assessment of the structure. In this way, the historical information, the present state and all acquired information, diagnosis, safety evaluation, interventions must be recorded and documented in an Explanatory Report. The Explanatory Report should contain:

- a) the type, form, dimensions and characteristics from outside and inside of the cultural heritage building;

- b) the intrinsic value of the monument (historic, cultural, artistic, scientific, etc), as well as the significance of the materials, elements, decorations, inscriptions, machinery, gardens, landscapes, etc.;
  - c) the technology and skills used during its construction and any relevant intervention;
  - d) history of the origins of the building including the date of construction, authorship, ownership, original design, decoration, use, etc.;
  - e) subsequent history of the building as different uses, historical events, alteration to the structure and architectural style;
  - f) the history of management and interventions (maintenance and repairs); and g) an assessment of the current condition of the building, including the conflicts and risks from human or natural causes (environmental pollution, actual use, etc.).
- Due to the large amount of information required for the Explanatory Report it is not always possible to have or to publish only one document. Therefore, the correct management of the different documents becomes compulsory.

It is noted that the ICOMOS Principles are open for new technologies such as multimedia and internet technologies, and they do not fix a specific format or media. This is important, because the advance of technology allows the incorporation of new media for appropriate handling of information (Romão, Paupério, Guedes, & Costa, 2006).

In 2002, on the occasion of the 30th anniversary of the Convention, the World Heritage Committee reviewed its Strategic Objectives and established, with the Budapest Declaration on World Heritage, four overarching goals:

- Credibility;
- Conservation;
- Capacity-Building;
- Communication.

These four goals sum up the challenges ahead:

- ensuring adequate representation for all types of cultural and natural heritage sites;
- promoting their effective conservation;
- raising the level of management and human skills for conservation;
- informing the public of the achievements and challenges ahead.

These important strategic directions, built on previous long-term orientations and resting on the solid experience gained over thirty years, today constitute UNESCO's main framework of action in the implementation of the World Heritage Convention.

The World Heritage Convention has achieved a great deal during the three decades of its existence. Today, it is among the foremost international tools of conservation, and certainly among the best known. Its impact has grown over time, inspiring ever greater involvement by governments, communities and individuals, universities, foundations and private sector enterprises. The key message of the Convention – the need to preserve and transmit cultural and natural heritage of 'outstanding universal value' to future generations – has found an echo in national and international policies worldwide. Today, the Convention is implemented through an extensive and still expanding system encompassing States Parties at all levels, from national government to site managers, UNESCO, the three Advisory Bodies, ICCROM, ICOMOS and IUCN, as well as many other specialized organizations and institutions worldwide. New actors and partners are continually being brought into the network. Each has an important role to play in shaping policies, advancing methodologies and management practices that need to be integrated in national policies, building capacity and extending the reach and the educational role of cultural and natural heritage. In a sense, this system is

the most important result of the Convention, ensuring its presence in today's world and its guarantee for the future.

Although the concept of cultural heritage was very old, this is still considered, in Europe, as a strategy for the preservation and the promotion of cultural heritage. In 2001, for example, in the Convention concerning the protection of the World cultural and natural heritage, the World Heritage Committee reaffirmed the Convention for the Protection and Cultural Heritage as an instrument of consensus, cooperation and accord between States Parties and takes particular note of Article 6 (1), Article 6 (2) and Article 11:

- Art. 6 (1): Whilst fully respecting the sovereignty of the States on whose territory the cultural and natural heritage [...], the States Parties to this Convention recognize that such heritage constitutes a world heritage for whose protection it is the duty of the international community as a whole to co-operate;
- Art. 6 (2): The States Parties undertake, in accordance with the provisions of this Convention, to give their help in the identification, protection, conservation and presentation of the cultural and natural heritage [...];
- Art. 11: Every State Party to this Convention shall, in so far as possible, submit to the World Heritage Committee an inventory of property forming part of the cultural and natural heritage [...].

In 2003, ICOMOS defines the principles for the Analysis, Conservation and Structural Restoration of Architectural Heritage, which the most important are the following:

- 1.1 Conservation, reinforcement and restoration of architectural heritage requires a multi-disciplinary approach.
- 1.2 Value and authenticity of architectural heritage cannot be based on fixed criteria because the respect due to all cultures also requires that its physical heritage be considered within the cultural context to which it belongs.
- 1.6 The peculiarity of heritage structures, with their complex history, requires the organisation of studies and proposals in precise steps that are similar to those used in medicine. Anamnesis, diagnosis, therapy and controls, corresponding respectively to the searches for significant data and information, individuation of the causes of damage and decay, choice of the remedial measures and control of the efficiency of the interventions. In order to achieve cost effectiveness and minimal impact on architectural heritage using funds available in a rational way, it is usually necessary that the study repeats these steps in an iterative process.

The UNESCO Draft Charter on the Preservation of Cultural Heritage, in 2003, presents a compelling case for digital preservation. It is included in the Guidelines to provide a clear link between the two documents, and to present those advocacy and public policy issues that are outside the scope of technical and practical guidelines, and proclaims and adopts this Charter, in which defines digital heritage (and then digital material includes texts, databases, graphics, software) as a common heritage. The purpose of preserving the digital heritage is to ensure that it remains permanently accessible. Accordingly, access to digital heritage materials, especially those in the public domain, should be equitable and free of unreasonable restrictions. In the second part of the Charter (Art. 3-4-5), there is the guarding and the attention against loss of heritage. For this reason, in the third part (Art. 6-7-8-9) measure required in order to preserve and protect digital heritage data.

## 2.5 The integration of Geomatics techniques for the survey of cultural heritage

In cultural heritage field, choosing and defining a priori the appropriate technologies and techniques is always a very hard question (Patias, Grussenmeyer, & Hanke, 2008). The main parameters are the size and the complexity of the object and the level of accuracy required. Nevertheless, the survey in the cultural heritage is associated to a restricted operative field, and the operations have different sizes: from the measurements of a building to those of a statue. In this context, cultural heritage is the most significant for the possibilities offered for every case study, also in function of conditions of work and time. For these reasons, it is useful and necessary a multi-disciplinary approach, starting from photogrammetric acquisition, to measurement techniques with laser or other 3D scanning (Vosselman & Maas, 2010). Nowadays the generation of a 3D model is mainly achieved using non-contact systems based on light waves, in particular using active or passive sensors. As mentioned, the importance of cultural and natural heritage documentation is well understood at an international level and the value of recording digitally in three dimensions is increasingly recognised. This continuous development of new sensors and the improvement of existing ones are contributing significantly to the documentation, conservation and digital presentation and to the growth of research in the cultural heritage field. This growth also derives from a continuous increasing demand for digital documentation in the form of three-dimensional surveys at different scales and resolutions with digital non-invasive techniques and methodologies. In general, objects can be measured by several different techniques, such as conventional close range photogrammetry (Gruen, Remondino, & Zhang, 2002), infrared thermography (IRT) (Clark, McCann, & Forde, 2003) image-based (Hutchinson & Chen, 2006), TLS (Pesci A., 2011), digital photogrammetry (Bitelli, Girelli, Marziali, & Zanutta, 2007); (Girelli, Tini, & Zanutta, 2005)). All Geomatics modern tools can be used and adapted in the cultural heritage field, although some are more suitable than others. In particular, in this field of research, surveying and documentation using non-invasive Geomatics techniques and methodologies, can be divided into four different broad scales (as shown in [Table 1](#)):

- Large scale: with the goals to give the context of analysis field, and the modelling of topography and orography of landscapes; airborne sensors are useful for this broad;
- Urban scale: where sites with historical and archaeological elements are recorded. Airborne sensors and terrestrial scanners provide suitable data for these tasks;
- Local scale: which includes buildings and archaeological and architectural complex objects; for these elements, terrestrial active and passive sensors are used;
- Object scale: the thorough recordings of artefacts enables new kinds of investigation, and facilitate the production of physical replicas, thus helping to preserve the original object or valorise them.

With a reduction of scale (from large to little size), geometric resolution and achievable Level of Detail gradually increase (Remondino & Lambers, 2008). Close range photogrammetry and terrestrial laser scanner, then, are used for objects with the same order of size, and for this reason especially in the cultural heritage field are closely related. The remote sensing, therefore, is used for example for mapping and classifications of an area, and with the integration of radar data.

This work will be focused on the use of terrestrial laser scanner TLS and close range photogrammetry CRP.

Types of survey	Object of interest	Available geomatics sensors and data
<b>Large Scale</b> (several km <sup>2</sup> )	Context	Aerial photogrammetry
	Landscape	Middle and high resolution satellite imagery
	Topography	Airborne laser scanning
	Sites	Radar and LiDAR Remote sensing GNSS
<b>Urban scale</b>	Archaeological sites	Aerial photogrammetry
	Excavation layers	Large scale aerial or terrestrial images
	Historical site	Radar ToF range sensors Total station GPS
<b>Local scale</b>	Complex object	Close range photogrammetry
	Building	Total station Terrestrial laser scanner GPS
<b>Object scale</b>	Excavated object	Terrestrial laser scanner
	Museum object	Photogrammetry
	Artefacts	



**Table 1:** Types of surveys with instruments for different sizes of operation are shown, with the related non-invasive geomatics sensors

The generation of a 3D model is achieved using active or passive sensors:

- Image-based sensors (i.e. photogrammetry), the very used method for its fast acquisition and because the contact with the object is not requested;
- Range-based modelling (i.e. laser scanning), acquiring thousands of points per second;
- combination of image- and range-based modeling, as they both have advantages and disadvantages and their integration can allow the generation of complete and detailed 3D models efficiently and quickly.

### 2.5.1 Terrestrial Laser Scanner TLS

A LASER (Light Amplification by Stimulated Emission of Radiation) emits a beam of highly collimated, directional, coherent and in-phase electromagnetic radiation. The sensor sends out this pulse, the signal is back scattered by ground surface or others objects and then recorded. It automatically collects 3D coordinates of an object surface in a systematic pattern, using laser light. The term 'laser scanner' is generally applied to a range of instruments that operate on differing principles, in different environments and with different levels of precision and resulting accuracy. A generic definition of a laser scanner, adapted from Böhler and Marbs is any device that collects 3D coordinates of a given region of an object's surface automatically and in a systematic pattern at a high rate achieving the results in near real time (Böhler & Marbs, 2002). Laser scanning generates a very dense point cloud with XYZ coordinates; the point cloud includes additional information, such as return intensity, colour values and reflectance. According to the principle of the distance measurement system, different categories are individuated:

- Short range 3D scanner: Short Range 3D scanners typically utilize a Laser triangulation or Structured Light technology (in this case laser technology is not involved). Systems based on the optical

triangulation principle are involved, in which the point is surveyed as the intersection of two lines. These tools are suitable for small or medium size objects, i.e. statues. The point cloud is very dense and accuracies down to some micrometres can be achieved;

- Optical triangulation scanner: they use a process called trigonometric triangulation to accurately capture a 3D shape as millions of points. Laser scanners work by projecting a laser line or multiple lines onto an object and then capturing its reflection with a single sensor or multiple sensors. The sensors are located at a known distance from the laser's source. Accurate point measurements can then be made by calculating the reflection angle of the laser light. The travel time required to the laser beam to reach the surface and come back is measured. Knowing its velocity, the distance can be calculated. These instruments allow the measurements of distances up to several hundreds of meters;
- Phase- comparison scanner: the distance laser-object is calculated by using the phase difference between the transmitted and received laser waves. They are more accurate and permit high frequency data acquisition but suffer from a limited range.

Principles and fundamentals of Laser Scanning techniques can be found in Shan & Toth (2008).

The different types of laser scanners involve differences in the measurement accuracies, in the acquisition methods, in the final resolution of the point cloud. There is not any instrument that can simultaneously satisfy all these requirements.

The choice of the instrument, in particular, must be based on the specific needs of use, on the basis of multiple characteristics as, for example:

- Accuracy;
- Fast acquisition;
- Range of measurement;
- Wavelength according to possible external noise signal (sunlight, humidity) and of the reflectivity characteristics of the external surfaces;
- Visual field of the instrument;
- Ease of transport;
- Type of power source;
- Quality of acquisition software.

A classification of laser scanning techniques, used in cultural heritage management activities, is reported in the following [Table 2](#).

Scanning system	Use	Typical accuracy/operating range
Triangulation based artefact scanners	rotation stage	- Scanning small objects (that can be removed from site) -To produce data suitable for a replica of the object to be made
	arm mounted	- Scanning small objects and small surfaces - Can be performed on site if required - Can be used to produce a replica
	Mirror/prism	-Scanning small object surface area <i>in situ</i> -Can be used to produce a replica
Terrestrial time-of-flight laser scanners	- To survey building façades and interiors, resulting in line drawing (with support data) and surface models	50 microns/0.1-1m  50 microns/0.1-1m  Sub-mm/0.1m-25m  3-6 mm at ranges up to several hundred meters
Terrestrial phase-comparison laser scanners	- To survey building façades and interiors, resulting in line drawing (with support data) and surface models-particularly where rapid data acquisition and high point density are required	c 5mm at ranges up to 50-100 m
Airborne laser scanning	- To map and prospect landscapes (including in forested areas)	0.05m+ (depending on the parameters of the survey) / 100m-3500m
Mobile mapping	-To survey railways and highways -For city models - To monitor coastal erosion	10-50 mm /100-200m

**Table 2:** Laser scanning techniques used in cultural management activities (Barber & Mills, 2011)

In the present work, systems based on the TOF method have been used.

In the TOF laser scanners, the principle of operation consists in the emission of a laser pulse towards the object. The distance between the emitter and the reflective surface is calculated as a function of the time spent by the pulse signal between the emission and the reception. 3D coordinates (X, Y, Z) are registered for each acquired point. Moreover, coupling the instrument with a photo camera it is possible to obtain also the RGB values of the acquired point cloud. The resulting data have to be georeferenced, firstly aligning the scans together and then globally, i.e. using a set of Ground Control Points (GCP). The alignment procedure usually consists of a preliminary rough registration, using homologous points and in a subsequent refinement, mainly obtained using the Iterative Closest Point (ICP) procedure ( Besl & McKay, 1992); (Chen & Medioni, 1991)). Depending from the final purpose, registration can be required in an absolute or in a relative coordinate system. Different approaches can be adopted, depending on the required accuracy, time, effort and cost constraints. For the global georeferentiation a GPS and/or a total station is required.

## 2.5.2 Close Range Photogrammetry CRP

The name "photogrammetry" is derived from the three Greek words phos or phot which means light, *gramma* which means letter or something drawn, and metrein, the noun of measure. Photogrammetry is the science of obtaining reliable information about the properties of surfaces and objects without physical contact with the objects, and of measuring and interpreting this information. The development of photogrammetry clearly depends on the general development of science and technology. It is interesting to note that the four major phases of photogrammetry are directly related to the technological inventions of photography, airplanes, computers and electronics. An important task of the photogrammetry is concerned with reconstructing the geometry of the object from the images. The success of reconstruction in terms of geometrical accuracy depends largely on the similarity of the image bundle compared to the bundle of principal rays that entered the lens during the instance of exposure. The purpose of camera calibration is to define an image space so that the similarity becomes as close as possible. Photogrammetry is based on the concept of stereoscopic parallax and collinearity equations. The stereoscopic natural vision allows the three-dimensional perception of the objects. It depends on stereoscopic parallaxes, that is the variation of the angles that make the visual of each eye on the observed point.

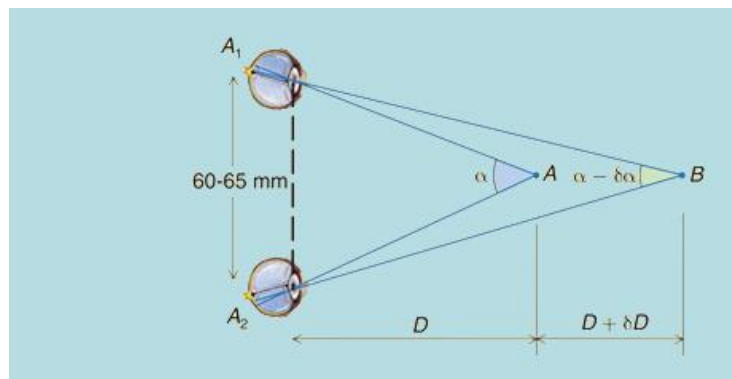


*Figure 1: Stereoscopic concept for the three-dimensional perception of the object*

The same concept is transferred to artificial stereoscopic vision: in photogrammetry, in fact, pair of frames exist, containing the same object took from different positions, in which homologous points will be identified.

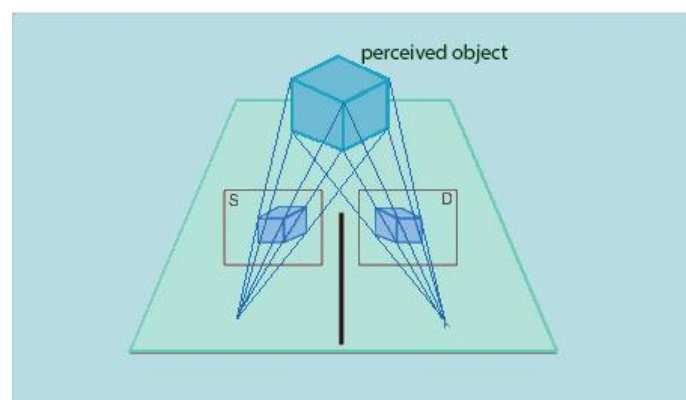


*Figure 2: Perception of depth with principles of collinearity*

Thanks to this, it can possible to perceive the depth. The principles of collinearity equations mean that the perspective centre, the image point, and the object point, must lie on a straight line. Theory of photogrammetry can be found in Slama et al. (1980) and Atkinson (1996), and in Schenk (2005). Photogrammetry is classified according to the type of acquisition, elaboration data and in function of the photos used, as shown in following **Table 3**.

Acquisition data	Elaboration data	Type of photo
<p><b>Terrestrial photogrammetry</b> The acquisition is made on the ground floor; in these cases, the objects are located at a distance less than 200m; for this reason, it is defined also photogrammetry of neighbours.</p> <p><b>Aerial photogrammetry</b> The acquisitions are made from a plane; in this case the terrain is located at greater distances of 200 m, and it is therefore called also Photogrammetry of distant (land survey).</p>	<p><b>Analogical photogrammetry</b> The reconstruction of measured objects is obtained with physical instruments (for example light rays), that reproduce the acquisition phenomena inverse.</p> <p><b>Analytical photogrammetry</b> The reconstruction of surveyed objects is obtained by making numerically (with modern calculation tools) appropriate measurements directly on the frames.</p>	<p><b>Classical photogrammetry</b> The photos are obtained on film or glass plates (in positive and negative).</p> <p><b>Digital photogrammetry</b> Photos are obtained numerically and organized in a grid of pixels. They can be got both from a digital machine, both for scanning of a traditional photo.</p>

*Table 3: Classification of photogrammetric acquisitions*

## Three dimensional modeling for structural analysis

### 3.1 Introduction

In many cases, an adequate model is obtained using a finite number of well-defined components. These are defined as *discrete*. In others, the subdivision is continued indefinitely and the problem can be defined only using the mathematical function of an infinitesimal. This leads to differential equations or equivalent statements which imply an infinite number of elements. These are defined as *continuous*. With the advent of digital computers, discrete problems can generally be solved readily even if the number of elements is very large. As the capacity of all computers is limited, continuous problems can only be solved exactly by mathematical manipulation. To overcome the intractability of realistic types of continuous problems (continuum), various methods of discretization have from time to time been proposed and all involve an approximation which approaches in the limit the true continuum solution as the number of discrete variables increases. It is the goal of *Finite Element Analysis (FEA)*, to link as a general discretization procedure of continuum problems, posed by mathematically defined statements. Finite element procedure is an indispensable part of engineering and design.

In this chapter, an introduction to the Finite Element approach has been carried out, with a particular attention for the linear static and dynamic analyses, faced in the case studies of this work of research. Furthermore, a study for existing FE models in the field of cultural heritage has been made, in order to analyse and compare different applications. At last, the legislative scenario in force in the field of structural analysis for cultural heritage is outlined, with a particular attention for the Italian decree laws.

### 3.2 Finite Element approach

In the analysis of problems of a discrete nature, a standard methodology has been developed over the years. Finite element approach is employed in the analysis of solids and structures and for transferring of fluids, in fact are very useful in every field of engineering analysis. Finite Element Analysis FEA was originally developed for solid mechanics' applications. FEM represents the confluence of three ingredients: Matrix Structural Analysis (MSA), variational approximation theory, and the digital computer. These came together in the early 1950. MSA came on the scene in the mid-1930s when desk calculators became popular, and variational approximation schemes akin to those of modern FEM were proposed before digital computers.

There was some theoretical formulation, by Ritz in 1906 in his "Lösung von Variationproblemen", "Weak formulation" by Galerkin in 1915, or "Mathematical foundation" by R. Courant in the 1943, and some others important by Argyris and Zienkiewicz. The definition "finite element" appeared for the first time in the paper by R. W. Clough (Clough, 1960). FEM analysis has achieved great development, because:

- Very complex geometry can be handled;
- It is very well suited for computers;
- It is useful for a wide variety of engineering problems (from mechanics to solid and fluids, to electrostatics etc...)
- Complex restraints and loading can be managed.

The FE method is used to solve physical problem in engineering analysis and design. The physical problem typically involves an actual structure or structural component subjected to certain loads, and the idealization of the physical problem to a mathematical model requires certain assumption that together lead to differential equations governing the *mathematical model*. The FE analysis solves this mathematical model. FEA is originally developed for solving solid mechanics problem.

### 3.2.1 Description

FEM cuts a structure into several elements (pieces of structure), then reconnect elements at *nodes* if nodes were pins that keep elements together. This process results in a set of simultaneous algebraic equations. Therefore, FEA is a numerical method that offers approximate solutions. According to the characteristics of a system, it could be distinguished in:

- Continuum model: with infinite elements
- Discrete model: which finite elements and nodes (hence the origin of *FEM*)

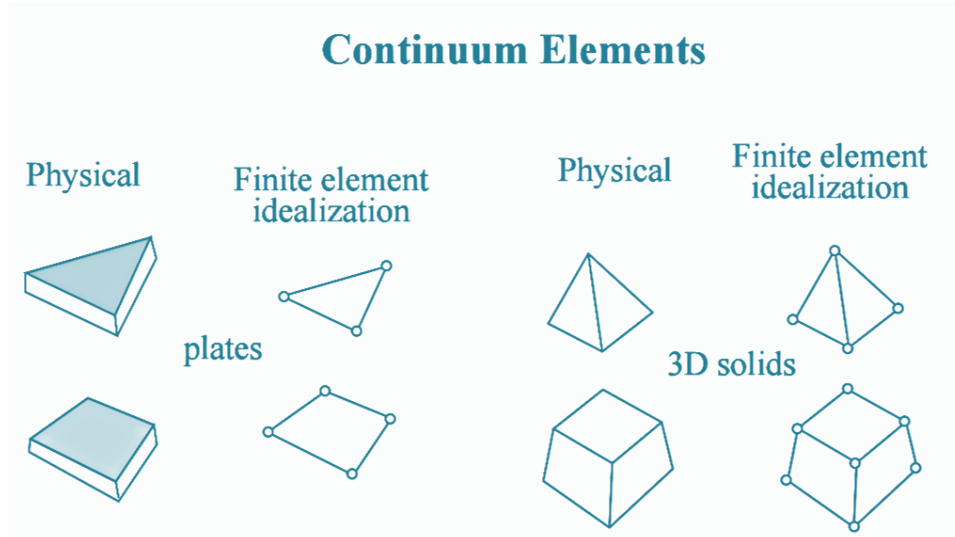


Figure 3: comparison between continuous and discrete element

Basically, FE method is a numerical technique for approximating the solution of continuous system. This is possible using a displacement based formulation, and a stiffness based solution (direct stiffness method). The continuum is discretized using a mesh of finite elements and element geometry is defined by node locations; this is valid in the domain 1D, 2D and 3D.

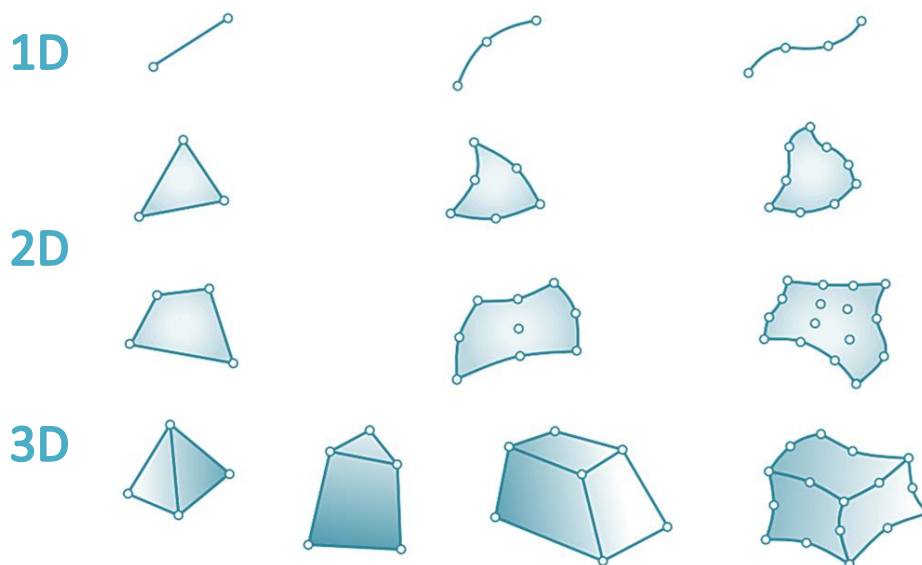


Figure 4: Example of discretized element in 1D, 2D and 3D domain

FEA is originally developed for solving solid mechanics problems. If we considered a generic solid, with an applied force:

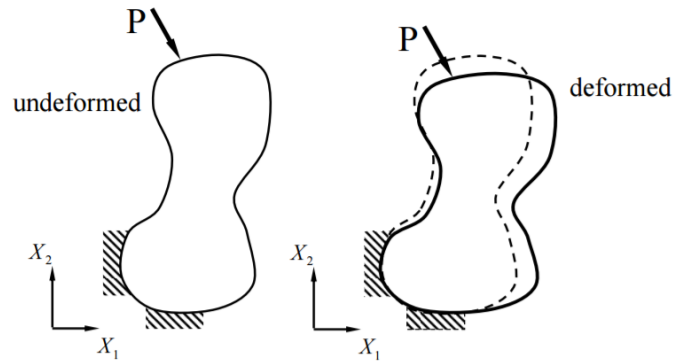


Figure 5: A generic object with an applied force P

we cannot calculate the value of displacement, stresses and strain for each point, because they answer to the following mathematical laws

$$e_{ij} = \frac{1}{2} \left( \frac{\partial u_i}{\partial X_j} + \frac{\partial u_j}{\partial X_i} \right)$$

$$\sigma_{ij} = 2G e_{ij} + \lambda e_{kk} \delta_{ij}$$

$$\frac{\partial \sigma_{i1}}{\partial X_1} + \frac{\partial \sigma_{i2}}{\partial X_2} + \frac{\partial \sigma_{i3}}{\partial X_3} + f_i = 0$$

For this reason, it is necessary to find a numerical method that approximate this solution. FEA method, in a numerical approximation, is based on some important concepts:

- Divide the interval of integration
- In each sub-interval, choose proper simple functions to approximate the true function
- The result will be an approximation of the exact solution
- The accuracy of the results depends on the number of sub-interval and approximate functions.

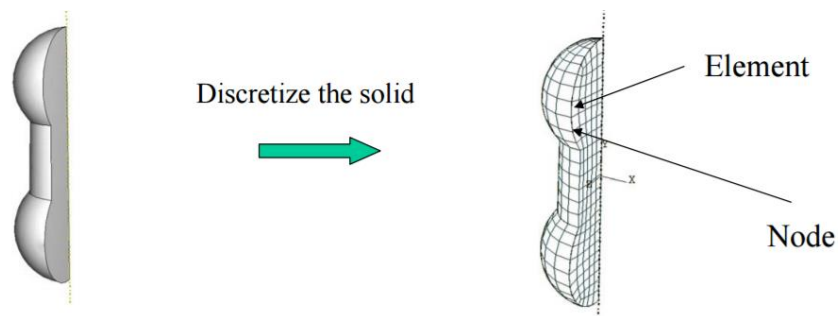


Figure 6: The image shows a quarter of previously generic solid object, a solid portion (left) and the discretized element (right)

If this approach is transposed on a generic structural and simple 2D element:

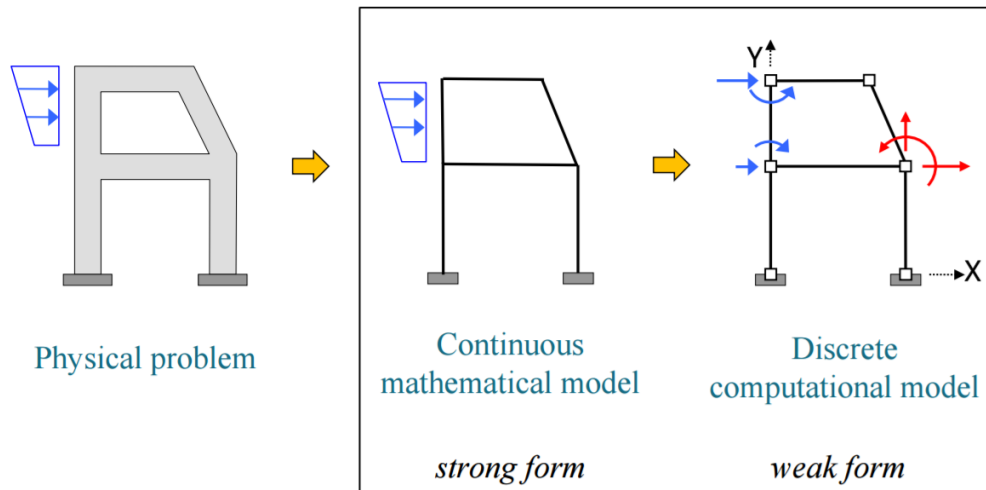


Figure 7: Computational structural analysis

The formulation of the equations governing the response of a system under specific loads and constraints at its boundaries, is usually provided in the form of a differential equation. The differential equation also known as the strong form of the problem is typically extracted using the following sets of equations:

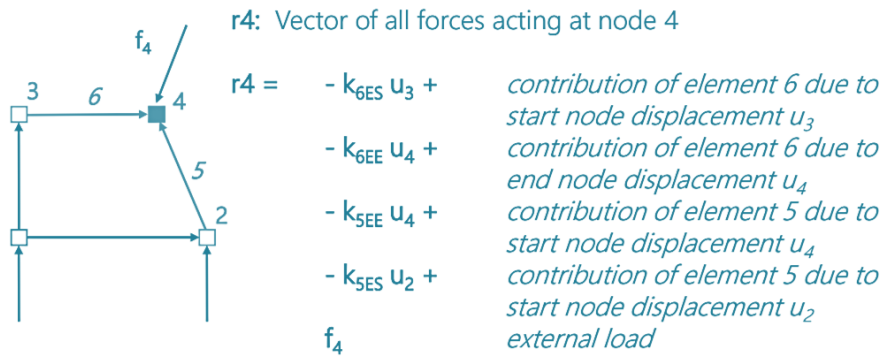
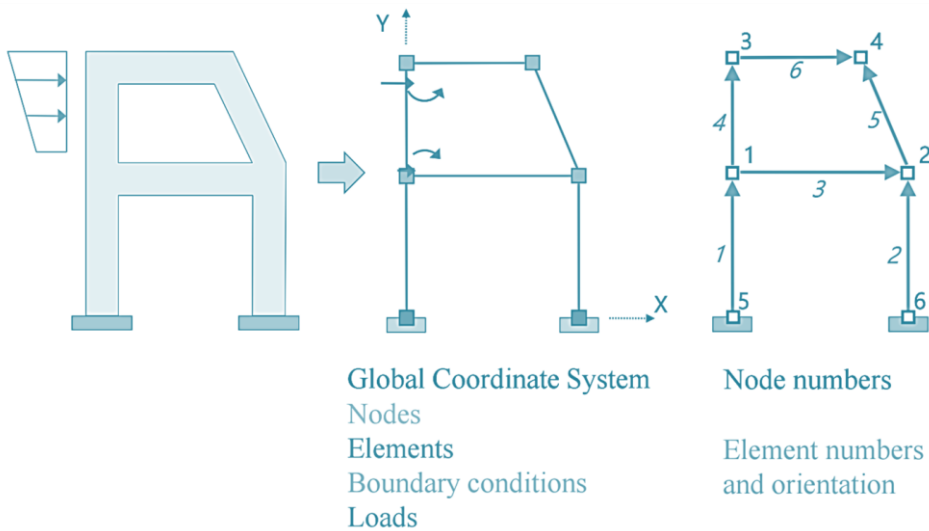
- 1 Equilibrium Equations  
ex.  $f(x) = R + \frac{aL + ax}{2}(L - x)$
- 2 Constitutive Requirements Equations  
ex.  $\sigma = E\epsilon$
- 3 Kinematics Relationships  
ex.  $\epsilon = \frac{du}{dx}$

The strong form requires strong continuity on the dependent field variables (usually displacements). Whatever functions define these variables have to be differentiable up to the order of the Partial Different Equations (PDE) that exist in the strong form of the system equations. Obtaining the exact solution for a strong form of the system equation is a quite difficult task for practical engineering problems. Using the finite element method on a weak form of the system this kind of problem is solved; it is usually obtained through energy principles which is why it is also known as variational form.

Three are the approaches commonly used to go from strong to weak form:

1. Principle of Virtual Work;
2. Principle of Minimum Potential energy;
3. Methods of weighted residuals.

Principle and fundamentals of Finite Element analysis procedure can be found in Bathe (Bathe, 1996). In the following scheme, it is shown the discretization of the previous structure:



Equilibrium at node 4:  $r_4 = -k_{5SE} u_2 - k_{6ES} u_3 - k_{5EE} u_4 - k_{6EE} u_4 + f_4 = 0$

	$u_1$	$u_2$	$u_3$	$u_4$	
$r_1 = -$	$\begin{Bmatrix} k_{1EE} + \\ k_{3SS} + \\ k_{4SS} \end{Bmatrix}$	$k_{3SE}$	$k_{4SE}$		$+ f_1 = 0$
$r_2 = -$	$k_{3ES}$	$\begin{Bmatrix} k_{2EE} + \\ k_{3EE} + \\ k_{5SS} \end{Bmatrix}$		$k_{5SE}$	$+ f_2 = 0$
$r_3 = -$	$k_{4ES}$		$\begin{Bmatrix} k_{4EE} + \\ k_{6SS} \end{Bmatrix}$	$k_{6SE}$	$+ f_3 = 0$
$r_4 = -$		$k_{5ES}$	$k_{6ES}$	$\begin{Bmatrix} k_{5EE} + \\ k_{6EE} \end{Bmatrix}$	$+ f_4 = 0$

$$-K U + F = 0 \Rightarrow F = K U$$

The global system of equations is:

$\mathbf{F}$  = global load vector = Assembly of all  $\mathbf{f}_e$

$\mathbf{K}$  = global stiffness matrix = Assembly of all  $\mathbf{k}_e$

$\mathbf{U}$  = global displacement vector = unknown

$$\mathbf{F} = \mathbf{K} \mathbf{U} = \text{equilibrium at every node of the structure}$$

The final equation system for solving the model, will become:

$$\begin{aligned} \mathbf{K} \mathbf{U} &= \mathbf{F} \quad \text{left multiply } \mathbf{K}^{-1} \\ \Rightarrow \mathbf{K}^{-1} \mathbf{K} \mathbf{U} &= \mathbf{K}^{-1} \mathbf{F} \quad \Rightarrow \mathbf{U} = \mathbf{K}^{-1} \mathbf{F} \end{aligned}$$

In general:

	Property K	Behaviour U	Action F
Elastic	Stiffness	Displacement	Force
Thermal	Conductivity	Temperature	Heat source
Fluid	Viscosity	Velocity	Body force
Electrostatic	Dielectric permittivity	Electric potential	Charge

In this work, elastic analysis with static and dynamic approach will be analysed, where:

$\mathbf{K}$ = stiffness matrix

$\mathbf{U}$ =displacement vector

$\mathbf{F}$ =load vector

### 3.2.2 Linear static stress analysis

Considering the equilibrium equation

$$[\mathbf{K}] \{\mathbf{U}\} = \{\mathbf{F}\}$$

The assumption is that this equation is in a standard form where  $[\mathbf{K}]$  and  $\{\mathbf{F}\}$  are known and  $\{\mathbf{U}\}$  is unknown, as previously mentioned, the solution for  $\{\mathbf{U}\}$  involves method related to inversion of  $[\mathbf{K}]$

$$\{\mathbf{U}\} = [\mathbf{K}]^{-1} \{\mathbf{F}\}$$

but inversion is not done. Since  $\mathbf{F}$  and  $\mathbf{U}$  may be functions of time  $t$ , the consideration as a dynamic equilibrium equations of a finite element system in which inertia and velocity-dependant forces have been neglected. In this case, since velocities and accelerations do not enter, the displacement can be evaluated at any time  $t$

independent of the displacement history. Principles and fundamentals of linear static procedures and methods can be found in Anderson (1994) and Bathe (1996).

In the Linear Static Analysis (1<sup>st</sup> order), the workflow for computer program is:

- System identification: elements, nodes, support and loads;
- Build elements stiffness matrices and load vectors;
- Assemble global stiffness matrix and load vector;
- Solve global system of equations (displacements);
- Calculate element results.

The output will be the exact solution for displacements and stresses.

### 3.2.3 Dynamic analysis

The equations of equilibrium governing the linear dynamic response of a system of finite elements is:

$$M\ddot{U} + KU(t) = F(t) \quad 1$$

where M and K are the mass and stiffness matrices; F is the vector of externally applied loads; and U, and  $\ddot{U}$  are displacement, velocity and acceleration vectors on finite elements assemblage. This expression represents the equilibrium at each node of the structure. It should be recalled that  $M\ddot{U} + KU(t) = F(t) \quad 1$

was derived from considerations of statics at time; i.e., the  $M\ddot{U} + KU(t) = F(t) \quad 1$  may be written as:

$$F_I(t) + F_E(t) = F(t)$$

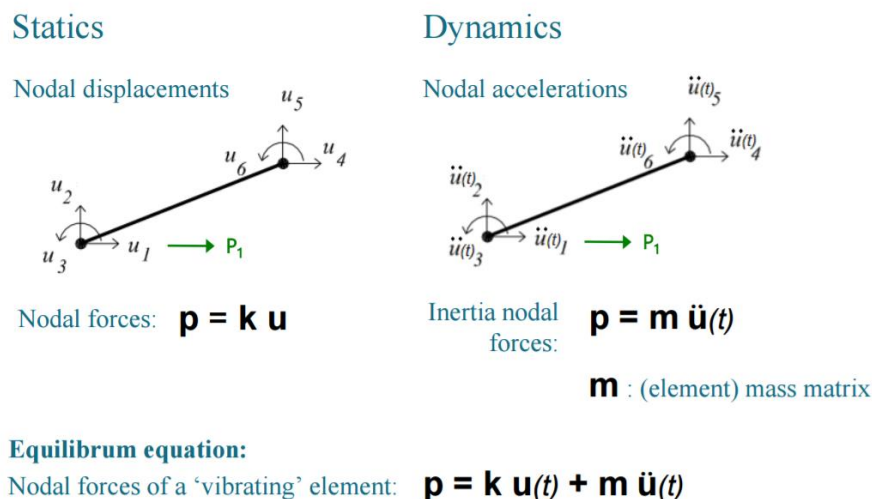
where

$F_I(t) = M\ddot{U}$  : inertia forces

$F_E(t) = KU$  : elastic forces

and all of the are being time-dependant.

With a simple example in 2D domain, and a comparison between static and dynamic analysis, it is:



The eigenmodes of a given structure are independent from the loads, and the displacement have harmonic function. For eigenmode I ( $E_i, \Omega_i$ ), the function is:

$$U_i(t) = E_i \cos(2\pi \Omega_i t)$$

$$(K - (2\pi \Omega_i)^2 M) E_i \cos(2\pi \Omega_i t) = 0$$

The solution of eigenvalue problem is:

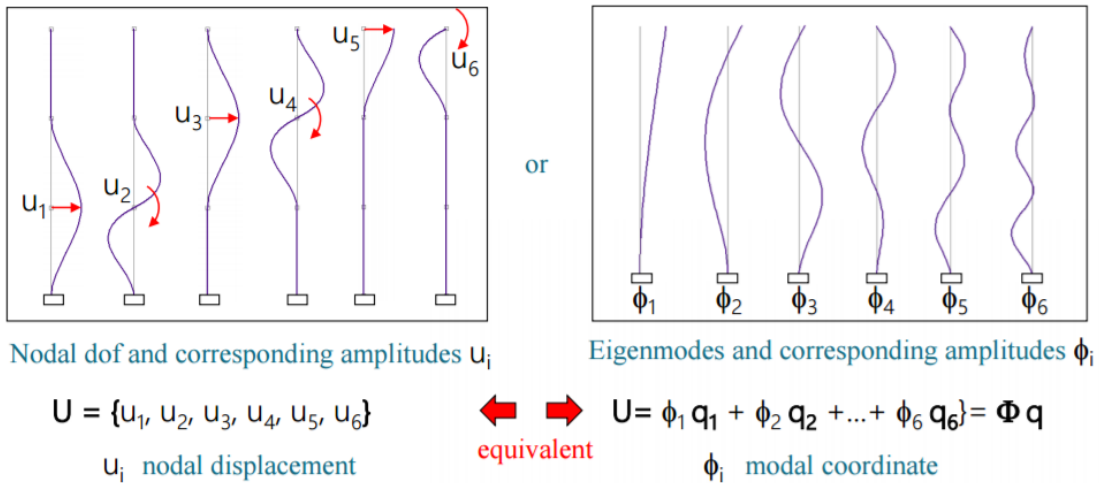
$\Omega_i$  = (dynamic) eigenfrequency

$E_i$  = (dynamic) eigenform

As we can see in the following figure, every mode is like an independent structure.

## Numerical structural model: Deformations of a structure

Every deformed configuration can be described as...



For the modal analysis, the workflow of computer program follows this procedure:

- System identification: Elements, nodes, support and loads;
- Build element stiffness and mass matrices;
- Assemble global stiffness and mass matrices;
- Solve eigenvalue problem for a number of eigenmodes;
- Perform further analysis (time-history or response spectra).

The output will be an approximate solution.

### 3.3 FE modeling

In the last twenty years, several studies have been taken on FEM for existing buildings of historical constructions. Boothby and Atamturktur (2007), for example, discussed some of the principles of masonry and provided basic instructions in preparing an FE model of complex vaulted masonry structures using widely available, modern tools of structural analysis. Masonry is highly anisotropic due to the presence of discrete sets of horizontal and vertical mortar joints. For this reason, in general, two main FE modelling approaches are possible for masonry structures: micro-modeling and macro-modeling (Lourenço, 2009). This distinction has been made by Lourenço (1996), Saadeghvaziri and Mehta (1993), Papa (2001).

Figure 8 shows details of micro and macro-modeling techniques. In particular, Figure 8b shows a detailed micro modelling where joints are represented by mortar continuum elements and discontinuum interface elements and Figure 8c shows simplified micro-modeling where joints are represented by discontinuum elements. Figure 8d shows macro-modeling where joints are smeared out in the continuum. In the micro-modeling techniques, it is possible to model the unit mortar interface and mortar joint which is responsible for most cracking as well as slip. Young's modulus, Poisson's ratio, inelastic properties of both unit and mortar are taken into account in the micro-modeling. The interface represents a potential crack/slip plane with dummy stiffness to avoid interpenetration of the continuum. Due to the zero thickness of the interface elements, the geometry of the unit has to be expanded to include the thickness of the joint. In the macro-modeling technique, mortar is smeared out in the interface element and in the unit. Therefore, micro focuses on the heterogeneous states of stress and strain using the properties of individual masonry units and mortar joints. For micro-modeling, the amount of computational effort necessary for analysis of an existing building is impractical. Macro-modeling, in contrast, assumes homogenous constitutive behaviour for the masonry and mortar assembly and, therefore, is commonly applied to model large-scale structures. The suitability of the homogenized material property assumption has been confirmed in numerous studies (Creazza, Matteazzi, Sassetta, & Vitaliani, 2002). This work will focus on macro-modeling.

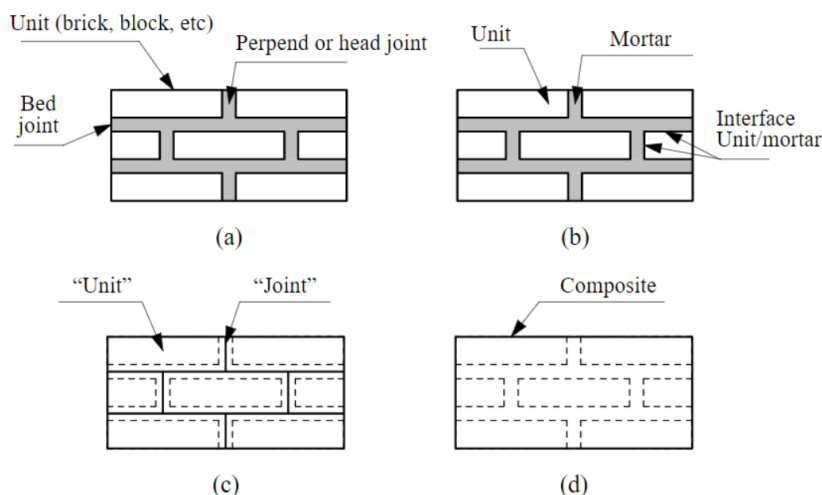


Figure 8: Micro and macro-modeling techniques

There are four main aspects to the structure that need to be defined by in FE model development: geometry, material properties, boundary conditions and loads.

Complex profiles, for example, are practically impossible to model accurately, and the effort spent on attempting to model these shapes often degrades the model accuracy because of unavoidable poor aspect

ratios in meshing. The physical geometries, in structural field, are typically simplified to rectangles that preserve the area and moments of inertia of the original cross section. **Figure 9** shows a simplification for the cross sections of ribs of Washington National Cathedral: the suggested principle is to simplify the geometry (Atamturktur, Verification and Validation under Uncertainty Applied to Finite Element Models of Historic Masonry Monuments, 2009). Lança et al. (Lança, Lourenço, & Ghiassi, 2015) analysed a masonry vault in Portugal, and they refined and reduced initial surveyed data about columns and ribs of the vault, in simple geometric element suitable for FE analysis (**Figure 10**).



**Figure 9:** In the left an highly ornamented rib, and in the right the simplified geometry for FEM

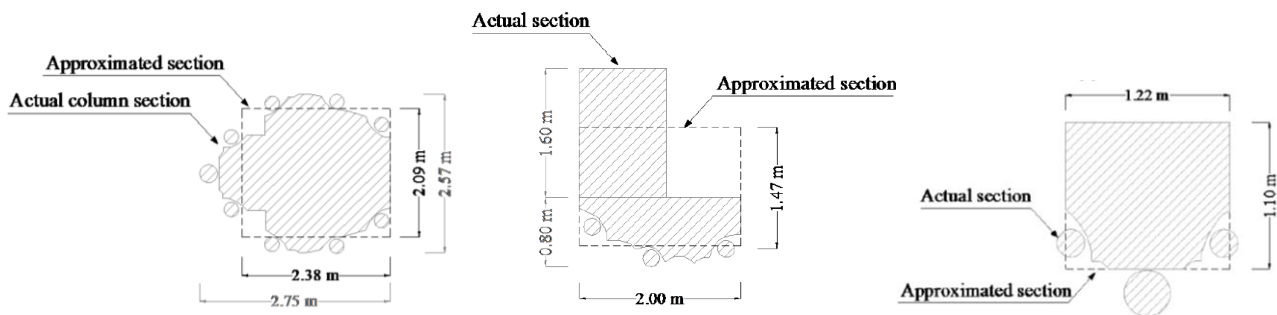


**Figure 10:** Example of overlap between approximated and real section

In both cases, the modeling is well approximated because there is attention for preserving the masses, the total area of the sections and the moments of inertia, but at the same time the accuracy of the data deriving from survey are compromised and neglected for structural purposes.

In this research, Abaqus software (Abaqus, Abaqus CAE/User's guide , v 6.14) will be used for FEA. The wide range of elements in the ABAQUS elements library provides flexibility in modeling different geometries and structures. In particular, each element can be characterized by considering the following:

- Family: shell, continuum, rigid, beam etc...;
- Number of nodes: depends on element shape and its order of interpolation (element shape, geometric order);
- Degrees of Freedom per Node: depends on the solution field of the analysis (Displacement, Rotation, Temperature, etc.) and the order of modeling space (1D, 2D and 3D);
- Formulation: applicable to some of the element families (e.g. small- and finite-strain shells) otherwise most elements provide both automatically;

- Integration: Reduced and full integration.

In this work, continuum element will be used.

Each element in ABAQUS has a unique name, and the element name identifies primary element characteristics.

As we will see in the next chapters, the most frequent element used for structural analysis, will be C3D8R.

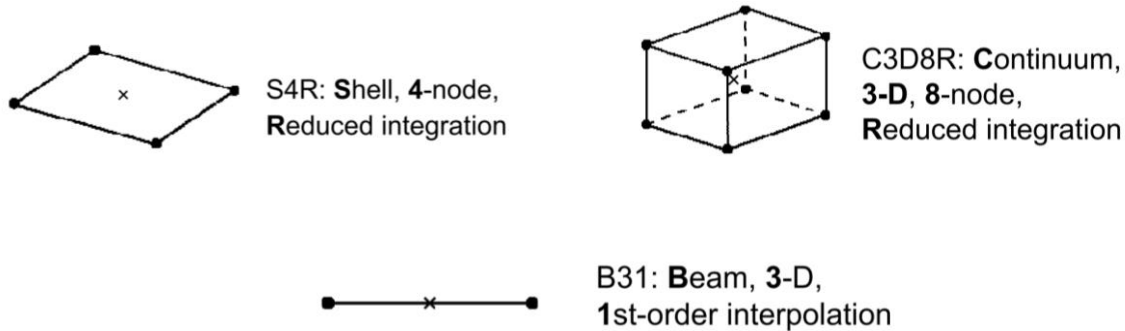


*Figure 11: Some element of Abaqus code*

C3D8R are three-dimensional hexahedral element, as shown in **Figure 11**: this is a linear element, because tetrahedral elements are geometrically versatile and are used in many automatic meshing algorithms, but however, a good mesh of hexahedral elements (C3D8R) usually provides a solution of equivalent accuracy at less computational costs. Application of three-dimensional hexahedral element, include C3D8R (8-node trilinear brick) are generally recommended whenever possible however these elements are geometrically less versatile and difficult to be used for complicated geometries. It should be noted that by effective use of different domain decompositions techniques (e.g. partitioning) it is possible use these elements even in complex geometries.

### 3.4 FEM in cultural heritage

In general, analytical modeling of masonry structures is very difficult, because the behaviour of the masonry, which mainly characterizes buildings of cultural heritage field, is nonlinear both in tension and in compression. On the other hand, as mentioned before, lot of progresses in the assessment of a masonry structure can be made assuming masonry as a linearly elastic isotropic and homogenous material (macro-modeling) (**Figure 12**). Recently, homogenization techniques have been effectively applied ( (Lourenço, 1995 b); (Milani, Lourenço, & Tralli, Homogenised limit analysis of masonry walls. Part I: Failure Surfaces, 2006 a); (Milani, Lourenço, & Tralli, 2006 b); (Cecchi, Milani, & Tralli, 2007); (Milani, Lourenço, & Tralli, 2007); (Milani, Milani, & Tralli, 2008)).

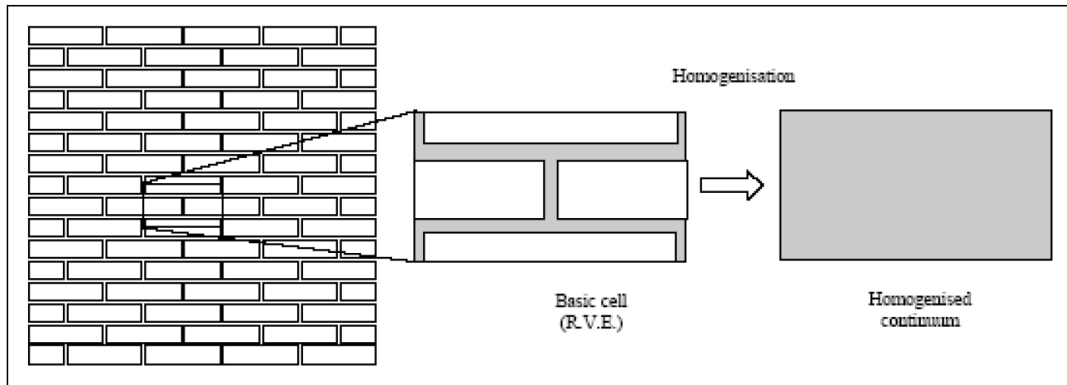


*Figure 12: Basic cell for masonry and objective of homogenization*

Since FE method was developed, many approaches of modeling and analysis have been improved and proposed.

The application of advanced computer methods to the analysis of historical structures was pioneered by the studies of the Brunelleschi Dome by Chiarugi et al. (1993), the Pisa Tower by Macchi et al. (1993), the Colosseo in Rome by Croci (1995), and Croci and Viscovik (1995), Mexico Cathedral by Meli and Sánchez-Ramírez (1995) and San Marco's Basilica in Venice by Mola and Vitaliani (1995), among others.

By then, the development of methods for accurate analysis of steel and concrete structures, including non-linear applications, was already at a very advanced stage thanks to the work of Zienkiewicz and Taylor (1991), Ngo and Scordelis (1964) and many others.

Specifically, in the Pisa Tower a Finite Element 3D global analysis has provided, in 1992, a comprehensive knowledge of the effects of permanent loads, wind, and circumferential pre-stress, which were only imperfectly known through the preliminary studies. At first, a numerical model was built, and then a FE mesh (Figure 13).

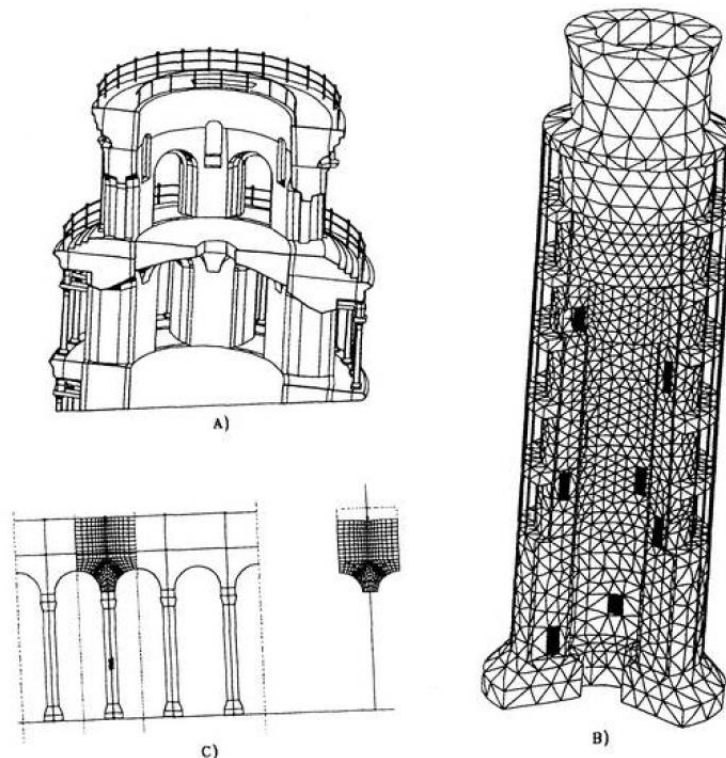


*Figure 13: Modeling of the tower: numerical model (A), FEM (B), sub-structuring of the colonnade system (C).*

The model takes into account all the relevant openings and stairs, based on a traditional survey. Nevertheless, the complexity and then the increasing of the order of polynomial shape function would be excessive if the colonnade would be modelled in detail (Macchi, Ruggeri, Eusebio, & Moncecchi, 1993); therefore (Figure 13c) the elements of the external colonnade (columns and arches) are simulated by trusses of equivalent axial stiffness. Hence, the three-dimensional modeling is greatly simplified, if compared with the real Tower, for computational needs of the epoch.

In the study of Mexico City Cathedral, developed in 1995, the effects of the temple represent a very severe action on the structure, the foundation and the soil and they have been studied mainly by finite element analysis of different structural model (Figure 14a). More detailed models of critical parts of the structure were studied mainly by bi-dimensional or three-dimensional isolated models (Figure 14b), as shown in the following figure, in which the supports of central vaults are analysed.

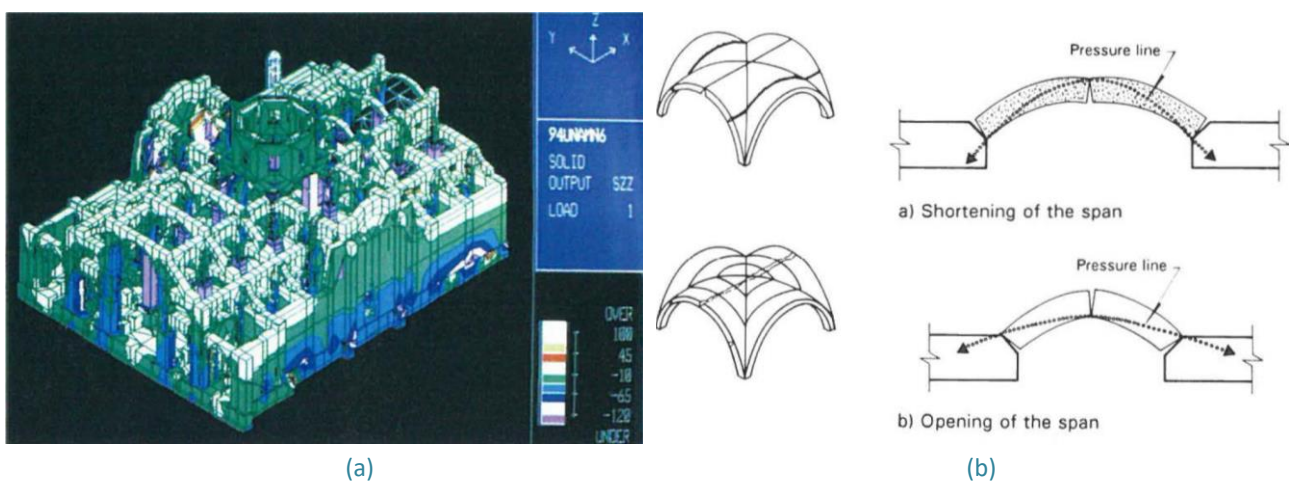
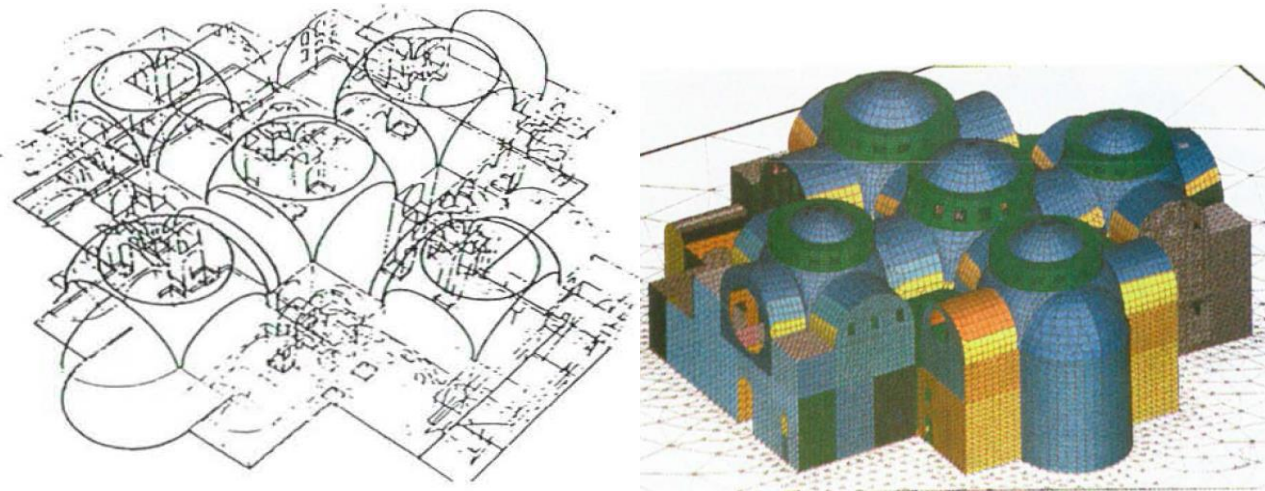
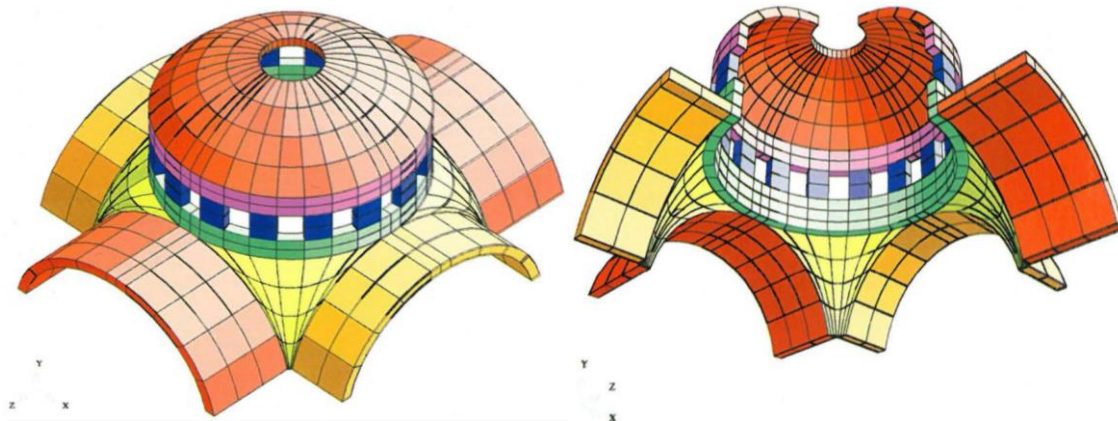


Figure 14: Finite element model of the central portion of the Cathedral (a); details of isolated 2D and 3D models (b)

Instead, for the three-dimensional model of St. Mark's Basilica (Mola & Vitaliani, 1995), a theoretical model for the structural analysis based of sub-assembling FEM techniques (Figure 15) have been realized; the geometrical discretization has been operated in CAD environment. The complexity of the model and the very high number of degree of freedom, has suggested to operate by means of the sub-assembly techniques. The structural complex has been subdivided into nine sub-assemblies. From structural analysis, concerning peak-stresses, there are differences between results of geometrical analysis (discretization) and theoretical test (three-dimensional modeling of some pillars). The suggest was to operate a convenient refinement of the three-dimensional model: this refinement should be accompanied by a more detailed geometrical description (par. 4 pag. 192, (Mola & Vitaliani, 1995)). In Oñate et al (Oñate, et al., 1996) a different approach for modeling of St. Mark's Dome have been proposed, using a common construction based on geometric measurements, using standard 20 node isoparametric hexahedral elements. The following figure shows different views of the finite element meshes of the structure (Figure 16).



*Figure 15: St.Mark's Basilica. From the left, sub-assemblies assumed for the mathematical model; FE global discretization*



*Figure 16: Three-dimensional FE model of St. Mark's Dome, based on geometric measurement.*

Methods then available were not yet prepared to tackle the specific problems of ancient constructions concerning materials, structural arrangements and real preservation condition. As can be seen in the above mentioned case studies, first studies related to cultural heritage analysed according FE models, were created mainly starting from simple geometries or from the elaboration of two-dimensional drawings (plans, elevations). For very complex buildings, it can be noted as sometimes it was necessary to realize the sub-models and this is a disadvantage for important elements of architectural building.

Actually, the difficulties posed by historical structures are still very challenging, and still reminiscent of those encountered by the pioneers, in spite of significant progress during the last decades.

At the beginning of this century, Roca (2001) proposed a study of structural analysis on gothic Cathedrals (**Figure 17**), with a comparison between three different case studies. In all three works, after an accurate but traditional survey, concerning geometrical elements, evaluating historical of the structures (linked to construction process, and possible natural or anthropic actions affecting the construction throughout its life time), three-dimensional models have been created. The accuracy of the survey, in this study, has been useful to verify the results derived from structural analysis. In fact, once created three-dimensional models (based on geometrical measurements), it was possible to verify that the most stressed parts, were also subject to degradation phenomena, having for example cracks, according with several analyses carried out before.

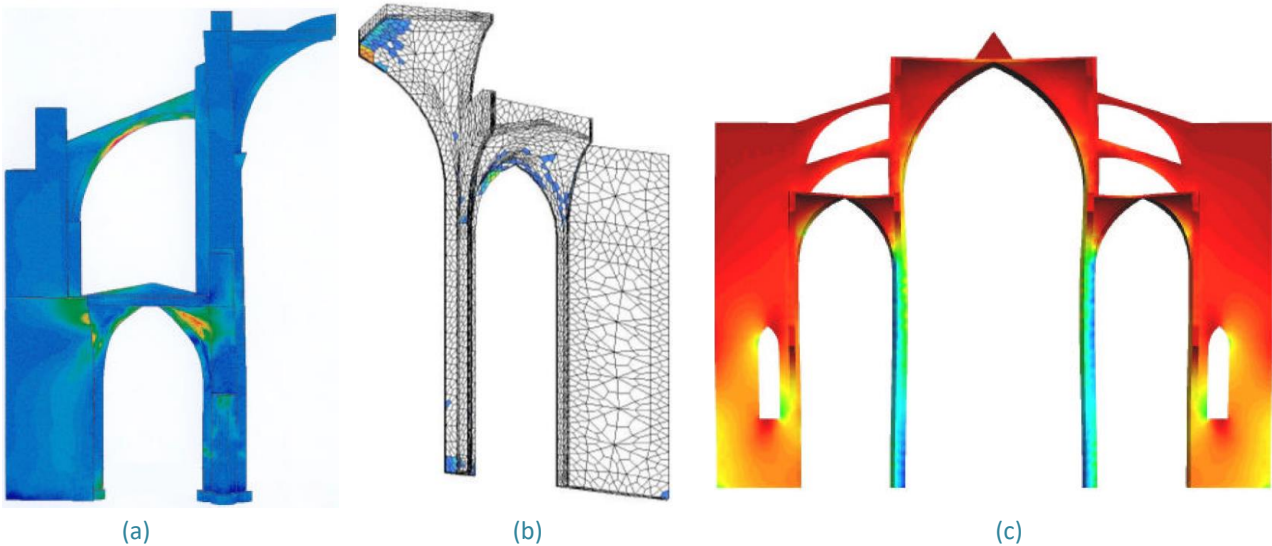
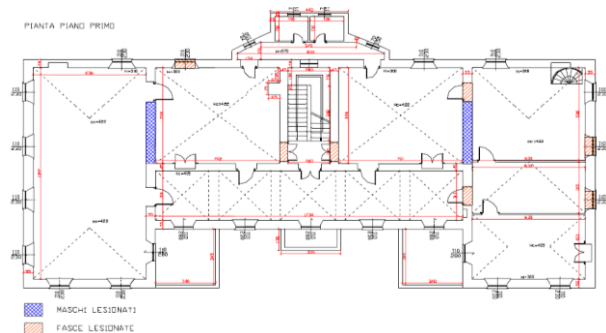


**Figure 17:** FEM continuous damage model of Tarazon Cathedral (a) with distribution of maximum tension stresses; Nave of Barcelona Cathedral subject to dead load (b); distribution of the principal compression stresses of Mallorca Cathedral (c).

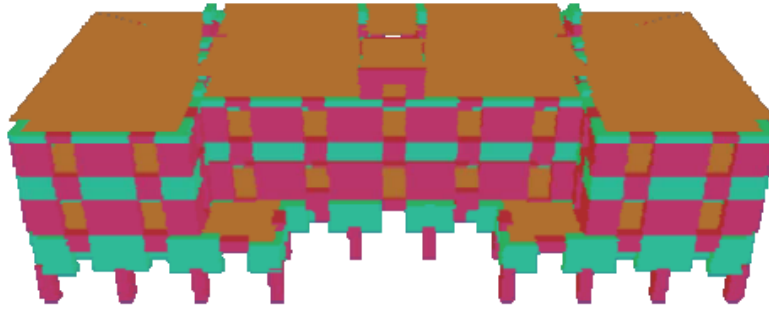
In a study of 2004 (Galasco, Lagomarsino, Penna, & Resemini, 2004), after an accurate and traditional survey of a building damaged by an earthquake, a complete three-dimensional macro-modeling has been used (Figure 18), in order to simulate the building response and the damaged pattern surveyed after earthquake. A finite element formulation for static analysis has been proposed in 2007 (Ozkul & Kuribayashi, 2007) with the historical Hagia Sophia in Istanbul. Starting from two structural systems (Figure 19), the basic system carrying the principal loads and the dome, and the secondary one that supports only itself and that depends on the basic system, the entire structure is modelled by using the same two-dimensional curved trapezoidal element. The analytical model includes all essential elements of the structural system; i.e. piers, two semi domes with the barrel vault on the end, upper and lower north and south arches, main east and west arches, the main dome. Structural characteristics of the building are considered for linear analysis.



(a)



(b)



(c)

**Figure 18:** Aerial view of the Castelnuovo Belbo Hall (Piedmont) damaged by the 2000 Monferrato earthquake (A); First floor plan of the building, survey with traditional methods (B); Perspective view of FE model (C).

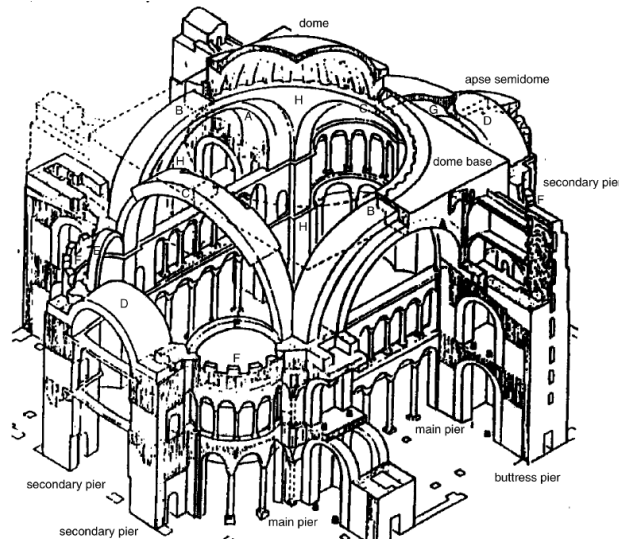


**Figure 19:** The primary structural system with the secondary ones

In general, in advance of the modeling effort, it is important to determine the level of simplification that will preserve realistic results. Boothby et al (2007) proposed guidelines for modeling and assessment of load-bearing masonry structures. Complex molding profiles are practically impossible to model accurately, and the excessive effort spent on attempting to model these shapes is not justified by the increased accuracy of the results obtained. It is convenient to reduce complex cross-sectional shapes to a simpler rectangular shape of approximately the same cross-sectional area and moment of inertia. An example of such reduction for the cross section of the piers of the Cathedral of Saint John the Divine is illustrated in **Figure 20**. Depending on the preferred FE software, a solid model can be created with modeling utilities in the structural analysis software or with alternative computer platforms, like CAD programs. There are significant interactions between the geometric model creation, solid model development and the choice of elements for use in structural analysis.

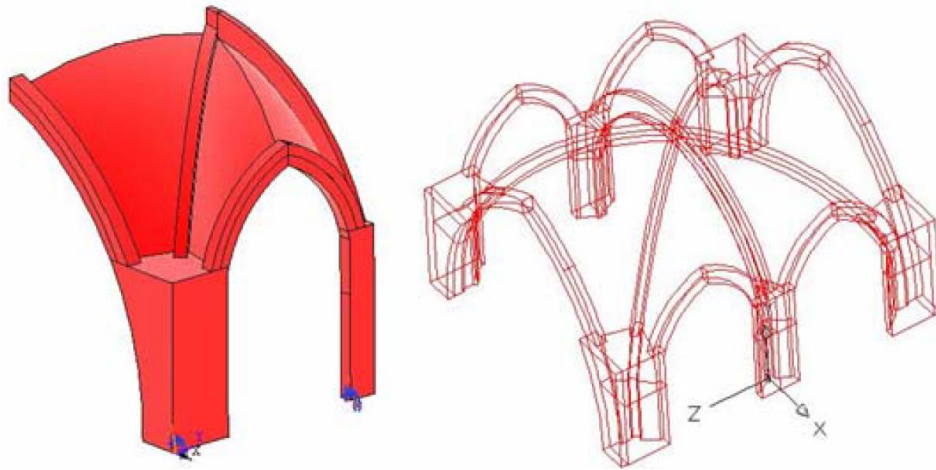


*Figure 20: The solid model in a specific structural Software (left); The AutoCAD drawing of the nave vaults (right)*

Generally, for structural modeling there are three types of elements available in most analysis programs: line, area and solid elements. The preference of one over another is dependent on the physical characteristics and scale of the members. Line elements represent a beam or bar by a single line, usually along the centroid of the member. Depending on the software, the element may be straight or curved. A spatial frame element has up to six degrees of freedom—three displacements and three rotations—at each end. Shell elements are three- or four-cornered elements, with nodes at each corner and are well suited to model singly curved or doubly curved surfaces of constant or varying thickness. The nodes of shell elements each have six degrees of freedom: three translational and three rotational. Alternatively, solid elements have three dimensions and hence a greater number of nodes than frame or shell elements. Tetrahedral solid elements with four nodes and so-called brick elements with a minimum of eight nodes are available in most FE software (Figure 21). Once realized the geometrical three-dimensional model, on completion of the solid model and selection of the element types, it is broken down into individual elements according to a systematic procedure known as meshing the model. The shape and size of the elements determines the solution. A mesh that is too coarse can produce inaccurate solutions, while a mesh that is too fine will result in problems with program limits on the number of nodes or elements or will result in excessive run times (Atamturktur, 2006).

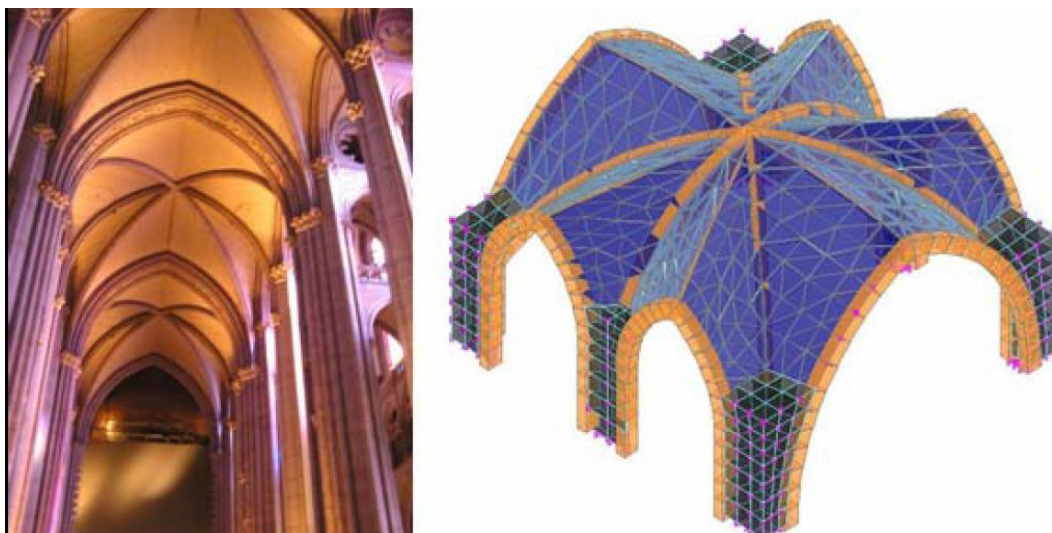


*Figure 21: View of Nave Vaults of the Cathedral of St. John the Divine (NY) showing Transverse Arches (left); The SAP 9.0 model of the vaults of the Cathedral of St. John the Divine in AutoCAD (right). This is an example of three-dimensional modeling with shell elements*

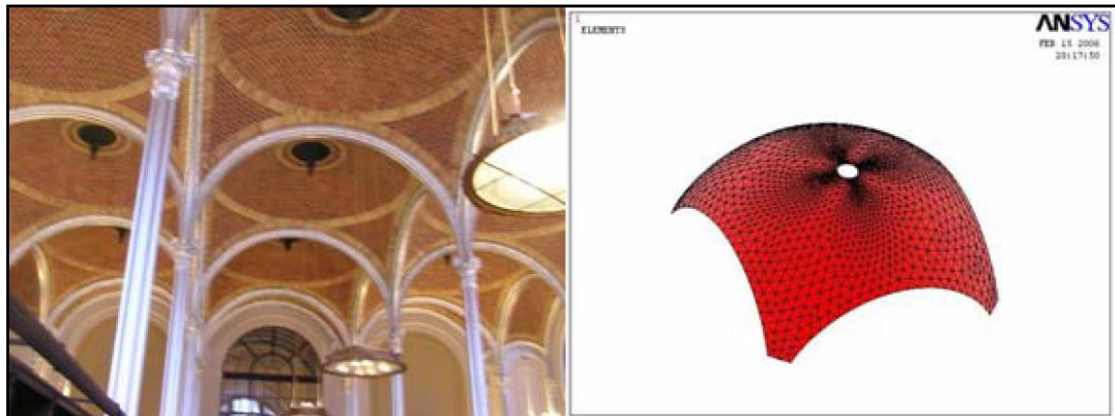
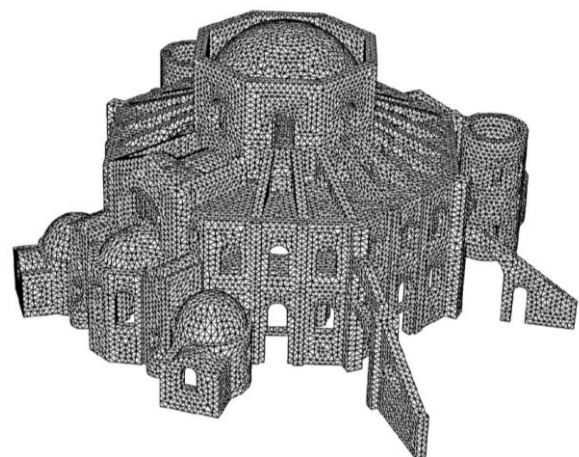


*Figure 22: In the left, the view of rib and dome construction of State Education Building, (NY); in the right FEM model of the single dome in ANSYS software. The dome has been modelled with classical geometric construction, and then separated into several elements.*

A FE model was developed to analyse the Basilica of San Vitale in Ravenna (Italy), a Byzantine building which suffers diffused cracking and excessive deformation. Thanks to previous topographical surveys of part of the building, to chemical and mechanical investigations, the geometry of the Basilica and the main physical properties of the materials are reasonably well defined and the topographic survey was the base for structural modeling. The authors built a complete finite element model of the Basilica conceived as a first step toward the understanding of the structural behaviour of the monument. Because of the complexity of the geometric model, a simplified (linearly elastic, isotropic) constitutive law had to be assumed to keep the computing time within reasonable limits. The geometry of the Basilica was defined as accurately as possible (Figure 23), according to available drawings, photographs, and the photogrammetric survey, and whenever no information was available, assumptions were made as reasonably as possible (Taliercio & Binda, 2007). The agreement between the geometrical model and the real building can be appreciated where the exedras in sectors of the women’s gallery are compared with their numerical counterparts.



(a)



(b)



**Figure 23:** View of the Basilica (a); View of the entire finite element model (b); Exedras in the sectors of the women's gallery (c) and geometrical modeling (d)

Another important study, related to historic cultural heritage and FE model, dates back to the 2010, which Peña et al (Peña, Lourenco, Mendes, & Oliveira, 2010) studied and modelled an old masonry tower. Since there were not three-dimensional surveys, three different numerical models were considered to evaluate the structural behaviour of the minaret. Two models use the well-known Finite Element Method; both are three-dimensional models (Figure 24), but one uses 3-D solid elements while the other one was performed with 3-D composite beams. The third model uses 2D in-plane elements based on the Rigid Element Method. Three results regarding frequencies, are then compared with experimental results, as we can see on the following Table 4.

The model that presents in general the smaller errors in the calculated frequencies (less than 5%) is the simplified Rigid Element model except for the vertical mode that has an error up to 10%. The differences between the final results derive also from different geometries of the three models: the true structure and the solid model, in fact, are not axisymmetric, meaning that a clear orientation of the modes in two essentially orthogonal directions  $x$  and  $z$  have been found. On the contrary, the Beam model is fully axisymmetric, meaning that the directions  $x$  and  $z$  lose their meaning. Finally, the Rigid model is two-dimensional, meaning that only one frequency is found for each pair of consecutive bending modes and a torsional mode cannot be found.

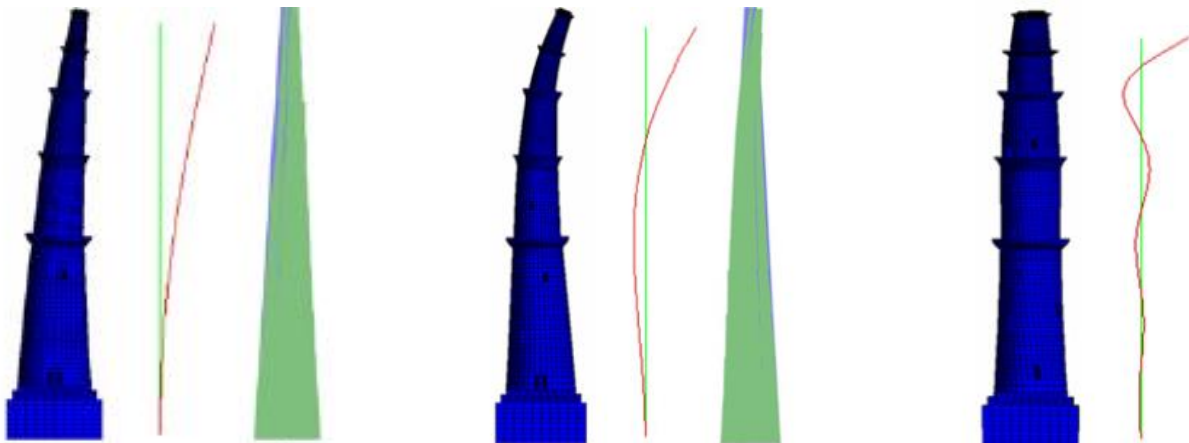
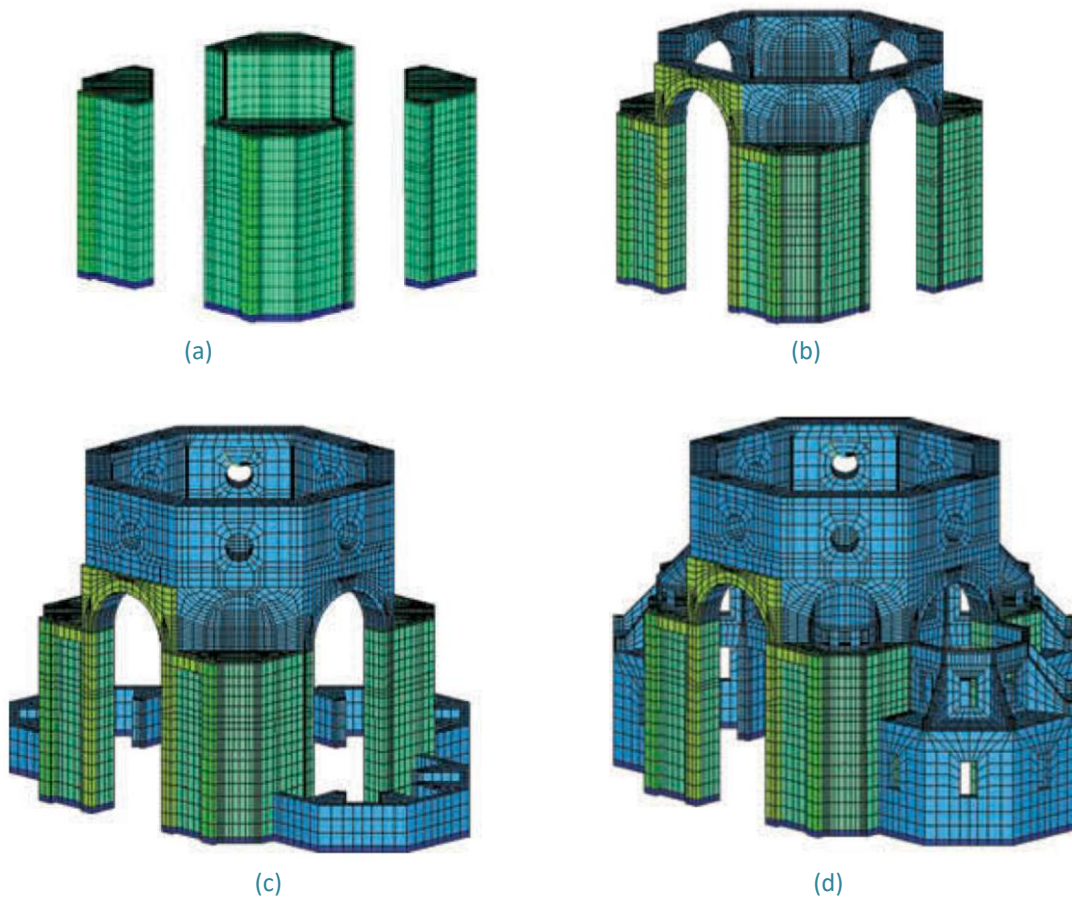


**Figure 24:** Modal shape for the models, solid (left), beam (central), and rigid (right)

Mode shape	Comment	Frequencies (Hz)						
		Experimental	Solid	Error (%)	Beam	Error (%)	Rigid	Error (%)
1	1st Bending, z	0.789	0.71	-10.01	0.734	-8.42	0.778	-3.17
2	1st Bending, x	0.814	0.71	-12.77				
3	2nd Bending, x	1.954	2.07	5.93				
4	2nd Bending, z	2.010	2.09	3.98	2.257	13.87	1.886	-4.84
5	3rd Bending, x	3.741	3.55	-5.10				
6	3rd Bending, z	3.862	3.59	-7.04	4.129	8.62	3.582	-5.77
7	1st Torsion	4.442	4.80	8.06	3.656	-17.69	-	-
8	4th Bending, x	5.986	5.98	-0.10				
9	4th Bending, z	6.109	6.02	-1.45	6.665	10.21	6.419	5.65
10	1st Vertical	6.282	5.35	-14.83	6.098	-2.93	7.061	12.41

**Table 4:** Comparison among experimental frequencies obtained with the three different models

Recently, an interesting study about structural behaviour of Brunelleschi's Dome of Santa Maria del Fiore has been proposed, in which new results concerning the static identification of the Dome, with the adopted modeling strategies, are reported. The new numerical model was built with the FE code ANSYS by using solid hexahedral isoparametric elements to discretize all the main geometrical components; the geometry of the new model was based on the results of a very accurate 3D topographic survey of the whole Dome. The analysis of the Dome under its own weight was performed through a step-by-step application of the self-weight to reproduce the effective stages of construction of the *fabrica*. The sequence of own weight application is reported in **Figure 25** and **Figure 26** (firstly the effects of the main pillars have been considered, next the arches, etc.). As shown, the structure changes at each step and at the end of each load step the new loads are applied over the deformed geometry so the nonlinear geometric effects are activated between each load step.



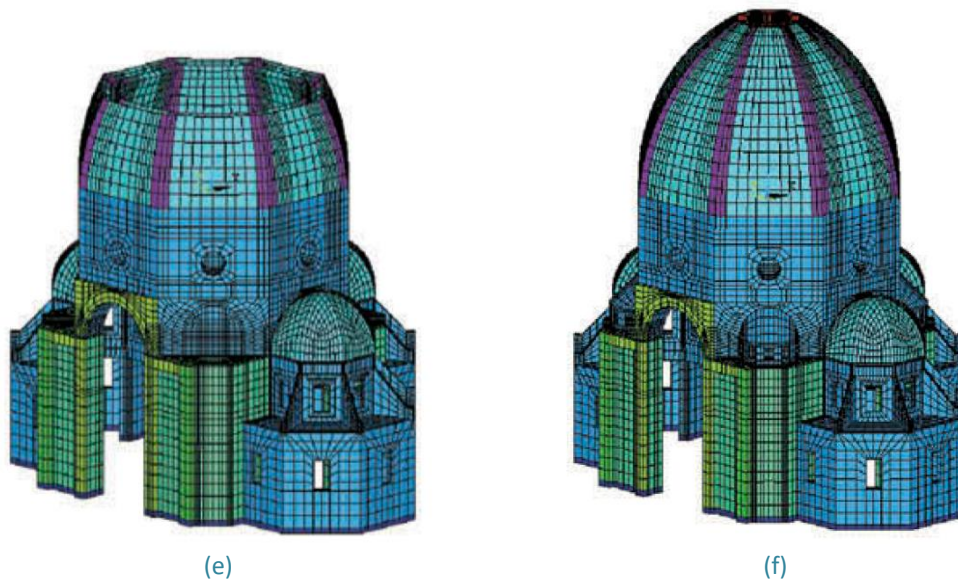


**Figure 25:** Sequence of self-weight application (a) Pillars; (b) pillars and main arches; (c) pillars, main arches and tambour; (d) pillars, main arches, tambour and lateral apses; (e) pillars, main arches, tambour, lateral apses and lower part of the dome; (f) final configuration.

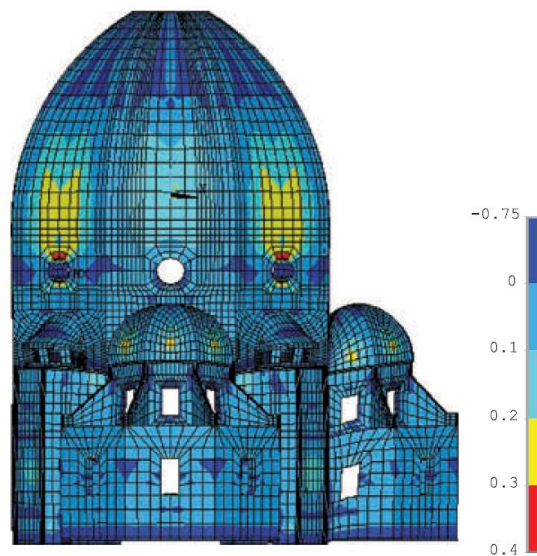


**Figure 26:** Self-weight applied step-by-step, according to the sequence of Figure 25

In these works, that have occurred in several years, we have seen that through the use of the finite element technique, the authors have provided an interpretation concerning the comprehension of the structural behaviour, more or less accurate. The study of the structure of historical constructions poses a number of very significant challenges. Difficulties are not only from the need to model complex geometries, materials and actions, but also from the significance of history and the need for linking the structural analysis with the historical events.

Traditional measurement methods of measurement, having a significant dependence with workers' skills (including an associated high cost of time) are reflected, therefore, on final results, which will be subjective and not perfectly objective parts. These subjectivities will determine the three-dimensional modeling, leading inevitably differences between the real object and structural one and then the final structural results. Studies on the structure of ancient constructions base on the combination of a set of activities which include:

1. the inspection and characterization of the present state of the construction, based both on visual recognisance and deep observation by means of (preferably) non-destructive techniques;
2. the historical research carried out by expert historians from the available historical documentation;
3. the monitoring of the building by means of different types of sensors;
4. the structural modelling and analysis of the building. These are, in short, the main elements of the study from which the conclusions on the condition of the building and on the need for repair or strengthening are to be drawn.

The fourth point, the role of the structural analysis within the frame of a general study and the requirements which should be taken into consideration to link it, in a profitable way, with the rest of the elements of the study (inspection, history, monitoring) is the most important point. From these works concerning structural analysis of cultural heritage, it seems clear that the connection between the first three points and the last one, is lacking or missing (Roca, 2005).

Therefore, from a complete and accurate point of view, all the activities should be the parts needed to develop a complete analysis based on scientific methods. The final numerical FE model is just the recipient of the hypotheses and the considerations about the physical and mechanical nature of the object. History, survey monitoring are activities oriented to the production of elements needed to validate the hypotheses and to improve, correct and complete the final product.

### **3.5 Legislative framework in the field of structural analysis for cultural heritage**

In this work of research, the procedure for transforming point cloud in three-dimensional FEM, will be applied and analysed in three case studies, two of which are located in Italy (and one, in particular, in a seismic zone). For this reason, a study about the current regulations has been carried out.

The main rules governing the structural analysis of masonry buildings are Structural Eurocodes published by CEN (Committee European Normalisation – European Committee for Standardization), with specifications listed in the National Appendices or, in lack of that, in the international EN (European Normalization).

Eurocode 6 concerns “Design of masonry structures”:

- Chapter 3: types and grouping of masonry units;
- Chapter 4: Durability of masonry;
- Chapter 6: Structural analysis.

Eurocode 8 (4.3.3) dealing with existing buildings, and gives the definition of seismic actions:

- EN1998-1 (definition of seismic action);
- EN1998-3 (existing buildings);
- Italian national annex regarding EN1998-1.

According to European code for the seismic design of building, Eurocode 8 ( (2005 a); (2005 b); (2005 c)), a seismic analysis of a masonry building can be carried out with different methods:

- “lateral force method”, that is a linear static analysis;
- “modal response spectrum analysis”, that is a linear dynamic analysis;
- “pushover”, that is non-linear static analysis;
- “non-linear time-history analysis” or non-linear dynamic analysis.

An important difference among the different methods is the way the seismic action is modelled; for example, in the first method static forces are schematized with equivalent horizontal while in the last one it is applied in form of accelerograms. These methods can be applied both for the design of new buildings and for the assessment of the existing ones.

In this paper the attention is focused on this last category.

As support at the analysis of existing building, the Eurocodes have introduced two important concepts: the knowledge levels (KL) and the confident factors (CF). Three different levels of knowledge are defined:

- KL1: limited knowledge;
- KL2: normal knowledge;
- KL3: full knowledge.

The level is assigned according to the available information on geometry, details, materials, and boundary conditions. If the level of knowledge is high, the uncertainties will be less and the confidence factor will be small, or even unitary. In the practice, the KL influences two aspects: the type of seismic analysis that have to be used and the values to be adopted for the confidence factors (CF). The Eurocode 8 recommends the following values:

- CFKL1=1.35,
- CFKL2=1.20
- CFKL3=1.00.

They are applied together with the coefficient for the material  $\gamma_M$  to reduce the masonry strength. The concepts of level of knowledge and confident factors have been introduced in other technical code, as for example the Italian National Technical Code for Constructions, shortly named NTC08 (NTC N. N., 2008), and the relative Guidelines (Circ. 09, 2009), which have been written in accordance with the Eurocodes.

### 3.5.1 Regulations and decree laws in Italy

As seen also in the first chapter, the task has always been to provide for the protection of national assets, and, from this point of view, the national decrees are at the forefront if compared to European decrees and standards.

In Italy, therefore, a lot of standards and guidelines dealing with the above mentioned arguments have been introduced. Specifically, it is worth to remember:

- Technical Rules for Constructions, proclaimed in 2008, shortly named NTC 2008 (as previously mentioned);
- OPM n. 3274 (2003), update with OPM. n. 3431 (2005);
- Circular of 2 February 2009, n°617- Indications for the application for “New technical standards for buildings” (previously mentioned);
- Guidelines about the preservation of historical and architectural heritage (2011);
- Rules DT/200 by National Research Council (CNR) dealing with the utilization of composite materials in retrofitting of existing buildings.

Analysing the most significant aspects faced by the Italian Code and ignored by Eurocode ([Figure 27](#)), it is possible to remember, above all (Borri & Maria, 2009):

- the deep attention dedicated to the question of masonry and its quality;

- the classification of the intervention in “seismic upgrading”, “seismic improvement” and “local interventions”, depending on basic criteria of extension of the intervention, transformation of the original behaviour of the construction and safety levels to be performed;
- the case of aggregated buildings is discussed; this is a typical configuration in the Italian historical centres;
- the case of historical and architectural heritage is discussed; this is another typical problem of retrofitting of buildings;
- safety factors depend on knowledge of the construction; three levels of knowledge have been defined; in such a way there is a direct correspondence between safety and knowledge;
- a range of possible values of the principal mechanical parameters are defined for masonry;
- the most common techniques of intervention are shortly explained.

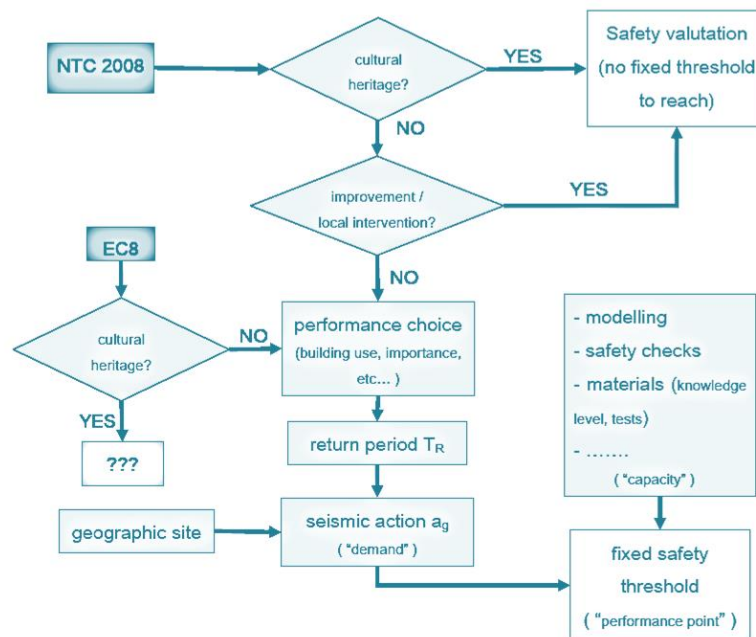


**Figure 27:** Flowchart explaining the procedure to determine the safety level. It is clear that EC8 cuts off the eventuality of seismic and local interventions and doesn't deal with cultural heritage

Italian NTC08 is divided in 12 Chapters, and the 8<sup>th</sup> concerns on existing buildings which introduces to general criteria on different types of buildings and the variables that allow to define the status of conservation.

In particular, the most innovative and complex topics of NCT 2008 regarding existing masonry buildings, have been explained by the further Circular 617 of 2 February 2009, in which level of knowledge and confident factors have shown (Table 5). In this document, definitions and guidelines for existing buildings are outlined (Circ. 09, 2009).

Therefore, the knowledge of buildings composing by masonry has a fundamental importance for a proper analysis, and it can be achieved with different level of study, according to the accuracy of survey operations, to the historical analysis and to the experimental measurements.

From Eurocodes and from Italian NTC08, levels on knowledge are defined as follow:

- **KL3:** is achieved when geometrical survey, extensive and comprehensive verifications and tests in situ for the construction details, extensive and exhaustive investigations in situ for the properties of materials are realized;

- **KL2:** is achieved when geometrical survey, extensive and comprehensive verifications and tests in situ for the construction details, exhaustive investigations in situ for the properties of materials are realized;
- **KL1:** is achieved when geometrical survey, limited verifications and tests in situ for the construction details, and limited investigations in situ for the properties of materials are realized.

Level of knowledge (KL)	Geometry	Construction details	Properties of materials	Methods of analysis	Confidence factors (CF)
<b>KL1</b>	Survey and measurement of masonry, vaults, floors, stairs. Identification of loads for each element on walls.	Limited checks in situ	Limited investigations in situ		1.35
<b>KL2</b>	Identification of types of foundations. Eventual survey of crack and deformation framework	Extensive checks in situ	Extensive investigations in situ	All	1.20
<b>KL3</b>			Extensive investigations in situ		1.00

*Table 5: Level of knowledge and confidence factor, from Circular 617 of 2 February 2009 (Circ. NTC08)*

The Italian body of laws and codes about constructions faces the problem of the artistic buildings in the “Guidelines for valuation and decrease of seismic hazard of cultural heritage referring to technical construction code”, which is an ordinance of the President of the Council of Ministers.

The purpose of the Guidelines is to match seismic-safety requirements with preservation requirements when the building is a unique and unrepeatable artistic construction. In Guidelines, much attention is pointed on survey and knowledge of the building, safety calculations to be performed, an adequate structural model (i.e. cinematic model) and monitoring the building after the realization of the intervention. In order to prevent the seismic collapse of objects and decorations in the building, an appropriate “artistic limit state” (SLA) has been introduced in the guidelines (paragraph 2.3). On the contrary, although EN1998-3 clearly admits (paragraph 1.1) that cultural heritage needs a different approach than ordinary existing buildings, no indication can be found in the European Code. It is evident from the flow chart in [Figure 27](#). Here the paragraph 1.1 of EN1998-3 is reproduced:

*“Although the provisions of this Standard are applicable to all categories of buildings, the seismic assessment and retrofitting of monuments and historical buildings often requires different types of provisions and approaches, depending on the nature of the monuments”.*

Decree law 6 June 2012, n. 74: A special mention deserves the regional law, issued in Emilia-Romagna after the earthquake of 20<sup>th</sup> May 2012, in which urgent actions in favour of populations affected by seismic events have been explained: this because of a case study dealt (Chapter 5), which was damaged just from this earthquake. In particular, in Art. 4, 1<sup>th</sup> point, measures for the property of artistic and cultural heritage are debated. Therefore, in this article, there are the rules for the implementation of a program of urgent

measures, in order to repair public buildings, damaged by the earthquake. In 2<sup>th</sup> point, Presidents of the region, in agreement with the Ministry for Cultural Heritage, within the available, provide the requirement related to:

- the safety measures involving the damaged property;
- the removal and recovery of cultural archival and mobile assets;
- the controlled removal and recovery of selected debris for the damaged cultural heritage;
- the beginning of reconstruction, recovery, conservation, restoration and structural improvement of the heritage.

These points have been adopted both to take on urgent actions, both for starting a next step of reconstruction.

Furthermore, in the Article 17, 3<sup>th</sup> point, it is emphasized that the damaged property of artistic, architectural and historical field, do not constitute waste. These materials are selected and separated at the origin, according to the dispositions of the competent authority, which also identify the place of destination.

### **3.6 Considerations**

The structural analysis in the field of cultural heritage, is a topic discussed very often. The importance to define a three-dimensional model, also for very complex structures have to be a priority. As seen, the difficulties to analyse the existing buildings is focused on the possible approaches in order to obtain a correct solution. Regardless of the method of modeling the structure (with macro-modeling or micro-modeling elements), the input data is the most important part because from this, the subsequent steps will derive. In fact, if the survey is accurate, the structural analysis will be closer to reality.

### 4.1 Introduction

As seen in the previous chapter, masonry walls are very used in the vast majority of existing monuments. Cracked elements, associated with different events (settlements and/or excessive displacement loadings) are a common problem that reduces the service life of these structures (Grimm, 1988). The structural behaviour is highly dependent of the structural geometry. This is why four conditions are required to carried out proper analysis (Sánchez-Aparicio, Riveiro, Gonzalez-Aguilera, & Ramos, 2008):

- Having a complete and accurate geometric characterization of the structure;
- Knowing the materials mechanical properties;
- Characterizing all the loads acting in the structure;
- Providing numerical models that correctly simulate the characteristic behaviour of the structure.

Modern restoration techniques for built heritage are characterized by minimal intervention, compatibility, durability and reversibility (ICOMOS, 2003). The Identification and monitoring of the pathological condition of the building, is very important for understanding the current behaviour of the structure and the choice of restoration methods to be accomplished (Vercher, Gil, Mas, & Lerma, 2013). The constant progress of the numeric method of finite elements and computer processing allows the generation of increasingly complex geometric models; that is why it is more and more imperative the necessity of relying on sensors capable to provide massive detailed data and features for the model. In this field, Geomatic sensors like terrestrial laser scanner ( Armesto, Roca-Pardiñas, Lorenzo, & Arias, 2010); (Pieraccini M. , et al., 2014)) or digital camera (Riveiro, Solla, De Arteaga, Arias, & Morer, 2013) have acquired important roles, due to the capacity to acquire accurate geometrical information needed by the numerical models.

Geomatics instruments, despite their high cost, are used today to perform numerous tasks: the sensor allows acquiring, in a short time, the current condition of the surveyed object and obtaining a snapshot of its geometry. This concept has been applied very often within the field of cultural heritage to support multidisciplinary studies: from simple documentation, to monitoring the condition of historical buildings and also in order to support restoration works or structural analysis checks. The three-dimensional model allows storing metric and qualitative information for further use. The possibility to have a complete coverage of a building changes the traditional concept of a survey, where only the data of some defined sections are available ( (Boehler, Heinz, & Marbs, 2002), (Núñez & Pozuelo, 2009)).

So, geomatic measurements and acquisitions allow to obtain, as well known, very realistic three-dimensional models that reproduce perfectly the real geometry. These techniques are nowadays used in many fields, but are not so often applied for Structural Engineering. Probably, this is because while the Geomatics seeks to get the best precision as possible, Structural Analysis aims to simplify. In this chapter, it will analyse how it is possible, therefore, to find a meeting point and a connection between Geomatics and Structural Analysis. In fact, most of geometric models used for structural analysis are really simplified, since are often developed starting from existing plants and sections obtained from direct surveying, and therefore poor of details. This simplification is acceptable for the largest part of modern constructions in concrete or steel, for their regularity and symmetry, but is not indicated for buildings and objects belonging to cultural heritage, because of very complex geometries.

In this chapter, the transformation from point cloud into a FE model has been analysed, with a deepening of existing studies. The problem of the automatic transformation of a large point cloud dataset to a simplified geometrical object is a well-known and studied topic. Several contributions are available in the literature, and some of them propose semi-automatic or automatic procedures specialized for a specific use. After an

analysis on the representative studies on this field, the second part of this chapter focuses on the identified methods in order to transform the input dataset (point cloud or polygonal model) into an output data, suitable for structural analysis.

## 4.2 The transformation of dense point cloud datasets

The problem of the transformation of a large point cloud dataset to a simplified geometrical object is a well-known and studied topic. Furthermore, the interest for the numerical modeling of historical building increased in the last years, for this reason FE modeling is considered a very useful method to investigate structural behavior of cultural heritage. The numerical modeling of historical monumental buildings is a challenging task for contemporary civil engineers. As seen from the literature, one of the main reasons for this is that the use of traditional simplified structural schemes is inadequate, due to the complex geometry of such historical structures. Therefore, it is necessary to resort to a fully 3D modeling technique that is often performed using Computer Aided Design (CAD). In general, CAD-based modeling is an expensive and complex process and it is often performed manually by the user, which inevitably leads to the introduction of geometric simplifications (defeaturing) or interpretations, to speed up the process.

Several contributions are available in the literature, and some of them propose semi-automatic or automatic procedures specialized for a specific use. In the context of an airborne laser scanner (ALS), the automatization aims to reconstruct simple shapes of buildings to use with textures from terrestrial and airborne images, and with its main geometric features. Consider, for instance, the study of Dorninger et al. (Dorninger & Pfeifer, 2008) where an approach for the automated generation of building models from ALS, comprising the entire sequence from extraction to reconstruction and regularization, is presented, or Africani et al (Africani, Bitelli, Lambertini, Minghetti, & Paselli, 2013), where the 3D simplified modeling of buildings is finalized to a study about solar radiation potential.

Recently, in the field of civil engineering, laser scanner surveys are gaining particular interest to generate structural models, since the increasing computational capabilities allow the manipulation of large datasets. Although there are several studies available in previous literature, in some cases, the cloud is simple or significantly simplified. In Chen et al (Chen J. , 2008), a pipeline to reconstruct the complete geometry of architectural buildings from point clouds obtained by sparse range laser scanning is presented for buildings that are made of planar faces. The proposed technique faithfully constructs a polyhedron of low complexity based on the incomplete scans, but does not resolve fine geometry details. In (Guarnieri, Pirotti, Pontin, & Vettore, 2006); (Guarnieri, Milan, & Vettore, 2013) ), a three-dimensional point cloud is used to generate a cross-section model that is applicable to structural analysis, and a finite element method (FEM) analysis of a whole building is carried out using laser scanning data.

(Armesto, Roca-Pardinas, Lorenzo, & Arias, 2010) presented a methodology to estimate the deformation of arches or vaults based on the symmetry of sections, obtained along the vault guideline. In this case, the accurate geometry of the masonry arches is obtained by means of a three-dimensional laser scanner survey, reduced to the inner arches' surface representation. Massive structures, such as masonry bridges, can also be investigated by summing the information obtained by Ground Penetrating Radar GPR, with the laser scanner survey (Lubowiecka, Armesto, Arias, & Lorenzo, 2009) or involving Close Range Photogrammetry CRP (Arias, P, Armesto, Lorenzo, & Ordóñez, 2006), obtaining a fine picture of the external and internal feature, as well as the development of finite elements based structural models. These works show a multidisciplinary approach to heritage documentation involving CRP or TLS and GPR techniques, as well as the development of finite elements based structural models. The geometric shape, the building material homogeneity and the current damages and its causes are obtained. A non-destructive test through GPR is employed for the interior

material homogeneity analysis and zones description. Resulting information related to the whole bridge geometry is taken as basis to develop different numeric models applying the finite elements method (FEM). These analysis involves different load hypothesis in order to obtain a stress distribution compatible with the detected damages which allows identifying likely causes of them.

A highly relevant contribution in this field, is proposed in several studies where a flowchart to precisely capture the building geometry by automatic reconstruction of its boundary is performed. Hackel et al describe two different methods for semantic classification (2016 a) and to automatically detect contours (2016 b), i.e. lines along which the surface orientation sharply changes, in large-scale outdoor point clouds. Contours, in particular, are important intermediate features for structuring point clouds and converting them into high-quality surface or solid models, and are extensively used in graphics and mapping applications.

Truong-Hong et al. ( (2013), (2014)) proposed an attempt to precise capture the geometry of the building through the automatic reconstruction of its boundary is presented (Figure 28), while in the contribution given by Hinks et al. (Hinks, Carr, Truong-Hong, & Laefer, 2013), a point-based voxelization method to automatically transform point cloud data into solid models for computational modeling is proposed. The method constructs a triangular irregular network (TIN) mesh by means of a voxel grid bounding the cloud region. The resulting model captures the three-dimensionality of the survey, but does not capture the whole structure, since it is designed for façades (Figure 29).

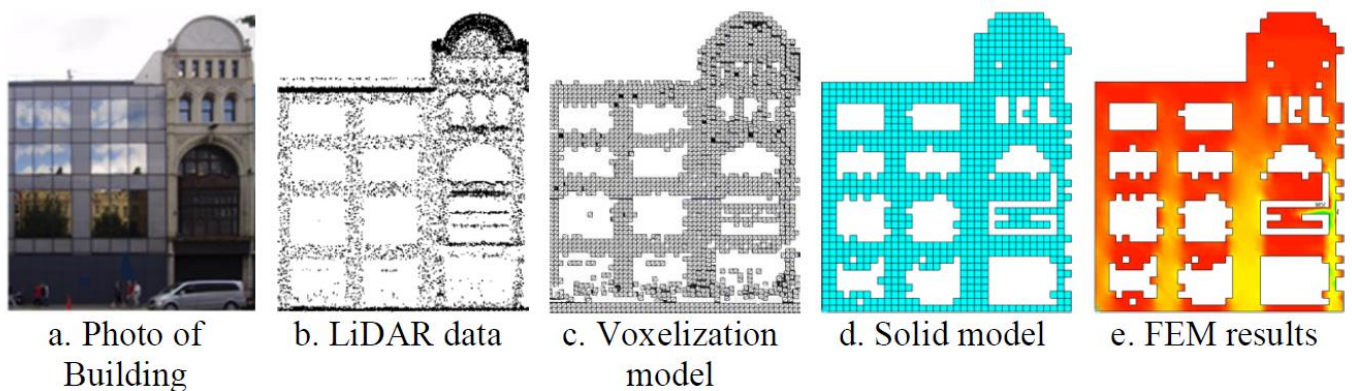
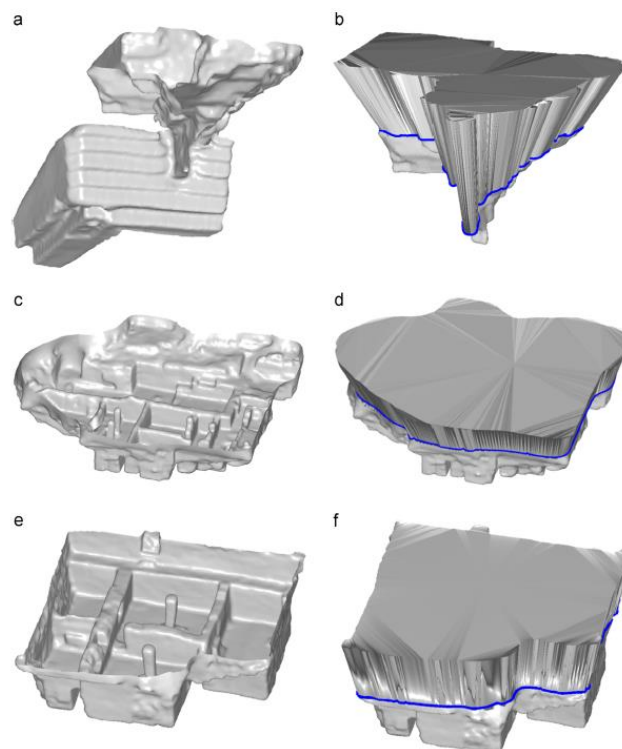


Figure 28: Solid model reconstruction of external façade from ALS data (Hinks et al., 2013)



Figure 29: Post-processing TLS data for a façade (Truong-Hong et al, 2013)

Regarding the reconstruction of buildings from point clouds, it is possible to update existing 3D models with accurate information acquired from TLS (Zvietcovich, Castaneda, & Perucchio, 2015). The authors, in particular, introduced a new methodology for updating solid models of monuments with information extracted from 3D local meshes built from point clouds. The procedure allows controlling each of the stages in an interactive fashion, and reduces considerably the time employed for a user to update the model manually in a CAD software (Figure 30). Moreover, since the creation, registration, segmentation and transformation of meshes to the solid model are managed by algorithms, the final outcome will preserve, as much as possible, the initial accuracy of meshes on the geometry of the resultant solid model. Anyway, preserving the same accuracy using manual procedures in a CAD software will be highly difficult and time consuming.



**Figure 30:** Mesh models of selected areas of Huaca de la Luna and corresponding solid features: decorated façade – mesh (a) and corresponding solid feature (b), mesh (c) and corresponding solid feature (d); and Hypostyle Hall – mesh (e) and corresponding solid feature (f)

An interesting approach is presented in Barazzetti et al. (2015 a) where the authors describe the use of building information modeling (BIM) derived from point clouds for the structural simulation based on FEM. Building Information Modeling is an object-oriented (and not only surface) organized space, managed from different available software, and consists of parametric objects representing building components, described through construction techniques, materials, historical data, photographs, audio, etc... ( Barazzetti, et al., 2015); (Eastman, Teicholz, Sacks, & Liston, 2008)). It is defined by international standards as “shared digital representation of physical and functional characteristics of any built object [...] which forms a reliable basis for decisions” (ISO standard, 2010). Starting from this concept, Chiabrando et al. (Chiabrando, Sammartano, & Spanò, 2016) define HBIM as a semantic-aware database regarding historical buildings, in which the geometric model is connected to descriptive information multi-source (Quattrini, Malinverni, Clini, Nespeca, & Orlietti, From TLS to HBIM. High quality semantically-aware 3D modelling of complex architecture, 2015).

Specific HBIM made up on existing historical buildings are able today to encapsulate into their own database a high level of multiple information, not only geometric but also the ones about historical evolution, material composition, stratigraphy, state of conservation, technological and structural behaviour of elements, and therefore they can be useful for different scopes. Research works in the field of HBIM can lead to many application and above all, for example: 3D detailed models for divulgative purposes; base models for historical constructive phases study; 3D models for interpretation, reconstruction and restoration design; management and monitoring of the state of conservation of structures and materials; base model for archive and relate various diagnostic test to the geometry; static and dynamic condition assessment by structural simulation and Finite Element Analysis (FEA). The authors observe that although BIM interoperability has reached a significant level of maturity, the density of laser point clouds provides very detailed BIM models that cannot directly be used in FE software. In fact, in order to achieve the expected FE model, several manual corrections or simplifications are needed to guarantee the mesh compatibility, to avoid mesh local distortions or small elements and to model complex architectural objects ( (Barazzetti, et al., 2015 a); (Dore, et al., 2015); (Sun & Cao, 2015); (Oreni, et al., 2014)).

Therefore, BIM models automatically produced from point clouds cannot directly be used in FE software. In fact, several manual corrections are needed to avoid mesh local distortions or small elements and to guarantee the correct representation of complex architectural objects. Providing algorithms that are both robust and capable to operate with few manual intervention, in order to fill holes, close gaps and remove intersection, requires an appropriate interpretation based on the object investigated (Attene, Campen, & Kobbelt, 2013).

#### 4.2.1 Restrictions

As seen in the previous paragraph, many works analyze and face the manual or automatic transformation for the treatment and the elaboration of the initial point cloud into two-dimensional contours, useful for three-dimensional modeling, Fe analysis etc... One of the most frequent problems when dealing with complex historical buildings, is the impossibility to generate closed surfaces with filled volume, starting from the point cloud of the surveyed object. Thereby, it is not possible to directly transform the TIN mesh surfaces into solid geometry and consequently into a FE model for a complex building. This approach for three-dimensional modeling may be right for element of small-scale: in this context, many interesting studies have been done, for example for Michelangelo's David statue (**Figure 31-Figure 32-Figure 33**) ( (Scopigno, Cignoni, Callieri, & Ponchio, 2003); (Callieri, et al., 2004); (Fastellini, Grassi, Marrucci, & Radicioni, 2005); (Borri, et al., 2005); (Borri & Grazini, 2006); (Corti, Costagliola, Bonini, & Landucci, 2014); (Forcellini, et al., 2015)), Socrate statue (Sorace & Terenzi, 2015), or the Bronzes of Riace (De Canio, 2012).

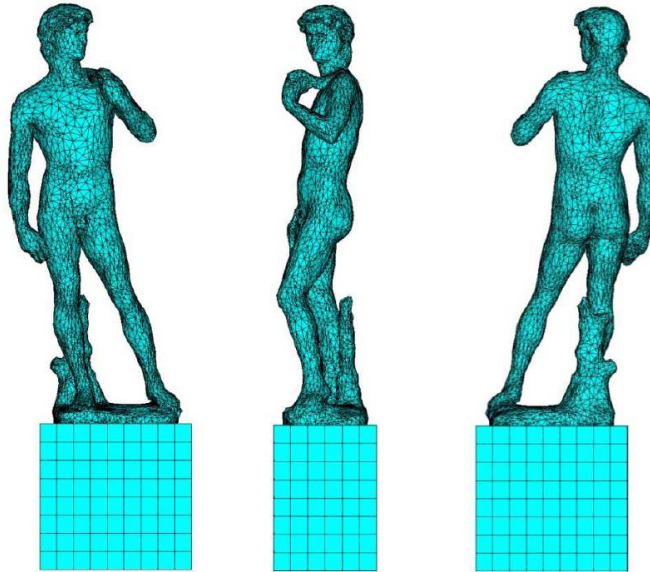


**Figure 31:** View of FE model made with ANSYS code, built with 40,205 isoparametric three-dimensional elements and 10,297 nodes; (Forcellini, et al., 2015)

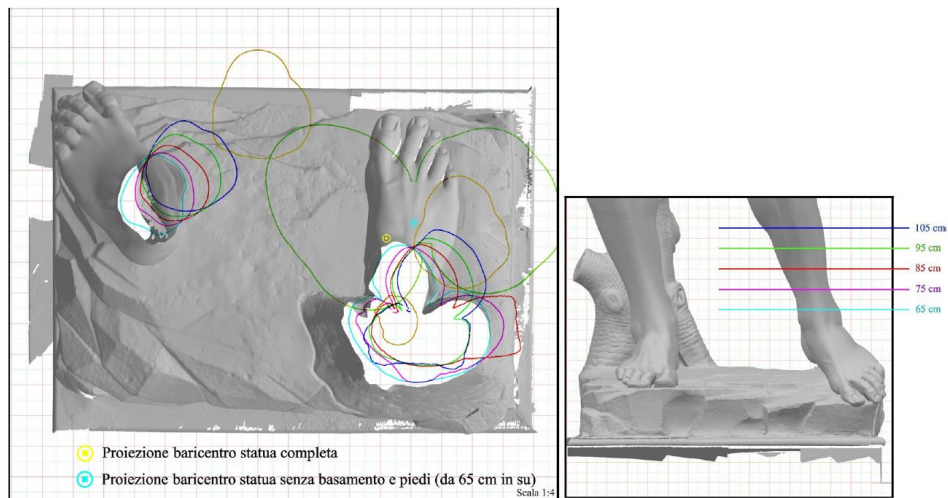


**Figure 32:** Visualization of the projection of the center of mass (marked by a yellow circle) and of the profiles of some cut-through sections (ankles, knees and groin); (Scopigno, Cignoni, Callieri, & Ponchio, 2003)

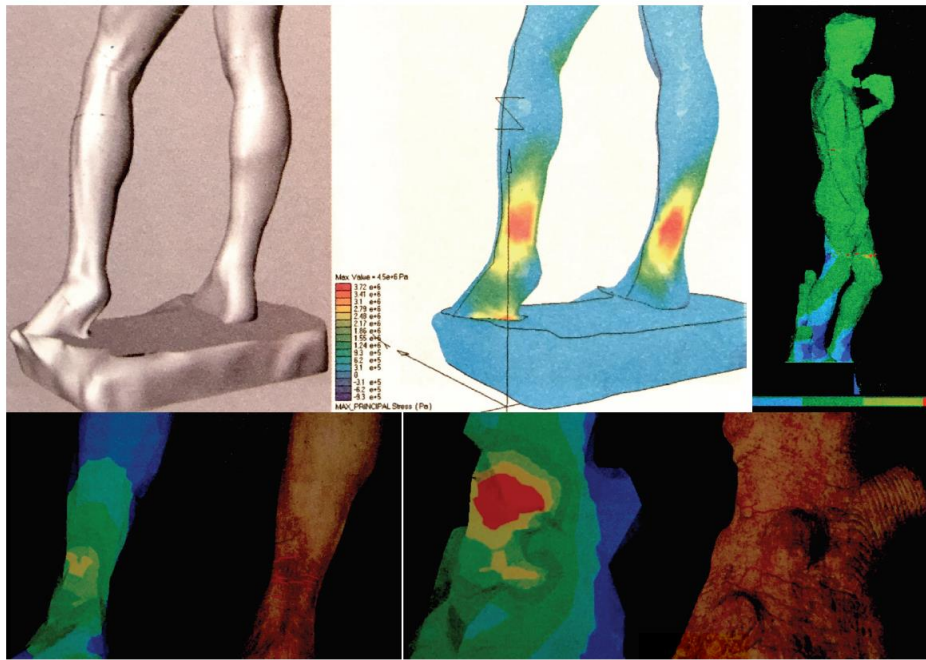


**Figure 33:** On the top left, the back view of 3D model. The analysis results, with ANSYS code, show the most stressed area from the back and of the entire statue. On the bottom the ankle model with stresses and the cracks (Borri, et al., 2005)

Yet, many approaches have been processed, in order to transform the initial point cloud in a three-dimensional FE model. This is also done in an attempt to achieve, as quickly as possible, a detailed and accurate model for a structural analysis.

An important recent work, was developed by Sánchez-Aparicio et al (Sanchez-Aparicio, Riveiro, Gonzalez-Aguilera, & Ramos, 2014): they proposed a methodology for generating precise finite-element numerical models for subsequent structural analysis. The point-clouds collected by laser scanning do not provide a sufficient amount of data for a full geometric characterization of the outer shell, and this requires a supplementary technology to the laser scanning, this is UAV + SFM. Besides, it gathers an extra supply of analyzable features, which makes it possible to get complete point-cloud models, which form the foundation for accurate and thorough CAD models. Then, the creation of a unique model is converted in to a valid CAD model of the building for the subsequent analysis. In a most recent work ( (Sánchez-Aparicio, Villarino, García-Gago, & González-Aguilera, 2015), the authors used only the photogrammetric methodologies (image-based modelling and digital image correlation) and the finite element method to understand the structural behaviour of these structures. Through the interpretation of the different obtained products, by the defined approach, they have been estimated and evaluated the causes of the structural damage that the analysed infrastructure, as a dome, can suffer and also design subsequent restoration mechanisms, always from a perspective of minimal intrusion to the structure.

In several contributes ( (Pieraccini M. , et al., 2014); (Szolomicki, 2015)) the point cloud is used, as base for the creation of three-dimensional model, by using CAD programs.

All works, however, are focused on three-dimensional transformation with different approach or based on CAD approach. No study, however, focuses on the full volumes of walls or elements (filled), but only on the exterior and interior part (meaning “skin”) of the surface. Even if the results might look correct, there is an approximation of the detailed initial model from the operator ( (Barrile, et al., 2015), (Almac & Pekmezci, 2016)).

Despite the huge advantages of the laser scanning technology for the geometric characterization of built constructions, as seen there are important limitations preventing more widespread implementation in the structural engineering domain. Even though the technology provides extensive and accurate information to perform structural assessment and health monitoring, the traditional processing times involved are prohibitive. Thus, new methods that can automatically process LiDAR data and subsequently provide an automatic and organized interpretation are required.

### **4.3 The transformation of point cloud dataset into FE model: procedures**

As previously said, the three-dimensional output data can reach a high level of detail and has to be synthesized to produced data input for FE modeling. This operation is not trivial, because the simplified model must retain all of the information regarding the structural elements.

In this research, different procedures are analysed and developed, in order to avoid approximation from initial data and loss of detail for structural analysis.

The proposed procedures can be distinguished into:

- Semi-automatic approaches, where the user input is necessary in some stage;
- Automatic approaches, where user input is mainly required to complement invisible parts and boundaries of the structure, and to assign meaningful approximate physical parameters.

The complexity of the dataset is arbitrary, since the procedure are designed for buildings with irregular geometry, such as historical buildings. It should be stressed, however, that these procedures do not require a particular methodology of acquisition of the cloud, which is therefore not limited to terrestrial laser scanning or photogrammetric acquisition, but can be obtained using any other suitable technique to define the geometry of the detected object.

In the following image, a workflow clarify how is the typical FEA procedure by Commercial Software.

The pre-process is a very important step in order to transform the initial point cloud in a model exploitable for any commercial software.

In the following paragraphs two semi-automatic approaches, and two automatic approaches will be presented, in order to transform three-dimensional point clouds of complex objects, into a three-dimensional finite element model. The proposed methods always guarantee the generation of a filled model ready to use for structural analysis purpose to produce data input for FE modeling.

In the automatic approaches, the operator input is limited exclusively to the choice of boundary conditions and physical parameters for the structural analysis, because of this the following procedures are considered fully automatics. No manual or semi-automatic operations are required by the operator for the treatment of initial dataset. These methods concern new procedures for fully automating point cloud segmentation of complex building in masonry, but suitable for any element.

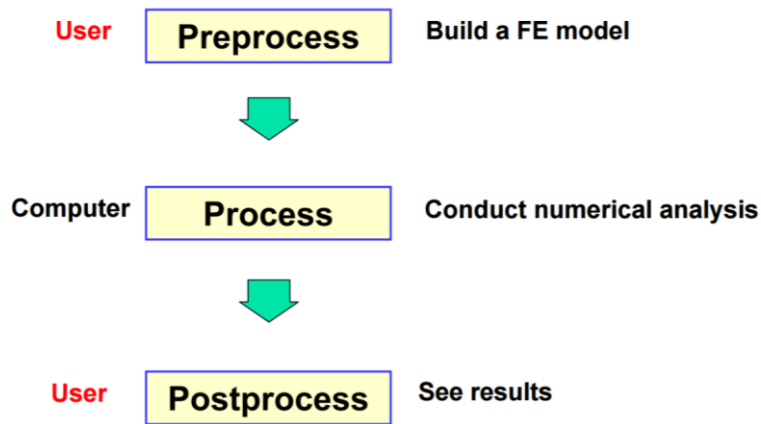


Figure 34: Workflow for a FEA procedure by Commercial Software

#### 4.3.1 Semi-automatic approach: Cloud2FEM procedure

This procedure is synthesized in the flowchart of Figure 35. The input data consists of generic point clouds, merged into a single point data file for the whole building surveyed. The workflow begins with a 3D analysis divided into sequential step and at the end of this first part, the building is described with a dataset of slices, each containing bi-dimensional points. These are subsequently analyzed in a 2D environment individually, and this phase includes some semi-automatic or manual analysis (highlighted in orange in the flowchart). All data are georeferenced using a unique local or global reference system; therefore, final datasets are stackable. Each pixel grid, obtained from the corresponding slice, contributes to the creation of the voxel model.

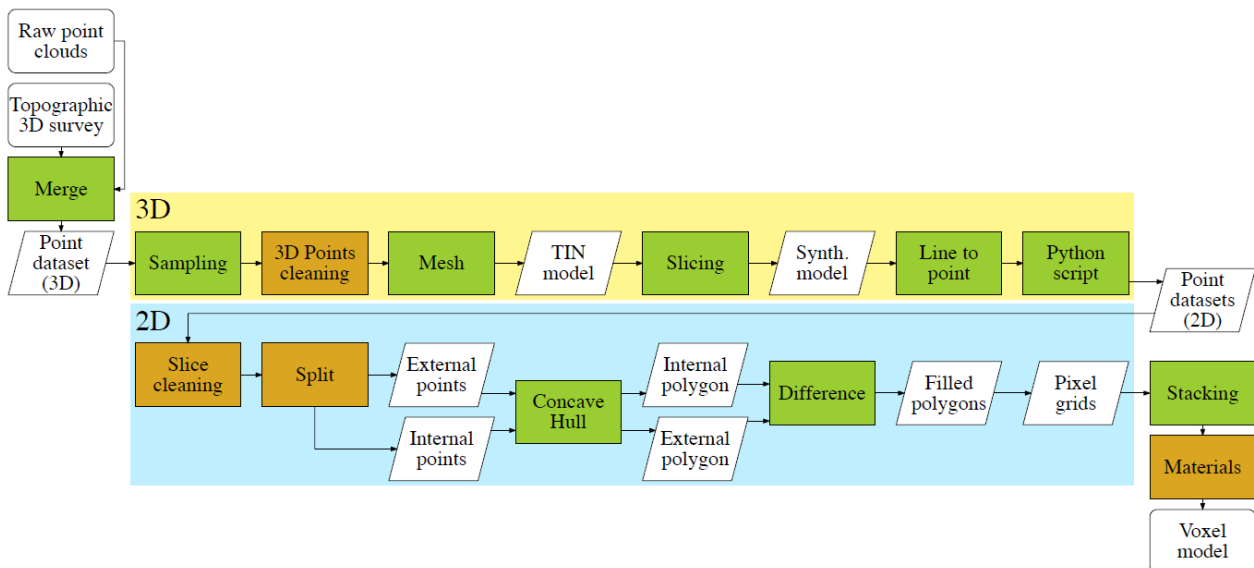


Figure 35: Flowchart for the proposed method: completely automated procedures (green) and semi-automated or manual procedures (orange).

A typical three-dimensional survey is composed by several stages; after the initial known steps to acquire the object, a specific software is then used to process the data surveyed and to align and merge all of the point clouds, applying a filter to eliminate any noise in the final point cloud. The robustness of the alignment can be enhanced using known coordinates from the acquired targets, producing a unique and optimized point

cloud. Point cloud slicing is a common procedure to extract sections and details from large point cloud databases. CAD based procedures are often used to transform sliced points into line-based models using automated procedures based on segmentation or using a manual extraction of profiles; see, for instance, Hackel et al (Hackel, Wegner, & Schindler, 2016 b) and (Martinez, Soria-Medina, Arias, & Buffara-Antunes, 2012) regarding the processing of building façades. Upon this condition, we conceive of the point cloud as a stacking layer sequence of “planar points”.

In **Figure 36**, a simple geometry is illustrated and referenced to the Cartesian system, where the axis Z is the principal direction of the stacking sequence (**Figure 36c**). The structure is subdivided by subsequent section planes  $\Pi_j^z$ , each one characterized by an incremental z-coordinate of  $\Delta z$ . Then, all of the points within the range  $[z_j - \Delta z/2, z_j + \Delta z/2]$  are projected to the mid-plane  $\Pi_j^z$  (see **Figure 36d**).

This method is inspired by techniques of computed tomography (TC) which, through the use of X-rays, the principle of representation of the body in slices is used. This technique, in fact, as output give the tomographic images (i.e. slices of bodily layers).

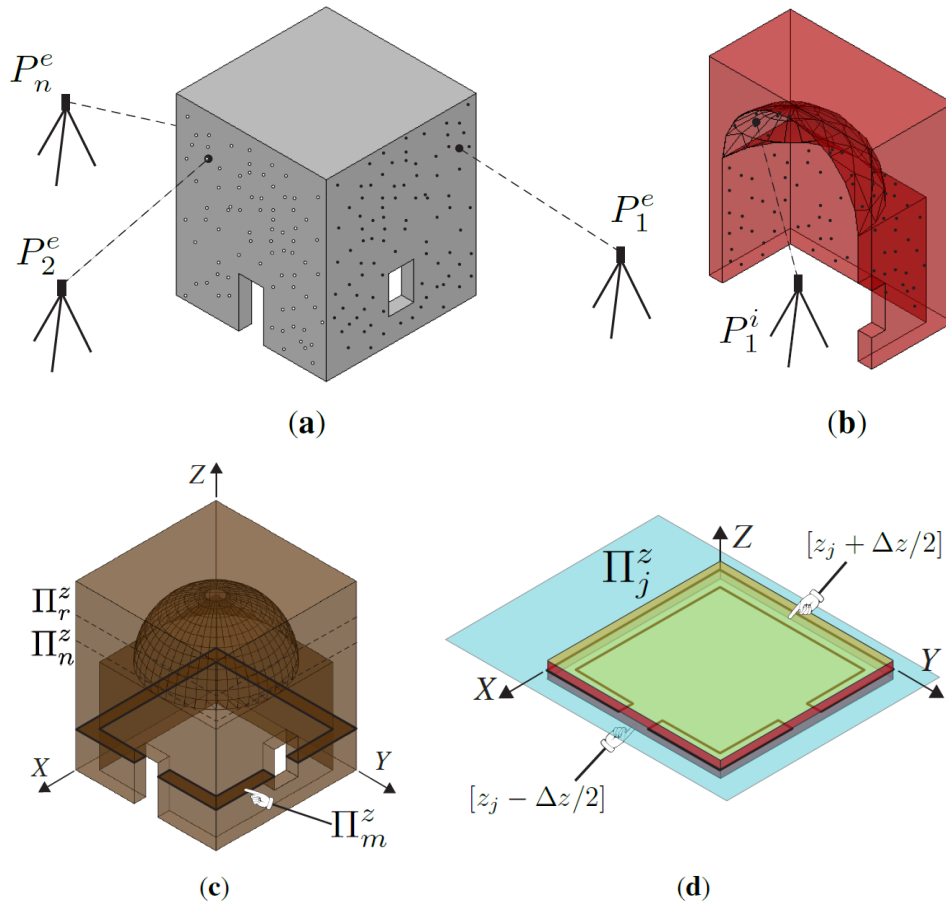


**Figure 36:** Visualization of the stacking layer sequence concept. (a) Point cloud survey of external façades; (b) point cloud survey of internal surfaces; (c) illustration of the  $m$ -th slice; (d)  $\Pi_j^z$  layer.

Therefore, the three-dimensional problem is reduced to a two-dimensional one. By means of a parsing algorithm that walks through the dataset and separates points belonging to each slice, it is possible to generate a number of two-dimensional layers describing the whole structure when they are stacked

together. In particular, as shown in flowchart (**Figure 35**), Python programming language (Python 2.7.13) is used to distinguish each slice and process them, therefore, separately.

This model is composed by slices containing only points with variable (x; y) coordinates and a constant zj coordinate. The distance between two adjacent slices has to be chosen according to the desired final resolution of the FE model.

It is possible to operate on each slice independently with effective techniques with a linear workflow using software for the management of spatially-referenced data (e.g., a GIS). The pattern of points located on the  $\Pi_j^2$  plane is generated from the points belonging to each section of  $\Delta z$  thickness. A sequence of points at a constant interval and high density is placed along the lines contained in each slice. A boundary polygon that encloses the points can be computed using a concave or convex hull algorithm (Edelsbrunner, Kirkpatrick, & Seidel, 1983).

In the case of a building, the slices contain two principal profiles: the first made by connecting the points that belong to the external point cloud (consider, for instance, the survey of the external façade of a building; see **Figure 36a**) and the second made by connecting the points that belong to the internal point cloud (consider, for instance, the survey of the internal rooms of a building; see **Figure 36b**). The first result is a filled geometry, the “external” one, because it envelops the whole building. This might also be composed of several islands that represent the outside face of the building walls.

Similarly, the second produces a boundary polygon called “internal” that is computed selecting only the points acquired in the internal rooms. It is important to emphasize that also this polygon, in the same way as the external one, is created using a concave hull algorithm (Moreira & Santos, 2007), enveloping the point selection from the outside. Additionally, this polygon may also be composed of several islands representing the various rooms of the building.

Now, there are two polygons, one external and one internal, and together compose a filled geometry. By subtracting the second from the first, we obtain our first result: a filled polygon for each slice of the building that describes the entire structure.

Until now all the data processed are in vector format: points, lines and areas. In this final step, each slice previously processed is finally converted into two-dimensional regular pixel grids at a constant resolution along X and Y axes. For this final step, we used Grass GIS + Python (GrassGIS, 7.2) for converting automatically each polygonal section into a raster model (**Figure 38**) that discriminates filled areas from void areas. All the pixel grids are then gradually stacked in sequence creating a complete voxel model of the whole structure. At this stage it is also possible to assign different values to pixels in order to define the materials of different structural elements of the model.

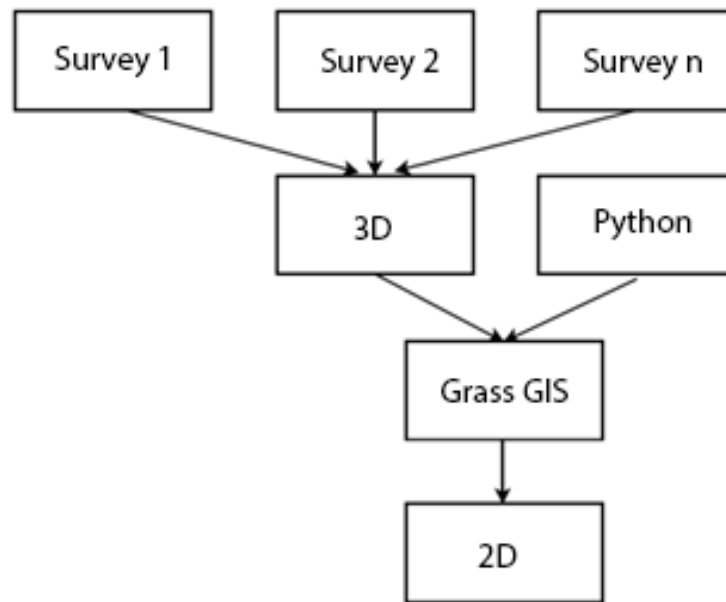


**Figure 37:** From different surveys, the initial dataset are merged into a unique three-dimensional model. Through Python programming language, two-dimensional slices can be elaborated into GIS environment. The final result, at this stage, will be given by the set of many raster images, one for each initial slice.

Once the slices have been created, we need to introduce the discretization procedure in order to set up the desired FE model. Thereby, we propose to discretize first the two-dimensional sections and then to use them to build the three dimensional discretized model. By using the CT approach (Malecki, et al., 2014) each slice has been idealized as a digital image, with a certain resolution, composed of picture elements (pixels), so the stacking of these slices generates the volume elements (voxels). This procedure allows the reconstruction of the original three-dimensional geometry by stacking all of its slices, so a complete volumetric representation of the object is obtained by acquiring a contiguous set of slices. The original polygon is then described by a  $N \times M$  pixel matrix corresponding to a grid of pixels with a particular resolution (Wang, Huang, Li, & Chen, 2014). With reference to **Figure 36c** and **Figure 38**, the pixel value will be, for instance, in an eight-bit grayscale, 255 for the filled area and zero for empty spaces. This transformation is performed automatically for each slice with a fixed region preserving the output resolution. Therefore, all of the grids are aligned, and we build the voxel model stacking them in the original order, following their coordinates.

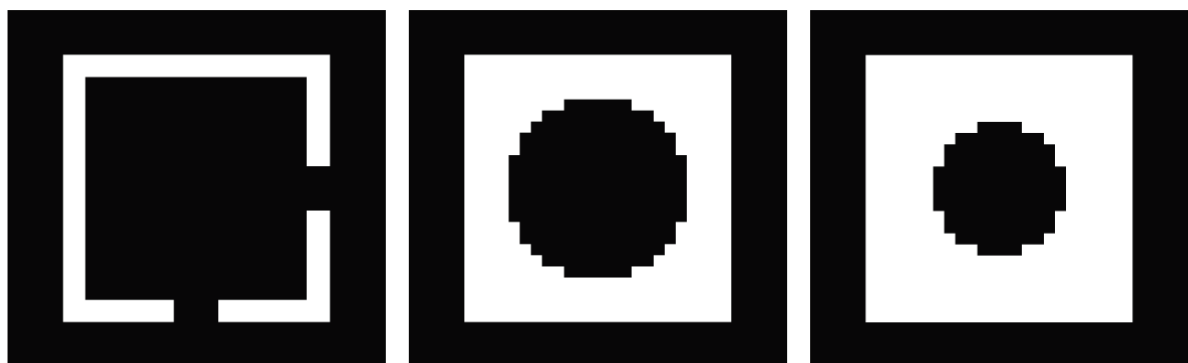


**Figure 38:** Two dimensional images obtained by slicing the structure illustrated in Figure 2:  $m$ ,  $n$  and  $r$  represent three generic slices located at the  $z_m$ ,  $z_n$  and  $z_r$  coordinates respectively; (a)  $\Pi^z_m$ ; (b)  $\Pi^z_n$ ; (c)  $\Pi^z_r$ ;

Voxels, as represented in **Figure 39a**, define a particular grid structure that possesses the following features:

- $\Pi_j^z$  planes are chosen with the normal along Z that is the building construction direction: features, layers and openings are conceived of by a stacking of elements (i.e., bricks) along the Z direction;
- $\Delta z$  is chosen according to the building complexity along the Z direction;
- $\Delta x$  and  $\Delta y$  are chosen according to the in-plane complexity and are totally independent of  $\Delta z$ ;
- The stacking procedure is here proposed as a linear stacking of contiguous slices, but can be, in general, considered as interpolated along the Z direction (i.e., considering more slices at a time);
- The resulting discretized volume does not need any particular further adjustment “to fill” the structure.

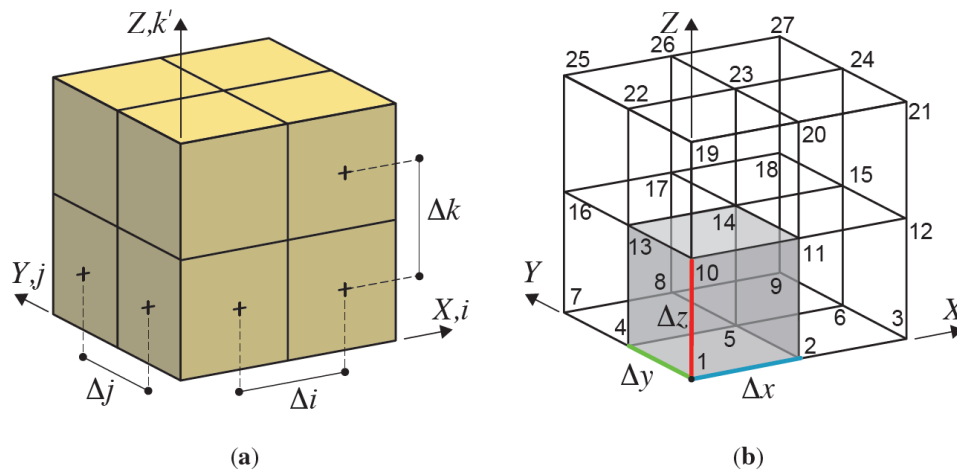


**Figure 39:** Voxel representation and finite element transformation:  $f_i; j; k$  and  $fX; Y; Z$  are the indexes of the voxels' three-dimensional matrix and the global coordinates of the structure, respectively. The coordinate  $k0$  means  $k0 = R - k$ , where  $R$  is the third size (along  $Z$ ) of the voxels' three-dimensional matrix ( $N \times M \times R$ ). (a) Voxel indexes; (b) hexahedral elements.

The resulting dataset is simple and easy to use with the finite element technique: each voxel is automatically transformed into an eight-node hexahedral finite element. By using a common space-partitioning data structure (KD-TREE), the scheme represented in **Figure 39a** is transformed into a finite element structure (**Figure 39b**) by simply generating the connectivity structure of each element. In theory, this operation can be performed for each voxel value (in this case, zero or 255) or only for a certain value of the voxel, i.e., only those with a value equal to 255. Therefore, it is possible to easily describe multiple properties of objects by setting multiple values for the voxel. For instance, if we assume that a particular voxel value corresponds to a particular material, we can describe, in addition to the geometry, also multiple mechanical properties. With these features, the resulting discretized geometry already contains all of the information to use with the FE model, including the mechanical properties associated with the material features. The proposed method guarantees, with a simple procedure, the construction of a fine discretized geometry and, then, an automatic generation of a reliable FE solid model. Since we are dealing directly with the definition of finite element nodal coordinates and with the connectivity matrix, the proposed method is generally customized to work with any commercial FE software. This rational organization is certainly the key novelty introduced by the method. **Figure 40** illustrates the FE mesh obtained by applying the procedure to the structure represented in **Figure 36**. As can be noticed, as long as the surface is regular and parallel to the axis directions, the resulting mesh precisely matches the original geometry (**Figure 40a**), but when the surface is irregular (curved) or not planar to an axis direction, the resulting FE mesh is a jagged representation of the original geometry (**Figure 40b**). Despite this fact, it is always possible to improve the mesh accuracy using a smoothing method to reduce the faceting; see **Figure 40c**.

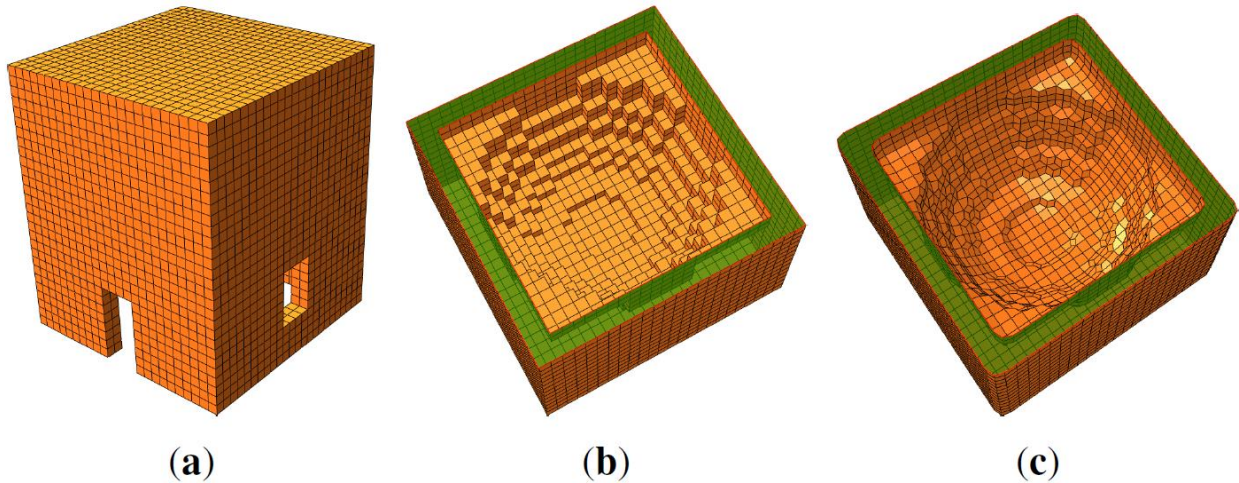


**Figure 40:** Finite element mesh obtained by applying the procedure to the structure represented in **Figure 39**.  
 (a) External restitution; (b) internal restitution; (c) smoothed internal restitution.

#### 4.3.2 Semi-automatic approach: HPC procedure

The procedure, summarized in the flowchart of **Figure 41**, has been developed with the Institute of Geodesy and Photogrammetry IGP of ETH (Zurich). Even in this method, the input data consists of generic point clouds, merged into a single point data file for the whole building surveyed. The FE model is generated from the registered and merged point cloud representing the entire surface of the object.

The goal is to have a very homogeneous point cloud, in order to directly transform the point cloud in a three-dimensional voxel model. As known, the original point cloud typically presents strong variations of density related to different parameters: the acquisition distance between the sensor and detected surface, the different techniques of acquisition, etc...

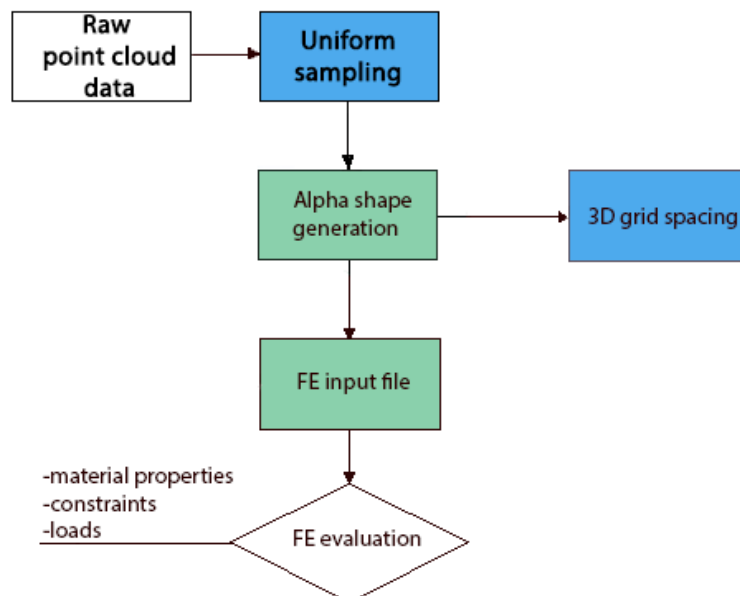


**Figure 41:** Flowchart for the proposed method: completely automated procedures (green) and semi-automated or semi-automatic procedures (blue).

Depending on the type of structure an appropriate type and dimension of three-dimensional finite elements is chosen. Herein we select eight-node cubic bricks (C3D8) which will likely be suitable elements also for a variety of other applications. The space contained within a three-dimensional bounding box of the point cloud is then filled completely with these elements; in case of cubic bricks, this corresponds to a voxel representation of the bounding box. Subsequently, the point cloud is used to select the elements actually corresponding to parts of the structure and discard the others. The result is a three-dimensional mesh that represents the structure geometrically within the FE software.

Starting from merged point cloud (three-dimensional initial dataset), a brief cleaning phase follows, with different tools but always supervised by an operator that has knowledge over the surveyed object, in order to delete all the points not useful for the subsequent analysis: close structures, vegetation, terrain and outliers.

Then a first polygonal mesh is computed from the point cloud using appropriate procedures and parameters (Figure 42). One of the main and typical problems is the presence of holes (Figure 43) due to data missing in the point cloud for occlusions in the line of sight between the sensor and the surface to acquire, and intersections from arbitrary triangle meshes (Figure 44a). At this stage, it is important to get a closed and topologically correct mesh, without overlaps, holes, noise or other types of defects which can occur in polygonal meshes (Attene, Campen, & Kobbelt, 2013). Nevertheless, it is not always possible to correct these gaps, for a whole complex building, using automatic procedures (Attene, 2014).

The scanned surfaces may not enclose the entire volume of the structure. Usually at least the foundation of the structure is hidden and it has to be reconstructed in order to represent the entire structure. Furthermore, there may be layers of the structure that need to be treated differently in the modeling; these boundaries within the structure need to be reconstructed using prior knowledge or assumptions.

The operator intervenes, at this stage, resolving eventual problems found during the mesh construction phase. Then a procedure for automatic decimation is performed, in order to reduce the complexity of the mesh, though ensuring the correct representation the specificities of the geometry of the structure (Figure 44b). The result is a continuous surface that represents the outer shell and interior shell of the entire structure.

The next step, consists in the conversion of TIN model into a point cloud data (Figure 45). This totally automatic transformation, starting from polygonal model, allows to obtain a totally homogeneous point cloud along its plan, for the external part and the internal one.

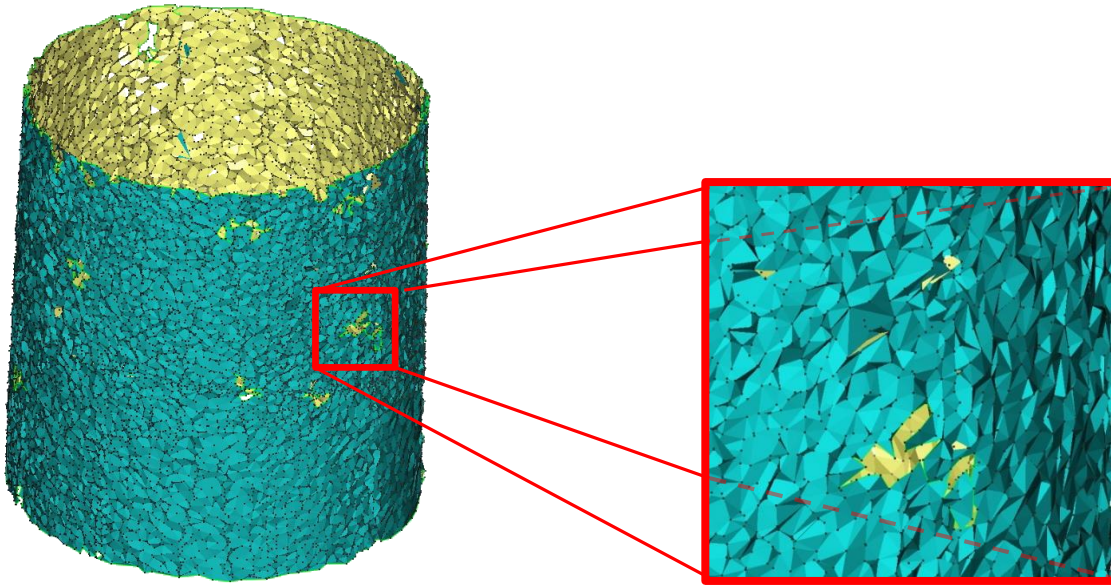


**Figure 42:** The raw polygonal model, in the first stage is characterized by uneven and messy elements, due to a rough surface, with non-manifold or singular edges, self-intersection, surface holes. Each point, vertex of triangles that composes the mesh surface are, subsequently, untidy and often are isolated. For these reason, they cannot belong to a continuous surface.

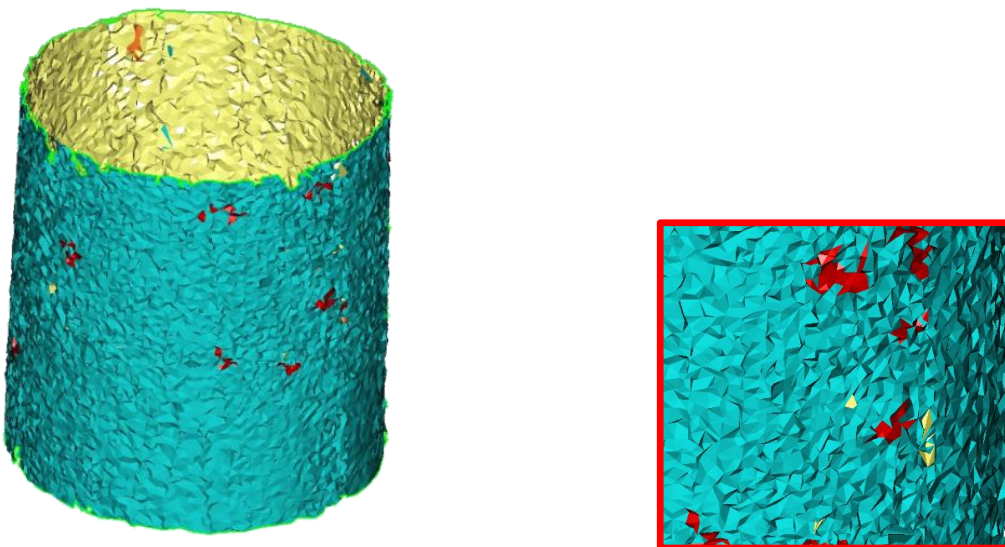


**Figure 43:** The manual input from the operator allows to fill holes of the surface. Nevertheless, self-intersections and inconstence orientations are still presents. As shown in the image detail, in the right, the external surface has two colors: the blu (external part) and some yellow triangles (tipical, in this example, for the internal part or for errors between polygons).

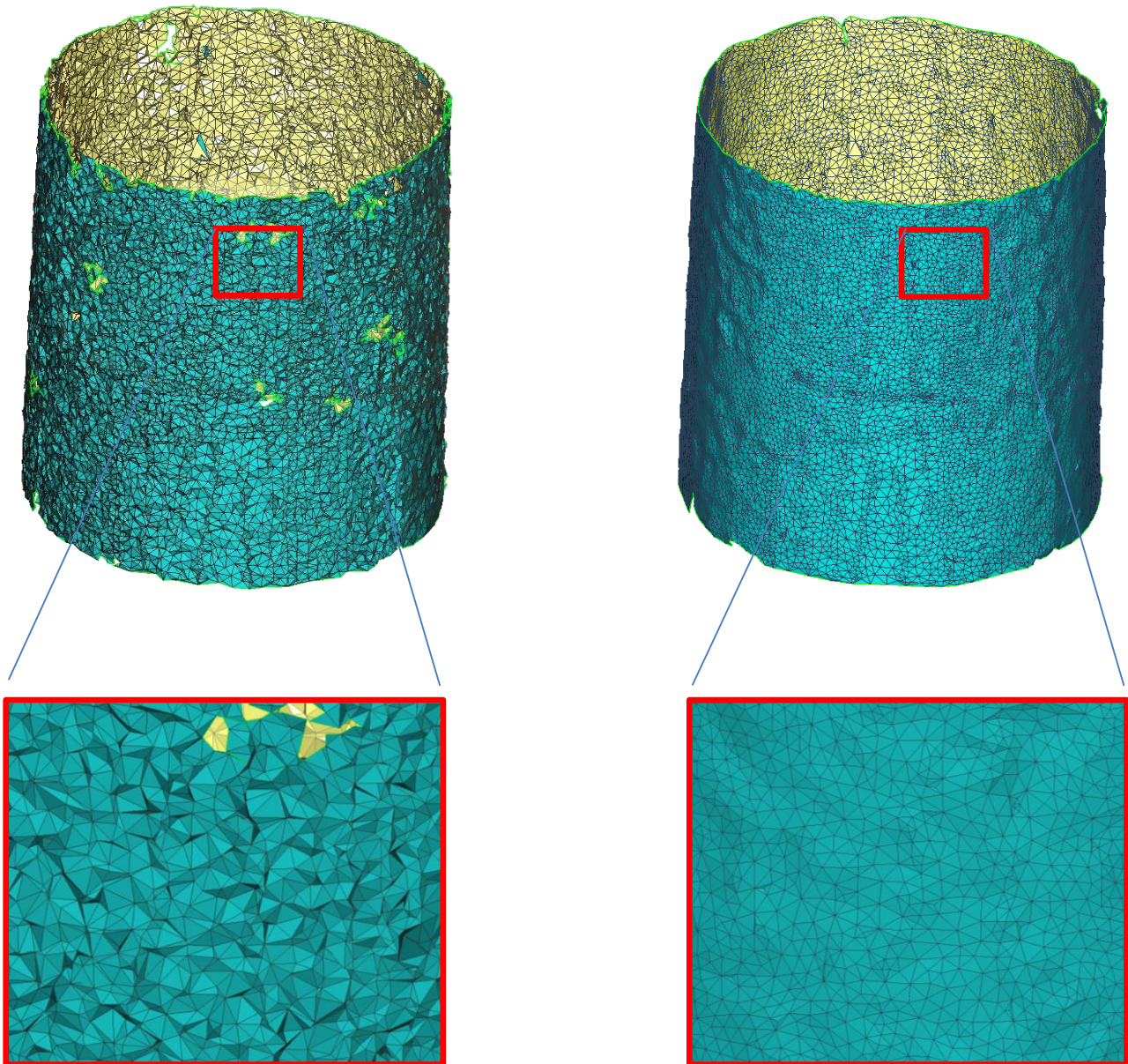


**Figure 44:** The next step, as shown in flowchart (Figure 41) is the automatic procedure to correct each error and flaw of the three-dimensional model. This can be solved with some common operations, through specific software or script for the treatment of three-dimensional polygonal models. Analysing the pictures on top, in which there is the overlap between the two-dimensional triangles and three-dimensional surface, the comparison between the initial polygonal model (left) and the final polygonal model (right) shows a final dataset improved and correct, with no errors described previously. (in Figure 42-Figure 43)

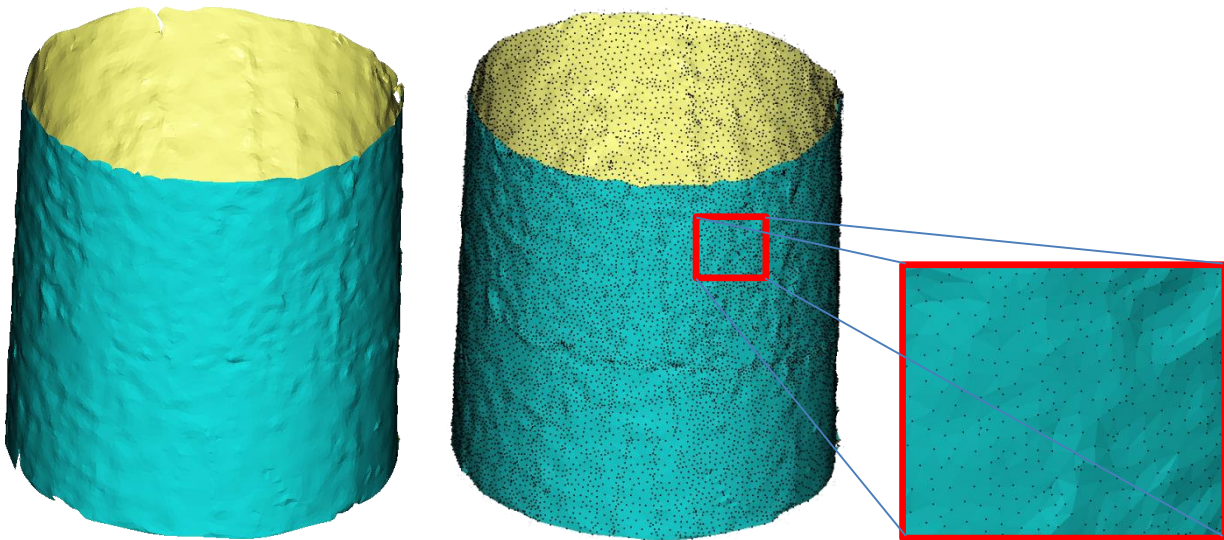


**Figure 45:** The last part of this procedure, for getting an homogeneous point cloud dataset, is the conversion from polygonal mesh to point cloud. Each point deriving from mesh model, is not casual: it is, instead, the vertex of every triangle of the mesh model. In this way, there is the assurance that all the points belong to the internal or external surface: in this specific example, there is the surface of the object, but in general it can be applied to buildings, considering the inner or outer part of a masonry, for example.

As previous said, this automatic process, starting from polygonal model, allows to obtain a very homogeneous point cloud, correcting and improving, therefore, the original non-homogeneous, discontinuous and noisy dataset. As shown in the images, the final point cloud will be homogeneous and suitable for automatic script, without data loss.

Hence, in the case of a building, the final dataset has contained two principal profiles: the first made by the points that belong to the external part and the second made by the points that belong to the internal part cloud. The point cloud is a discrete representation of the visible surface only, and an algorithm is needed to distinguish interior and exterior of the surface. We propose to use an alpha shape (Edelsbrunner, H., & Mucke, 1994) of the point cloud as a continuous representation of the surface. An alpha shape can be intuitively defined as a generalization of the convex hull of a point set in the sense that it also allows for concave shapes with curvature below a certain threshold depending on a chosen parameter. The bricks whose center lies within the alpha shape are selected as part of the FE model. For more details, see Edelsbrunner (1983) and (1995). A clarifying sketch of the 3d mesh generation (Figure 46) highlights the key elements involved, and solutions to two practical challenges.

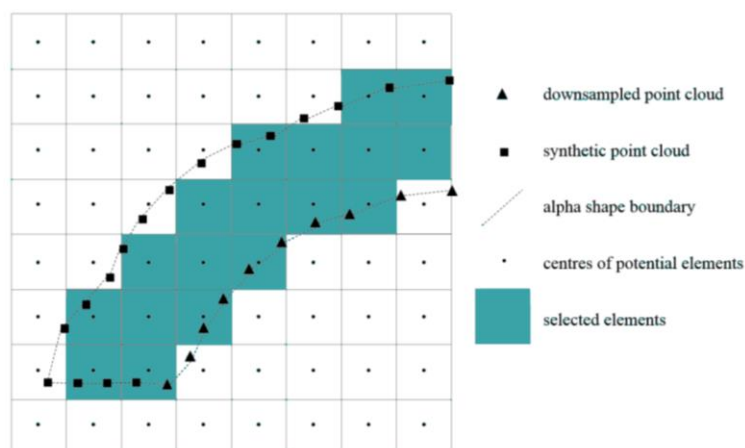


**Figure 46:** Two-dimensional sketch illustrating the generation of a voxel model out of the original point cloud.

Considering, for example, a masonry, the code reads every point as the centre of each linear element. Once identified each centre, through alpha shape function, the generation of the eight-node hexahedral elements will be obtained. The resulting point cloud fully describes the surface enveloping the structure, which is automatically discretized/meshed in chosen size-wide cubic eight-node brick (C3D8) elements. The mesh generation is followed by the choice and definition of the constitutive relations, material properties, constraints, and internal and external loads. This step requires understanding of the main physical properties of the structure and cannot be automated except for the assignment of concrete values to the individual finite elements based on a classification of these elements (e.g., different but individually homogeneous parts of the structure) and on generation of the corresponding input files for the FE software.

### 4.3.3 Automatic approach: From raw point cloud to FE model

This method was developed with the idea to automate as more as possible, the management of initial point cloud, for transforming of geomatics data, suitable for structural engineering field. In this case, a totally automatic method and very fast is used, through (Matlab, R2016a) programming language, but it could be used in any others programming languages. Through this procedure, the raw point cloud is imported and analysed. Therefore, no transformation is necessary from point cloud to polygonal model, or treatment of dataset (spacing uniform data, etc...) because it has been designed just for working with initial raw object, then non homogeneous. Once the point cloud has been imported, the code reads the position of every point and identifies a set of strips with constant or variable step (vertical or horizontal, according to the characteristics of case study and to the final results). In this way, according on the axis of own-interesting (in this case, in the [Figure 47-Figure 48](#), Z axis has been considered), the object is divided in  $-n$  sub-structuring, one for every strip.

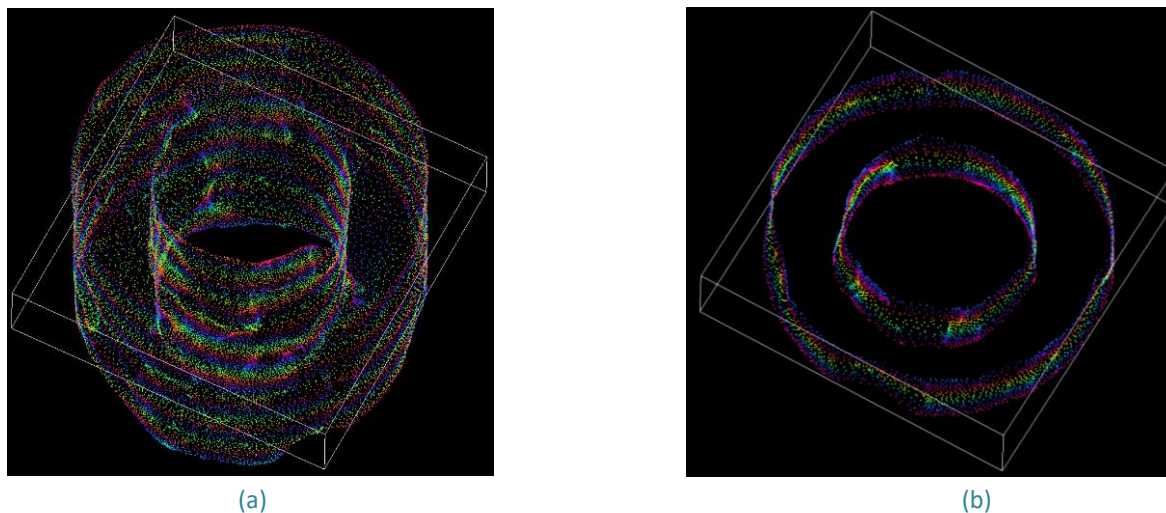


*Figure 47: Isometric view (a) with one of  $-n$  strips along Z axis; subsequently, a sub-structured (b) element has been considered.*

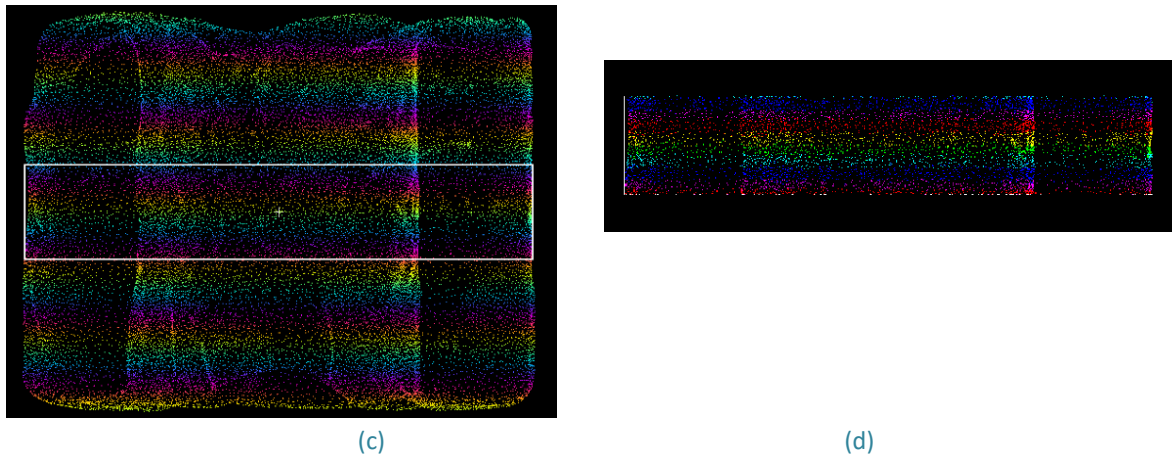


**Figure 48:** Front view (a) with one of  $-n$  strips along  $Z$  axis subsequently, a sub-structured (b) element has been considered.

Afterwards, every sub-structured element can be considered, and with the identification of external and internal edges, through alpha shape function, the final FE model is created.

#### 4.3.4 Automatic approach: Discretization of the three-dimensional space

Also this method focuses on using the geometric data of 3D point clouds, regardless if surveyed by laser scanning or photogrammetric techniques. Since the proposed method aims to be a tool for linking Geomatics with structural field, it starts with a registered point cloud of the element, because it is the most primitive product delivered by the surveyors.

This idea has been carried out with the goal to exploit the initial point cloud, in a new approach of three-dimensional visualization and transformation. In general, as known, the input data is a point cloud with a very non-homogeneous and different data. For this reason, using directly the initial data is difficult because the dataset is very heavy. Inspired from “Minecraft” game, and from different methods existing in literature ( (Ruizhongtai, Hao, & Mo, 2016) (Garcia & Ottersten, 2014); (Alsadik, Gerke, & Vosselman, 2014)), the goal is to transform the input data in elements with the same shape (cubes, for example), starting from initial raw point cloud. Moreover, the three-dimensional transformation will be exploited for different purposes: structural analysis and real-time visualization. Thanks to this kind of procedure, in fact, the transformation of initial dataset may be used also for visualizing point clouds in real-time.

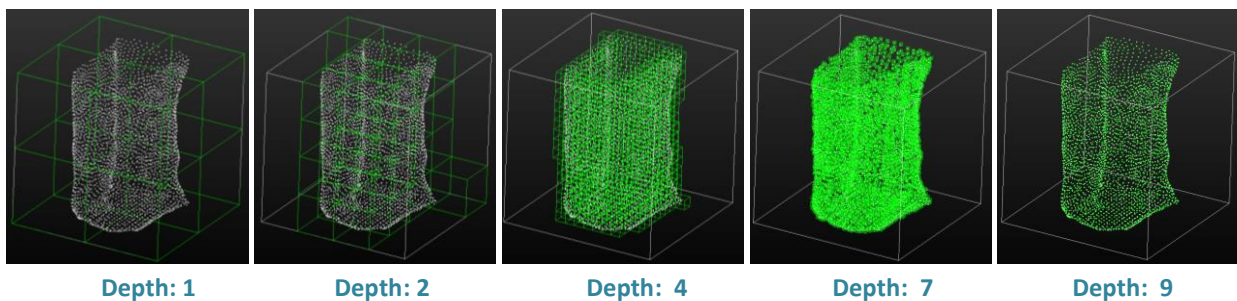


**Figure 49:** The initial raw data is immersed into a 3D grid of space; the basis functions and the width of the grid are modified depending on the object and the boundary conditions. From left to right, the three-dimensional grid is characterized by a discretization of the environment gradually reduced.

Game-engines perform primarily two types of computations: physical simulation and visual rendering. For this reason, two main type of object have been identified: particles and rigid-bodies. In this work, we concentrate only on rigid-bodies, that is the mainly topic of this research. Rigid-bodies are actual 3D objects with mass properties and a specific number of faces (minimum four). Since usually point-clouds representation of buildings comprehends millions of points, the first task will be the definition of the maximum number of particles for both types of objects. The second task will be the definition of an appropriate converter and output structure for the point cloud.

The basic idea is simple: create separate geometric and physical representations of the model in question and combine them when necessary.

The analysis model is constructed on a (typically, but not necessarily) uniform orthogonal grid of space that initially knows nothing about the model being analysed, based on octree approach. An octree corresponds to the recursive partition of a cubical volume of space. From an initial box, octree cells are formed by dividing cubes into 8 equivalent sub-cubes ([Figure 49](#)).

It can be thought, therefore, of as a 3D “graph paper”. The usual (variety of) basis<sup>1</sup> functions are associated with the vertices of this mesh, or point cloud data. The geometric model exists in the same space, in its native unaltered form, and is not aware of the mesh surrounding it. The geometric model can come from any source, as long as it is clear which points in space belong to the model and which do not, and it is possible to compute the distance from any given point to the model’s boundary.

The bottom limits and the top limit for the number of particles has to be defined for the point cloud. The top limit is set by the computational power and the type of visualization desired. In the case of rigid bodies, the maximum number of entities, which can be simulated by a standard computer (Intel i7, 2.9GHz) is around 1’000.

Since the point cloud will be converted into a regular 3D grid, with a discretization of the environment, the required number is dependent on the size of the point cloud dataset. The first step consists into the resizing of the point cloud from the full size to a more suitable size, depending on the final goal, such as Rigid body. To perform resize of the point cloud, a python script has been used. The script parses the point cloud and subdivides the points in a regular 3D grid with the specified block size. The second step is different depending on the desired visualization format. In case of a rigid body visualization, the resized point cloud will be converted in Blender format, suitable for printing or Unity3D visualization, while in case of structural analysis, the process will be managed by a script for the conversion in a file, suitable for structural software.

To perform analysis on a geometric model, such as structural analysis, the boundary conditions have to be specify, such as restraints and loads on the boundary of the native geometric model. The analysis problem will then be solved on the uniform orthogonal mesh, but the usual FEA procedure is modified at run time to account for the existence of the geometric boundaries, restraints, and loads.

This new approach is useful because the workflow is very efficient and it is not dependent on the acquisition of the initial dataset, as we have seen. The advantage of this procedure is that starting from the discretization of the three-dimensional input data, is exploitable directly in structural field. In fact, the resulting discretized geometry with the same shape (for example cubes) and size, contains all the information to use with a finite element method procedure, including the mechanical properties associated with the material features. Then, with a conversion from the three-dimensional model described by cubes, in a file format suitable for a specific software, it will be possible to analyze the model from a structural point of view. Otherwise, this would not be possible because of the initial raw file that is very accurate and as a consequence too heavy for any structural software. The proposed procedure is a very rough and quick solution for complex structures,

---

<sup>1</sup> Basis functions are often called “shape function” in FEA terminology

especially in the field of cultural heritage, and is furthermore designed to be independent of any particular software.

With this approach, there is no pre-processing, and thanks to the automation and the speed, the reach of FEA or simple real-time visualization of data (polygonal mesh, or point cloud) can be extended throughout engineering and beyond, including art, medicine military etc.

#### **4.4 Considerations**

A study through different contributions has been made, in order to analyse and verify how it is possible to transform the initial point cloud dataset, and the importance to automatize as much as possible, in order to obtain a model with a high level of detail and accuracy, by avoiding to loss important data.

In the second part of the chapter, the identified procedures have been explained. In fact, in order to transform the initial point cloud into a Finite Element model, available for structural analysis, different methods have been studied. The distinction has been made, depending on whether the contribution of the operator is or minimal or necessary.

In the first case, two methods have been grouped in the automatic procedures; in the second case, two other procedures have been identified as semi-automatic.

For the semi-automatic procedure, in particular, the HPC method previously explained, has been developed in the Institute of Geodesy and Photogrammetry of ETH, Zurich, with the PhD student Eugenio Serantoni, and the supervision of Prof. A. Wieser. As a study object we chose a large igloo made of compacted snow and covered by non-compacted snow (Serantoni, Selvaggi, & Wieser, 2017). The igloo had deformed – mainly in terms of differential settlements – by more than 1 m at its top over the course of 76 days. Although the code was developed specifically for a very particular object, like an igloo, it can be easily adaptable to other field, like cultural heritage.

The Cloud2FEM procedure, has been carried out through a collaboration between the Structural and Geomatics areas of Department of Civil, Chemical, Environmental and Materials Engineering (DICAM) of University of Bologna (Castellazzi G., D’Altri A. for the Structural area, and Bitelli G., Lambertini A., and Selvaggi I. for the Geomatics area); for more details, see (Castellazzi, D’Altri, Bitelli, Selvaggi, & Lambertini, 2015); (Castellazzi, et al., 2016); (Castellazzi G. , et al., 2016).

All the four proposed methods always guarantee the generation of a filled model ready to use for structural analysis purpose to produce data input for FE modeling.

In order to validate and show the capabilities of the proposed techniques, different case studies are presented and discussed in the next chapters.

## The San Felice sul Panaro Fortress case of study

### 5.1 Introduction

The interest for the study of historical buildings and their analysis through survey and modeling has been developing gradually more, especially since arose the awareness that the heritage could be damaged by earthquakes or by events of other kinds. It is therefore increasingly clear the need to give, on the one hand the study for the safety of these objects, from another side the storage of digital three-dimensional models able to reproduce exactly the objects. Just consider all those sculptures or elements from historical assets destroyed, or otherwise damaged beyond repair, by the earthquake. This is the case, for example, of the Fortress studied in this chapter, hit by the Emilia earthquake, in May 2012. The Fortress has been object of several studies that aim to preserve its integrity; after the earthquake, the Fortress presented lots of cracks, and parts partially collapsed.

In this chapter, techniques related to acquisition using TLS have been analysed and portrayed and some problems, related to the three-dimensional modeling, have to be faced in order to deal with a very complex case study, as a fortress severely damaged by an earthquake, and then composed by non-continuous surfaces.

The study has been concentrated on the transformation of initial dataset, a very dense point cloud dataset. The main difficulties have been the transformation from initial point cloud into the polygonal model, in order to apply the Cloud2FEM procedure. From this, the final complete voxel model has been obtained. Once analysed the entire Fortress, the most characteristic elements of the building have been studied as single element: The Mastio Tower and the North tower.

The work, with the original development of the Cloud2FEM procedure, has been carried out through a collaboration between the Structural and Geomatics areas of Department of Civil, Chemical, Environmental and Materials Engineering (DICAM) of University of Bologna.

### 5.2 Historical description

The San Felice sul Panaro Fortress is a monumental historical building located near the city of Modena, in San Felice sul Panaro (Italy).



*Figure 50: Emilia-Romagna area (red) and position of San Felice sul Panaro (MO)*



*Figure 51: San Felice sul Panaro with position of the Fortress*

The first information about a fortification in San Felice dates back to a document in 927, which the “Castellum Sancti Felicis” is cited. This “Castellum”, actually was probably without walls, but simply made by an embankment. In XIV century, the Fortress was realized, at the request of marquis Orbizzo, on the South-West perimeter: the definition of “Fortress” was used for defining the principal tower (Mastio) and the four perimetral towers, instead of “castle”, which is used for the ensemble of Fortress, church, perimetral walls and bridge. The Fortress is the most important building of San Felice sul Panaro, characterized by a typical quadrilateral plan, with corner towers, of which the principal tower (Mastio) is in the Southeast corner.

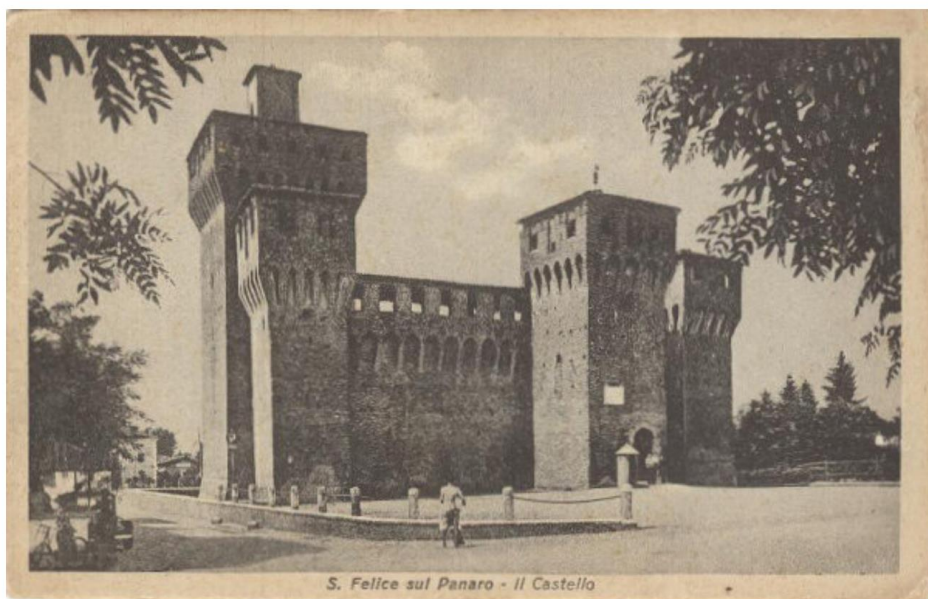


*Figure 52: Historical image of San Felice sul Panaro Fortress*

Following, the phases of construction are shown, useful to understand the historical layers, seismic analysis etc...

- Phase 1 (XIV century): in 1340 there was the construction of the first element of the Fortress, the main tower placed in southeast. The Mastio tower is, in fact, previous to the adjacent elements. Probably, in this epoch there is also the construction of the central North tower;
- Phase 2 (mid XIV century): in this epoch the smaller towers and perimetral wall to connection between the towers were realized;
- Phase 3 (beginning of XV century): the towers were completed, with the higher part;
- Phase 4 (end of XV century): elevation of the basement near the wall located in the West zone;
- Phase 5 (XVI-XVII century): the connection walls between the towers were built and a window in the Mastio tower was created;
- Phase 6 (XVII-XVIII century): the roofs of the towers were completed;
- Phase 7 (XVIII-XIX century): an element, located in North East was built, in the courtyard; the stairs were created in the courtyard and in the South. The South element was elevated.
- Phase 8 (beginning of XX century): the elevation of West element was done, up to the height where it currently appears.

### 5.3 Seismic vulnerability of the Fortress

In 2012, the Fortress was hit by the Emilia earthquake with two magnitude peaks on 20 May (MW = 5.86) and on 29 May (MW = 5.66) (Scognamiglio, et al., 2012), and it is object of several studies that aim to preserve its integrity. After the earthquake, the Fortress presented lots of cracks, and parts partially collapsed, but it was the only Fortress in the earthquake area not completely collapsed after the event. The roofs of the Fortress, after the earthquake, are partially collapsed (Figure 53). The Mastio, as the North tower, was damaged in the external and internal part.



*Figure 53: In these images, we can see an overview of the area before and after the Emilia earthquake. It is possible to see that the roofs of the fortress, in the centre of the image, as some roof of the adjacent building, are collapsed, and now covered with large plastic sheets to avoid water infiltrations.*



*Figure 54: View of the North East front before the earthquake (a), after the earthquake (b) and currently (c)*



*Figure 55: View of the North front before the earthquake (a), after the earthquake (b) and currently (c)*

Irregular plans and elevations of the Fortress, denote a high seismic vulnerability. The towers are connected, as previously seen, by perimetral walls without continuity, and this causes bending and torsional effects. Furthermore, the different height between the perimetral walls and the towers, determines a different dynamic response of the structures. The connections between the walls and the towers (which can result in more or less effective reality constructively) determines a seismic behavior different from that isolated. The characteristics of seismic impulse at the surface, with significant components to low frequencies, are penalized by a low own frequency, as in this case the towers. The seismic behavior of the Fortress derives from its geometry and also from the type and quality of its materials. The entire Fortress is built of masonry and mortar, with a minimum thickness of 30 centimetres, to a maximum of 250 centimetres, in the basement of Mastio tower. Being masonry, the thickness of the walls decreases from the bottom to the top. The horizontal elements are characterized by vaults and, in the roofs, by wood with principal and secondary frame.

## 5.4 Measurements

After the earthquake, as the first intervention the municipality of San Felice did a fine survey of the damaged building by using geomatic techniques, mainly laser scanning and photogrammetry, obtaining different products, like point clouds, orthophotos and immersive visualization. A morphological and structural survey for the San Felice sul Panaro Fortress was planned by request of the Municipality in order to generate a functional representation of the actual state of the building. The survey was performed by ABACUS s.a.s., using a FARO Focus 3D x 330 laser scanner and a total station Trimble S6. The building has a complex structure due to its construction, which took place in several stages over several centuries, forming an irregular geometry. The analysis has become more complex after the earthquake, because of the presence of debris in some interior rooms. Numerous targets were then placed, for precise identification of correlation points

between scans, for both the exterior and the interior of the fortress. A closed polygonal topographic network was prepared, to detect the position of each target using the total station. This network has been properly calculated and compensated. Subsequently, 163 point clouds have been acquired by different scanning positions using the laser scanner. These scans are aligned to the topographic network through correlation with the reference targets, resulting in millimetric precision. Following the first decimation, the aforementioned clouds were merged into a unique cloud containing more than 40 million points (Figure 56). The input data is a comprehensive three-dimensional point cloud for the whole building, both from the exterior and interior spaces. Each point of the cloud is conveniently referred to a reference system with X, Y, Z coordinates.

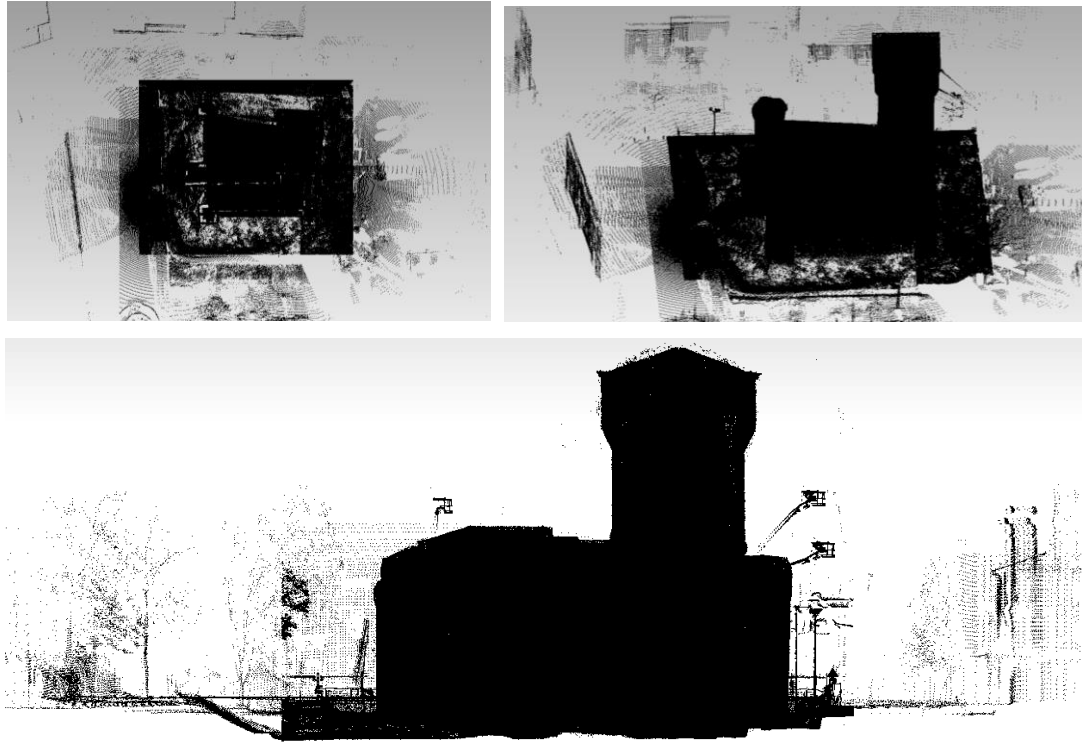


*Figure 56: Initial point cloud with more than 40 million of point*

In order to simplify this initial point cloud and to produce a new point cloud with a more regular density, a particular algorithm (Corsini, Cignoni, & Scopigno, 2012); (Ebeida, Mitchell, & Patney A., 2013)) was used to populate a new dataset with a point sampling generated according to a Poisson-disk distribution (Bridson, 2007) (Figure 57) using the open source mesh processing system MeshLab (Cignoni, et al., 2008)). Starting from the original that typically presents strong variations of density (related to the acquisition distance between the sensor and detected surface, the result is a new point cloud reduced to 3.2 million points, with a regular spatial sampling of 0.050 m, suitable for further analysis. The next operation was to clean the point cloud (three-dimensional point cleaning in Figure 57), mainly removing all neighbor points not belonging to the building of interest. In fact, other surrounding buildings were acquired during the initial scan, in order to align all of the different point clouds. These buildings can be removed from the point cloud, reducing it further down to 2.7 million points. This algorithm has been applied for all the dataset, both in the outer part than the inner part, in the same way (Figure 57).

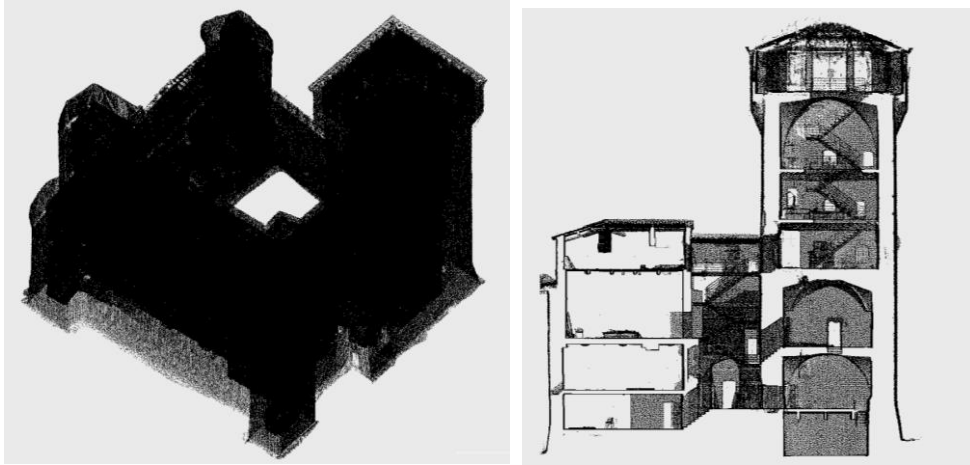


Figure 57: Isometric view (left) of point cloud with regular spacing (3.2 million points); section of point cloud (right)

## 5.5 Fortress: numerical model and structural analysis

Once obtained the dataset with a regular spacing, the point cloud was then transformed in a polygonal model using triangular irregular network (TIN). Considering the points  $(x; y; z)$  in space, the conjunction between them is realized with lines forming adjacent triangles in order to represent the object with a continuous surface. The mesh consists of a total of 4.8 million triangles. This model describes all of the surfaces surveyed with the laser scanner, but it cannot be considered a correct closed model from the topological point of view; consider, for instance, the roof surfaces in [Figure 58](#) (green). Regarding the interior part of the model, we must account for the fact that, at the moment of the laser scanner acquisition, there were furniture in different rooms, as well as rubble and debris in some areas. Every disturbing element increases the complexity of the building. The special conditions of the building must be considered. Regarding the exterior part of the model, there were problems with the roofs that were partially collapsed, and these were covered with large plastic tarpaulins in order to avoid water infiltration. Furthermore, in the surroundings and in the internal courtyard of the building, there was piles of rubble and debris. All of these elements hide the actual geometry of the building from the laser scanner point of view. In fact, in the three-dimensional point cloud, these elements are acquired and then intrinsically fused with the proper model of the building, and there is no automatic procedure to perform a full cleaning in advance ([Figure 57](#)).

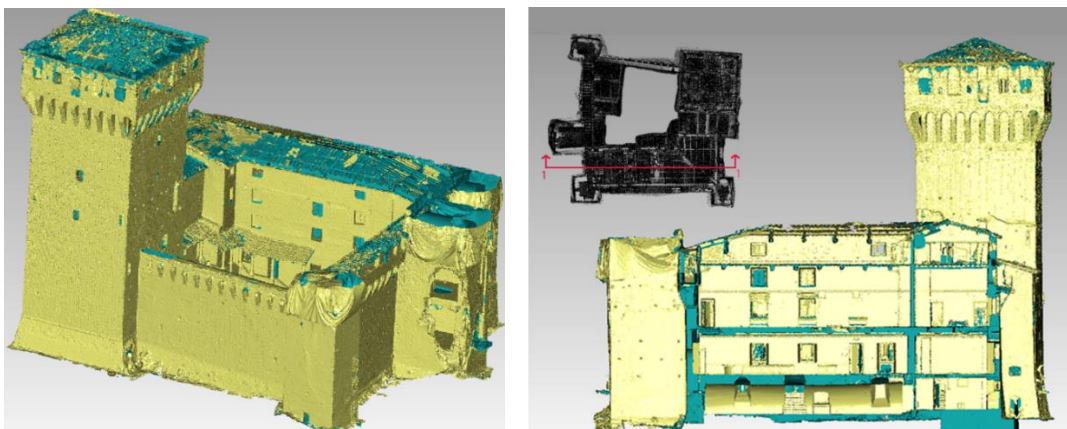


Figure 58: Isometric view (left) and sectional view (right) of polygonal model. The green part is the not continuous surfaces (missing parts, cut elements etc...), as opposed to the yellow part.

The polygonal model of the complex building, is composed by 5 million of triangles.

One of the main problems in this phase is the presence of holes in the mesh, due to data missing in the point cloud for occlusions in the line of sight between the sensor and the surface to acquire; this problem is furthermore present for buildings damaged after disasters or in a serious state of decay. At this stage we do not care to obtain a perfectly closed and topologically correct mesh, since it would require a great amount of manual intervention in a three-dimensional environment by a qualified operator in relation to the complexity of the structure. Nevertheless, these holes do not allow to properly define, for a whole complex building, an accurate filled model using automatic procedures. The operator intervenes at this stage resolving eventual problems found during the mesh construction phase. Then an automatic decimation procedure is performed in order to reduce the complexity of the mesh, though ensuring the correct representation the specificities of the geometry of the structure.

### 5.5.1 Cloud2FEM procedure

The resulting TIN model fully describes the surface enveloping the Fortress inside and outside. After having obtained the shell of the structure, it is possible to define the volume of the structure to be filled (**Figure 59**). In order to create a volume model, an overlap between polygonal model and slices with a constant step of 25 centimetres has been done. Afterwards, by inspecting every single slice in GIS software (in this case, QGIS has been used), it is possible to find and properly clean every slice from points that do not belong to the building, but have been inevitably acquired during the scanning. Using this procedure, by creating a concave hull that envelops the internal points from the outside, the presence of internal debris or any furniture located inside the room is irrelevant, because each new shape is based on the peripheral points. This operation is fundamental to obtain a closed shape for each slice, directly using the geometry provided from the previous step, without any smoothing. This part of the procedure is semi-automatic. Some manual intervention is essential at this stage for an accurate separation between internal points and external points: this is especially true with data from complex buildings, such as the one analysed.

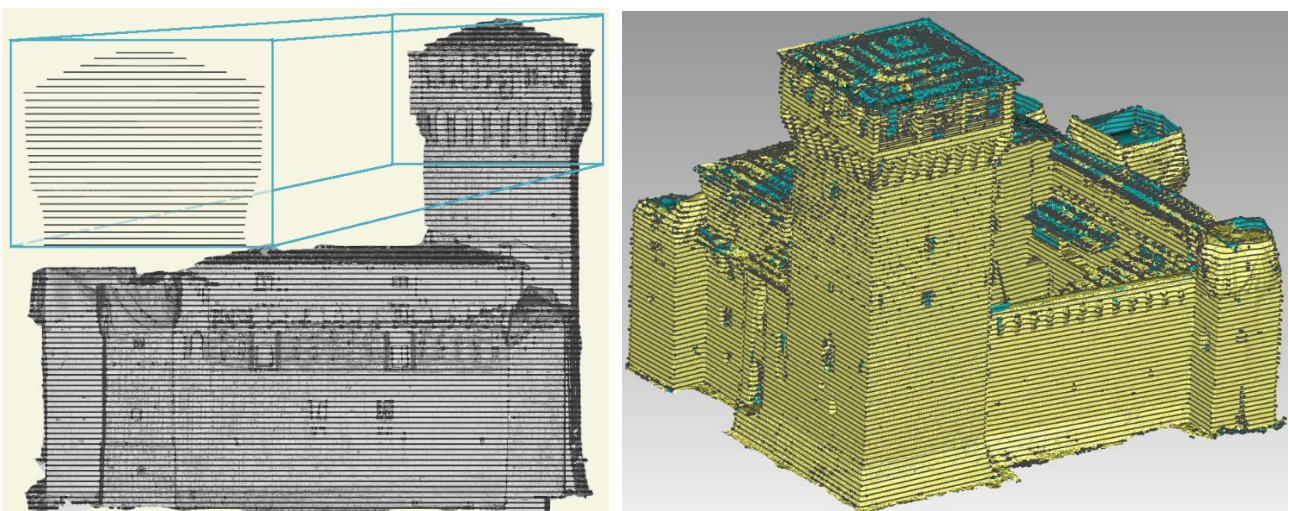


*Figure 59: Isometric and front view of the Fortress with the overlap of the slices*

The proposed workflow aims to minimize manual intervention in terms of time in order to maximize the efficiency of the procedure itself. Based on the Fortress geometry properties, a fine description of the

Fortress can be done by slicing the complex building height with a  $\Delta z = 250$  millimetres, and 121 digital slices have been stacked. In this way, there is almost always the intersection with the horizontal floors (characterized by vaults or wooden beams). The resolution of each slice is set to have a bi-dimensional resolution in the horizontal plane of  $\Delta z=250$  millimetres. The dimension of each pixel was set as 250 x 250 millimetres: in this way the third dimension is the distance between each slice, and the final result will be cubic voxels.

In **Figure 60** some examples of digitalized slices of the fortress is shown, with a sketch of their stacking sequence. The output of this process, that represents the input for voxel model, will be, then, a set of 121 slices, in which the 255 is for the filled area and 0 for empty spaces.

The resulting mesh is characterized by 409,900 hexaedral (**Figure 61**) finite elements (each one 250x250x250 millimetres) and 1.512.444 degree of freedoms (dofs). Thanks to the material properties survey, the structure has been entirely described by using five different material properties, the mechanical properties of which are set according to (NTC, 2008) and (Koponen, Toratti, & Kanerva, 1991), shown in the following **Table 6**.

Material	Elastic Modulus (MPa)	Poisson's Coefficient	Density (kg/m <sup>3</sup> )
Masonry	1500	0.20	1800
Reinforced masonry	1900	0.20	1800
Terrain	-	-	-
Timber	8000	0.37	415
Air	-	-	-

*Table 6: Materials mechanical properties*

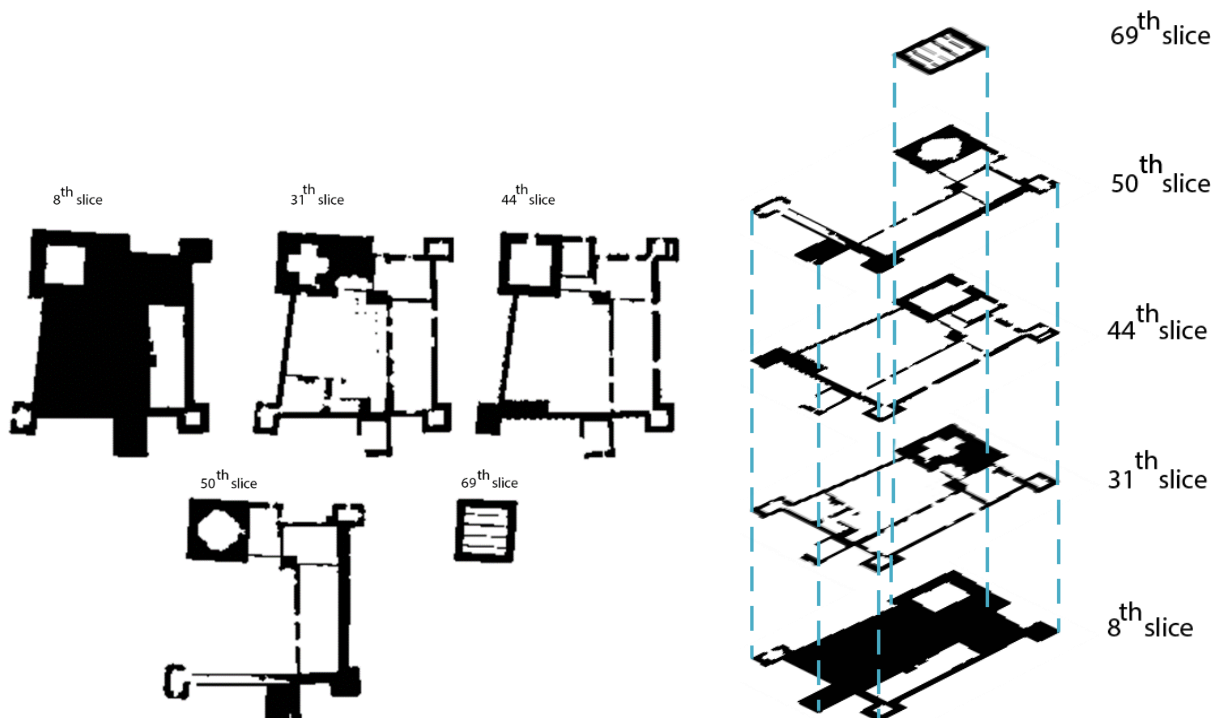


*Figure 60: Exemple of digitalized slices of the Fortress (left), and their stacking (right)*

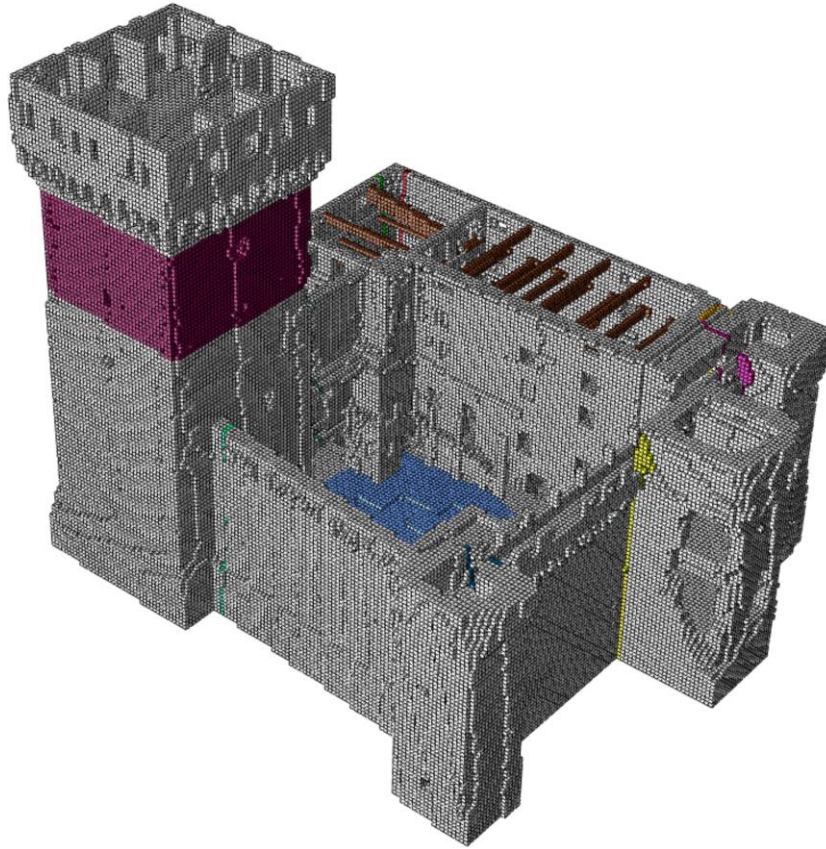
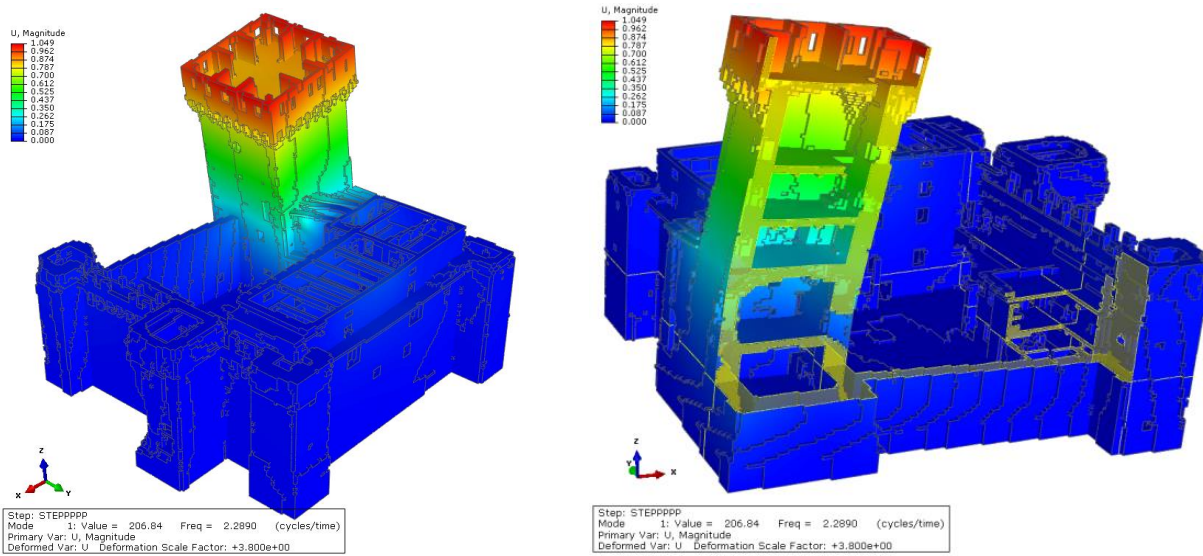
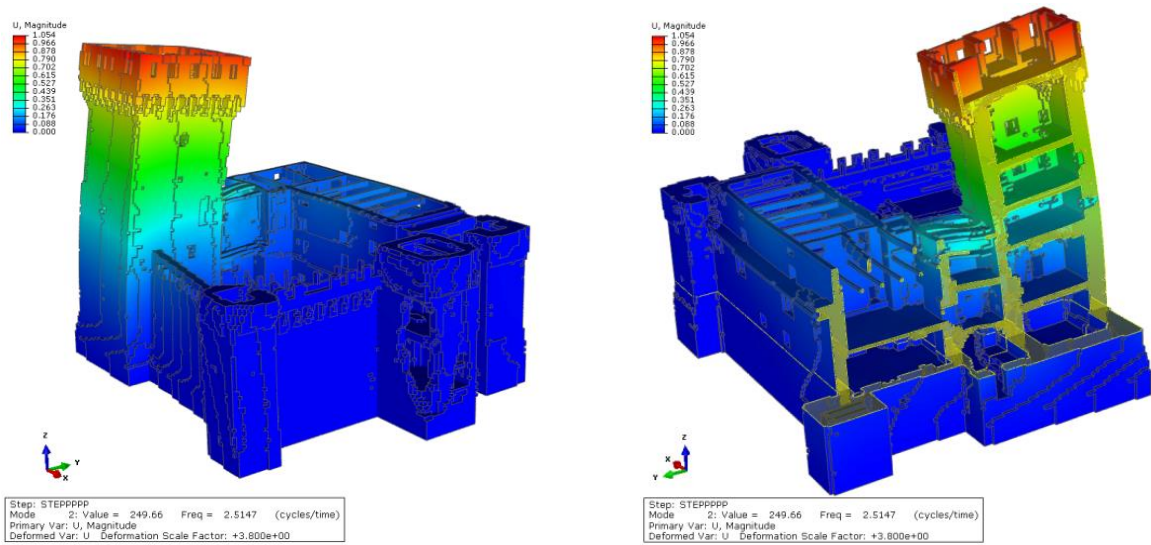


Figure 61: San Felice sul Panaro Fortress FE mesh. The colors are different for each material.

Through the voxel three-dimensional model, it is possible to analyse the structure with static or dynamic analysis. The following figures show the modal shape.



(a)



(b)

Figure 62: modal shape of mode 1 (a) and 2 (b)

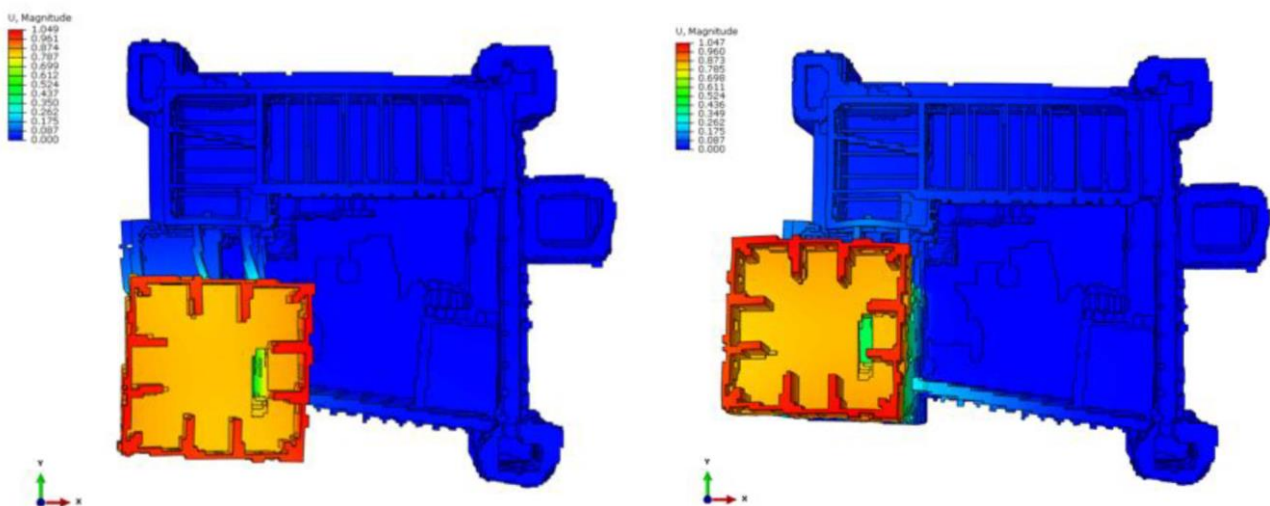


Figure 63: In the Mode 1 (left) the Mastio is along the Y axis; in the Mode 2 (right) the Mastio is along X axis.

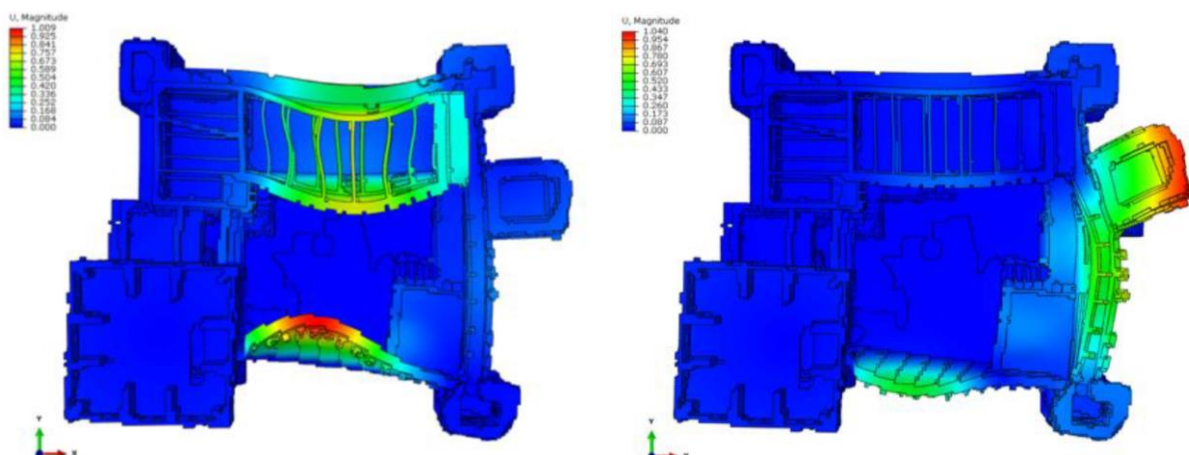
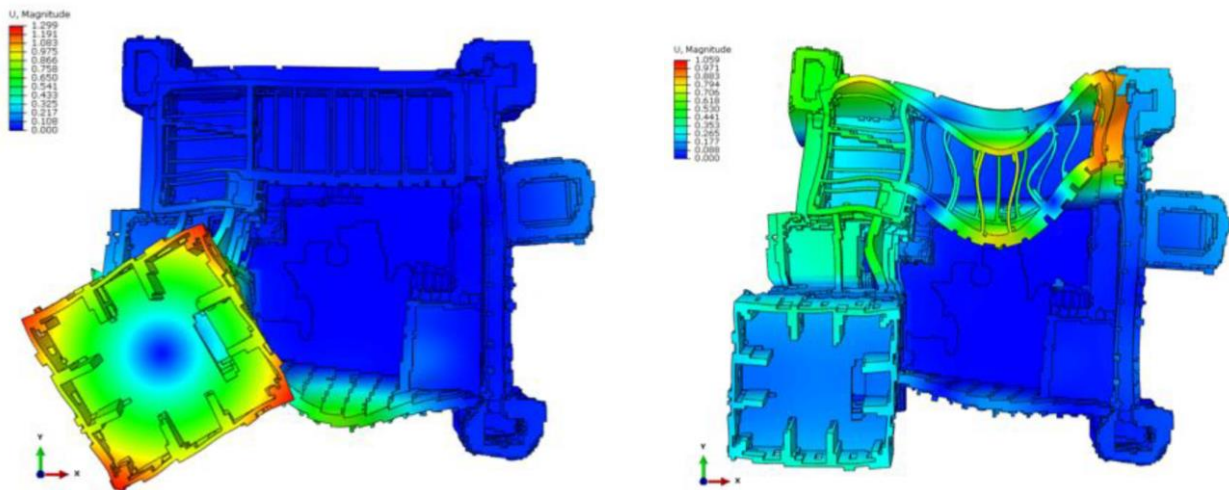
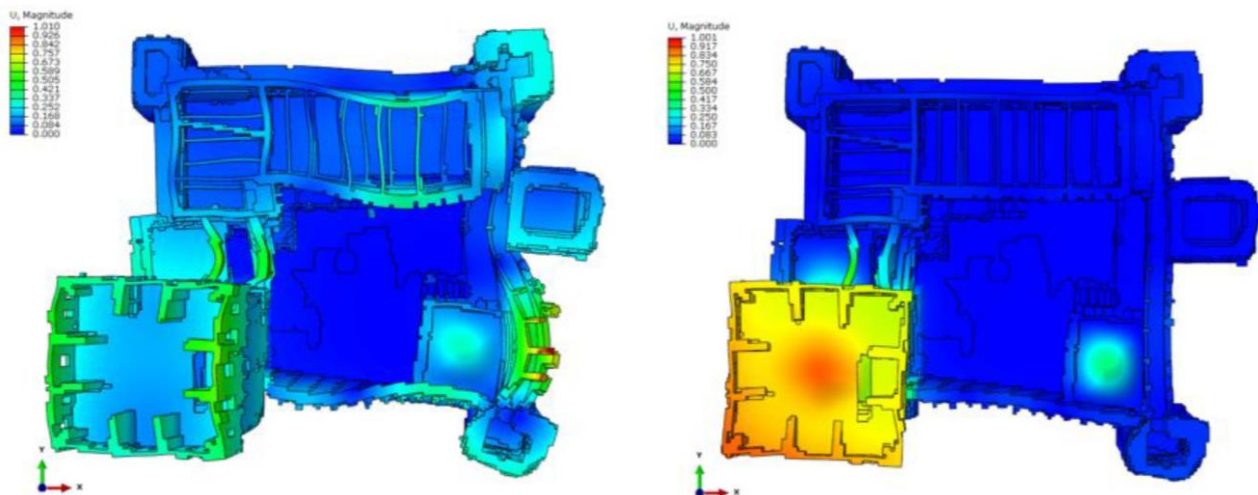


Figure 64: In the Mode 3, there is the vibration of perimeteral East wall and the building leaned with perimeteral West wall (left); in the Mode 4 (right), there is the maximum stress with the North tower and perimeteral North wall.



*Figure 65: In the Mode 5 (left), a torsional stress of the Mastio is resulted; in the Mode 6 (right), the maximum stress concerns Mastio tower and the building leaned perimetral West wall.*



*Figure 66: In the Mode 7 (left) all perimetral towers of the fortress are stressed; in the Mode 8 (right), the most stressed part of the Fortress is the Mastio.*

Considering the results of dynamic analysis, and according to the vibration modes for the entire Fortress, the Mastio tower is the most stressed part. For this reason, it was studied also as an isolated element, and in more detail.

## 5.6 Mastio tower

The Mastio tower has an overall height of about 32 meters, with wooden roof and variable wall thickness, that is thinner in the highest part. As shown in [Figure 67](#) the tower is composed of six layers of different kinds: cross-vaults, wood slabs with old and remodeled structures. Each level is then characterized by irregular dimensions and thickness. By inspecting the south front illustrated in [Figure 67a](#), it is shown how the seismic shock hit and damaged the tower by producing a lateral and torsional oscillation and residual

displacements on the actual configuration. Openings are placed irregularly on the structure and also have irregular shapes and sections (Figure 67c,d) Summing up, the structure is not regular.



Figure 67: San Felice sul Panaro Fortress principal tower. From left: South front; East front; E-W section; S-N section.

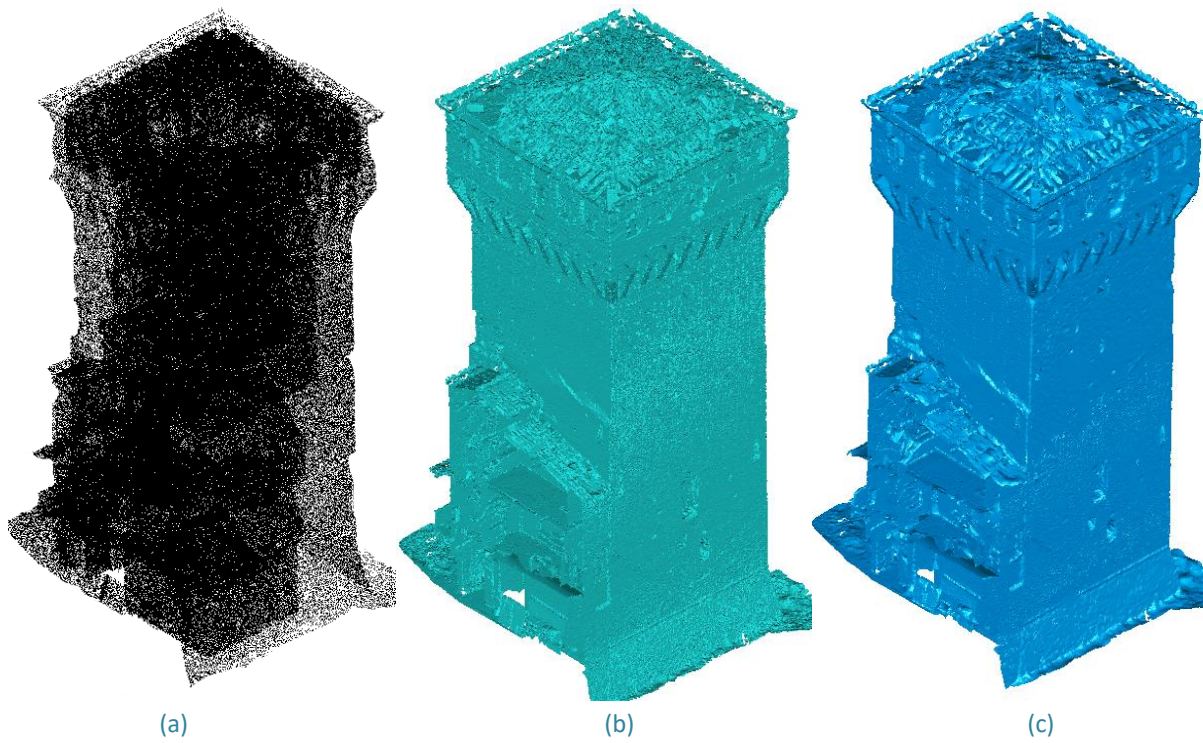
### 5.6.1 Cloud2FEM procedure

From the point cloud of the Fortress, a subset of 0.8 million points related to the Mastio has been extracted and analyzed; see Figure 68a. As represented in Figure 68b, the survey finely describes every single feature of the structure. The point cloud has a very heterogeneous density, primarily related to the distance between the single scan positions and the object acquired. The first polygonal model consists of about 1.670 million triangles (Figure 68b). After decimation and cleaning, the TIN model consists of about 1.120 millions of triangles (Figure 68c).

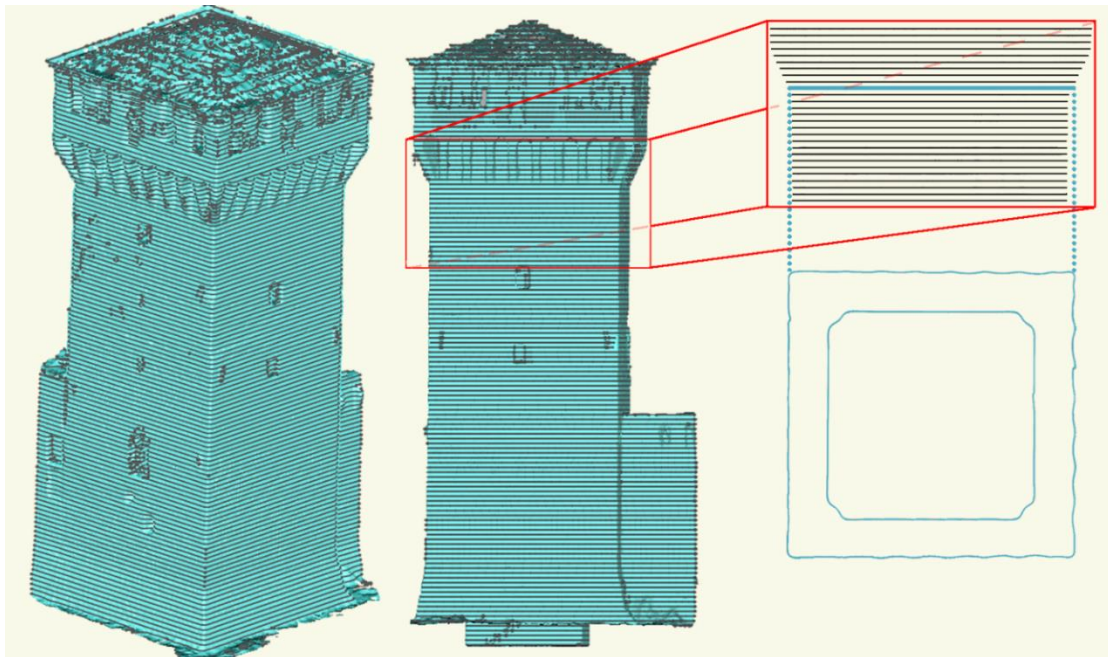
Regarding the interior part of the model, there are furniture in different rooms, as well as rubble and debris in some areas. Every disturbing element increases the complexity of the building, as illustrated in Figure 70. By inspecting every single slice in GIS software (in this case, QGIS has been used), it is possible to check every element from points that do not belong to the building, but have been inevitably acquired during the scanning. Using this procedure, by creating a concave hull that envelopes the internal points from the outside, the presence of internal debris or any furniture located inside the room is irrelevant, because each new shape is based on the peripheral points. This operation is fundamental to obtain a closed shape for each slice, directly using the geometry provided from the previous step, without any smoothing.

Figure 70a represents the points that are located within the range  $[z_j - \Delta z/2; z_j + \Delta z/2]$ , at a given  $z_j$  coordinate. In Figure 70a, the lower left corner is magnified to show the original point cloud density. Based on the Mastio geometry properties, we consider that a fine description of the tower can be done by slicing the tower height with a  $\Delta z = 0,200$  m, which corresponds, more or less, to three layers of bricks and two layers of mortar. On the other hand, the resolution of each slice is set to have  $\Delta x = \Delta y = 0,115$  m, which corresponds to the short dimension of the brick (half-brick). The resulting stacking sequence is composed of 153 horizontal slices (Figure 69Figure 57). The slices are located with a regular step for all the tower.

Each slice is represented by a  $N \times M$  grid of  $116 \times 107$  pixels. **Figure 69**, **Figure 70** and **Figure 71** illustrate the procedure starting from the polygonal model, and the i-slice representative of a generic section.



**Figure 68:** Three-dimensional models of Mastio Tower. Point cloud dataset (a); initial polygonal model (b); final TIN model (c)



**Figure 69:** The two-dimensional slices are overlapped to the three-dimensional polygonal model, for all the height of the tower. In detail, a two-dimensional slice is shown (right)

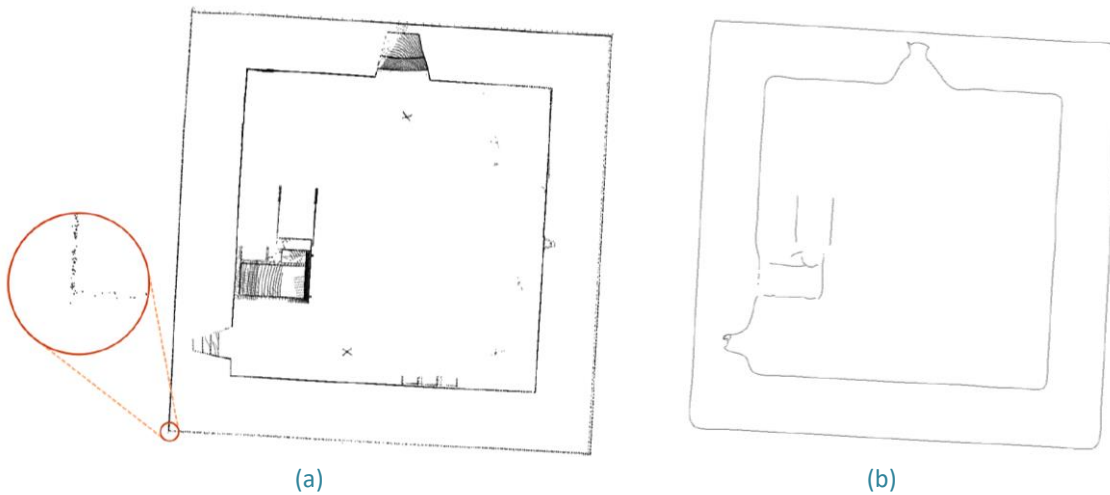


**Figure 70:** First part of the slicing workflow (3D data): the magnified portion shows the uneven density of the raw data. (a) Points within the  $_z$  increment; (b) final processed slice of points.

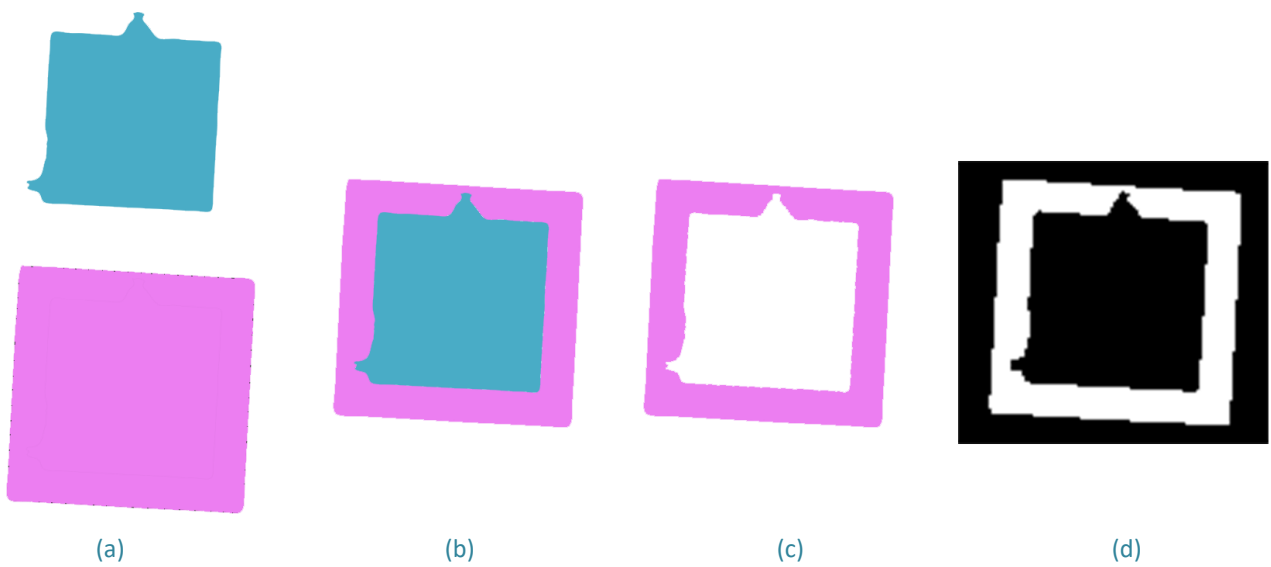


**Figure 71:** Second part of the slicing workflow (2D data). (a) External slice (pink) and internal slice (green); (b) overlap between external slice and internal slice; (c) difference between external slice and internal slice (filled slice); (d) bitmap: 116 x 107 pixels.

Thanks to the material properties survey, the structure has been entirely described by using five different material properties, the mechanical properties [Table 7](#).

**Figure 71** describes the generic section representation where the user can visualize and set the material properties based on his knowledge, which might have been acquired from direct inspection or available images. The resulting three-dimensional matrix is visualized by plotting its pattern by means of RGB colors in [Figure 73](#).

MATERIAL	Color (0-255)	Elastic Modulus (MPa)	Poisson's Coefficient (-)	Density (kg/m <sup>3</sup> )
Masonry	255	1500	0.20	1800
Reinforced Masonry	150	1900	0.20	1800
Terrain	125	--	--	--
Timber	100	8000	0.37	415
Air	0	--	--	--

Table 8: Mechanical characterization of the materials by colour

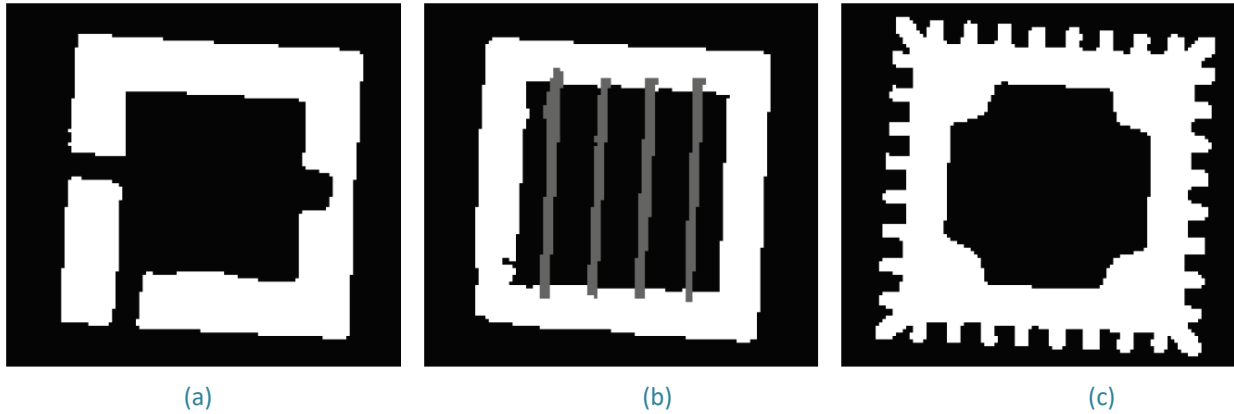


Figure 72: Example of bitmap slice. a) 42<sup>th</sup> slice; 84<sup>th</sup> slice; 128<sup>th</sup> slice.

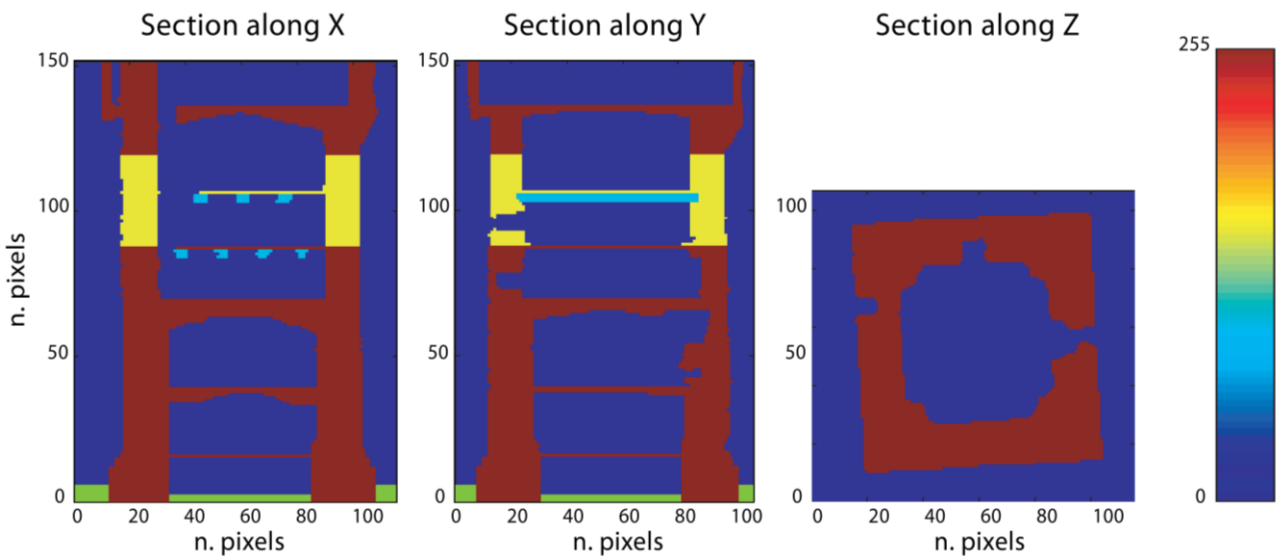
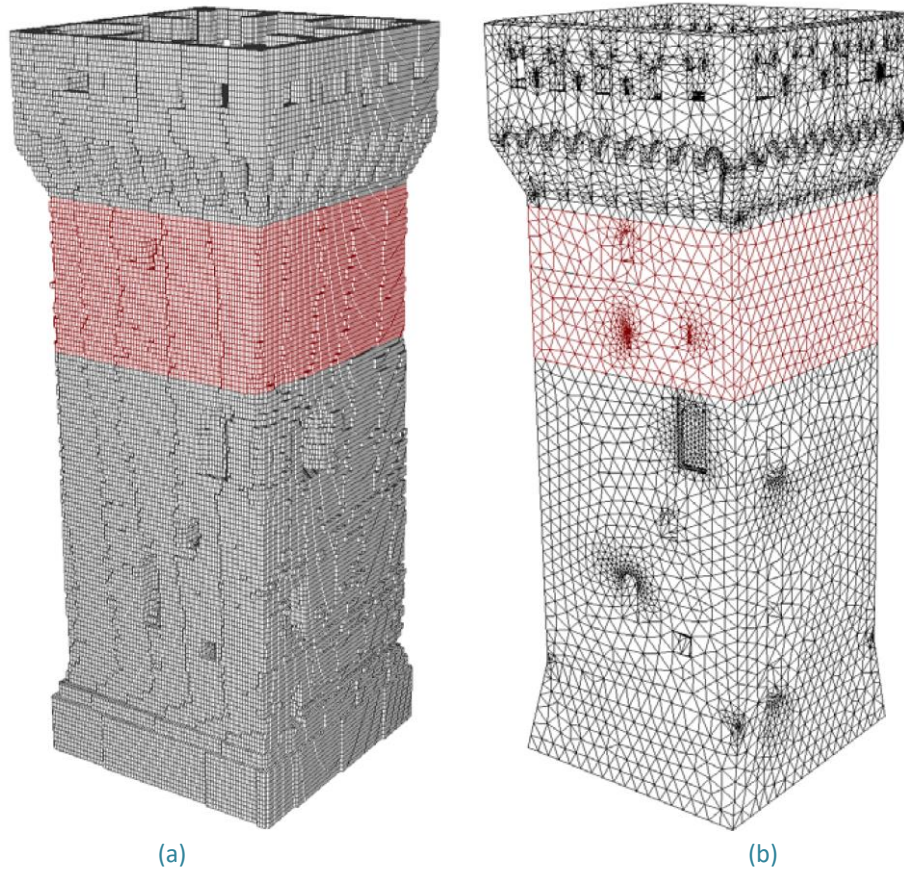


Figure 73: Visualization of the three-dimensional material matrix: voxels possess unitary dimension. Five materials (colors) are used to represent the structure, according to mechanical characterization of given in Table 1.

Voxels are plotted by transforming row and column indexes to a unitary coordinate. Then, the generation of the eight-node hexahedral FE model is done by associating their coordinates respectively to the  $\Delta x$ ,  $\Delta y$ ,  $\Delta z$  volume. It is important to notice that the three-dimensional matrix contains volumes for any arbitrary index (i; j; k) combination, i.e., values are also assigned to empty spaces (surrounding air, terrain, etc.). The user

can choose, according to the FE model purposes, to filter out some of the values. For instance, here, the voxels corresponding to the air and terrain properties are excluded by not being processed during the mesh generation procedure. The final mesh is then characterized by 745,668 nodes and 661,105 elements (Figure 74a).



**Figure 74:** Finite element discretization comparison; colors are set according to the material properties: gray and red colors are used to illustrate the masonry and the reinforced masonry elements, respectively. (a) CLOUD2FEM discretization; (b) CAD-based discretization.

The finite element model obtained by using the proposed procedure is tested within a structural analysis. A comparison is performed using a very accurate finite element model obtained through a precise CAD procedure based on the same laser scanner dataset; see Figure 74. The reference model (Orlando, 2014.) is obtained by means of tetrahedral four-node elements to model the masonry walls and four-node shell elements to model vaults and layers, counting 54,340 nodes and 215,938 elements.

In order to assess the accuracy of the proposed model, a linear natural frequency analysis (eigenvalue analysis) is performed. Clamped boundary conditions have been considered for nodes located at the ground level ( $Z = 0$ ).

The linear natural frequency analysis is a common tool for the characterization of structures' dynamic behavior and also used for historical masonry structures ( (Pieraccini M. , et al., 2014); (Roca, Cervera, Gariup, & Pela', 2010); (Casolo & Sanjust, 2009). The natural frequencies and the natural mode shapes of vibration, which are the characteristics of the structure, are given by the solution of the following eigenvalue problem:

$$K\Phi = \lambda M\Phi$$

where  $M$  is the mass matrix,  $K$  is the stiffness matrix,  $\lambda$  is an eigenvalue and  $\Phi$  is its relative natural mode shape of vibration (eigenvector). The eigenvalue problem does not fix the absolute amplitude of the vector  $\Phi$ , but only its shape.

It is evident that both  $M$  and  $K$  are highly conditioned by the correct representation of the geometry and by the accurate mass and stiffness distribution along the structure. **Table 9** summarizes the computed mass and the overall dimensions for both models. By inspecting **Table 9**, it is clear that the application of the proposed technique produces a finite element model that accurately describes the building geometry and its mass distribution.

MODEL	Mass (tons)	Max Dimensions [L x B x H] (m)	$h_g$ (m)
CAD	3055.78	9.97 x 9.97 x 30.64	13.67
Voxel	3032.11	9.90 x 9.79 x 30.60	14.07

**Table 9:** Mass. Overall dimensions and center of mass height

**Table 10** collects the obtained results in terms of computed frequencies and computed errors. It appears that, for the first six modes, the computed error is always less than 4%, and it is less than 0.1% for the fundamental modes (Mode 1 and Mode 2). The discussion is limited to the first six modes according to the structural meaning associated with the frequency and the corresponding mode shape (Chopra, 1995). The tower dynamically acts as a cantilever beam whose fine description can be summarized by two bending modes in each horizontal direction plus a torsional mode and an axial mode. **Figure 75** illustrates Mode Shape 1, where colors are associated with the magnitude of the computed amplitude (normalized). Mode shapes are in very good agreement as concerns the overall behavior, and they slightly diverge as concerns the local displacement distribution of the top part: in the CAD-based model, some simplistic assumptions have been introduced on this specific part, due to the high complexity of the geometry. Some parts of the structure have been considered adding the corresponding mass values to the model. In this regard, the  $z$  coordinate of the center of mass has been computed for each model in order to check the overall mass distribution; see **Table 10**.

Mode No	Voxel Frequency (Hz)	CAD Frequency (Hz)	Error (%)	Mode Description
1	1.9131	1.9137	0.031 %	1 <sup>st</sup> bending mode (E-W)
2	1.9276	1.9289	0.067 %	1 <sup>st</sup> bending mode (N-S)
3	4.5437	4.4253	2.675 %	Torsional mode
4	7.0804	7.3518	3.692 %	2 <sup>nd</sup> bending mode (E-W)
5	7.1654	7.3665	2.730 %	2 <sup>nd</sup> bending mode (N-S)
6	8.1623	8.0055	1.959 %	Axial mode

**Table 10:** Natural frequencies analysis: frequencies of the main mode shapes of the Mastio tower of the San Felice sul Panaro Fortress. Comparison between the voxel-based model and the CAD-based model.

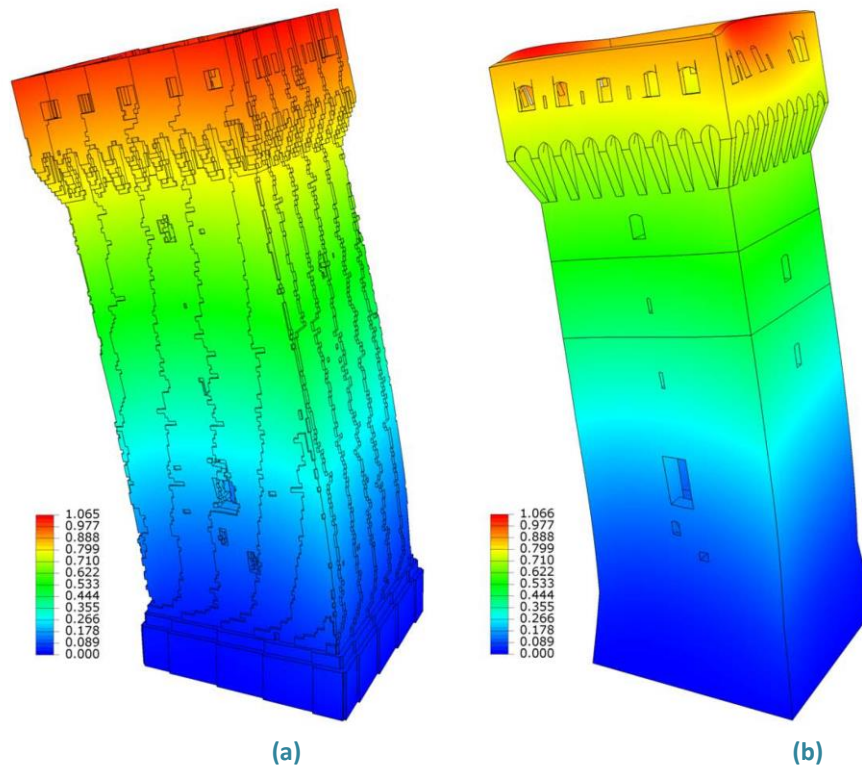


**Figure 75:** Mode 1: bending mode shape. Displacement magnitude.  
 (a) Voxel frequency = 1.9131 Hz; (b) CAD Frequency = 1.9137

On the other hand, the voxel-based model captures every single detail of the geometry precisely, thanks to this semi-automatic procedure, avoiding the user interpretation or the necessity to defeature the complexity of the model. This fine description obviously introduces a higher number of degrees of freedom (dof): the voxel model counts 2,237,004 dofs, whereas the CAD-based model enumerates 163,020 dofs. Despite the larger number of dof, the proposed procedure allows one to transform the user time into computational time. Moreover, a more effective FE model prone to optimizing the computational cost, preserving the accuracy, might be obtained by coarsening the resolution of the voxels. The voxel discretization introduces a simplified description of the geometry and leads to a finer finite element model able to precisely capture the geometry features and the corresponding mass properties. The mechanical properties are defined by a punctual characterization, which leads to a very accurate description of the structure, since each voxel can be, generally, automatically associated with a particular property definition, whereas for the CAD-based model each material or property needs a partition of the whole solid model. Further enhancements of the capability to simulate the structural behavior (i.e., introduction of special elements or interface elements) can be easily done manually or automatically through simple selections of elements or nodes, due to the rational database organization, whereas for the CAD-based model, any enhancement of the structural model has to be preliminarily designed along with the geometry.

Furthermore, **Figure 76** illustrates the detail of the vault of the 6th level, which is in particular a groined vault (**Figure 76a**). As can be noted, when the surface is irregular (curved) (e.g. for vaults) the resulting FE mesh is a jagged representation of the original geometry (**Figure 76b**). Despite this fact, it is always possible to improve the mesh accuracy using a smoothing method to reduce the faceting, see **Figure 76 c** and **Figure 76d**. These methods decrease high curvatures variations (jag) and have to be chosen in order to not produce shrinkage, see for instance (Taubin, 1995). Despite the geometrical improvement, the mesh enhancements are limited by the performance of the parametric finite elements. Nevertheless, if we aim to assess the global behavior of a historical structure, the geometrical accuracy of the raw mesh can be considered satisfactory

even if vaults are present. Furthermore, the recovered fields can be improved by standard recovery procedure ( (Castellazzi, et al., 2016), (Castellazzi, D’Altri, Bitelli, Selvaggi, & Lambertini, 2015)).

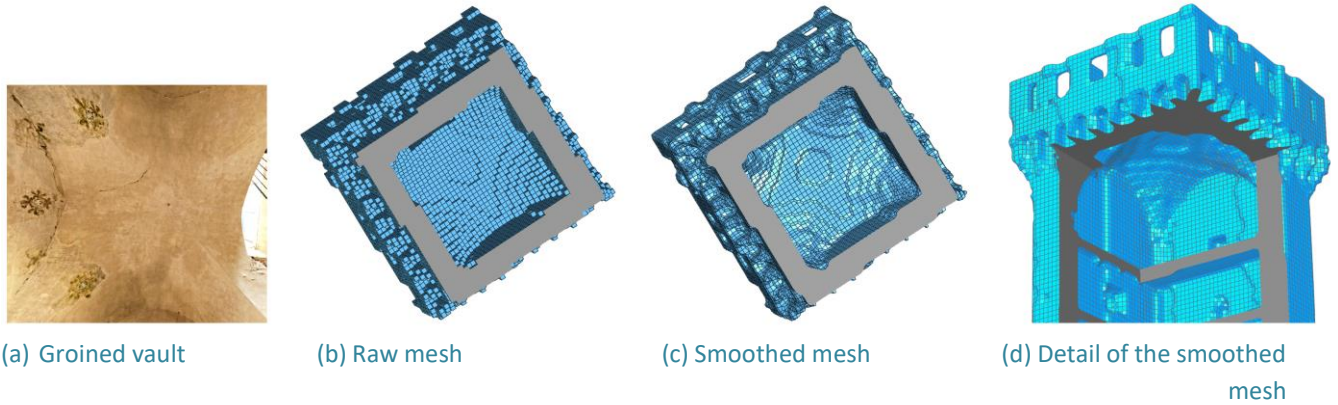


*Figure 76: Detail of the groined vault of the 6<sup>th</sup> level.*

## 5.7 North tower

A further analysis has been carried out for the North Tower, which was damaged in a greater part of its external walls **Figure 77** as well as the roof almost completely collapsed. The North tower is composed of three floors, with inter-floors characterized by vaults (**Figure 78**).

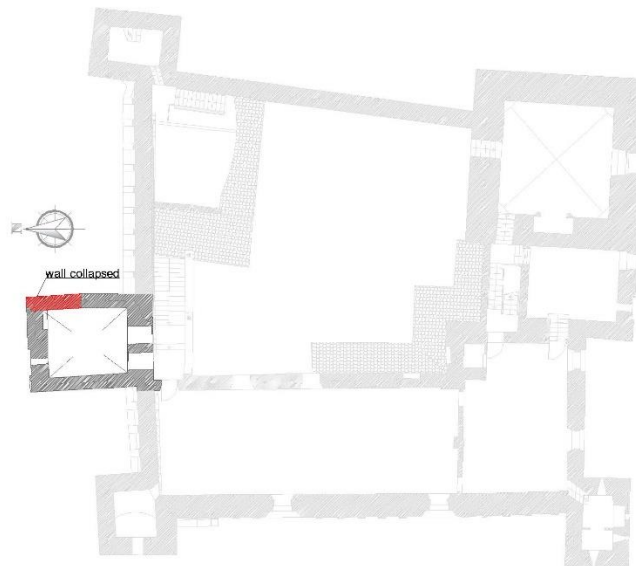


*Figure 77: Floorplan of the San Felice sul Panaro Fortress: North Tower highlighted*



*Figure 78: Seismic damages to the North Tower of the San Felice sul Panaro Fortress*

Since the global processing time, in CLOUD2FEM procedure, is directly correlated to the number of slices to process, the main challenge for the approach was to lower the number of slices to process, while strictly describing the whole structure surveyed. The approach can be efficiently applied to different structures and contexts. The basic idea is to define a principal extension of the structure to process and to slice the point cloud along that direction. In order to achieve this result, the data is processed in different detail and resolution, depending on the context. Initially the structure is sliced with a parameter  $2\Delta$  as the distance between any given slice and the following (Figure 79). The specific value of the parameter  $2\Delta$  is carefully chosen for the context of operations and depending on the result to achieve during the structural analysis. An automatic script parses all the slices converted in pixel grids and compare the adjacent ones with image analysis techniques. If the difference between the two compared slices is evaluated under a certain threshold, then the algorithm proceeds to compute the following couple of adjacent slices. Only when the difference between the couple of slices is over the threshold, then the algorithm detects a significant variation in the structure between the two levels. In the example shown in Figure 80, it is possible to observe how the section selected with the slice changes: from 'S1a' to 'S2a' and from 'S3a' to 'S4a' there were significant variations over the threshold. For this reason, new slices 'S1b' and 'S3b', highlighted in red, should be processed respectively. Therefore, in this particular case a distance of  $2\Delta$  between the two slices is subdivided equally and another slice is added at a step of  $1\Delta$ , as visualized in Figure 80.

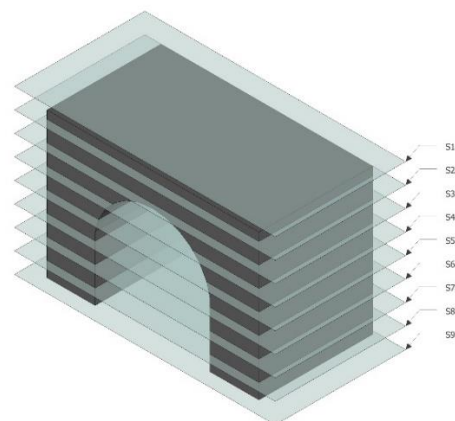


*Figure 79: Visualization of the stacking layer concept*

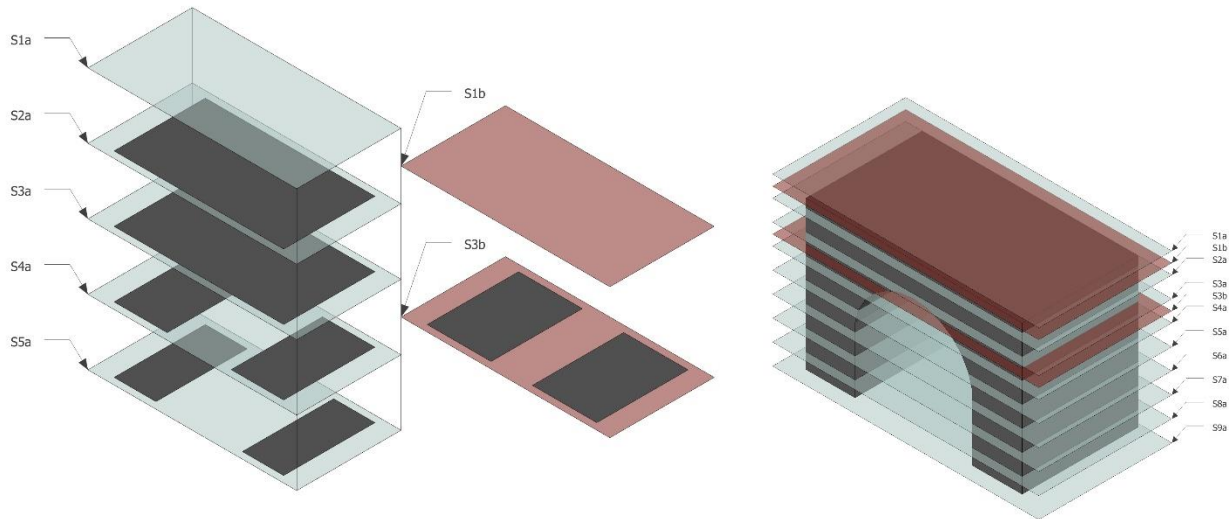


*Figure 80: From the left: concept of slicing threshold; new displacement of the slices.*

This procedure allows to process less data and reduce the time needed to analyze the simpler and regular part of the structure. At the same time, it allows to describe with a higher precision all the special features of the building: curved surfaces, vaults, floors height or walls thickness. This is achieved by having a variable resolution of the analysis along the axis perpendicular to the slices. This approach was applied to a simple structural element with a vertical extension: the north tower of the San Felice sul Panaro Fortress. Nevertheless, the tower presents interesting features to analyze, such as the different vaults at various levels and the whole building has an irregular geometry and a complex structure due to its construction, which took place in several stages over different centuries. Furthermore, the tower was heavily damaged during the earthquake (**Figure 78**).

From the initial point cloud of the entire Fortress, a dataset of about 990 thousand point have been extracted, removing all point except those of North tower. Then, the polygonal model is created, that consists of 1.9 million of triangles. In order to reduce the number of triangles, a series of operations (such as decimation) were made to simplify the three-dimensional model which guarantee the correct geometry of the structure. Others operations (self-intersections of triangles, closure of small holes...) have been carried out to solve problems defined during the creation of mesh model. Through these operations, the final model obtained consist of about 1.5 million triangles. The north tower, as already mentioned, shows some issues, such as the collapse of the roof and damage to much of the structure along its height. For these reasons, in order to obtain the full volume of the structure, filling the gap between the external and internal surface, it has been necessary an interim operation. Therefore, the polygonal model was cut along the Z-axis through horizontal slices ( $x, y$ ) at a constant distance from each other ( $2\Delta = 250$  mm) for the entire height of the tower. In the most significant areas, in the specific case the vaults, more slices with  $1\Delta = 125$  mm increment have been inserted, to better define their variable geometry. The distance between two adjacent slices has to be chosen according to the desired final resolution of the FE model. The resulting stacking sequence is composed of 70 horizontal slices (**Figure 81**).

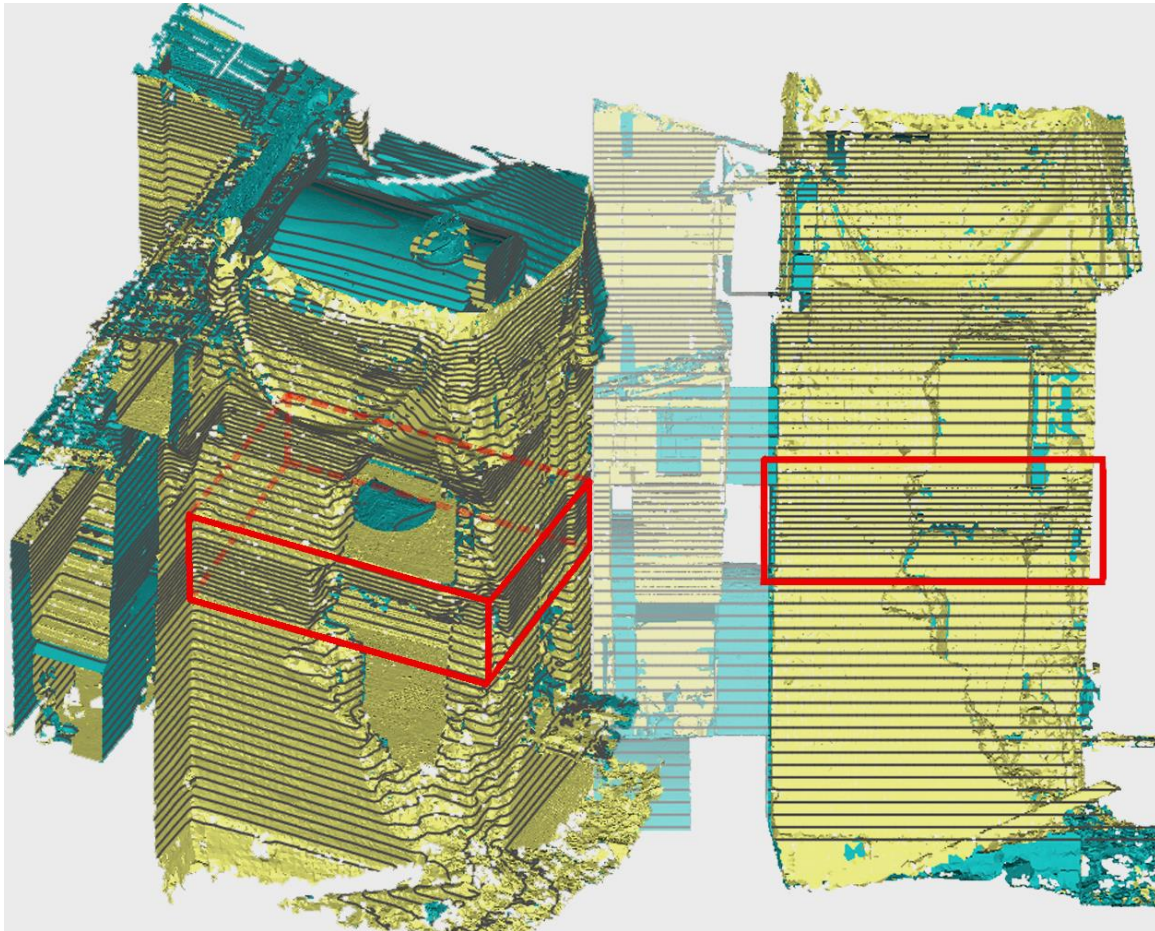


*Figure 81: Isometric and frontal view of North tower mesh with slices at variable distance (red)*

As previously mentioned, by creating a concave hull that envelopes the internal points from the outside, the presence of internal debris or any furniture located inside the room is irrelevant, because each new shape is based on the peripheral points. This operation is fundamental to obtain a closed shape for each slice, directly using the geometry provided from the previous step, without any smoothing. This part of the procedure is semi-automatic: the manual intervention is essential at this stage for an accurate separation between internal points and external points: this is especially true with data from complex buildings, such as the one analysed. The proposed workflow aims at minimizing manual intervention in terms of time in order to maximize the efficiency of the procedure itself. Therefore, the three-dimensional problem is reduced to a two-dimensional problem.

Afterwards, the reconstruction of the original three-dimensional geometry by stacking all of its slices has been carried out with a resolution of digitalization of each slice of 125 mm: this value is chosen according to the characteristics of the object to be analysed. In this case of study, in particular, it is more or less the half of a brick that composes the masonry (**Figure 82**).

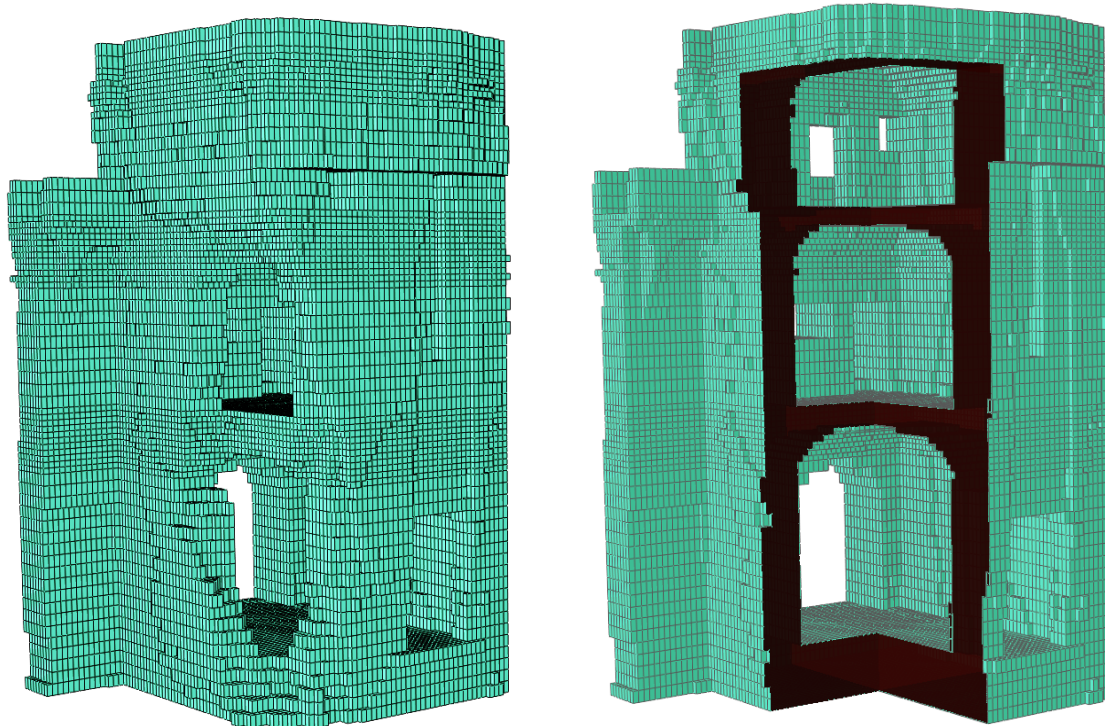


*Figure 82: Voxel model, the whole model (left); a section cut where the different floors and their vaults are shown.*

The resulting dataset is simple and easy to use with the finite element technique: each voxel is automatically transformed into an eight-node hexahedral finite element. This assumption produced a fine FE model which counts 119547 elements and 141525 nodes. Such a model is simple to be used for every kind of FE analyses. The obtained three-dimensional voxel model is tested with a structural analysis. In order to evaluate the effectiveness of the proposed method, a preliminary linear static analysis under dead loads is performed. From a practical point of view, this procedure is very efficient and can be considered expeditious since allows to immediately identify critical stress states peaks that a building with collapsed portions may present also under dead loads. The results of the analysis in terms of maximum principal and vertical stresses are collected in Figure 9a and 9b, respectively.

In particular, **Figure 83a** shows that relevant tensile stress peaks appear in proximity to the collapsed parts indicating a critical structural condition. Similarly, **Figure 83b** points out the resulting stress peaks, in terms of vertical compression, which are clearly due to the lack of some portions of wall of the tower.

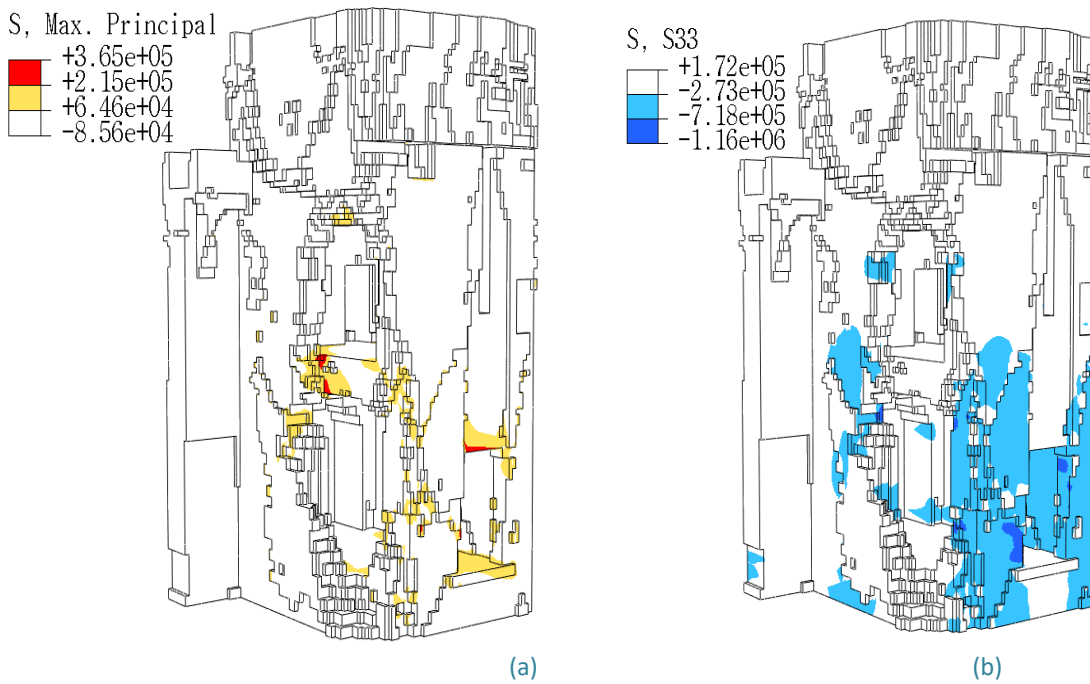


**Figure 83:** (a) Maximum principal stress contour plot (MPa); (b) Vertical stress contour plot

Therefore, through the proposed procedure it is possible to straightaway understand the main criticalities of the structure which can be very useful, for instance, to address first-aid structural interventions. Furthermore, more advanced structural analyses with complex constitutive models as well as a comprehensive vulnerability assessment of the structure, could be performed on the same FE mesh (Castellazzi G. , et al., 2016).

## 5.8 Considerations

Starting from a very dense point cloud dataset, acquiring using TLS, a complete polygonal model has been obtained. It is possible to highlight how the models, with due care, could be used for structural analysis, exceeding then the oversimplification typically of structural analysis for cultural heritage modeling, and too many details deriving from acquisition using Geomatics techniques.

This new technique, called Cloud2FEM, to generate an FE model from a laser scanner survey of a complex building has been applied to study a fortress damaged by the 2012 Emilia earthquake. This procedure has been applied for the entire Fortress, and then for the Mastio tower and the North tower, studied as single elements.

For the Mastio tower, the development of an FE model obtained using the mentioned procedure has been shown and compared with a CAD-based FE model. The resulting discretized geometry contains all of the information to use with a finite element method procedure, including the mechanical properties associated with the material features, and guarantees the automatic generation of a reliable FE solid model. To assess the accuracy of the proposed FE model, a linear natural frequency analysis has been performed. Results, illustrated by means of computed natural frequencies, show very good agreement. An estimation of the global time spent to generate the FE model of a complex structure for both CAD-based and Cloud2FEM-based procedures has been evaluated.

Also for the North Tower, the resulting discretized geometry contains all of the information to use with a FEM procedure, including the mechanical properties associated with the material features, and guarantees

the automatic generation of a reliable FE solid model. The generated models are currently used to support the conservation for the damaged building. The proposed procedure furthermore designed to be independent of any particular software.

## The Baptistery of Aquileia case of study

### 6.1 Introduction

In this chapter, the structure composing the Basilica of Aquileia have been analysed with a particular attention for the Baptistery. The historical analysis allowed to analyse the different changed and modifications that the complex was subjected to the time. After an accurate study, through several historical old data and documents, a data acquisition of the complex, in its internal part and external one, have been carried out. Different instruments have been used, in order to obtain a complete dataset suitable for several analyses. In particular, the final point cloud dataset was obtained using two different terrestrial laser scanners, two different DSLR cameras, a total station and an action camera. Thanks to all these instruments, a very detailed three-dimensional model has been obtained. The survey was a collaborative effort between the Geomatics groups from Bologna and Udine Universities.

The three-dimensional acquisition, deriving from different techniques of acquisition, showed issued related to very non-homogeneous data, and for this reason the realisation of a three-dimensional model has been performed in several phases. After the cleaning and merging of the data, a unique dataset has been obtained, and some operations (as cleaning noisy parts etc..) have been made in order to have a correct final dataset. After all these operations, the three- dimensional point cloud of the entire structure has been ready to be transformed in a polygonal model. This has been exploited for a comparison between old data, and they show discrepancies, especially in the dimensions of the baptistery (height and weight) and for the baptismal font, which is translated.

In order to define the 3D Model of the Baptistery it was necessary, once separated the surface of the Baptistery, to reconstruct manually those parts occluded to the scanning, but also to close those holes formed by the missing parts of the surface model that was eliminated.

Starting from historical description available, with a conversion between old units of measurement and current one, two three-dimensional models have been created: the first one, in the first configuration of the Baptistery, with the dome cover and some openings, that in the second reconstruction do not exist more. Thanks to these reconstructions, comparison of results in term of accuracy and change detection have been possible, for the entire model and the baptismal font.

Regarding the baptismal font, all the pictures acquired have been used for the photogrammetric elaboration, in order to reach the maximum possible detail and to evaluate the behavior of different software tools in processing CRP. In fact, some tests are presented, performed with the purpose to analyze the possibility to compare different software packages that follow different workflows. Therefore, the acquired images were processed using some of the different software tools implementing photogrammetry and computer vision algorithms, in order to evaluate their behavior in the processing and results. The final models have been compared to the TLS point cloud. Also in this case, a comparison with old data has been done and discrepancies have been underlined. Other geometric considerations, and from a static point of view, have been carried out for the six columns around the hexagonal baptismal font.

The three-dimensional polygonal model deriving from the data acquisition, and those reconstructed by simplified geometries, have been analysed with different approaches in order to evaluate static and dynamic behaviour of the structure. Some comparisons in terms of displacements and natural frequencies are shown.

## 6.2 Historical description

Aquileia is a small city near Udine, in Friuli-Venezia Giulia region (Italy). The entire structure including the Basilica of Aquileia, dates back to the fourth century and the actual configuration is the result of transformations and different reconstructions during the centuries.

The Basilica of Aquileia ([Figure 86](#), [Figure 87](#)) is composed by the Church (called “Church of Pagans”), the Bell Tower, the Baptistery (object of this study).

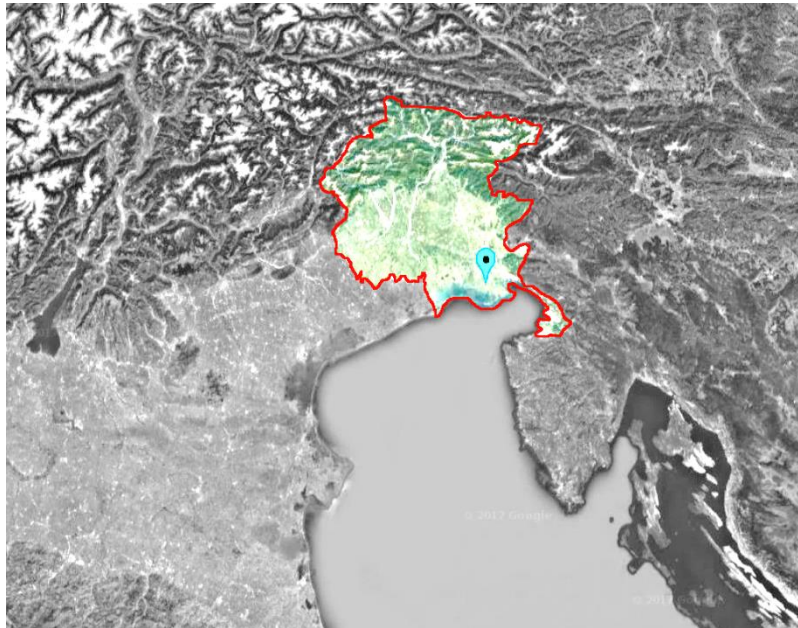


*Figure 84: Friuli-Venezia Giulia area and position of Aquileia (UD)*

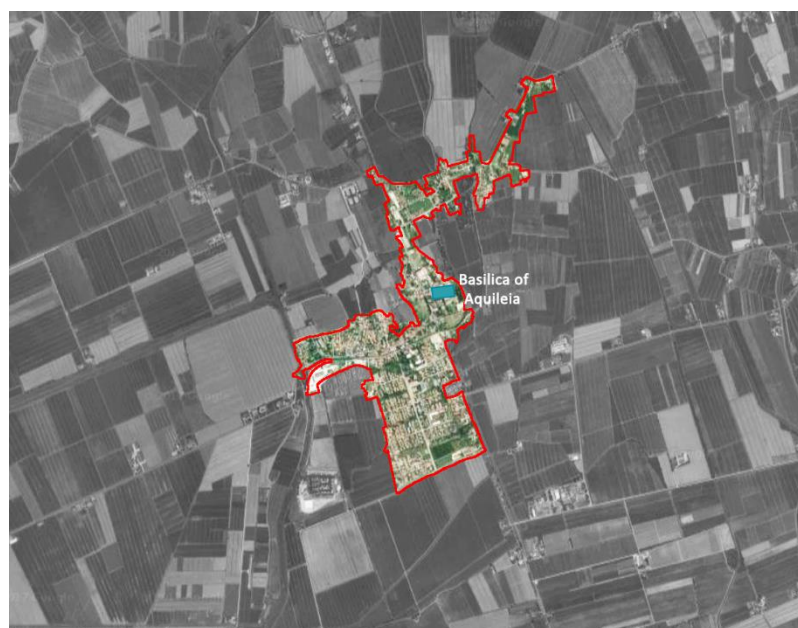


*Figure 85: Aquileia with the position of Basilica*

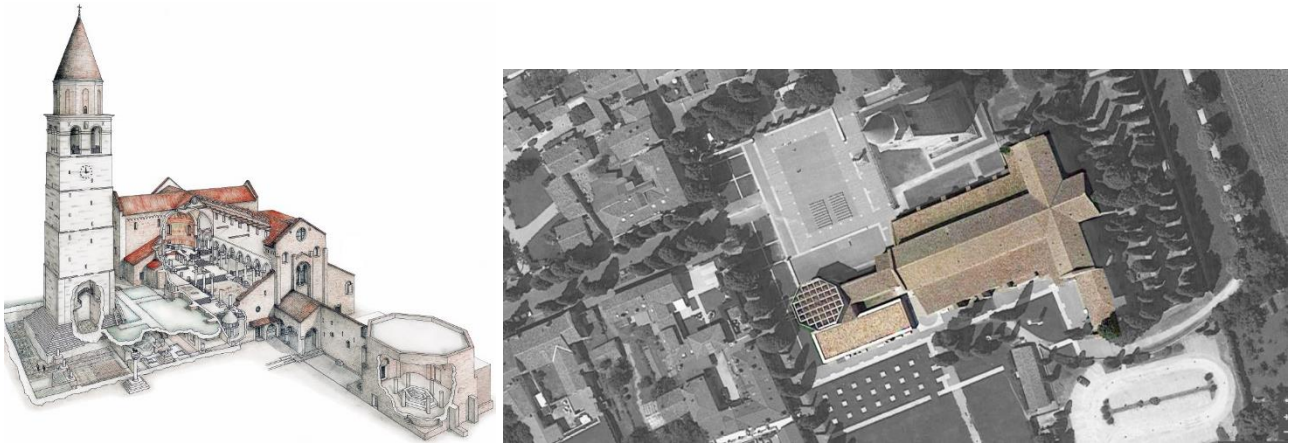


**Figure 86:** Axonometric cross section of Basilica structure (left), and ortoview (right)



**Figure 87:** View of the Baptistery from the North East side (left) and South West side (right)

The Basilica and all the closed buildings have undergone several interventions throughout the centuries; after the destruction of the first bishopric, it was rebuilt four times, overlapping the new building to the previous ruins.

It is possible to distinguish the different phases in:

- Theodorian, first half of IV century;
- Post-Theodorian North, half of IV century;
- Post-Theodorian South, end of IV century until half of V;
- Maxentian, IX century;
- Poponian, first half of XI century;
- Marquardian interventions, (reconstruction of the roof) XIV-XV century.

In the first phase, the primary configuration of the Baptistery (**Figure 88**) consisted of a quadrangular room with elliptical baptismal font.

During the Post-Theodorian phase, the Baptistery was located in another position, the actual one. From the Basilica, through a hallway with mosaic floor, there is the Baptistery, also called “Cromatian Baptistery”, since its construction is attributed at the time when Cromazio was bishop of the diocese (from 387/388 to 407/408), even if the exact date remains doubtful. As shown in **Figure 88**, the initial configuration of the baptistery was different from the present one: the building was initially octagonal, with a recess for each oblique side (four); this octagon was inscribed in a square. It was enclosed between two arcades, that

encompassed the baptistery in a larger building, likewise squared. These two wings are historically called Nordhalle and Sudhalle, from the excavation realized at the end of the 19<sup>th</sup> century by George Nienmann and Heinrich Swoboda, and were connected to the baptistery with two pairs of doors on the north and the south side. The remains of the mosaic floor of one of these two lateral halls are still visible, in the new construction called “Mosaic Hall”, hosting the former Sudhalle. To the east, where the Baptistery is currently connected to the Church of Pagans, a further door, probably larger than the actual opening, led to the courtyard outside the building.

The lower square building had an height of about nine meters; there was also an upper part that stuck out from the base structure. The octagonal shape was maintained even at the top of the building, which towered over the rest of the same. The original parts of this phase are recognizable by the use of a rather regular masonry clay bricks, with the insertion of few sandstone blocks.

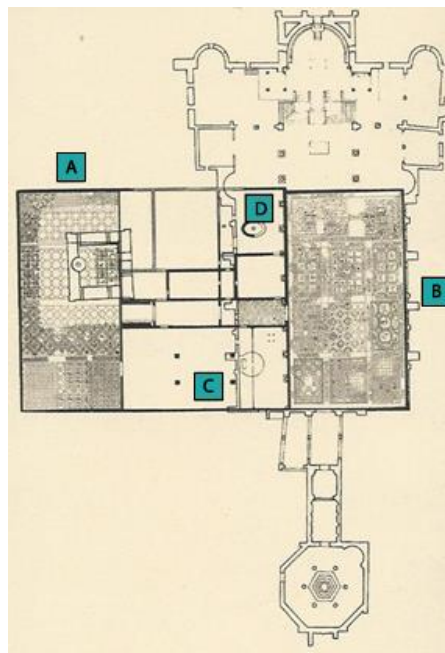


**Figure 88:** Plan of Theodorian structure, the first construction phase (of about 320), overlaid to the current configuration. A: Northern Theodorian hall; B: Southern Theodorian hall; C: cross hall; D: primary baptistery

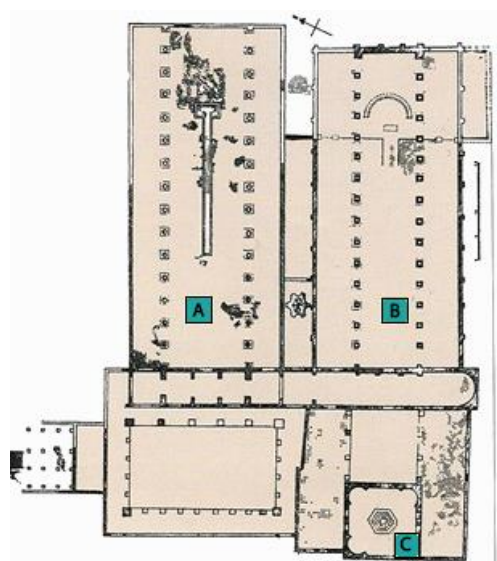


**Figure 89:** Plan of the Post-Theodorian phase. A: Post-Theodorian Basilica, at the half of IV century; B: Southern post-Theodorian or Cromatian Basilica, end of IV century; C: end of IV century, Cromatian baptistery.

From the V to the IX century, there were different transformations (**Figure 93**): three of the four apses were closed, and six arches (**Figure 92**) were realized from the boundary of the hexagonal baptismal font to the exterior wall in order to support a second floor. The fourth apse remained open for ritual occasions (**Figure 93**). New arches were inserted in the masonry, in order to unload the weight, since the closing walls of apses had no foundations (Bertoli, 1739). To the early of ninth century, a portico consisting of three naves was built, composed by five arches that connected the Baptistry to the Basilica (**Figure 91**); a close space, the “Church of Pagans”, was also created, covered by vaults and dome, with entrance in front of the Basilica door. This portico consisted of two layers (**Figure 91**): the upper floor was accessible from inside the Basilica, through a stair. The masonry of this intervention is more ordered and varies between regular clay bricks and some stone blocks.

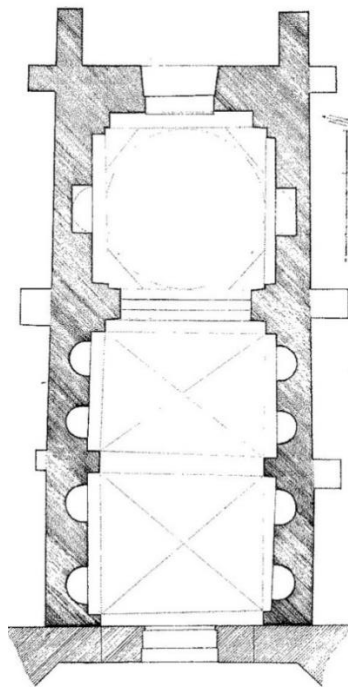


**Figure 90:** Plan of “Church of Pagans”

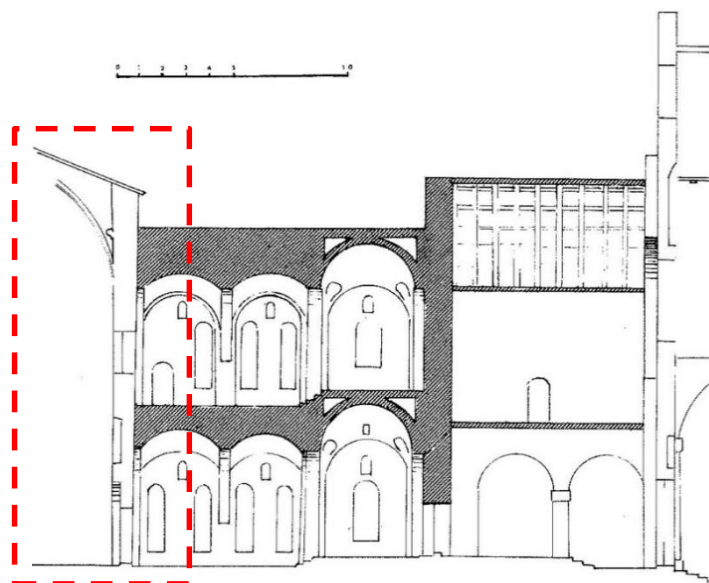


**Figure 91:** Cross section of Church of Pagans; in red the common wall between Baptistry (left) and the portico on two floors.

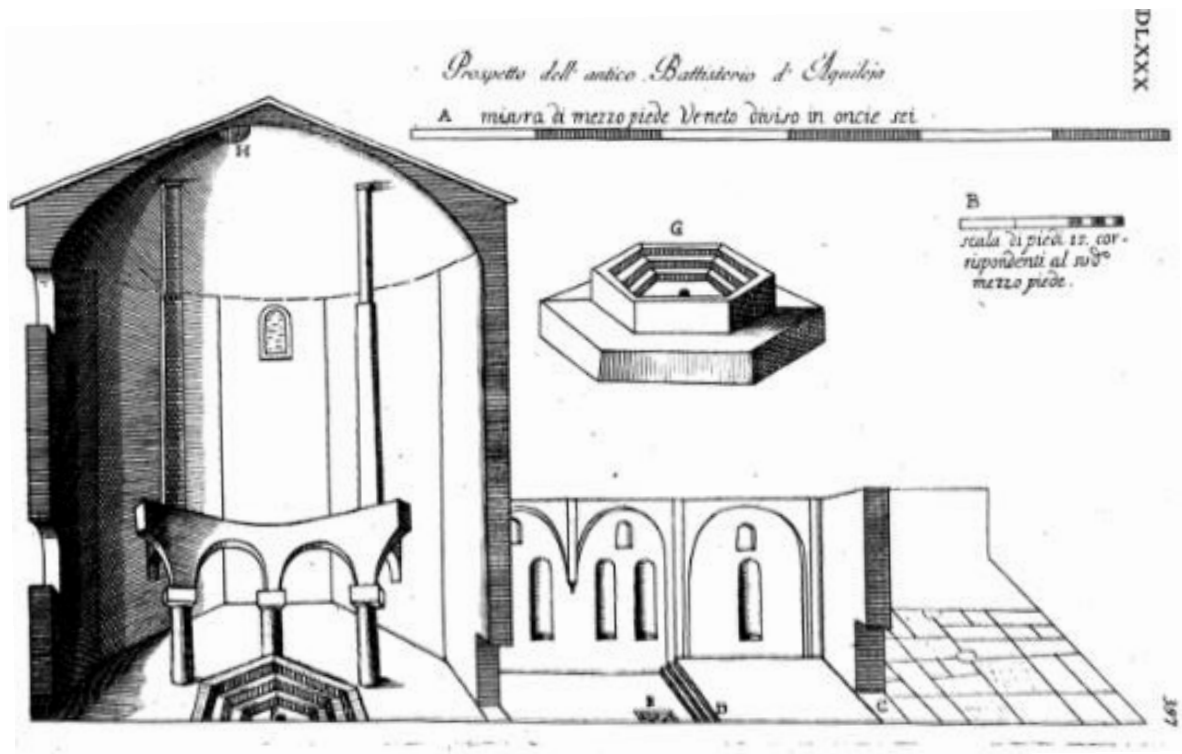


**Figure 92:** Cross section of Baptistery. The previous internal configuration, as shown, was characterized by the dome as roof, and supported by four squared columns leaned on transversal arches.

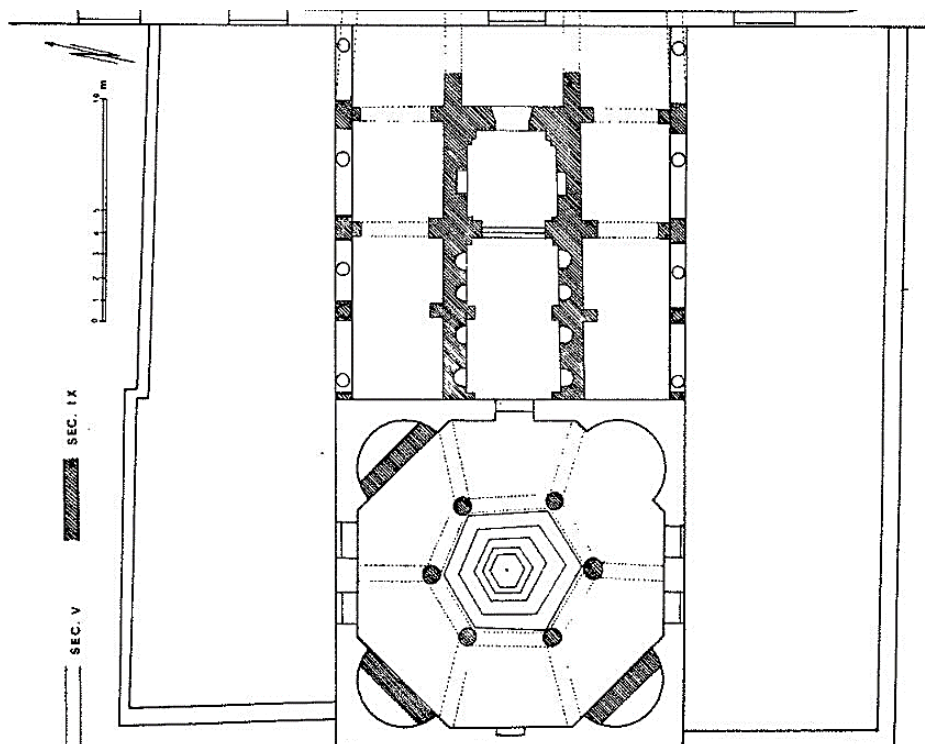


**Figure 93:** Plan of Baptistery about the transformations from V to IX century

Nowadays, it is possible to visit only the lower floor of the Church of Pagans, because the second floor collapsed at the end of eighth century. Regarding the Baptistry, it is now composed only by the lower floor, that is characterized by an octagonal internal and external shape. Certainly the baptistry is the result of a succession of phases: the latest documents available on this argument are the results of the archaeological excavation of Paola Lopreato (Tavano, 1972), (Tavano, 1996), and an analysis on the structure of the walls held by Olof Brandt (Brandt O. , 2009).

From the excavations lead by Lopreato, there is an initially squared foundation with an offset brick all around the niches, on which rested both the first floor and the bases for the columns set at the corners, which had no static function. The first excavations are shown already at the end of IX century, by Lanckoronski (Lanckoronski, 1906), in a survey on the foundation, as shown in the [Figure 94](#). Therefore, the excavations lead by Lopreato ([Figure 95](#)) were made inside the Baptistry; they are non-accessible excavations, but documented by a drawing of the plan. It is important, although it has some limits: the external part of the foundation is not documented, and the baptismal font has a different shape if compared to the other plans and to the reality. Although the plan is not detailed, the excavation gives some important information: the foundation is square with an offset brick all around the niches, on which the first floor placed, and there were the bases for the columns set at the corners, which had no static function. In the excavation, a sequence of baptismal font is identified. It is possible to note a decagonal irregular foundation, on which a probably first hexagonal font leaned, and then it was replaced by an octagonal one and at last by the hexagonal actual one. The analysis of masonry carried out by Olof Brandt, in a more recent formulation, takes advantage of earlier studies and analysis in situ; the stratigraphic analysis, performed according to the method formulated by Harris, which defines the age of an archaeological excavation according to the order of overlapping of the pattern and according to the continuity of phases, is unfortunately not so accurate, because of the impossibility to dismantle the wall. For more details, see (Brandt, 2012).

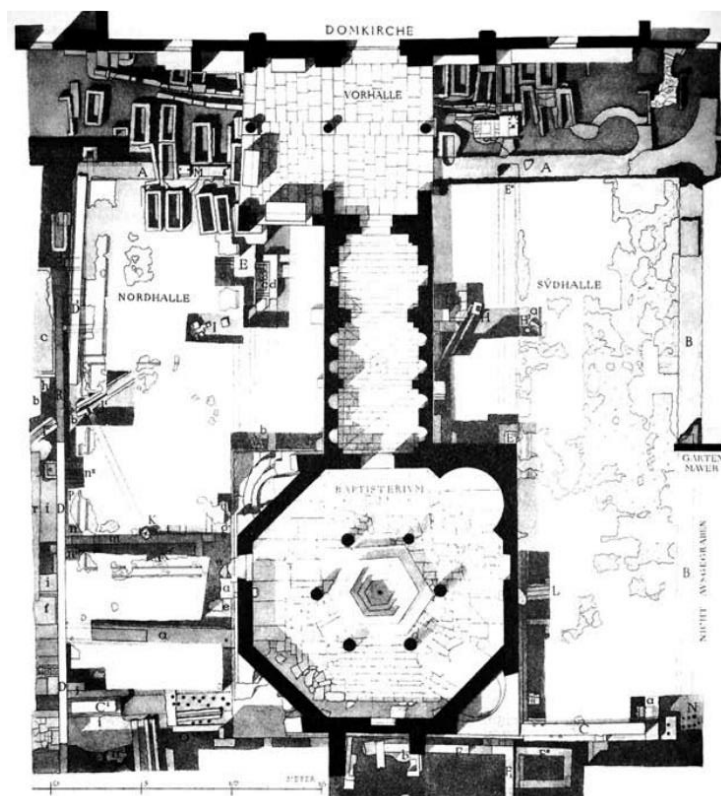


**Figure 94:** Plans Of the archaeological excavations in a survey of 1894, by (Lanckoronski, 1906), Table VII

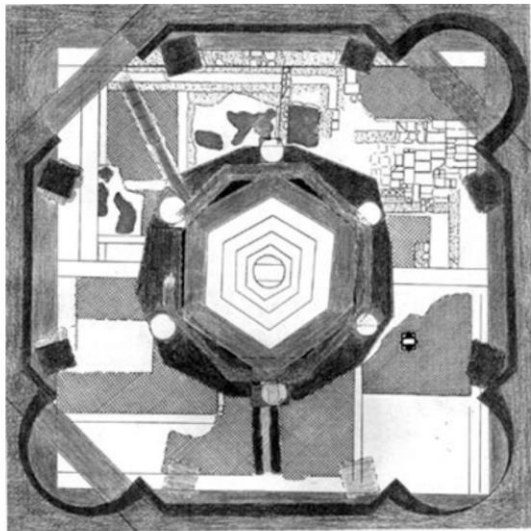


Fig. 5 - Aquileia, Battistero, Pianta.

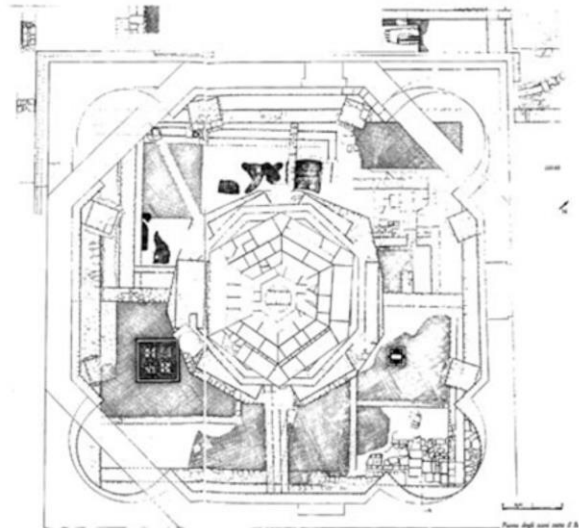


Figure 95: Plans of the excavation in the Baptistry, made by Lopreato in 1989 and 1991

### 6.3 Data acquisition

The surveying of the Baptistry has been realized in a campaign organized together with the staff of the Department of Civil, Chemical, Environmental and Materials Engineering of the University of Udine, since a research on analogous arguments is currently held there, in order to compare and evaluate the obtained results.

In order to acquire a complete description of the object, and therefore not only of its surface, but also of those characteristics that assume a high importance in the structural definition and for geometrical analysis and considerations - and among all thickness and inclinations of walls - the survey involved both the interior and the exterior parts of the building, with different instruments.

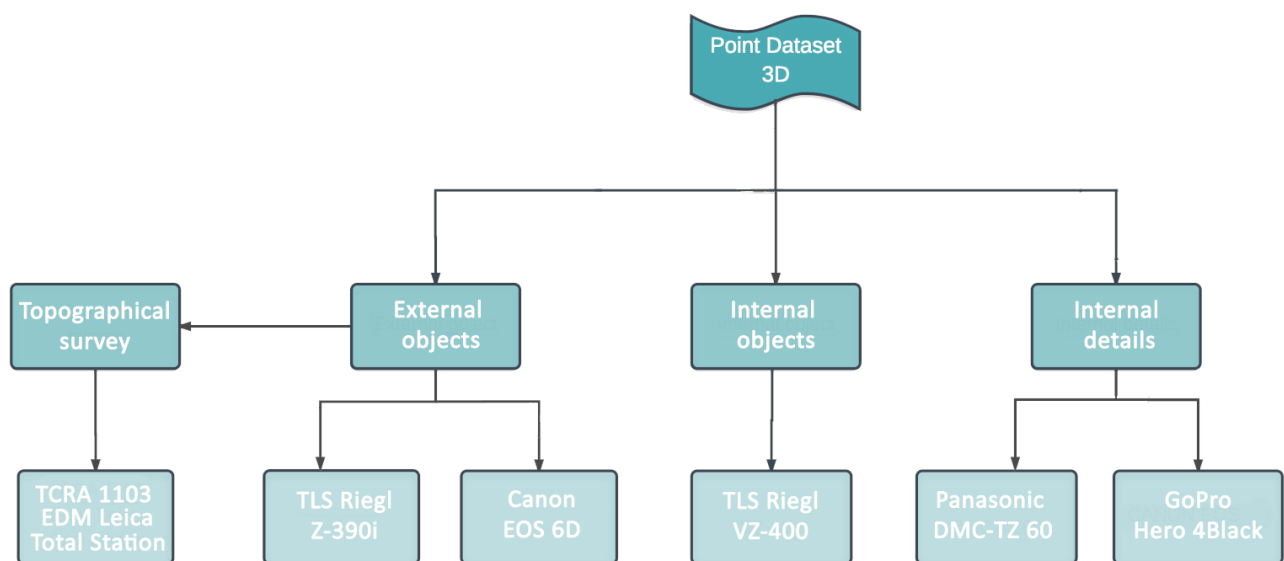


Figure 96: Workflow about the acquisition data

### 6.3.1 Terrestrial Laser Scanner

The surveying of the exterior part, using the laser scanning has been carried out by the staff of University of Udine with the TLS system Riegl Z390i (Figure 96), integrated with a Nikon D200 calibrated camera. Eight scans were acquired from eight different stations, previously defined through a preparatory project (Figure 98), in order to have a complete measurement of all the surfaces of the building. Since the building is strictly connected to the Church of Pagans and to the Mosaic Hall, these building have been surveyed as well. The total number of points acquired amount to 3.219.815 and 759.793 belongs to the Baptistery.



Figure 97: Acquisition of the external part using TLS

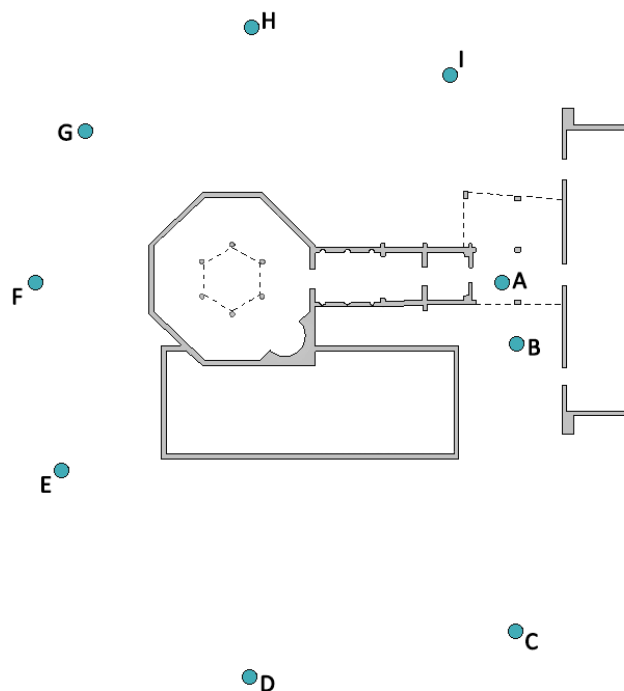


Figure 98: Scan position of external part of the building, carried out by the staff of University of Udine



**Figure 99:** Point cloud dataset of the exterior part after registration and merging  
Perspective view of the North front (top) and South front (below)

In order to proceed with the registration of the scans, 15 cylindrical ( $\Phi 10$  cm) reflective targets and 55 disk targets ( $\Phi 5$  cm) have been placed over the external parts of the structure. Anyway, these acquired points were not sufficient for the registration of the internal scans; therefore, it was necessary to proceed with a topographical survey of all the placed targets. Also the topographical survey has been carried out by the staff of University of Udine, with a Leica reflectorless TCRA 1103 EDM total station.

Once processed all the values of the topographical survey, a net has been obtained as represented in [Figure 100](#), with a coordinate value ( $x, y, z$ ) for each point. The compensated values were therefore assigned to the targets recognized in RiSCAN software, in order to proceed with the registration of the points clouds, that succeeded with a residual medium value of 1,54 centimetres. This result can be considered more than satisfactory for the purposes of the thesis and in relation with the dimension of the building.

Instead, the staff of the University of Bologna surveyed the interior part of the building. The surveying was realized with the TLS system Riegl Z400 from 18 different scan positions ([Figure 101](#)), acquiring the same number of scans; in detail:

- 5 scans of the Church of Pagans ([Figure 102](#));
- 2 scans of the Mosaic Hall;
- 11 scans of the Baptistery.

The result of each acquisition has been a point cloud dataset with a very high density, of about 5.600.000 points. The total of collimated points, with large redundancy, was 95.200.000 points (see [Figure 105](#) and [Figure 106](#)). After this, the residual error has been calculated; the precision of the instrument is about 3-5 millimetre, and the results obtained for each dataset were very good (see as example the [Figure 105](#)).

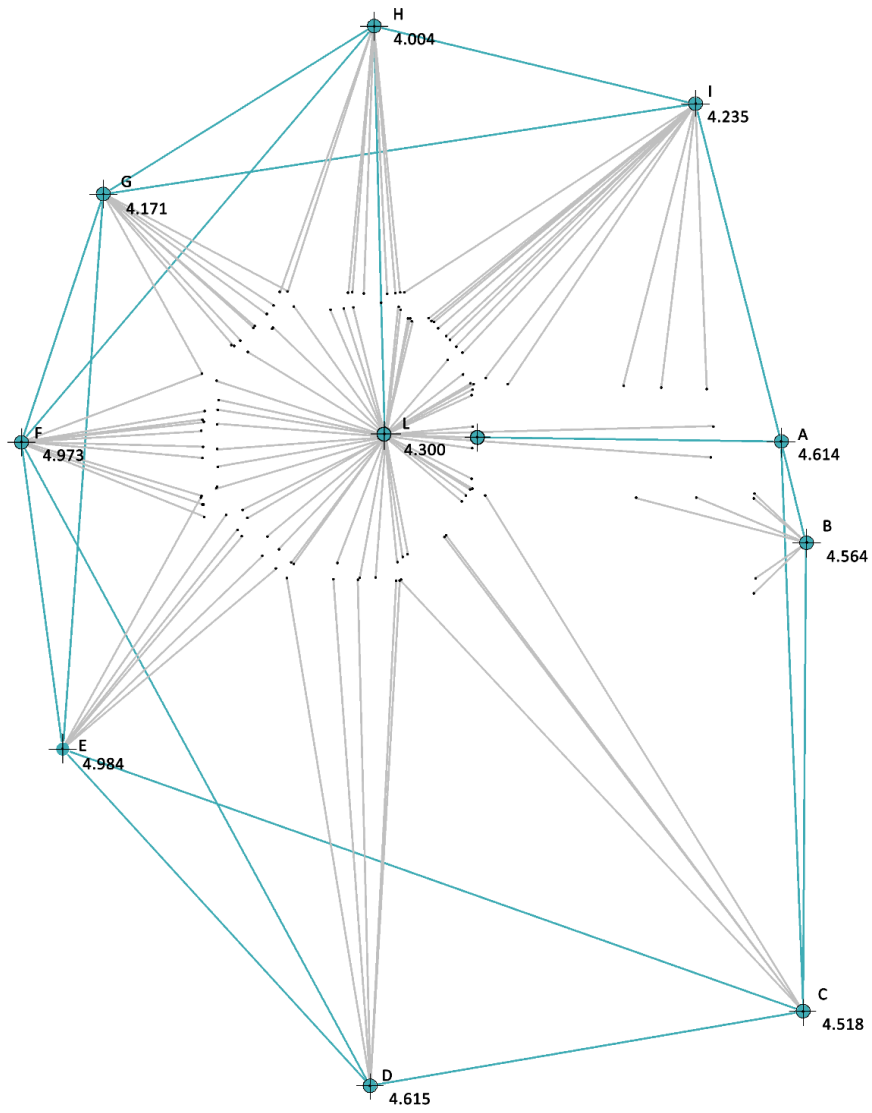


Figure 100: Net of targets and station points

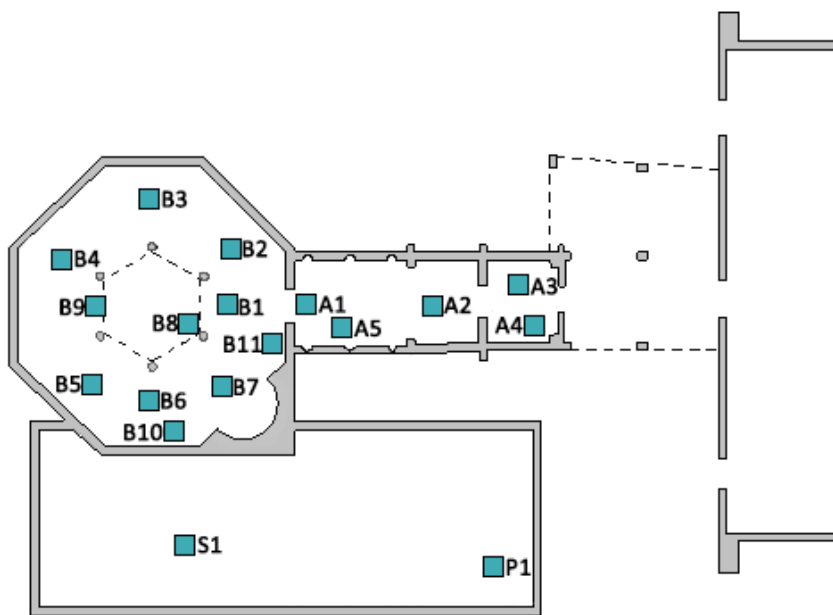


Figure 101: Scan positions of the inside



Figure 102: Internal acquisitions from Church of Pagans (left, position A3 ) and from Baptistry (right, position B3)



Figure 103: Scan B4 position with individuation of targets

Find corresponding points

Settings | Filter | Results

STATUS

State of calculation: **Not running.**

Number of corresponding points: **20**

Standard deviation of residues: **0.0022**

MATRIX

Calculated matrix:

-0.895145204	0.445772766	-0.001305617	2.911712937
-0.445773369	-0.895145834	0.000199145	-0.024553932
-0.001079944	0.000760273	-0.999999128	5.494455587
0.000000000	0.000000000	0.000000000	1.000000000

INFO

Click on the button **[Start]** to start calculation.

Start Close Help

Figure 104: Residual error scan B1



Figure 105: Registered and merged point clouds from the outside



Figure 106: Registered and merged point clouds from the inside

### 6.3.2 Close Range Photogrammetry

The Baptistery has a height of about 11 meters, therefore it is not possible to reach its highest parts using TLS, as for example its modern roof or the external walls in its upper parts (the South East front and the high part in front of the Basilica). In fact, the highest parts of external walls are characterized by very poor data, due to the distance between the instrument and the structure. For these reasons, the staff of University of Bologna proceeded with the integration of the lacking data, with the acquisition through a photogrammetric survey (*Figure 107*), adopting an extensible tripod linked to opportune devices in order to remotely control the camera (*Figure 109*).

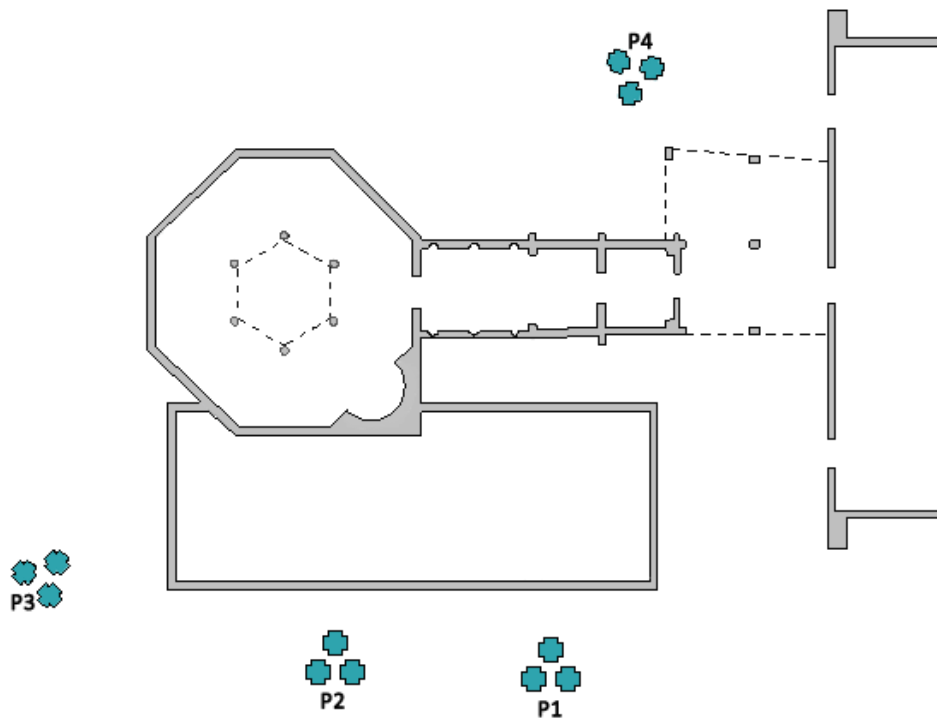


Figure 107: Surveying positions

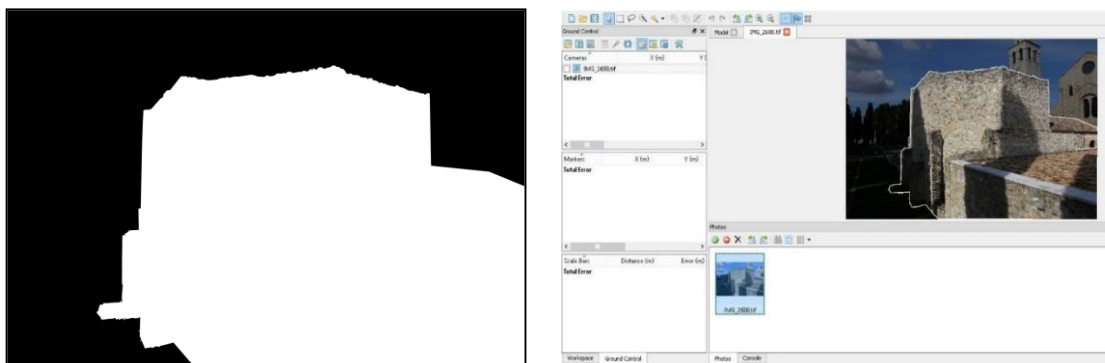


Figure 108: Acquisition from P2 position

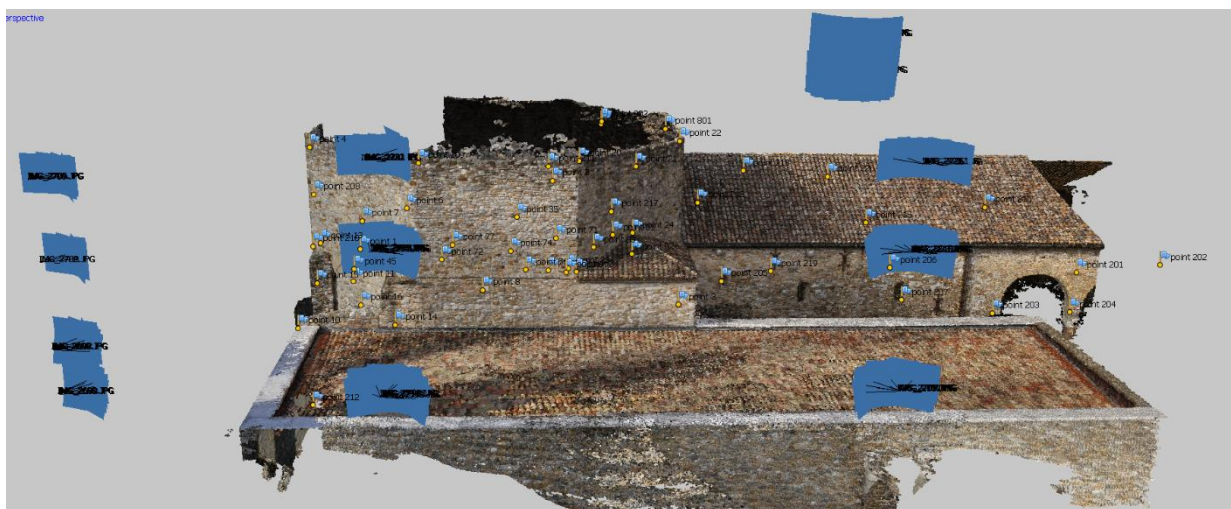


Figure 109: The tripod has a system of telescopic extensible rods that reach an high of about 14 meter. In the left, the tripod during its manually extension, in the right, the tripod extended with a height of 12 meter, enough for the acquisition of the roof and the missing elements acquired before, using TLS

So, an image-based method was applied: it was decided to execute a photogrammetric survey of the roof (and so even of the highest part of the masonry walls) by means of a full frame Canon EOS 6D DSLR camera fixed on an extensible tripod (a survey by UAV was in fact not possible). The tripod has 14 meter as total maximum extension (through a system of telescopic rods) and is equipped with opportune devices for the remote control of the camera and real-time visualization of the acquired images (*Figure 108, Figure 109*). This operation required four different positions of acquisition (*Figure 107*): three (P1-P2-P3) from the southern side of the building and another one (P4) from the northern side, for a total of 77 images acquired. For each station, pictures from three different heights were taken, following the strategy of orthogonal and converging directions. Once acquired all the photos, they have been processed, masking all around (vegetation, sky, buildings etc.) not useful to the three-dimensional model purposes; in this way, leaving empty only the structures object of study, when the images have been uploaded, the software adopted (Photoscan) identifies immediately the elements to consider, so obscuring the environment around. Therefore, a point cloud dataset has been obtained, resulting from the photogrammetric acquisition. In order to get a good alignment, essential for the following stages, and to obtain the correct size of the model, markers have been placed (*Figure 112*), associated to known coordinates derived from the topographic survey and from the TLS survey. The residual error is less than 1 pixel and about 3 centimetres. Considering that the acquisition has been made only from four positions, and the object of study is very large, this is a satisfactory result.



*Figure 110: Masks are used in order to specify the areas on the photos which can otherwise be confusing and lead results with incorrect reconstruction. In the left, mask of an acquired picture in which the white is the object of study and the black is the external environment which does not have to be considered. In the right, the identified mask on the picture inside the software.*



*Figure 111: Dense point cloud with the position of photogrammetric acquisition (blue) and markers points, from the North side*

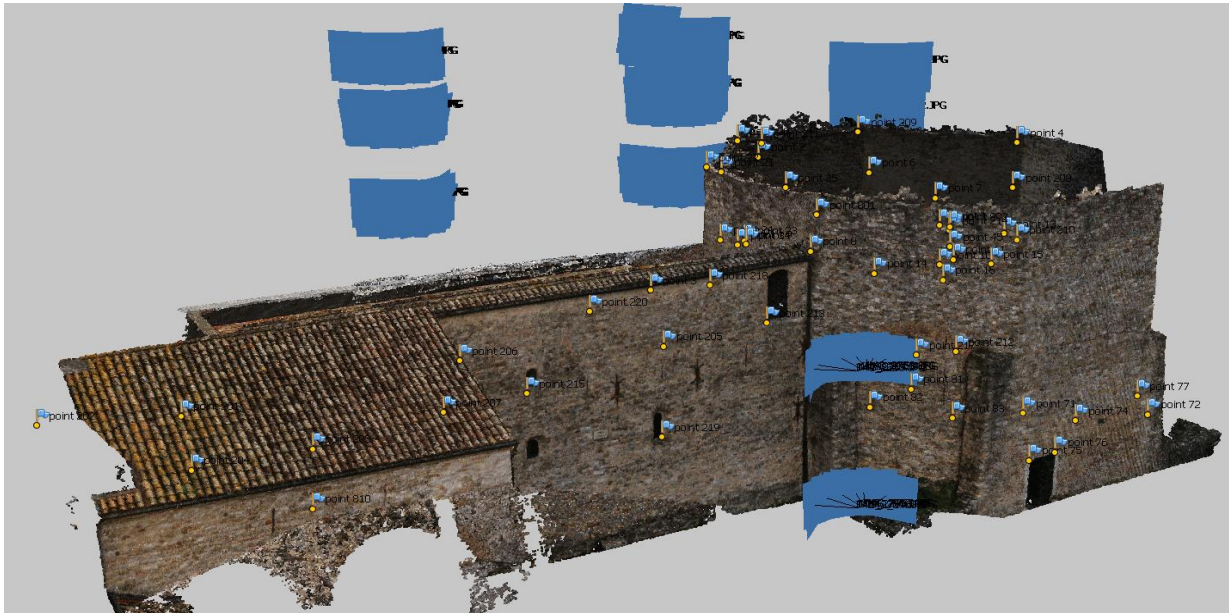


**Figure 112:** Dense point cloud with the position of photogrammetric acquisition (blue) and markers points, from the South front

The interior of the Baptistery is characterized by recesses and ledge elements in masonry. For this reason, the only internal laser scanning acquisition did not result the best solution because the thicknesses and higher parts could not be surveyed in an appropriate way. Thus, the internal survey has been supplemented by photographic acquisition. In particular, the pictures have been take through an action camera GoPro HERO 4 Black on a high rod (**Figure 96**). From all the images captured, 18 pictures of a bulge element were selected, with a constant timing of three seconds, and then processed for obtaining a three-dimensional detailed model.

The images captured and selected, were calibrated using a specific software (Calib3V). This is a software for the calibration of full frame images and of cameras with quadrangular lenses. After entering the specific parameters of the instrument used, the software will give the parameters of calibration of digital camera. Therefore, uploading images, the distortion will be deleted with calibration parameters. After the calibration (**Figure 113**), the selected pictures are ready for the next step of alignment.



**Figure 113:** Two images calibrated with a specific software. The images do not have a high quality, because if the rod extends (on which the GoPro is fixed), the oscillation increases. In this case, however, there was the need to acquire some specific elements, like the internal thickness of the recess, or a ledge of masonry (red) with this instrument. Despite this, satisfactory results have been obtained, as will be seen later.

## 6.4 Three-Dimensional complete model

### 6.4.1 Numerical modeling

In total, 40.703.765 points, covering the exterior and interior surface of the structure and the acquired details, compose the final point cloud, which represent the union of all point clouds obtained from each scan and from each different acquisition technique (Figure 114, Figure 115).

Once merged all point cloud dataset, the issues were due mainly to:

- the high number of data to process, which led to a slowdown of the computing processes;
- the overlap between different point dataset, derived from different techniques, as for example the external walls of the baptistery with the dataset deriving both from TLS and from CRP;
- the different density of dataset, as for example the external acquisition using TLS and CRP (Table 11).

In order to solve the listed problems, it was necessary to set an operative strategy for avoiding losing of important data; in particular:

- cleaning of the data, from noises, outliers and isolated points;
- choosing of the best dataset according to the density, and deleting of poor or missing parts;
- resampling and homogenizing only of the very dense point clouds.

The first step of cleaning data was obtained through software (CloudCompare), partially in automatic way and partially with manual procedures, where all the points considered useless (like the ones too far) or even not useful for the next elaborations have been eliminated. These operations led to a strong reduction of the number of points for each point cloud, as it is possible to note in Table 11.

The second step of choosing of the best data was the most important step: in fact, a first test was made without this stage, but the result has been inaccurate because of the difference of density using different instruments, as mentioned before. In the overlap and merged data, this has caused a difference of millimetres especially in the upper part of the exterior walls of the baptistery, where resulted the noise that compromised the quality of final three-dimensional model. For these reasons, an accurate selection by the operator has been carried out, in order to choose manually the data to be deleted, the data to be stored and finally how to combine and merge different dataset in the best way.

The third phase concerns the resampling of the point clouds adopting a constant distance between each point, for very dense point cloud dataset. In particular, this operation has been made for dataset derived from CRP for the external part and the TLS of the internal one, because there was a difference in terms of density with the other datasets. Considering that the point clouds had a very high level of detail, the operation of resampling did not compromise the data quality. This operation, besides having regularized the density of the points, allowed a further reduction of their quantity (Table 11) and with an operation of data uniforming, with a spacing of 1 cm, the whole information was reduced for having more suitable datasets.



*Figure 114: Point cloud of the entire structure, South front*



*Figure 115: Point cloud of the entire structure, North front*

After these operations, the three-dimensional point cloud of the entire structure has been ready to be transformed in a polygonal model (**Figure 118**). This model is still in a raw form and has to be processed in order to obtain a clean surface with no incongruences, holes or errors. In the **Figure 117** and **Figure 118**, it is possible to see how the model is complete, in the external part and in the internal one.

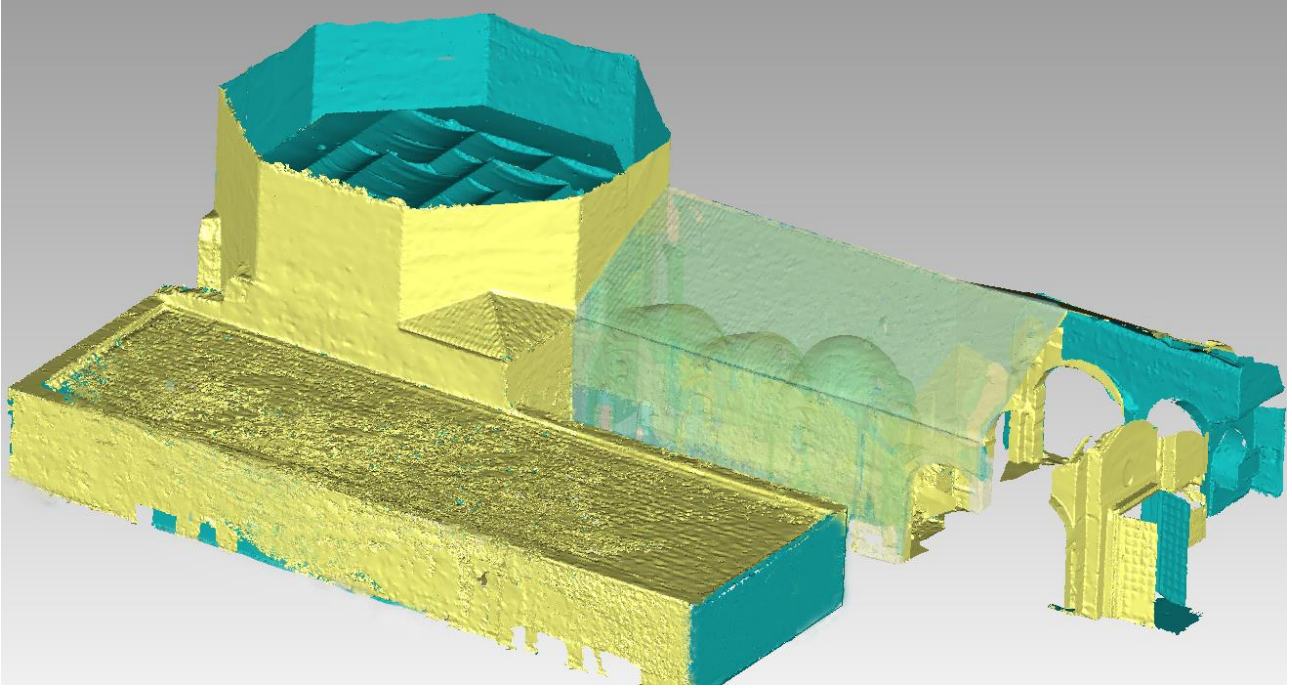


*Figure 116: View of the model from the South front. The transparent mode is set in correspondence with the Church of Pagans, where it is possible to observe therefore the external surface and the internal one, with the vaults of the hall.*

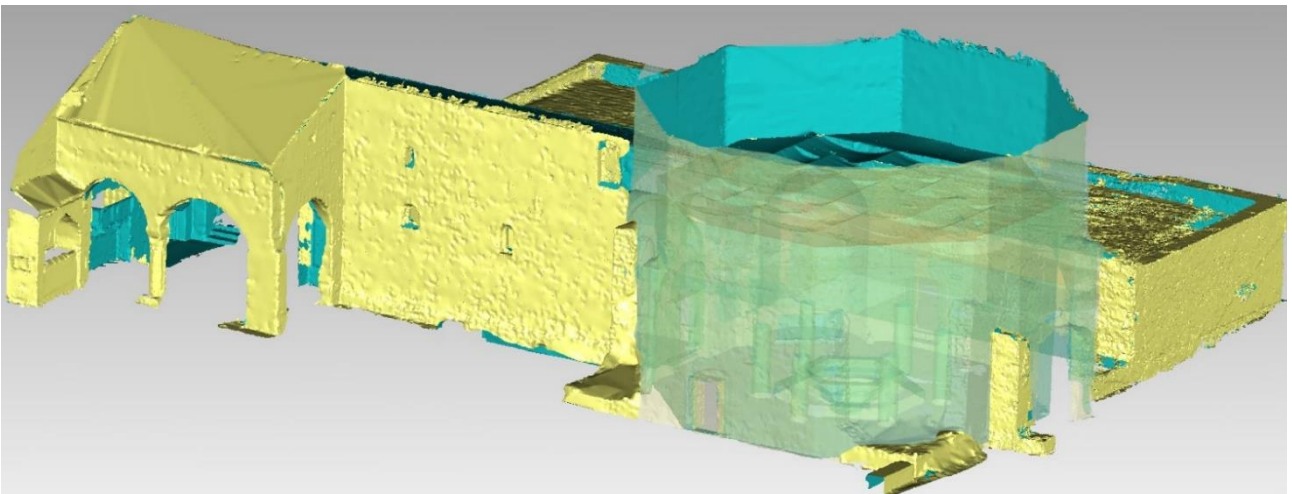


*Figure 117: The model is seen from the North side and the transparent mode is set on the Baptistry.*

POINT CLOUD		Original dataset (no. points)	Cleaning dataset (no. points)	Polygonal model (no. triangles)	Final polygonal model (no. triangles)		
Outside	TLS	3.219.815	2.488.845	47.845.279	46.369.814		
	CRP	8.204.440	7.165.287				
Inside	TLS	24.155.312	22.751.491				
	CRP	5.124.198	4.621.135				
TOTAL		40.703.765	37.026.758				

*Table 11:* Transformation from point cloud dataset to final polygonal model



*Figure 118:* Three-dimensional final polygonal model with texture

#### 6.4.2 Comparison with old data

The only cross section of the entire structure dates back to 1906, in the Lanckoronski book (Lanckoronski, 1906), in which the Church of Pagans is composed by two layers, divided by the vaults and dome. This section has been used for evaluate the differences and changes with the actual conformation of the structure. In fact, there are discrepancies between the old section and the new generated profiles. The Baptistery is more high now, but its length between opposite sides (in plan) is less than the historic document. Consequently, the baptismal font, which is located in the centre of the Baptistery, is shifted in the overlap.

Regarding the Church of Pagans, the height of the roof for the two vaults are coincident; instead, the dome has a same height but is narrower that the present one.

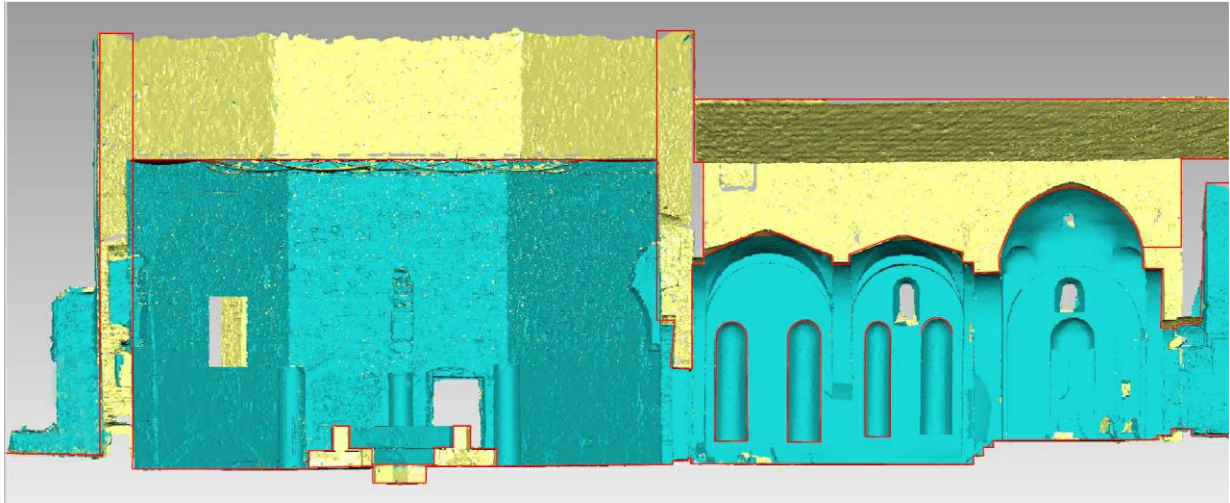


*Figure 119: Cross section obtained from the complete three-dimensional polygonal model. The red lines represent the sectioned parts*

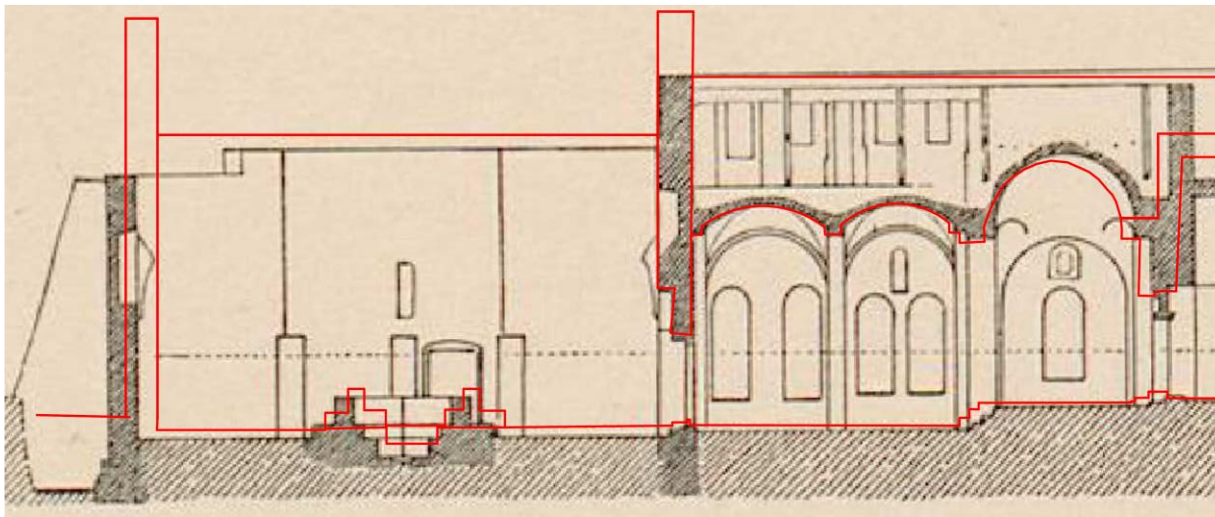


*Figure 120: Cross section of the Baptistry and the Church of Pagans, from Lanckoronski (1906). The red lines are the sections obtained from polygonal model*

## 6.5 Three-dimensional model of the Baptistry

In order to define the three-dimensional model of the Baptistry it was necessary, once separated its surfaces from that belonging to the close structures, to reconstruct manually those parts occluded to the scanning. Furthermore, also the holes formed by the missing parts of the surface model have been filled.

The three-dimensional model was composed by 8.824.126 million of points, concerning the internal part (**Figure 121** in the right, and **Figure 122**) and the external one (**Figure 121**).

The transformation from the point cloud dataset into a polygonal model, has generated a dataset of more than 5 million of triangles (**Figure 123**). A decimation and the manually reconstruction was necessary, of those parts occluded to the instruments.

As mentioned before, thanks to different acquisition techniques, a very complex three-dimensional model is obtained. All the details are represented in the complete model. Some elements are shown in the following figures (from **Figure 124** to **Figure 127**).

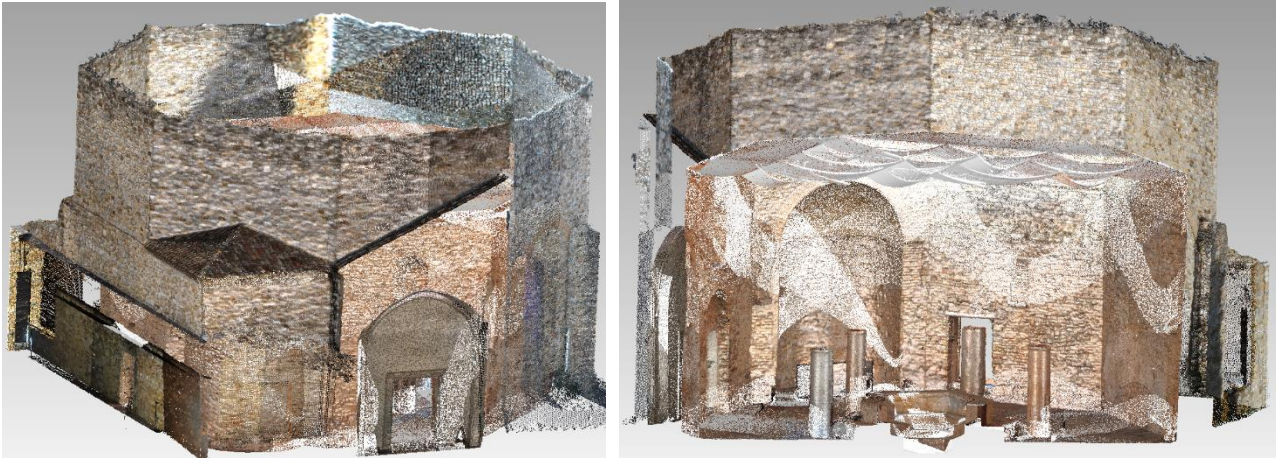


*Figure 121: Complete dataset from the external part and the internal one, only of the Baptistery. In the left, a perspective view from the external East front; in the right, a perspective view of the internal complete dataset.*

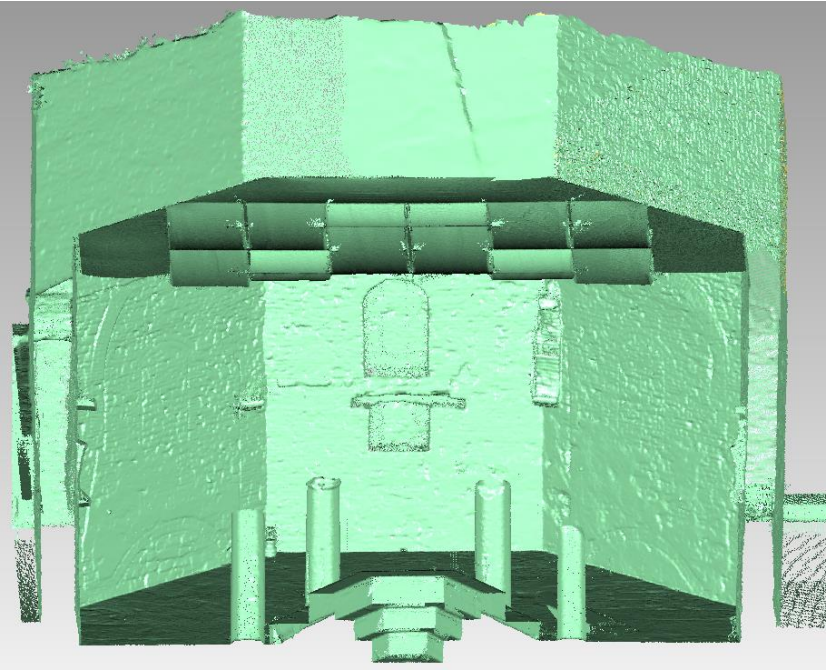


*Figure 122: View of the internal part of dense point cloud without texture. As it is possible to see, the final dataset, after an accurate process and elaboration, is very homogeneous and dense*



**Figure 123:** Cross section of the polygonal model of Baptistery

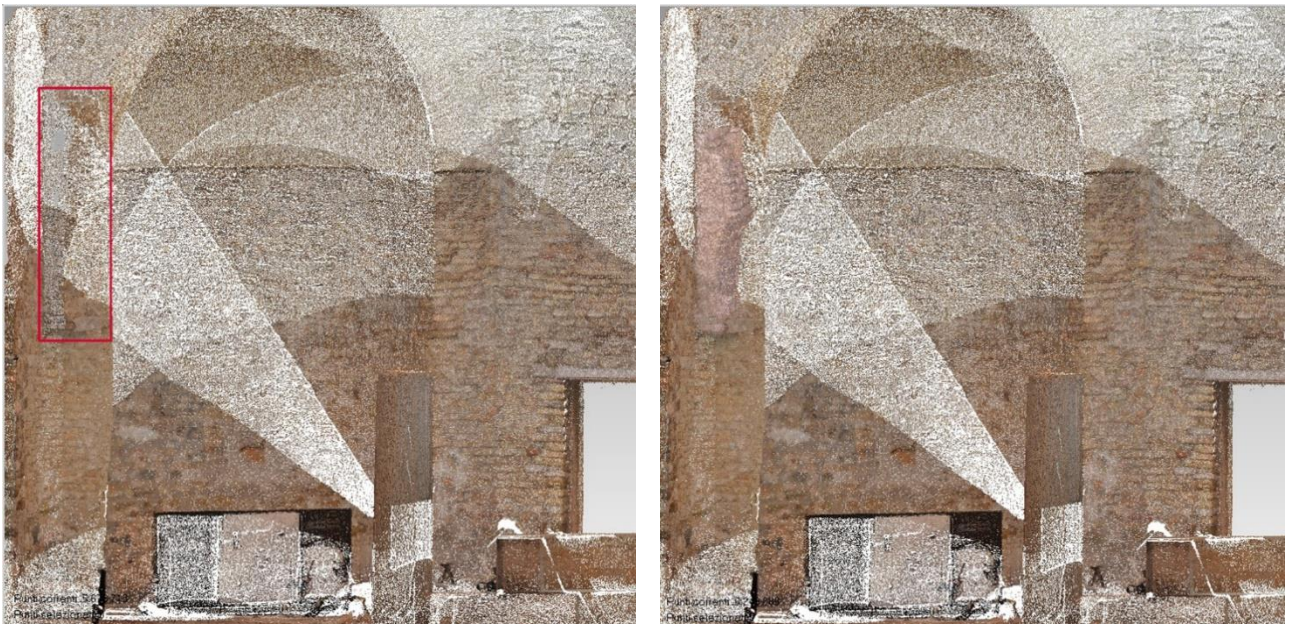


**Figure 124:** View of point cloud from internal of baptistery. In the left, one of the recess (red) that characterize the historical structure, acquired using TLS. As it is possible to see, the acquisition is not accurate, due to the height of the instrument, compared to the element. In the right, the overlap between the point cloud acquiring using TLS and CRP (using GoPro). The element is correctly defined without noise.

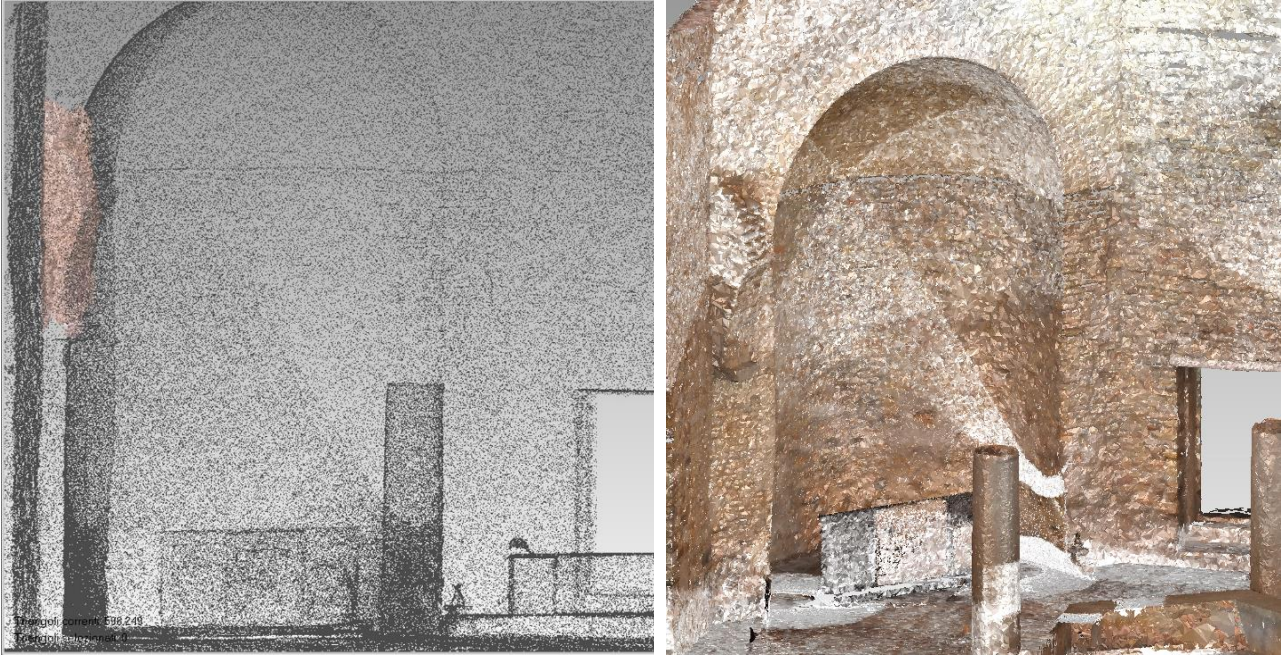


**Figure 125:** In the left, the point cloud deriving from CRP, is overlaid to the dataset acquiring using TLS (black) in order to show the accuracy and the density compared to the internal dataset; in the right, a perspective view of polygonal model with the global texture of inside.

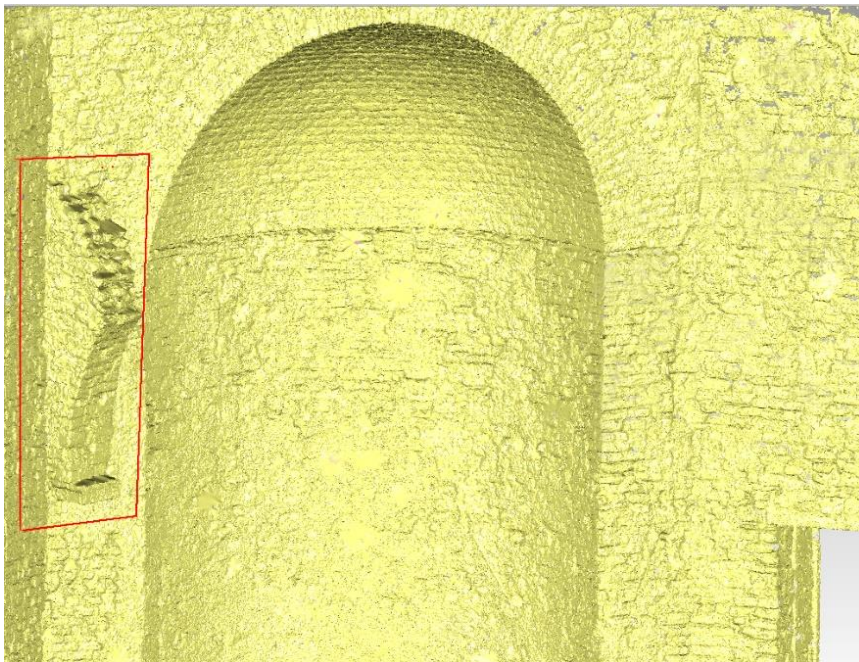


**Figure 126:** Perspective view of the internal part. As it is possible to see, the final polygonal model, after some operations (closing holes, decimation etc...) is homogeneous even if derived from different instruments.

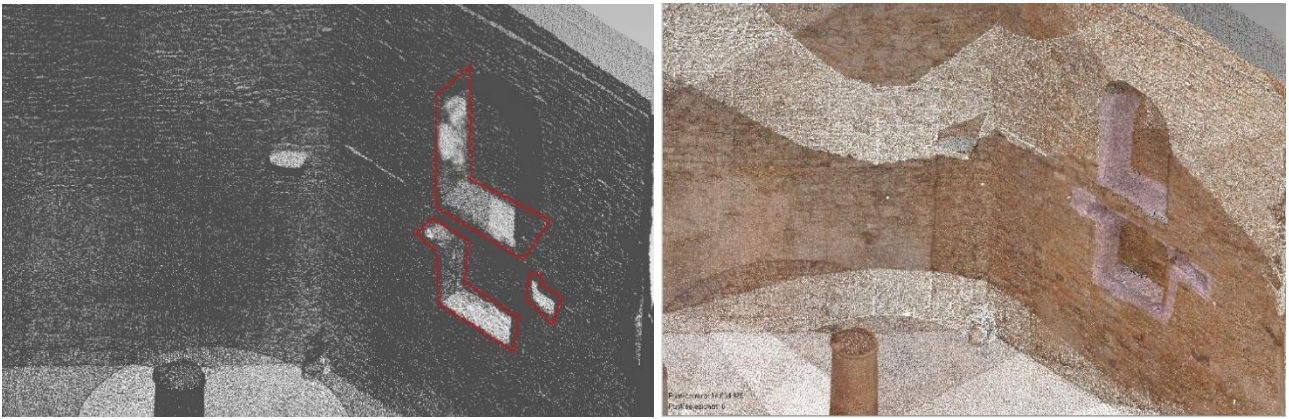


**Figure 127:** In the left, the missing or poor parts are underlined with a red line. In the right, the point cloud derived from TLS, integrated with CRP acquisition. The colour is more homogeneous and the final model is complete and correctly defined.

For some tests, which will be discussed later (as, for example, 6.5.2 and 6.7), all those unnecessary parts have been deleted, like the modern glass and the coverage curtains, the baptismal font with the internal columns and all the furniture. In fact, the target model to reach, has to represent only the masonry belonging to the Baptistery. This operation was done manually and the transformation from initial model to “emptied” one, is represented in Figure 128. The following step was related to the reconstruction of the lacking parts and in particular, as regards to the interior model, of the surface of the wall over the curtains, as reported in Figure 129, considering as reference the height of the exterior model and extruding the upper border of the model.

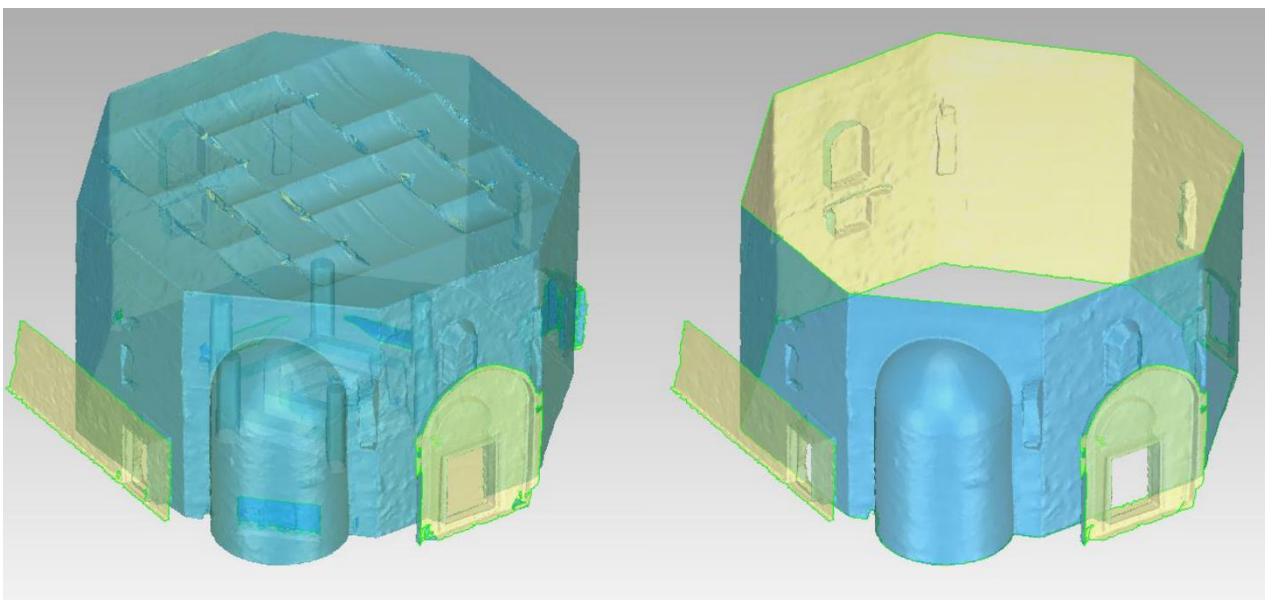


**Figure 128:** From the left: the polygonal model complete of inside; the interior model without unnecessary parts

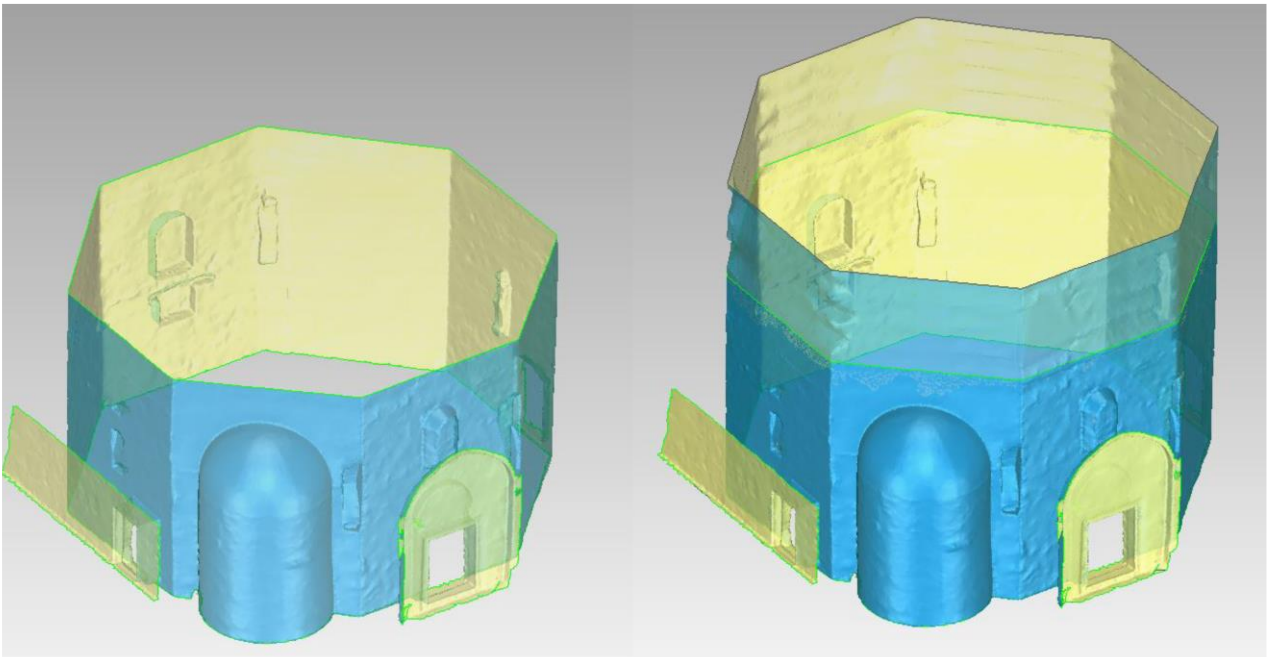


*Figure 129: Adding of the lacking surface of the interior wall*

The next and final step was the merging of the two models, the internal one and external one, obtaining an open surface (**Figure 130**) that needed further operations in order to close those holes existing between the two surfaces. As final result, a three-dimensional model with continuous surfaces has been achieved; the model is composed by 3.291.952 triangles (**Figure 131**).

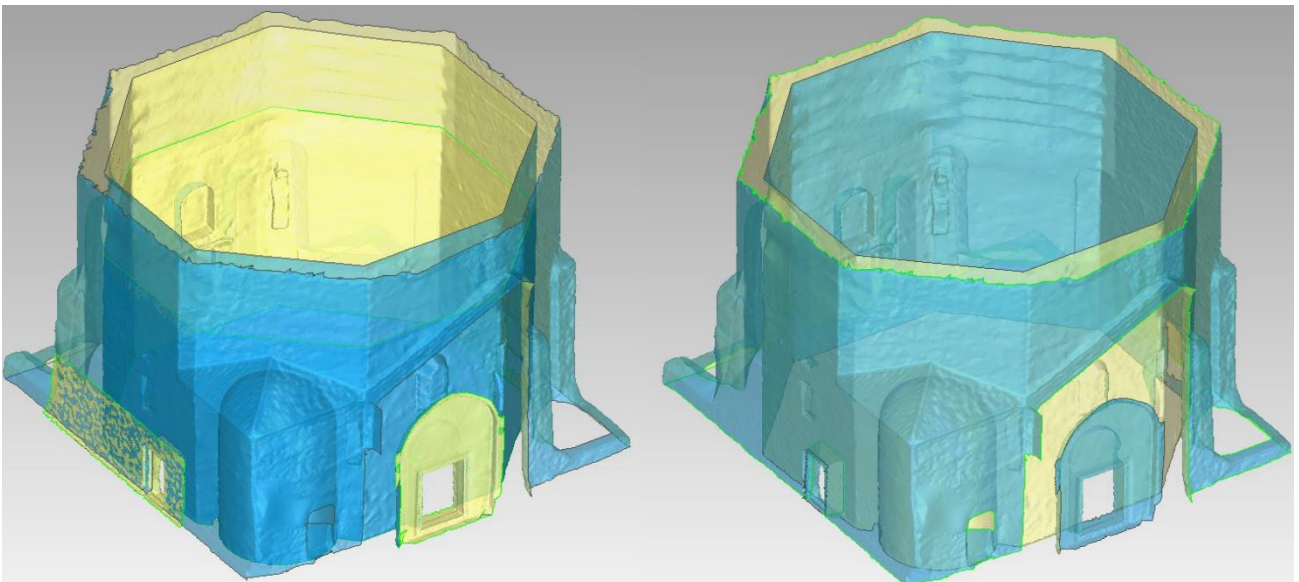


*Figure 130: In the left, internal and external surfaces still separates; in the right the model with the merged surfaces*

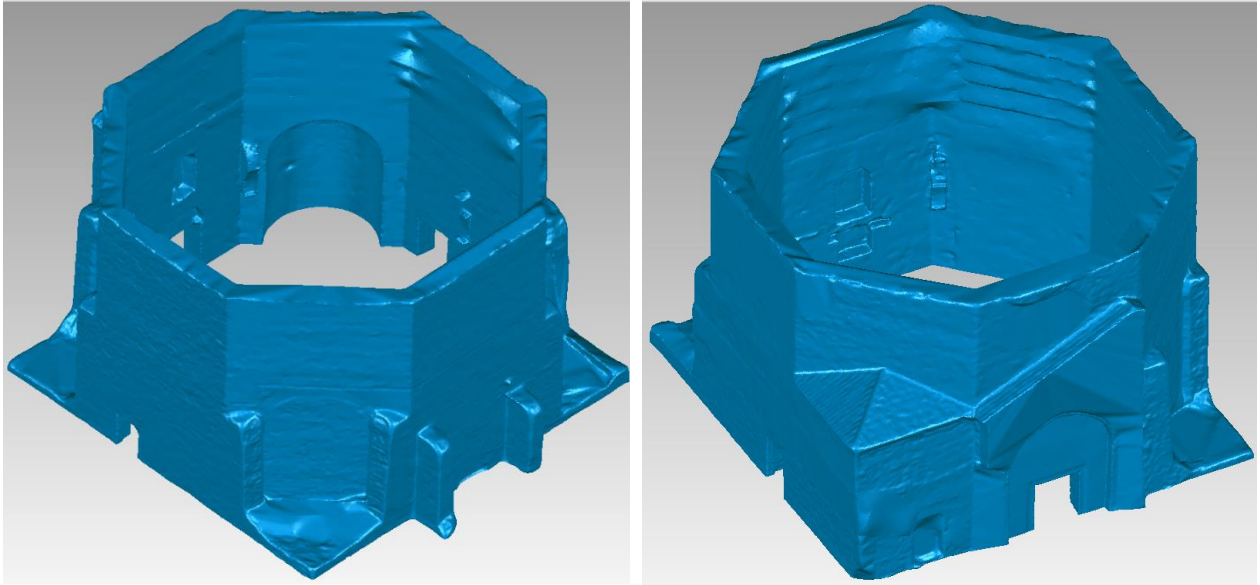


*Figure 131: The final three-dimensional model of the Baptistery*

### 6.5.1 Geometrical modeling from old data

Starting from the plans and the sections available from existing documents, two three-dimensional models have been realized. Thanks to the historical description, in fact, it has been possible to reconstruct one of the initial conformation of the Baptistery, characterized by the dome cover. Analyzing the documents and the descriptions made by Bartoli, and using the only section available before the 18<sup>th</sup> century, a reconstruction was made with a good level of detail and accurate dimensions. Therefore, this result is obtained following the description of Bartoli, in which the interior part of the Baptistery has been explained in detail, and also through metric measurement of that historical period, in particular “*steps*”, “*once*” and “*venetian foot*”. In the following table, a correspondence between old units of measurement and the actual one, in metres, are reported.

Old unit	Metres
STEP	1.715
ONCE	0.1429
VENETIAN FOOT	0.343

*Table 12: Correspondence between old units of measurement, used for the description of the internal spaces of the Baptistery, with the actual one.*

Through the conversion of measurements, it has been possible to date back to the correct dimensions of the initial configuration of the structure (**Figure 132**). The Baptistery at first was characterized by a dome cover, supported by four vertical columns with square section (**Figure 134**).

The six columns were already placed in each corner of the hexagonal baptismal font, but they were connected to each other with six arches, and from each column another transversal arch connected the perimetral wall (**Figure 135**).

The three-dimensional model was realized with (Rhinoceros, 5.0), a well-known software for three-dimensional modeling.

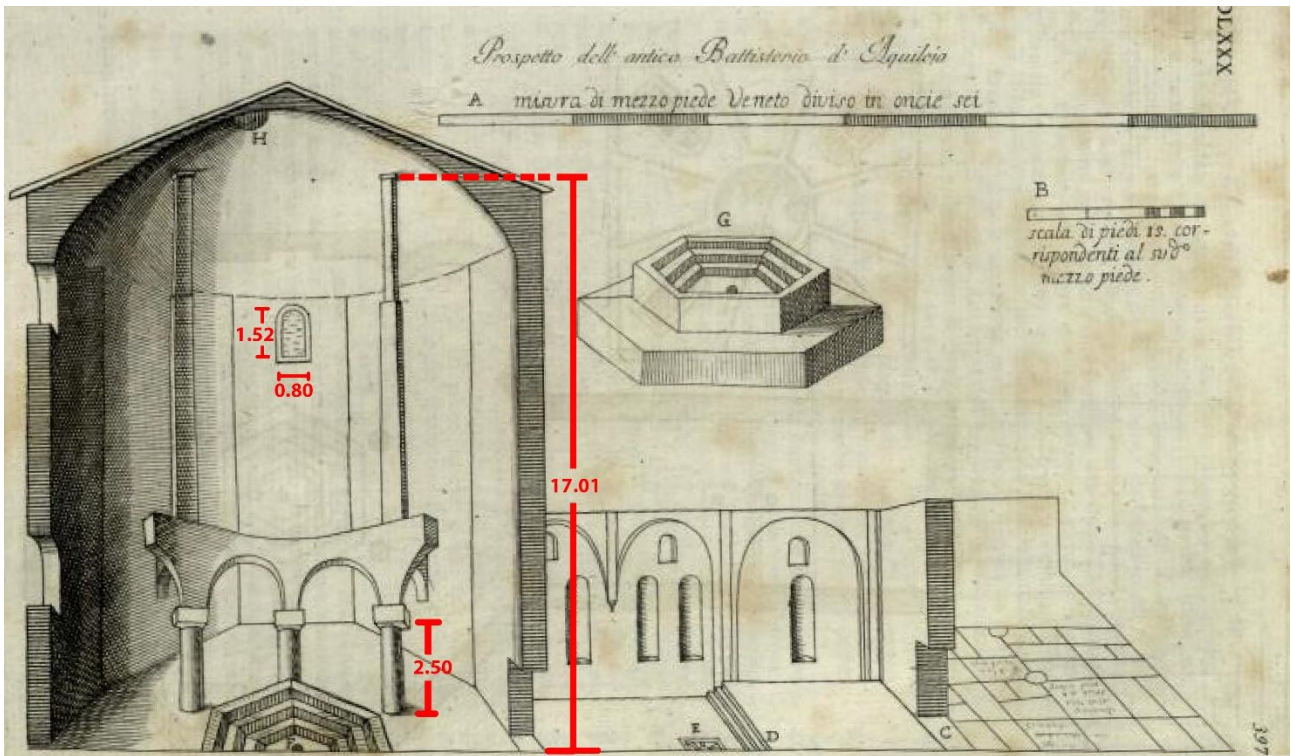


Figure 132: Old cross section, with measurements in metres

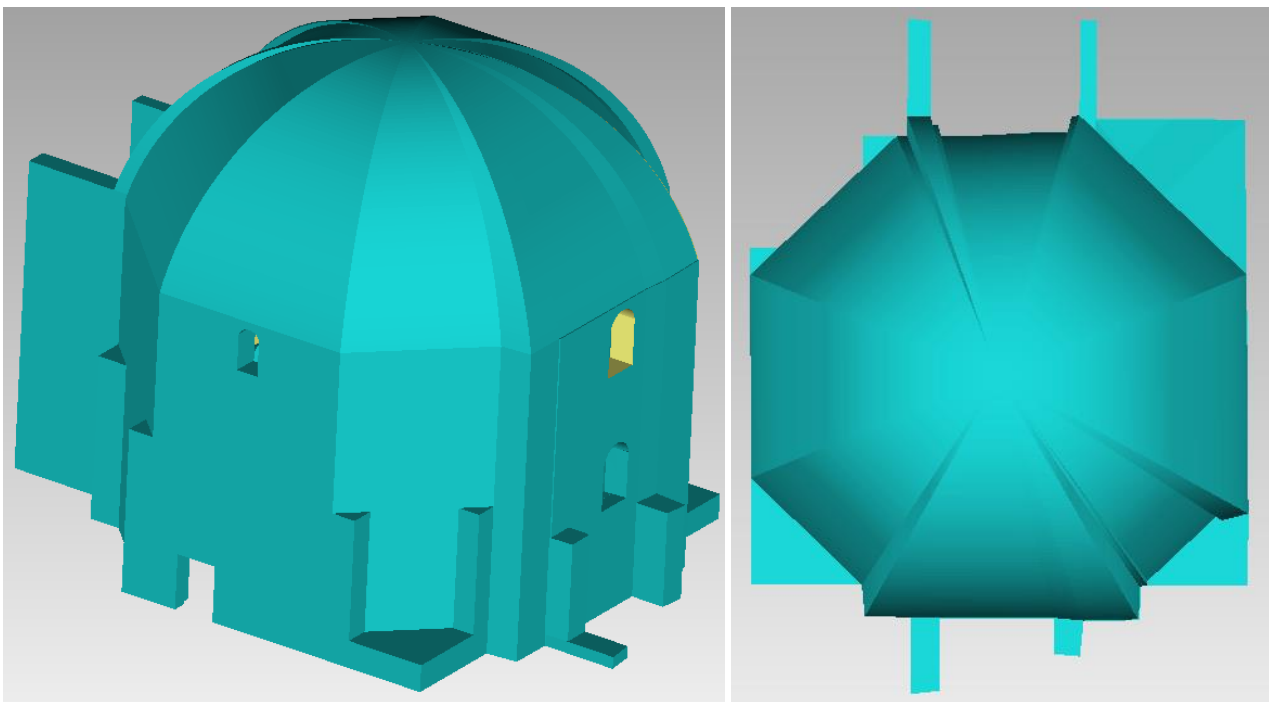
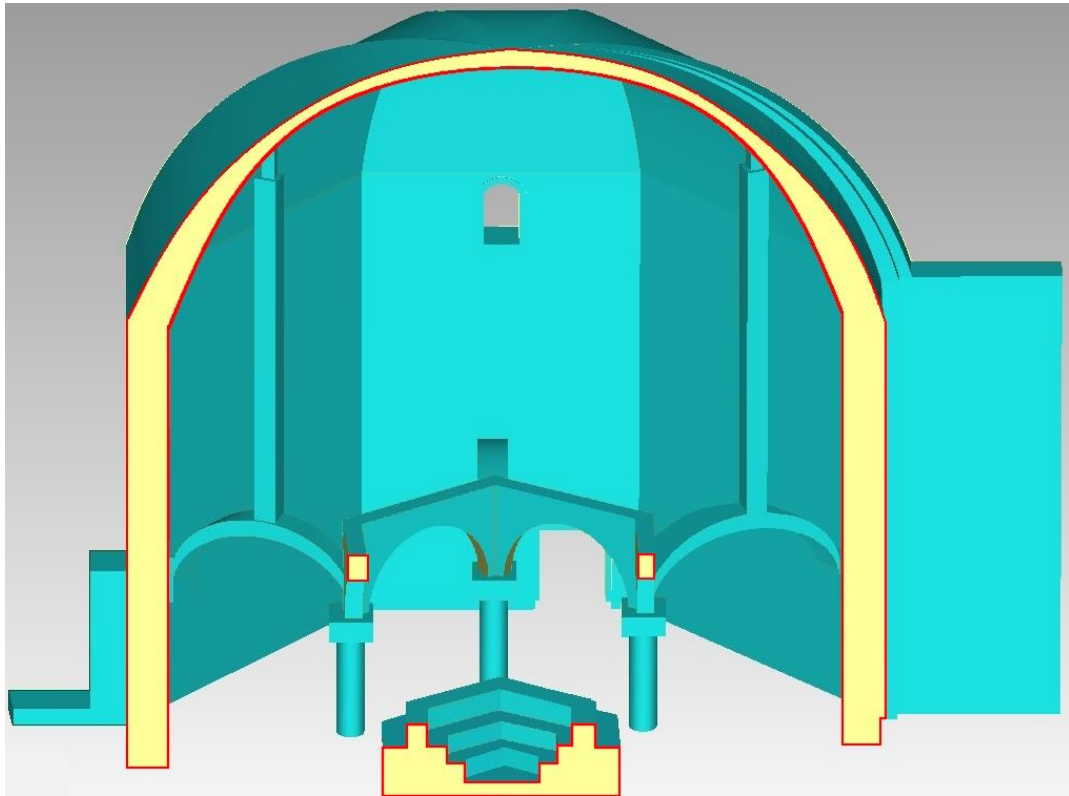
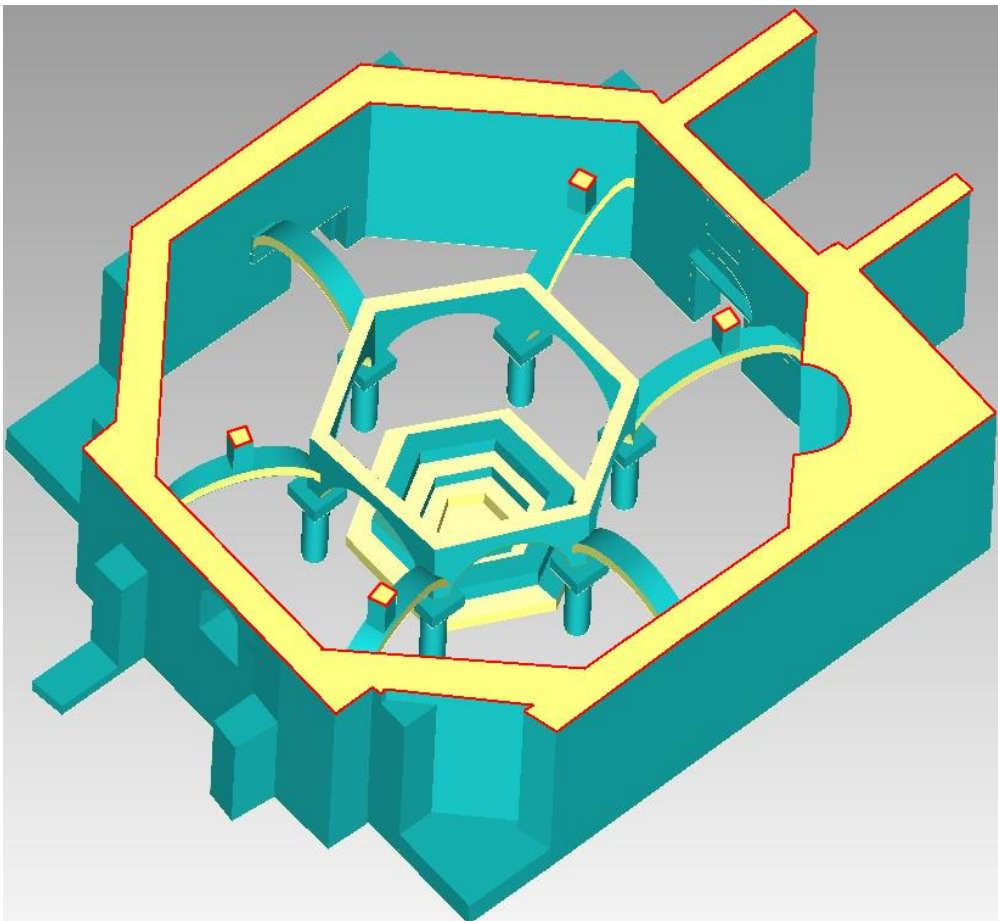


Figure 133: The three-dimensional model reconstructed as its first configuration. In the left, external view from the South front, in the right, view from the top.



*Figure 134: Vertical section, in which it is possible to see the column linked to the internal surface of the dome*



*Figure 135: Horizontal section at 2.60 of height. The six arches are connected to the perimeter walls, and the columns in each corner of the font are characterized by the capital on the top*

Another simple three-dimensional model was realized starting from the measures obtainable by the plans and sections derived from existing documents of the Baptistery (**Figure 136**), more recently than the Bartoli one, obtained from previous direct surveying. This reconstruction well represents the typical level of detail usually realized in general for example of reconstruction, or adopted for the models used in structural analysis. This was also realized with Rhinoceros 5.0 software.

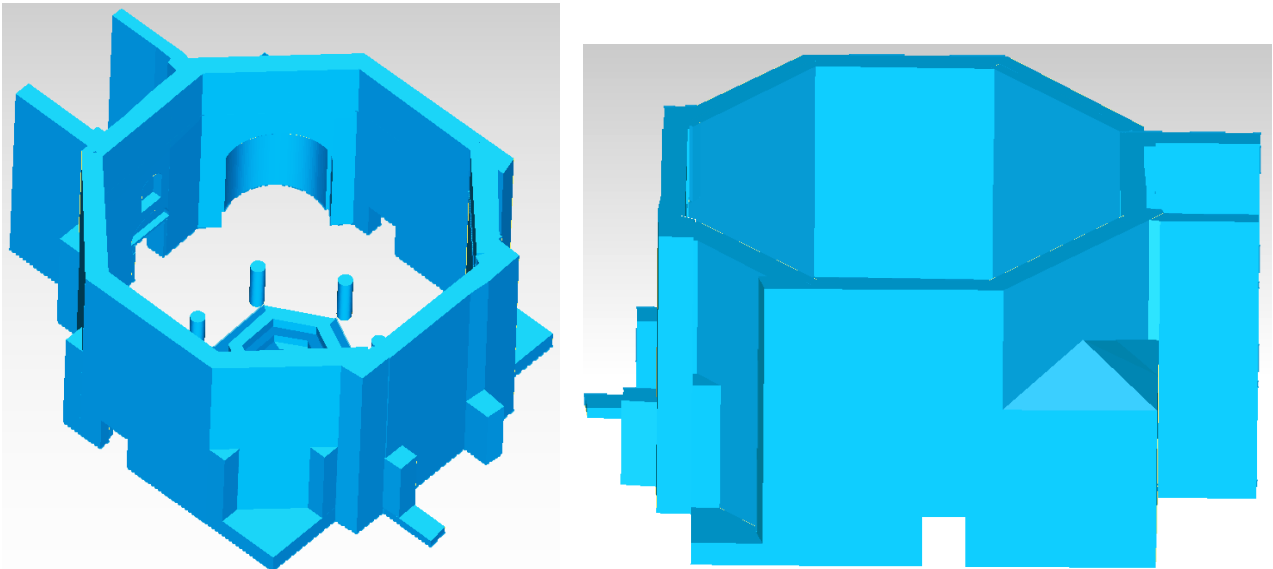


*Figure 136: Reconstruction of three-dimensional model in the configuration without the dome*

### 6.5.2 Comparison of results

The comparison between numerical model (point cloud dataset or polygonal model) with the geometrical one, is very important in order to evaluate the accuracy obtained from three-dimensional surveys. Starting from the polygonal surfaces concerning only the Baptistery, three horizontal sections have been realized at three different heights, in particular the first one to a level of 0,50 metre, the second one to five meters, and the last one to 10,75 meters (**Figure 137**). In order to analyse the area of the masonry at different layers, the sections have been transformed into images, then composed by pixels. The change detection procedure is followed; as known, it concerns the object based, in particular the grouping of pixels. Through a decisional tree (**Figure 138**), parallel maps are identified.

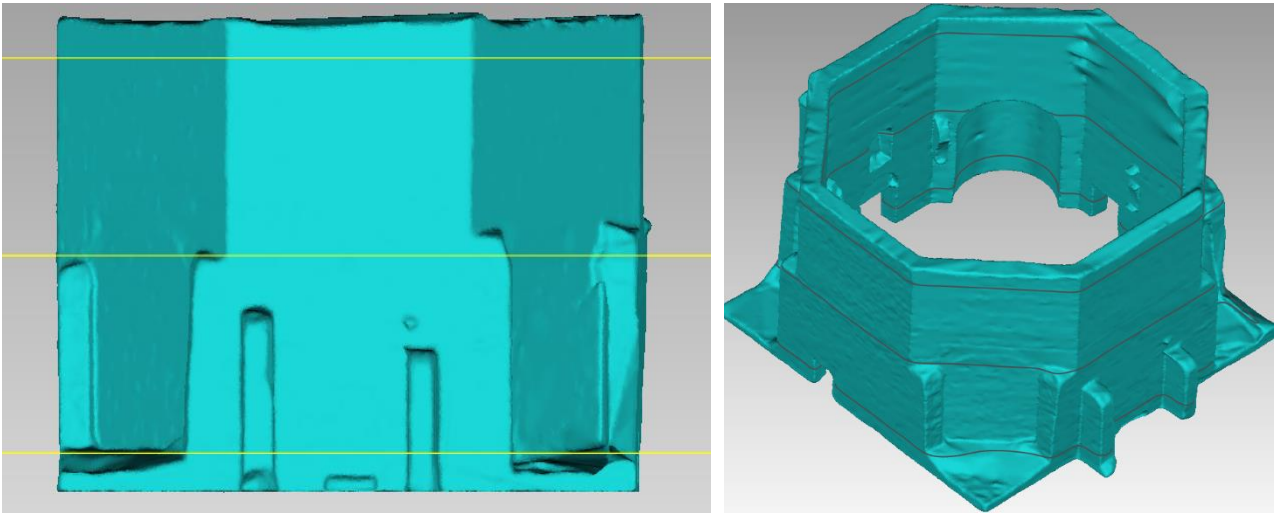


**Figure 137:** The polygonal model of the Baptistery with the overlap of the three horizontal section in different layers

The first step has been to classify the sections in two portions, 255 for the filled area and 0 for the empty space (in this case, 255 is the masonry that compose the building). This procedure is carried out through the object based approach, or classification of objects, that segments the image for the section considered, and assigns the grouping of pixels to different categories.

Once obtained the segmentation and classification for the two sections analysed (the first one and the second one), they could be compared and the change detection procedure (increase, decrease or no change of elements) is classified (**Figure 139**) directly through the software (eCognitionDeveloper). An automatic procedure compares two input data each time.

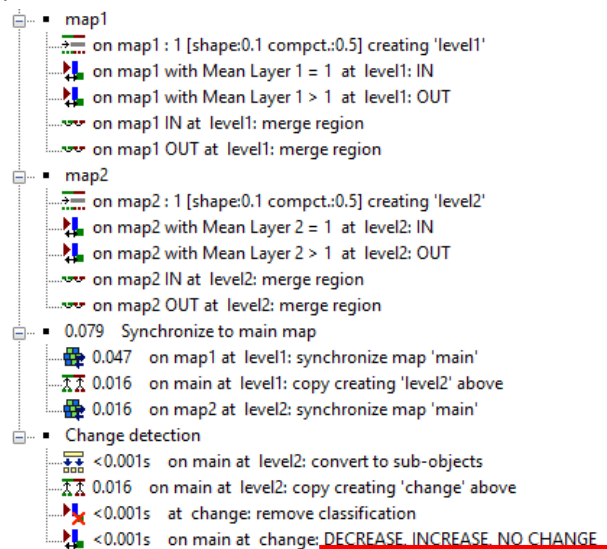


**Figure 138:** Process tree of the first section and the second one. As shown, each section is considered as a map (map 1, map2), the filled area is identified as “IN”, and the external area as “OUT”. The final results, obtained by change detection, are underlined with a red line

The same procedure has been applied also between the first section and the third one, as shown in **Figure 140**. Therefore, with the overlap between the sections of the baptistery at different layers, several elements can be calculated with accuracy, like decrease, increase and no change between the sections. Through this procedure, it is possible to calculate the precise areas of the masonry, that in a geometrical model is pretty constant because the three-dimensional model derives from the measures obtainable by the plans and the sections of existing documents, and only with traditional survey.

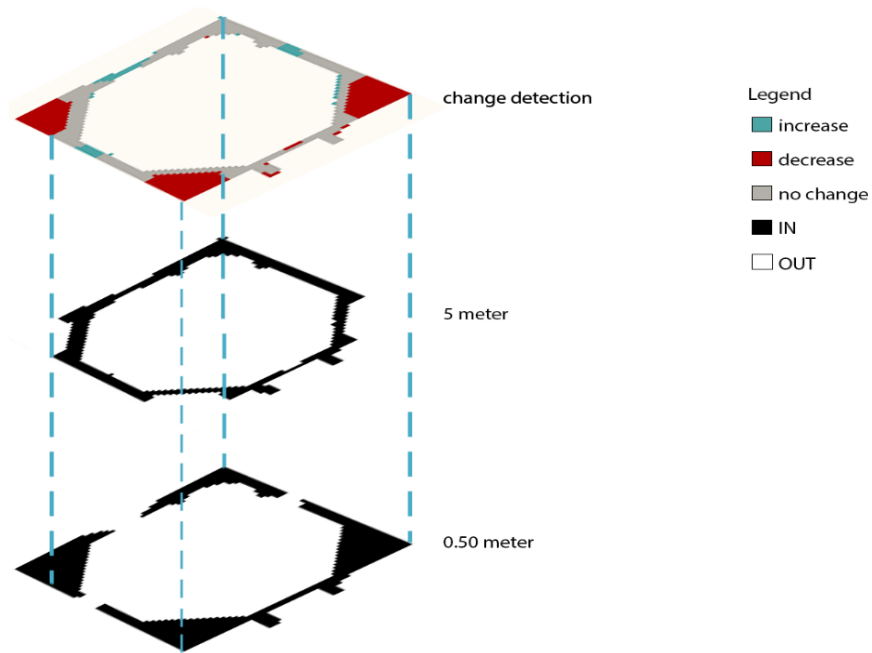


Figure 139: Change detection between first and second section

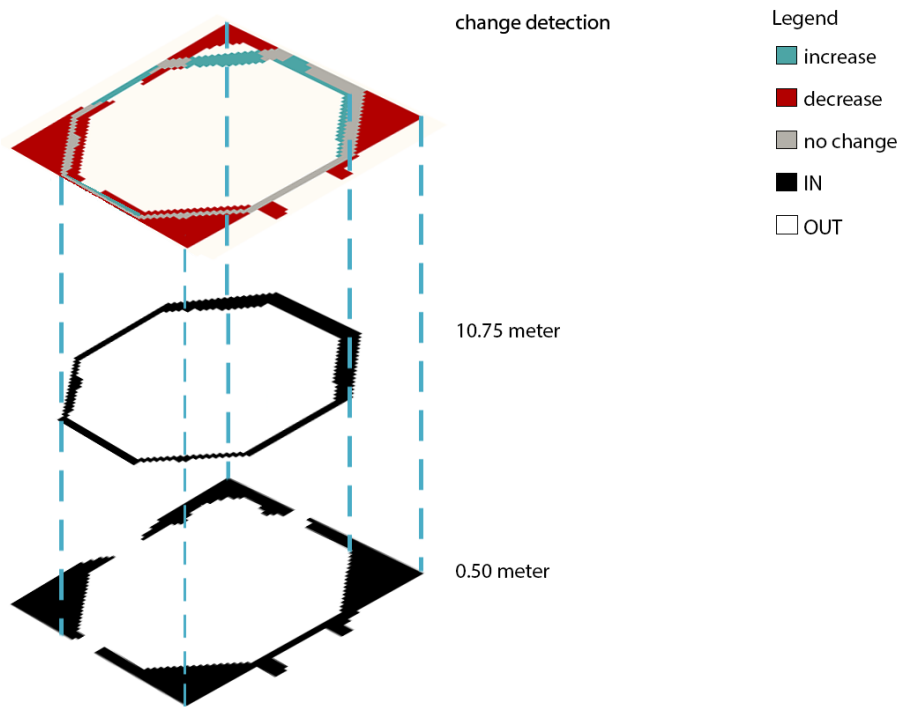


Figure 140: Change detection between first and fifth section

	Area (m <sup>2</sup> )
Decrease	98.5
Increase	26.6
No change (IN and OUT)	577

Table 13: Change detection between the first and the fifth section, i. e. between 0.50 meter and 10.75 meter

Another comparison has been carried out between the polygonal model (Figure 131) and the geometrical one (Figure 136), in order to see the differences between the three-dimensional model deriving by manual reconstruction and the one obtained from three-dimensional survey. This is an interesting comparison also because, without a precise three-dimensional survey, this geometric reconstruction well represents the typical level of detail usually adopted to obtain geometrical models, as for example those used for structural analysis.

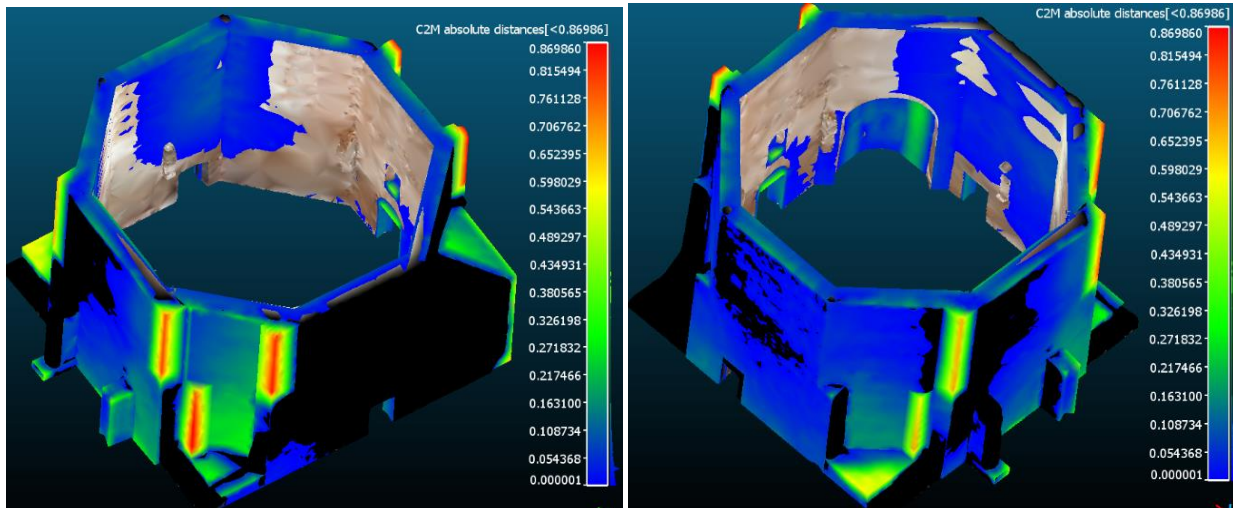


Figure 141: The 3D reconstructed model compared with the polygonal numeric model. In the left, view from the north-east side; in the right, view from the south-east side.

From the analysis of the two models, how it is possible to see in the Figure 141, the geometric differences are really relevant, reaching, in some point, the value of 0.86 metres, identified with red color. Beside these macro-differences, the most significant variances depend on the reconstructed three-dimensional model, which does not take into account the slope and the irregularities of the surfaces, but has been realized with a central symmetry and a perfectly regular shape. Furthermore, some parts reconstructed through the drawing of Lanckoronski (1906) do not exist anymore, and this justifies the greater discrepancies.

As seen in the Figure 141, the most evident differences (red) are located in the corners reproduced with perfect geometry in the reconstruction, but in reality they cannot be with a perfectly shape squared. Another evidence of these regular shapes, is present in the aps and in its vaults, where the difference between the two surfaces is quite constant over 0,16 metres. On the other hand, this result could be more than expectable, since it is quite hard to proceed with measurements of such a surface with direct methods, and usually it is simplified with a circular shape surface.



**Figure 142:** Cross section and overlap between the three-dimensional polygonal model, and the reconstructed one. The black parts are the section of the polygonal model, the blue part is the section of the geometric reconstruction.

On the other hand, with the overlap between the input model and the reconstructed one, from a cross section it is possible to observe how the blue lines (reconstructed model) are perfectly vertical, on the contrary in the reality, where the perimetral wall in the left, for example, (Figure 143) is slightly inclined outwards, of about 2,5 centimetres how it is possible to see in the following section.

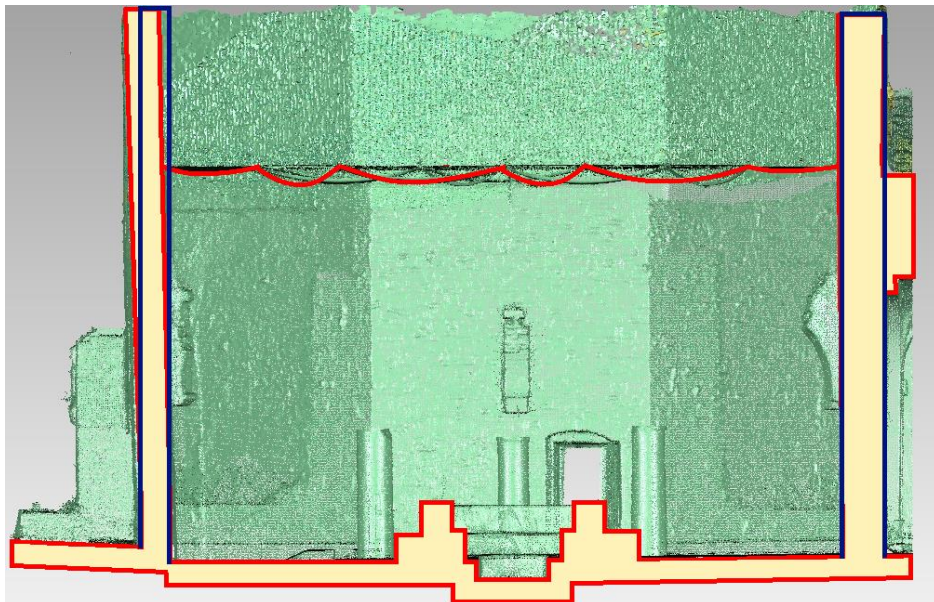


**Figure 143:** Overlap between cross section of point cloud dataset (red lines and yellow parts) and reconstructed model (blue lines).

## 6.6 Geometrical evaluation of baptismal font

As seen, the baptismal font is the most characteristic element in the internal part of the baptistery; furthermore, its center coincides with the center of the entire building (Figure 144). For these reasons, it offers ideas for several and different analyses.

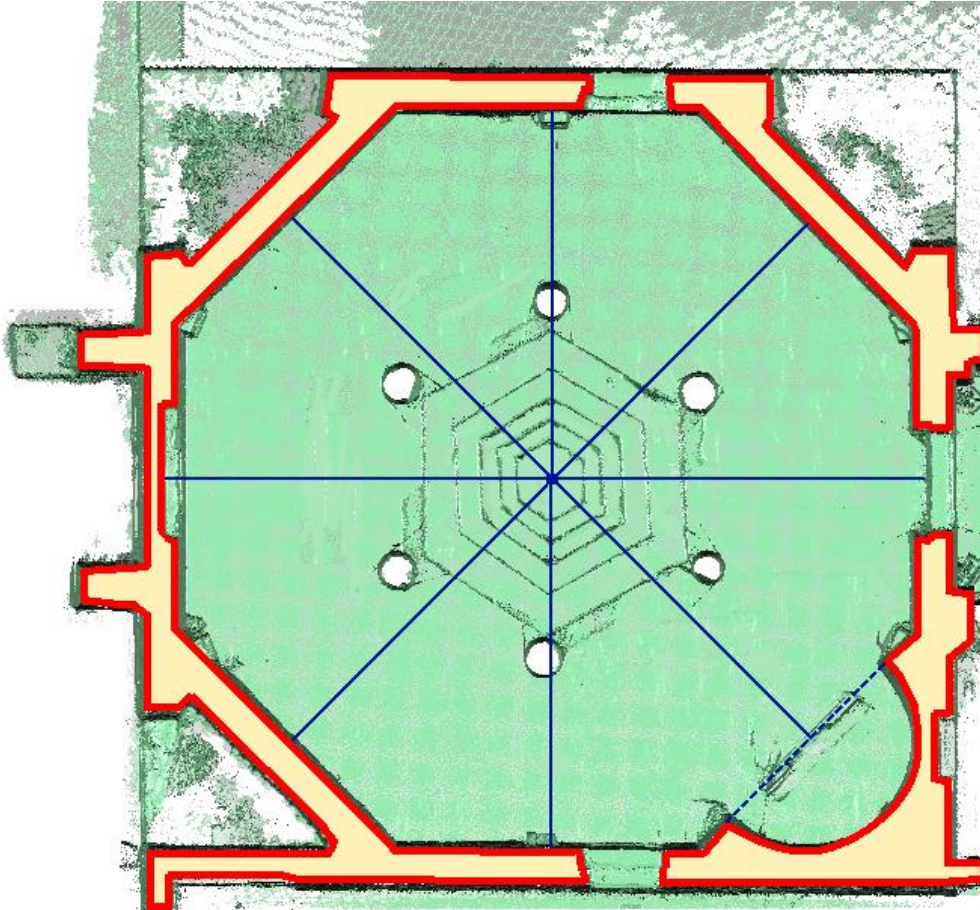


*Figure 144: Horizontal section of point cloud dataset, at a height of 1.60 metres. The red lines and the yellow parts identify the sectioned walls. By drawing lines from the middle of each side of the internal wall (blue lines), it is possible to see how the centre of each line coincides with the centre of the Baptistery (that is also the centre of the baptismal font)*

### 6.6.1 Photogrammetric data: acquisition, processing and results

Photogrammetry is characterized by a relatively rapid data acquisition phase, but followed by a time consuming manual measurement, and computational data processing stage. An architectonic or archaeological object is usually characterized by sharp edges, with a high level of detail. This means that many series of complex photographic blocks have to completely describe the object of study. When a detailed element has to be surveyed, the use of speed and automatic workflow that reduce as much as possible the user interaction, allows to minimize the elaboration phase. As shown in the flowchart (Figure 96), internal details have been acquired not only with GoPro camera, but also with a Panasonic DMC TZ60 non-metric camera. Photogrammetric elaboration has given very satisfactory results, despite the instrument used is not professional. To have a complete description of the object, 36 pictures have been acquired around the hexagonal element. All the pictures have been used, and a close range acquisition is performed, in order

to reach the maximum detail as possible, and to evaluate the behavior of different software tools in processing CRP. In fact, some tests are presented, performed with the purpose to analyze the possibility to compare different software packages that follow different workflows, in order to evaluate their effectiveness and weaknesses.

The acquired images were processed using some of the different software tools implementing photogrammetry and computer vision algorithms, in order to evaluate their behavior in the processing and results. The models were then georeferenced in the same reference system using the measurements deriving from TLS survey. This also allows to easily compare the different results. The resulting dense point clouds have been finally compared using as reference the TLS point cloud. In particular, the acquired data have been processed using the Structure from Motion (SfM) approach implemented in different software tools: Agisoft Photoscan Professional, Context Capture and Visual SfM package. The process is carried out almost automatically by these software tools, based on algorithms of photogrammetry and computer vision that allow to process a large amount of images in a fast and easy way, with a limited influence of the user on the resulting dense point cloud. The analysed software are commercial, proprietary solutions, except Visual SfM (Wu, 2011) with the integrated algorithm CMVS/PMVS (Furukawa Y., 2010). All these software tools differ in the algorithms used for the image processing and matching, and in the different possibilities on the various parameters setting. However, they all lead to the images alignment, generation of dense point clouds. Generally, the input data required by these tools to perform the 3D model reconstruction process are only the acquired images and some GCPs. According to the acquired data, the obtained point clouds offer a complete 3D model. In **Figure 145**, two views of the achieved point clouds are reported.

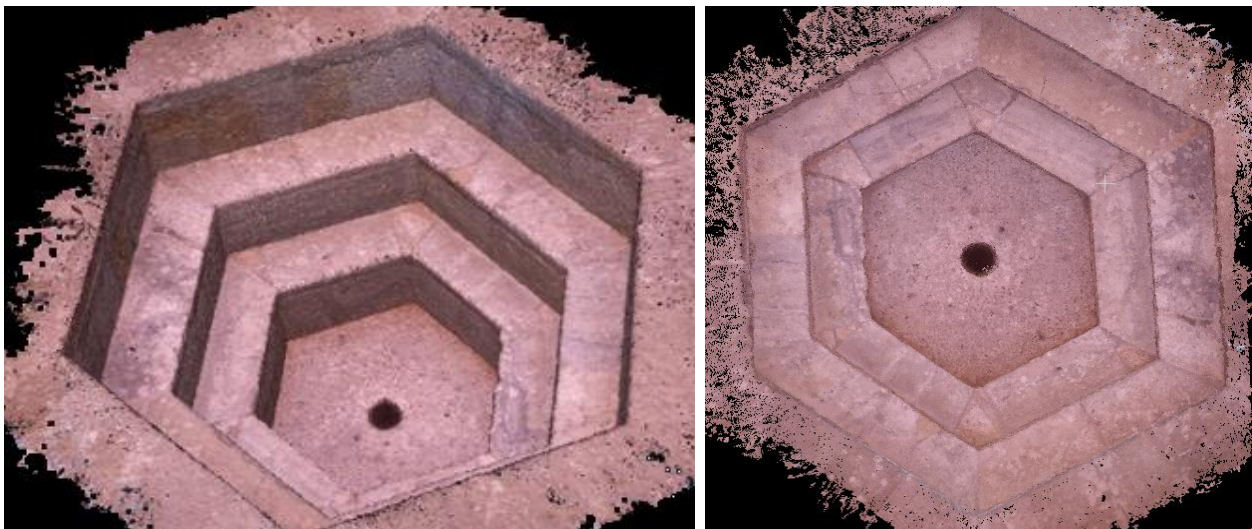


**Figure 145:** Point cloud dataset deriving from Photoscan software

Different density of points are characteristics of each software and processing parameters. In the following **Table 14** a summary (in terms of millions of points) of the generated clouds is reported. The denser cloud was obtained by the Context Capture software, more than 139 million of points, despite the lower derived from Visual SFM.

	Photoscan	Context Capture	Visual SFM
Number of points	4.270.839	139.711.711	575.189

*Table 14: Number of point for each 3D model*

The comparisons and the results have been performed using the software CloudCompare, on a part of the generated point cloud, considering as reference the TLS point cloud (**Figure 146**). In fact, despite the TLS is not the most appropriate instrument for the acquisition of such a detailed element, by acquiring the interior of the structure, also the baptismal font was measured using TLS. For this purpose, a portion of a baptismal font measured using TLS has been exploited for reference in the comparison between the different photogrammetric elaborations. For this reason, this evaluation has to be considered only as an initial test.

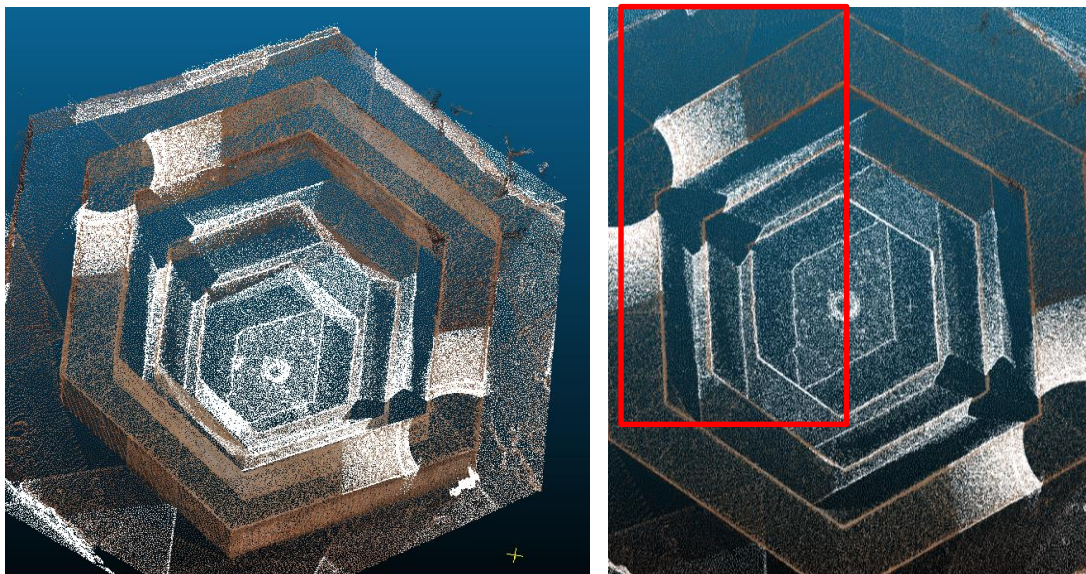


*Figure 146: Acquisition of the baptismal font with TLS. As shown, some parts are very noisy. In red, the portion used for a comparison with photogrammetric approach.*

A quantitative result is given by the computation of the minimal distance between every point of the models using the Nearest Neighbour algorithm. The software allows also to calculate statistical values, such as minimal distance, maximal distance, average distance, standard deviation.

These values are reported in **Table 15**.

**Figure 147**, **Figure 148** and **Figure 149** report the maps of the discrepancies. The scale bars on the right part of the images also show a graph of the error distribution. How it is possible to observe from the maps of the discrepancies, the differences between the point clouds have quite constant, from 6 millimetres to 2 centimetres (blue and green colors).

Software	Photoscan	Context Capture	Visual SFM
Min dist. [cm]	0	0	0
Max dist. [cm]	1.08	1.27	2.24
Average dist. [cm]	0.09	0.13	0.16
Standard deviation [cm]	0.09	0.14	0.20
Max error [cm]	0.08	0.10	0.10

*Table 15: Values of the comparison between the TLS data and generated point clouds from photogrammetric acquisition (CRP)*

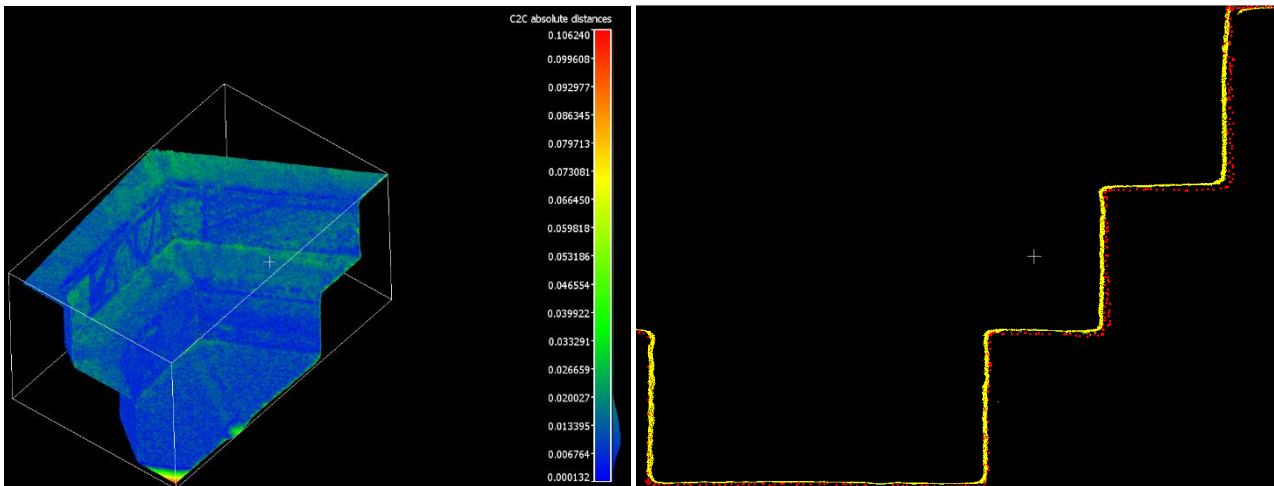


*Figure 147: Overlap and differences between 3D point cloud dataset deriving from Photoscan software, and TLS dataset with the graph of error distribution (left). In the right, overlap of two sections: the yellow one is from photogrammetric model, and the red one from terrestrial laser scanning.*

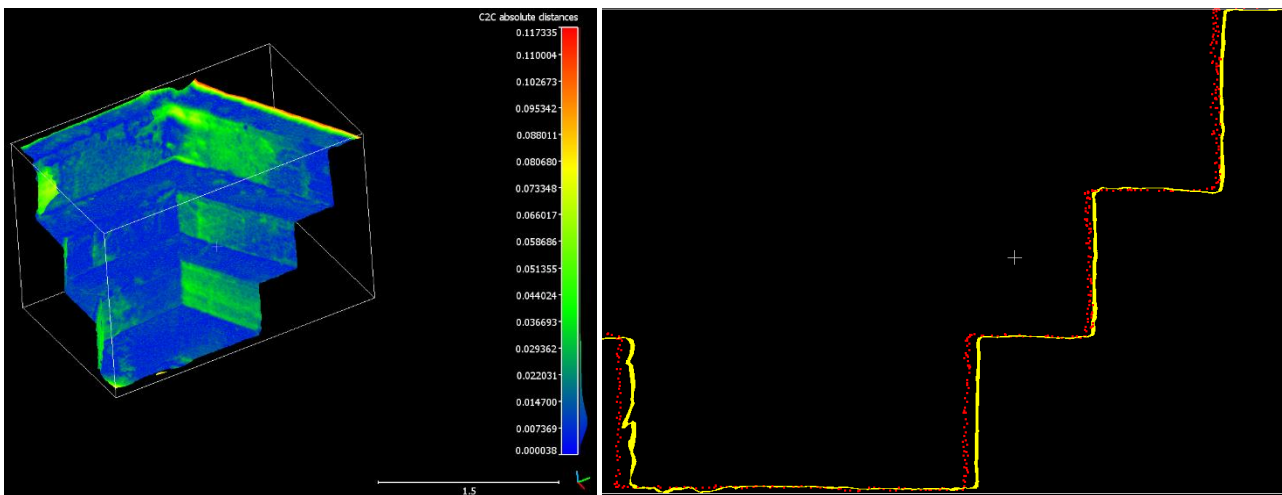


*Figure 148: Overlap and differences between 3D point cloud dataset deriving from Context Capture software, and TLS dataset with the graph of error distribution (left). In the right, overlap of two sections: the yellow one is from photogrammetric model, and the red one from terrestrial laser scanning.*

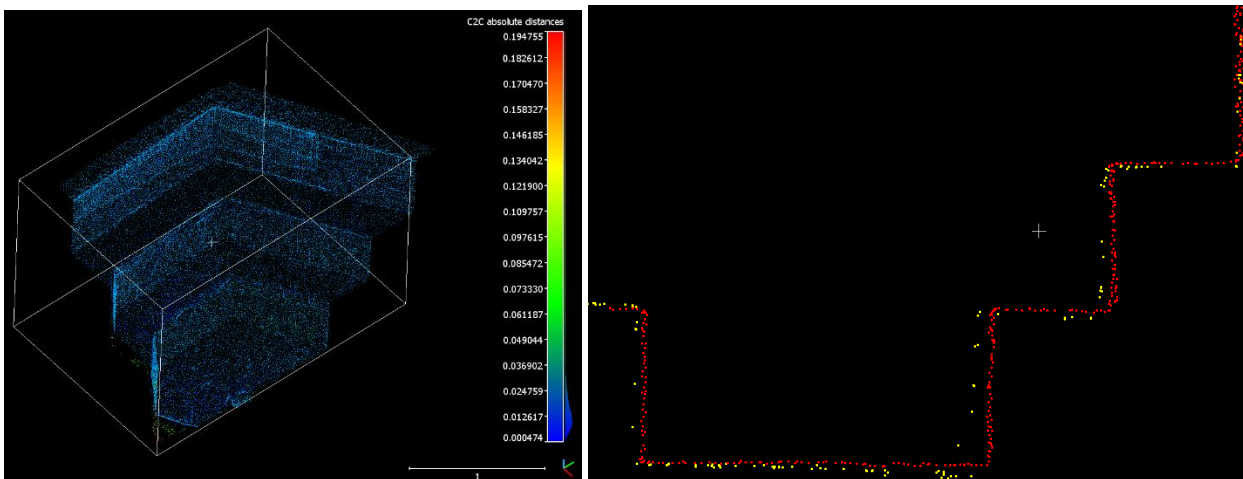


Figure 149: Overlap and differences between 3D point cloud dataset deriving from Context Capture software, and TLS dataset with the graph of error distribution (left). In the right, overlap of two sections: the yellow one is from photogrammetric model, and the red one from terrestrial laser scanning.

By comparing graphs and data referring to each point cloud dataset, it is possible to observe very different quality deriving from each software. In order to underline some pros and cons according to the achieved outputs it is possible to state that the point clouds generated by Visual SFM has the main error as final Standard deviation (close to 2 cm). According to the achieved results, with (Photoscan, 2013) the results obtained are closer to the point cloud dataset derived from TLS (Figure 147). With Context Capture software, the generated output point cloud was more than 130 million of points, without noise. Visual SFM is an open source software and it is not the best instrument for the generation of very dense point cloud; nevertheless, the results in terms of average and max errors, are similar to the others. The used software tools are able to realize suitable product in a quite similar way although some slight differences appear in the results.

### 6.6.2 Comparison with old data

The historical research, and the documents and data available, have allowed to develop further analysis concerning the baptismal font. In the following Figure 150 and Figure 151, an overlap between the two-dimensional point clouds extracted from point cloud dataset and the historic documents, show differences not only in the baptismal font, but also in the columns around it.

The intersecting plane is adjusted manually to the extent of the old plans, and the profile was rotated and translated. So, the profiles are compared to the old plans in the software AutoCAD. Through visual inspection, same points on the profiles and on the old plans are identified to define the transformations. The old plans are transformed through a translation, scaling and rotation to the profiles. In Figure 150 and Figure 151, the generated profiles are overlaid to the old plans. There are discrepancies between the old plans and the new generated profiles.

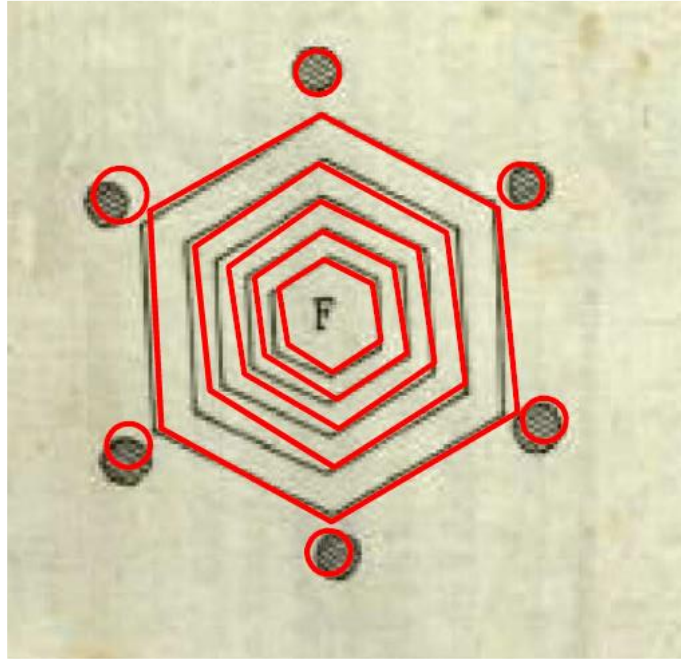


*Figure 150: Comparison between old plan from Bertoli illustration, and profiles of the baptismal font*

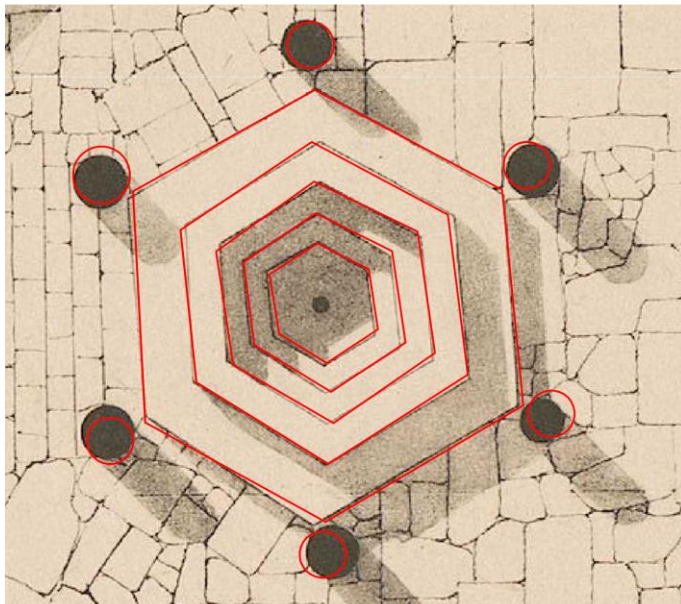


*Figure 151: Comparison between old plan from Lanckoronski illustration, and profiles of the baptismal font*



In order to analyze the discrepancies not only in two-dimensional space, but also in three-dimensional space, the model of the baptismal font has been carried out in (Rhinoceros, 5.0). In particular, starting from the old drawing and descriptions made by Bartoli, the three-dimensional model has been created and then compared with the polygonal model derived from photogrammetric dataset and elaborated with Photoscan. As mentioned before, the initial point dataset was about 4 million of points, and after the transformation, cleaning and decimation, the final polygonal model was characterized by less than 2 million of triangles. The comparison has been developed with CloudCompare. From the overlap between the two models (**Figure 155**), there is an absolute distance lower than 29 centimetres

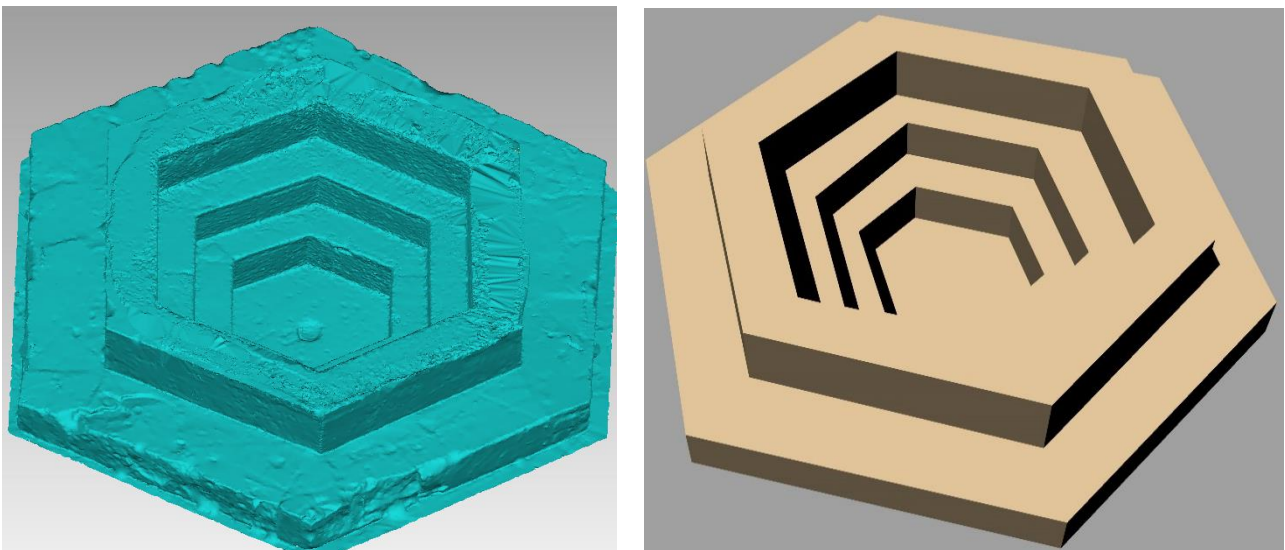


**Figure 154:** Polygonal model deriving from photogrammetric elaboration by Photoscan software (left), and geometrical model carried out in Rhinoceros software (right) starting from measurements and profiles found in the historical documents (Bartoli).

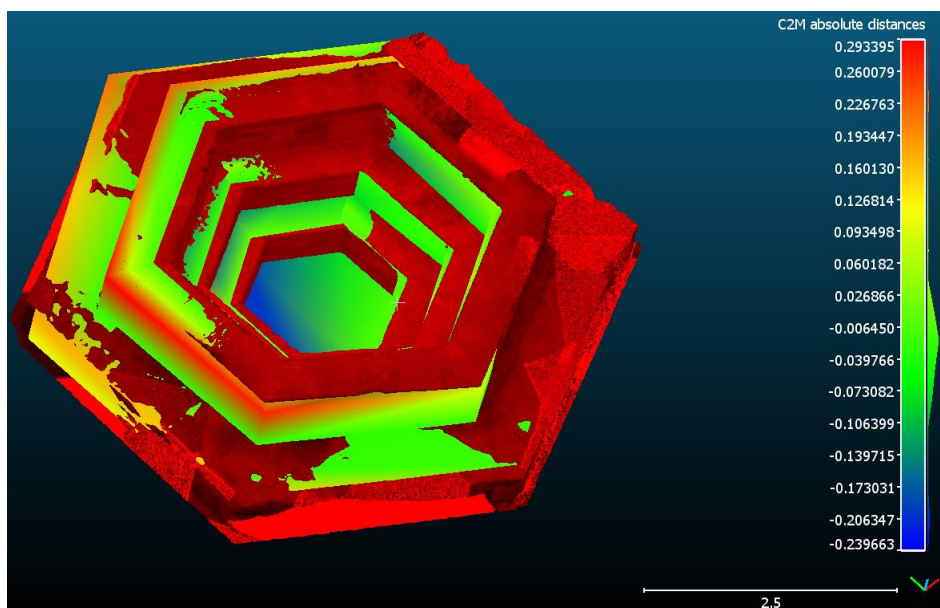


**Figure 155:** Comparison between geometrical and polygonal model, in Cloud Compare. It is possible to see how, as in plan (**Figure 152**), the maximum discrepancies are lower than 30 centimetre. The red mesh is the polygonal model of reference.

### 6.6.3 Columns: geometrical analysis and static considerations

As previous seen, the columns around the baptismal font are six, each in its corner. Although they seem with the same section, thanks to the point cloud it is possible to analyse how each section has different and non-constant dimension, and consequently also the central core of inertia. As it is known from the literature, for a generic circular section the central core of inertia is a circular section, with the diameter equal to a quarter of the section considered. Hence, it is evident how the central core of inertia is strictly conditioned by the correct geometry of the element. This analysis is very important because, considering for instance the [Figure 134](#), it is clear how the columns were subjected to a vertical force due to the arches that transferred their loads. For each arch, the resulting thrust have to be in the central core of inertia, in order to avoid tensile loads. In order to have precise values of the diameters for each column, starting from the polygonal model an overlap between the three-dimensional model and horizontal planes has been made, with a range of 30 centimetres for the entire height of the elements, as shown in the pictures.

An interesting work is offered by (Cannella, 2015), where is shown an interesting extraction of geometrical data, from the polygonal model obtained with a TLS surveying. The research explains the methodology applied to the representation of the column shafts and capitals of the Temple C in Selinunte Archaeological Site. Using mathematical auxiliary surfaces and NURBS modelling tools, textured highly-detailed meshes, produced with photogrammetry and laser scanner 3D data, was unwrapped onto a reference plane.

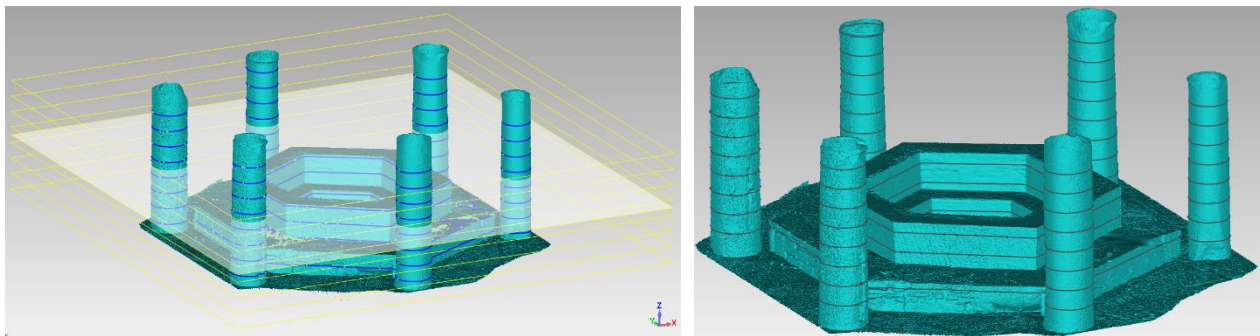


*Figure 156: The polygonal model has been overlaid with horizontal planes, with a spacing of 30 centimetres. In this way, the columns are wholly described by two-dimensional sections.*

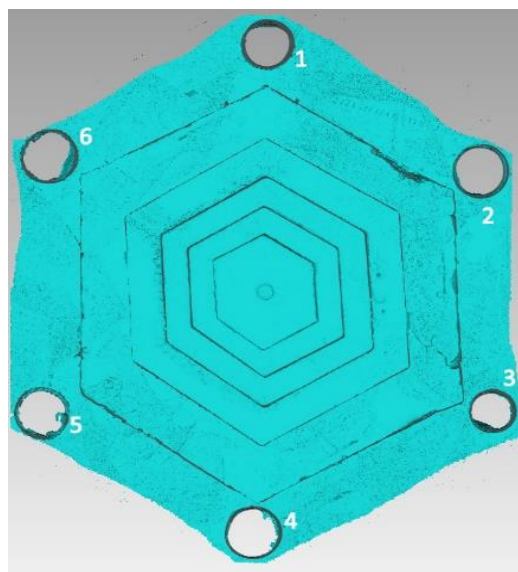


*Figure 157: Plan of baptismal font and columns with the numbers as reference*

Layer of each horizontal plan (centimetre)								
No of column	30	60	90	120	150	180	210	240
1	69.5	65.4	63.5	63.4	61.4	61.3	61.3	59.3
2	70.5	71.3	70.5	68.9	68.1	67.1	66.3	65.9
3	60.6	60.1	59.3	58.7	58.3	57.6	56.8	56.1
4	72.0	71.7	69.8	66.7	65.9	62.5	62.0	61.0
5	65.5	64.6	62.3	59.0	58.7	53.7	52.6	51.6
6	71.9	67.6	65.3	62.1	60.4	56.7	57.5	54.1

*Table 16: Diameter of each column, changing the horizontal plane of reference*

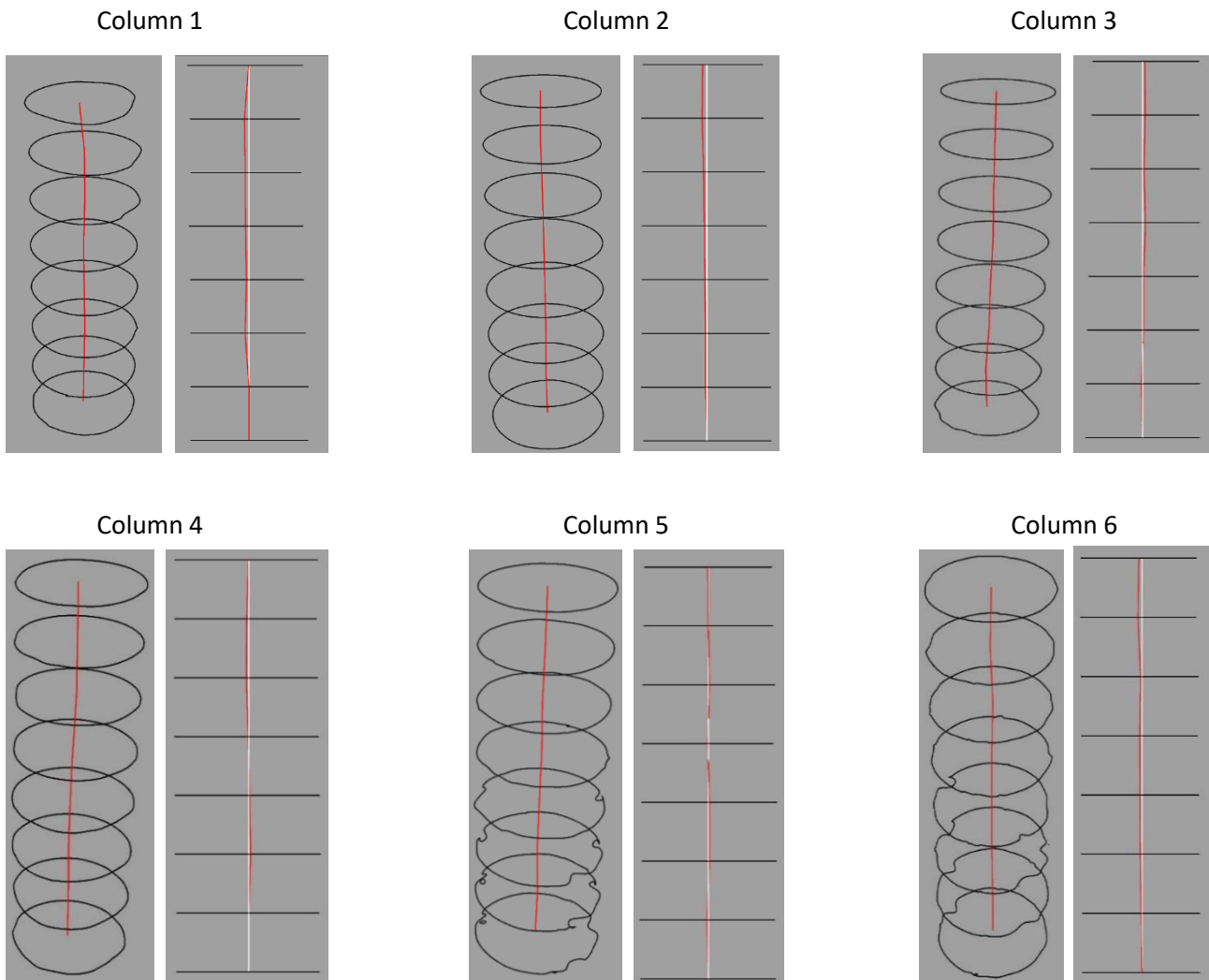


*Figure 158: The columns described by two-dimensional lines, with a step of 30 centimetre. The red lines represent the connecting axis between each centre of the circumference. The white lines are the vertical axis of reference. In this way, it is possible to note the discrepancies between the real axes (red) with the vertical one (white).*

Analysing a column on which there are two different loads (the connecting arch between each column and the transversal one by connecting to the perimeter wall, as shown in [Figure 134](#) and [Figure 135](#)), for example the no. 2 ([Figure 157](#)), the comparison between the geometric construction and polygonal model has been done, in order to highlight the differences also in three-dimensional space. The geometric construction has been carried out in (Rhinoceros, 5.0) software: starting from the two boundary profiles (upper and lower) obtained using TLS, a three-dimensional column has been created, by revolving the two profiles of circumferences around a vertical axis, as shown in [Figure 159](#).

As it is possible to see, an overlap between geometrical model and polygonal one of the columns no. 2 has been made, in order to analyse the discrepancies also for an element of little size, as is a column. Despite the lower and upper profile of the geometric model have the same size of that of polygonal model, from the analysis between the polygonal textured model with the wireframe geometric model, in some points a maximum discrepancy of 4 centimetres has been measured. In general, the medium value measured is 1 centimetre.

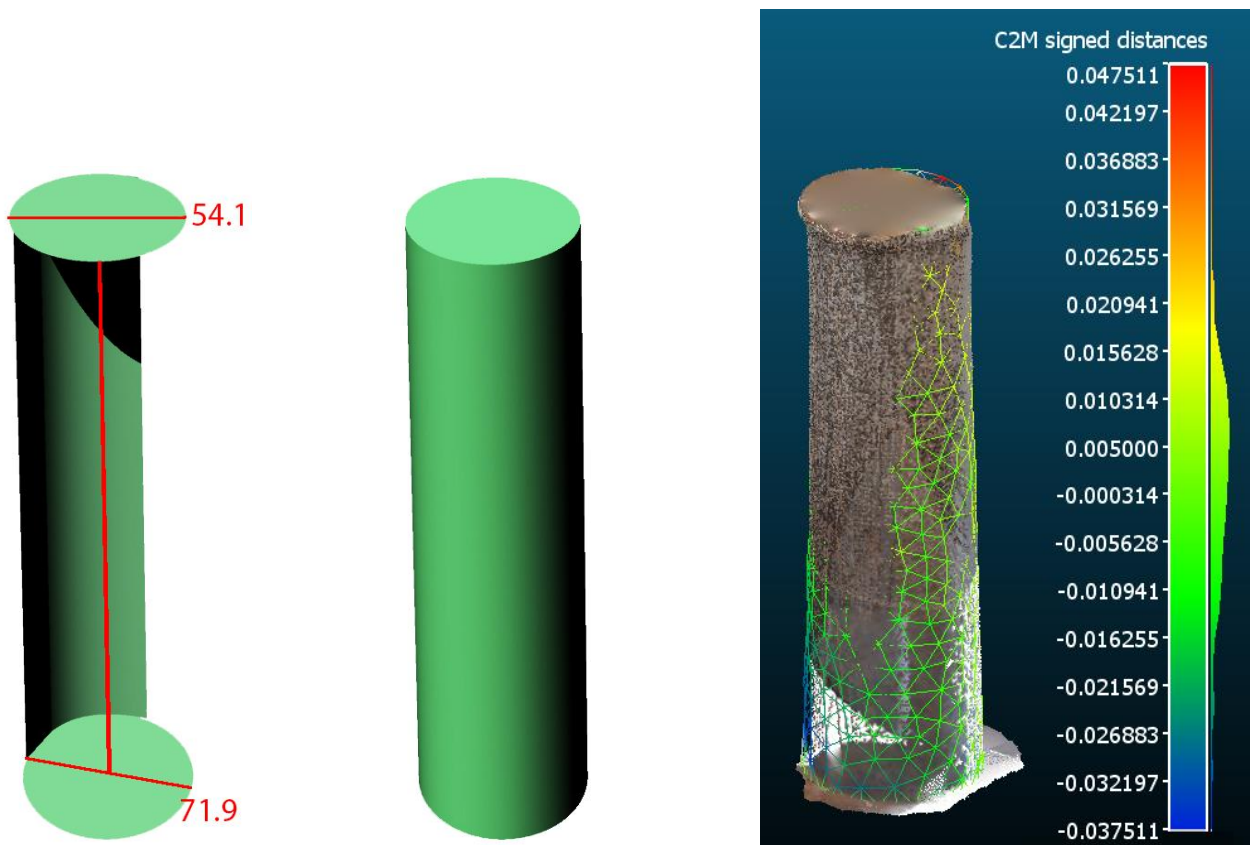
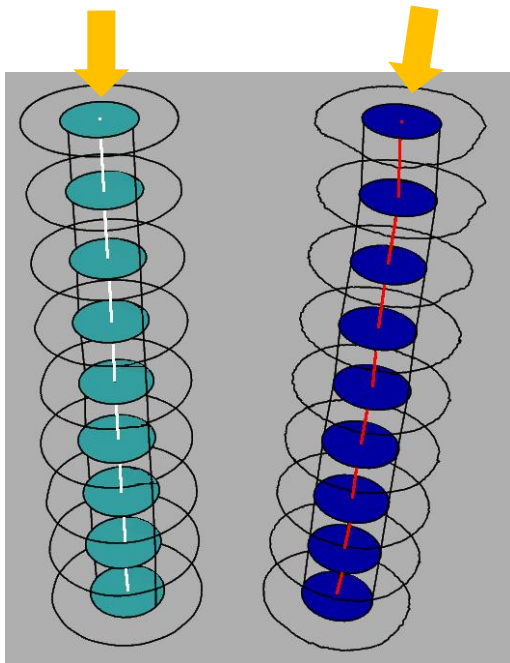


**Figure 159:** Geometric construction of a column and comparison with polygonal model. Left: the revolve curve with a rail in Rhinoceros software, considering a quarter of two profiles. Middle: column with a complete surface, with a rail of 360°. Right: the overlap with the scale bar of the discrepancies between polygonal model and geometric construction

The reason is that the geometrical model is very simplified, and the material wear, geometric lacks, or corrosion deriving from humidity etc. over the centuries, cannot be considered.

Starting from these discrepancies, a further analysis has been made. In fact, the central core of inertia has been calculated and represented in the overlap of horizontal section of the column no. 2, as shown in the following [Figure 160](#). In particular, the green sections are the diameter of the central core of inertia for the geometric model, and the blue sections are referred to the polygonal model. As indicated in the following

table, despite the dimension of each section may seem the same, from the bottom to the top they have different measurements. This may change the static condition of the structure because, considering for example the initial configuration of the baptistery (see [Figure 135](#)), the weight of each arch on the column, have to be within the central core of inertia, in order to avoid tensile stresses on the columns that could cause buckling stress.



Diameter of central core of inertia (cm)		
Level of plan	Geometrical construction	Polygonal model
30	34.2	35.9
60	34.0	33.8
90	33.4	32.6
120	33.0	31.05
150	31.1	30.2
180	30.9	28.3
210	30.1	28.7
240	29.6	27.05

**Figure 160:** In the left, overlap between slices for the column 6, with a step of 30 centimetre. The white line is the vertical one and the green one identifies the diameter of central core of inertia for each layer, for the geometrical construction. The blue surfaces identify the central core of inertia for the polygonal model, and the red line is the real state of the axis. The two arrows symbolize the thrust: it has to be inside to the central core of inertia in order to avoid tensile stresses, and thus could compromise the eventual upper structure. The corresponding measures are reported in the Table in the right.

## 6.7 Structural analysis with different procedures

The three-dimensional model has been analysed with different approaches, in order to transform the initial dataset into a FE model. Although this is not strictly a work of structural field, lots of analysis have been carried out, shown in the next paragraphs, in order to evaluate static and dynamic behaviour of the structure. Regardless of the following procedure for the structural evaluation and for transforming the input dataset in a FE model, three common aspects have to be defined:

- the characteristic of the material;
- the boundary conditions to apply;
- the forces acting on the object to analyse.

According to the Italian legislative framework, the characteristics of the masonry are choosing according the table C8A.2.1 of the (NTC N. N., 2008) , concerning existing masonry.

Type of masonry	$f_m$ (N/cm <sup>2</sup> )	$\tau_0$ (N/cm <sup>2</sup> )	E (N/mm <sup>2</sup> )	G (N/mm <sup>2</sup> )	w (kN/m <sup>3</sup> )
Masonry stones with good texture	260	5,6	1500	500	21
	380	7,4	1980	660	

**Table 17:** Reference values of the mechanical parameters (minimum value and maximum one), and medium weight for masonry stones

In which:

$f_m$  is the average compressive resistance of masonry

$\tau_0$  is the average shear strength of masonry

E is the average value of the modulus of normal elasticity

G is the average value of the modulus of shear elasticity

w is the average weight of the masonry.

As shown in **Table 5** of par. 3.5.1, if only the geometry is known, but there are not precise tests about all the materials that compose the building (masonry, mortar, etc...) the level of knowledge is limited (for more details, see the table C8A.1.2 of the circular (NTC N. N., 2008), and the confidence factor CF is 1.35. This means that the minimum parameters of the

**Table 17** has to be considered, and they have to be divided for the confidence factor. In this way, the resistance of the materials is reduced, in favour of the level of safety. Instead, for the modulus of normal elasticity E, the medium value of the

**Table 17** has to be considered. Ultimately, the values to use are:

Type of masonry	$f_m$ (N/cm <sup>2</sup> )	$\tau_0$ (N/cm <sup>2</sup> )	E (N/mm <sup>2</sup> )	G (N/mm <sup>2</sup> )	w (kN/m <sup>3</sup> )
Masonry stones with good texture	192,6	4,15	1740	580	21

**Table 18:** Reference values of the mechanical parameters, in function of the confidence factor (CF)=1,35 and level of knowledge KL=1

Once defined the material, it is necessary to define the boundary conditions (constraints). Some observations have been made:

- the foundations condition is not well defined but, from the excavations made by Lopreato, it is known that the walls continue for little less than a meter underground. Of course, this is not even similar to the condition of an elastic continue foundation, but assuming that the structure will not move at its basis, it was decided to insert built-in supports in correspondence of the ground floor;
- the connection with the "Church of Pagans" was simulated through the introduction of appropriate constraints, in order to simulate the function of direct connection between the two buildings;

- the connection with the “Mosaic Hall” was not considered since this building was later built and, even if physically attached to the Baptistery, it has its own supports and does not contribute anyway with the structural behaviour of the Baptistery itself.

By concerning the forces on the building, the only load imposed for the analysis is the gravity force.

All the structural analysis (static and dynamics) have been carried out through Abaqus software (Abaqus, Abaqus CAE/User's guide , v 6.14).

### 6.7.1 CLOUD2FEM procedure

For the Cloud2FEM procedure, starting from the emptied polygonal model (Figure 131), horizontal slices with a step of 25 centimetres for all the height of the building have been created.

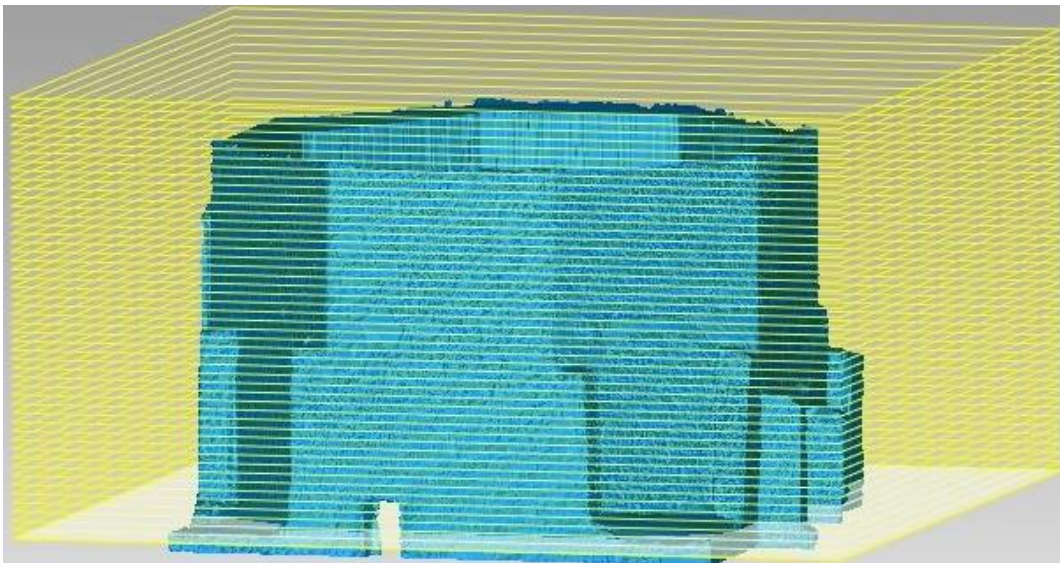


Figure 161: Overlap between the horizontal plans and three-dimensional polygonal model, with a step of 25 centimetre

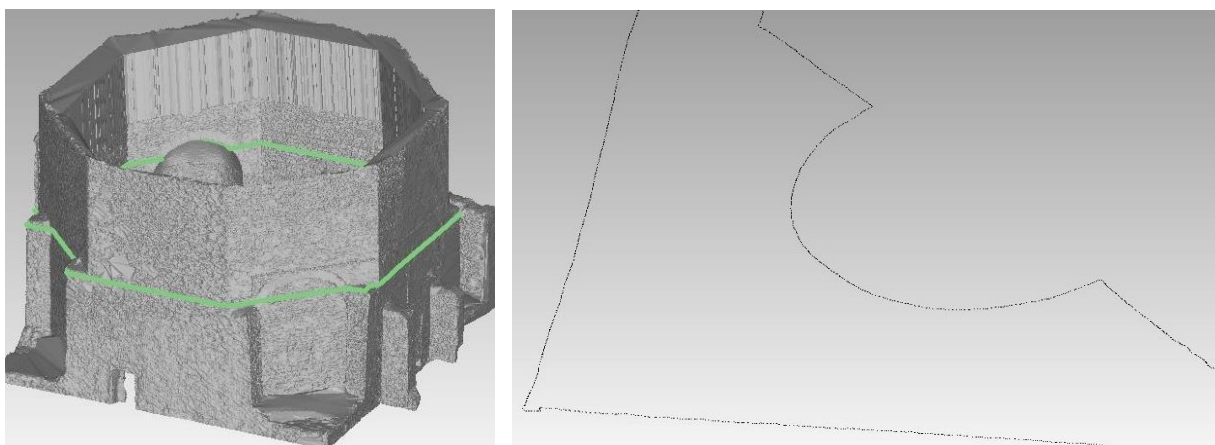
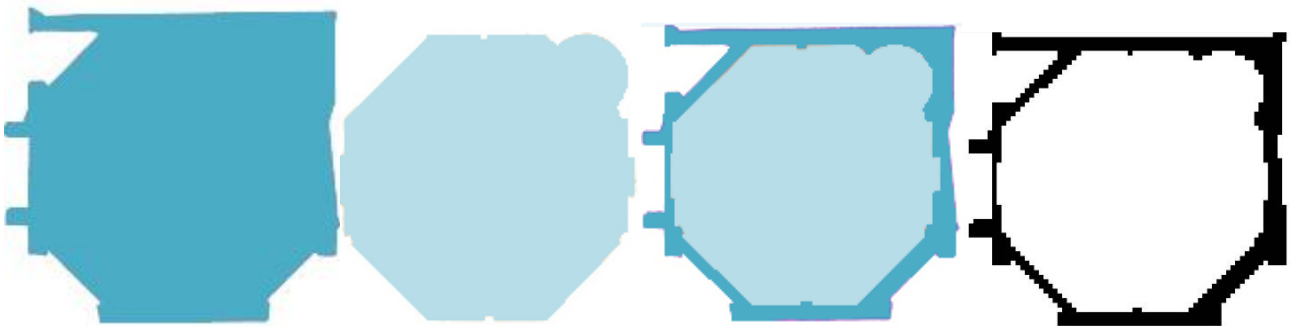


Figure 162: As explained in par. 4.3.1, all the 2D polylines are then transformed into points. A sequence of points (right) at a constant interval and high density is placed along the lines contained in each slice

In total, 43 slices have been elaborated and, through python code and convex hull function (Figure 163), the final dataset is composed by 43 images with a resolution of 250 x 250 millimetre, in which black pixels (value 255) is the inside (masonry, full volume), and white pixels (value 0) is the outside (empty).



*Figure 163: Example of elaboration of a slice, from left: convex hull of the external and internal perimeter, difference between external part and internal one, and transformation into an image with a resolution of pixels of 250 x 250 millimetre.*

Once obtained all the slices, the creation of a three-dimensional voxels model has been created in Matlab programming language. In particular, for each pixel that compose the dataset of images, Matlab code (Matlab, R2016a) identifies the centres and these will be also the centres of the three-dimensional voxels, as shown in the following figure.

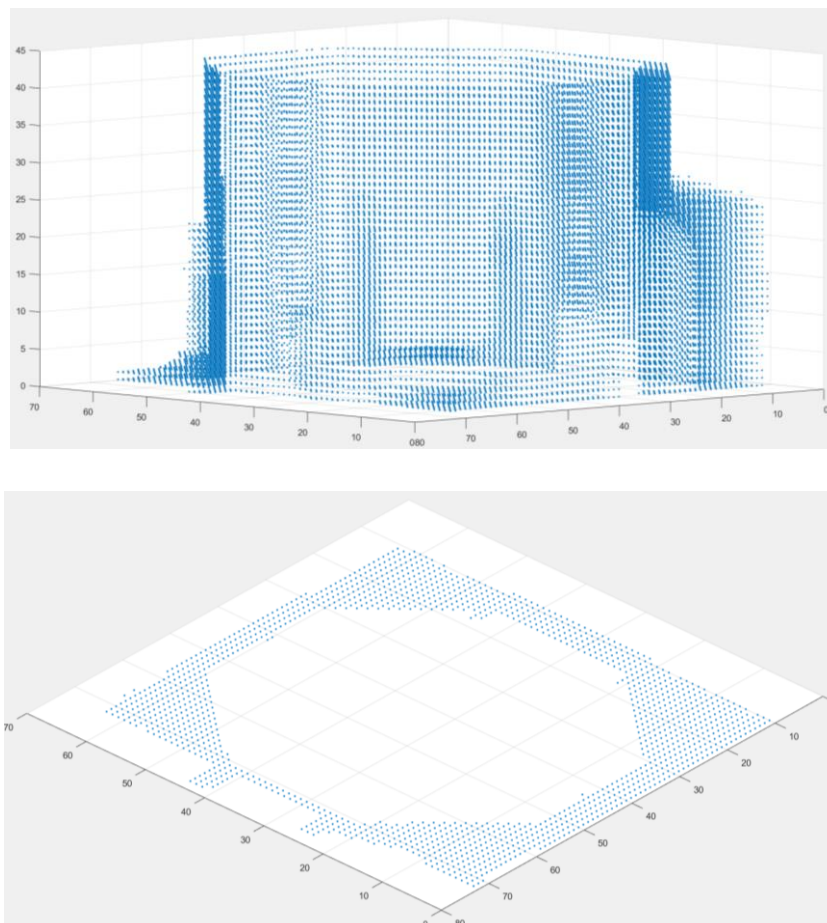


*Figure 164: The three-dimensional model in Matlab code, in with the points are the centres of each voxel*

With the overlap of each slice, the two-dimensional pixels are transformed into three-dimensional voxels, each with dimensions 250x250x250 millimetre. In total, 32409 voxels compose the entire building.

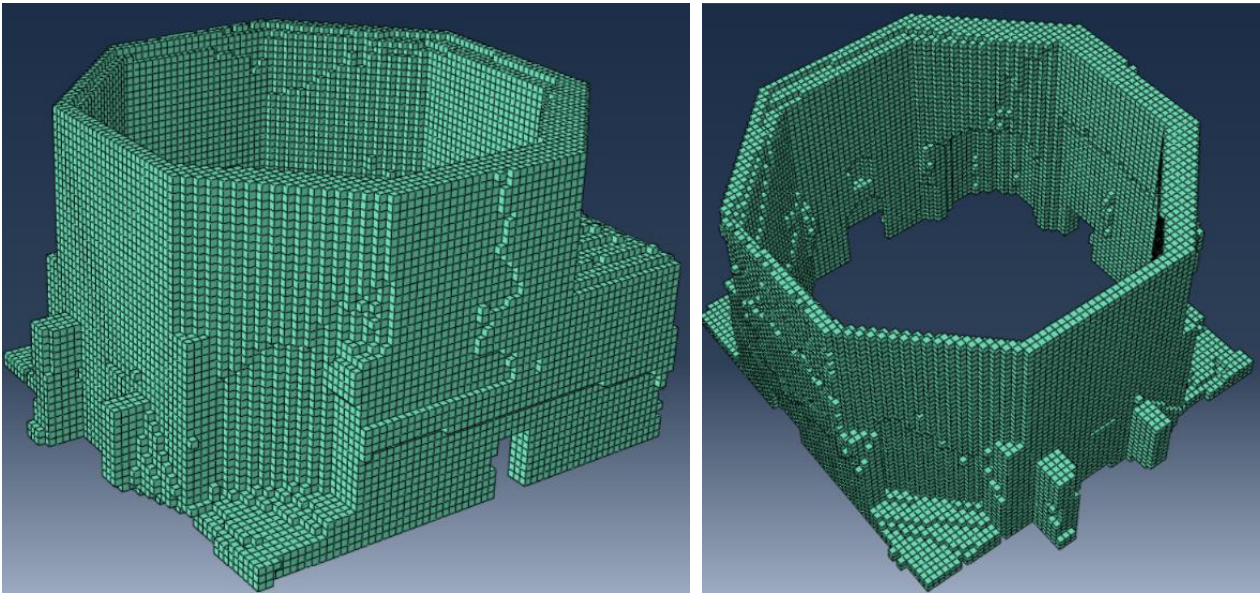


*Figure 165: Three-dimensional voxel model. The output of Matlab code will be the input for the structural analysis*

The FEM model deriving from initial point cloud dataset is now ready for the structural analysis.

### 6.7.2 HCP procedure

As explained in par. 4.3.2, for this procedure, the input data is the polygonal three-dimensional model transformed into a three-dimensional point cloud dataset. For the Baptistery, at first 3.291.952 triangles composed the building. As seen previously ([Figure 131](#)), the final model is very accurate, for this reason a decimation has been made, in order to reduce the number of triangles to about a million. After this, the input data for Matlab code has been a text file.

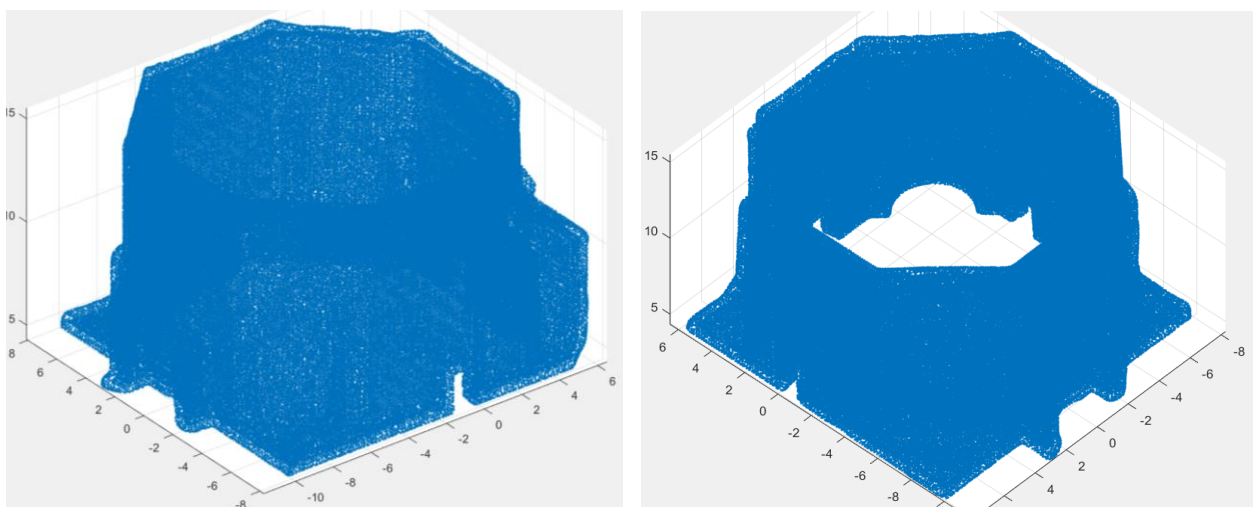


*Figure 166: Point cloud dataset read and plotted in Matlab*

As it is possible to observe in the previous [Figure 166](#), the input dataset is very dense. Nevertheless, it has no noise because it is distributed along the external perimeter of the structure, following a grid with a spacing of 2 centimetres. This ensures the uniform distribution of the dataset only in the external part (“skin”) of the entire building. This is a very important step: in fact, otherwise, the following alpha shape function used does not work. As mentioned, once read the input dataset, the next step has been to apply the alpha shape function. Before arriving to the final mode, some attempts have been made because the Baptistery is composed by niches and doors, and it has been necessary to specify a suitable alpha shape, which did not close these elements of the building. In this case, the most appropriate alpha radius has been 0.28. As comparison, a wrong attempt ([Figure 167](#)) and the correct one ([Figure 168](#)) have been reported.

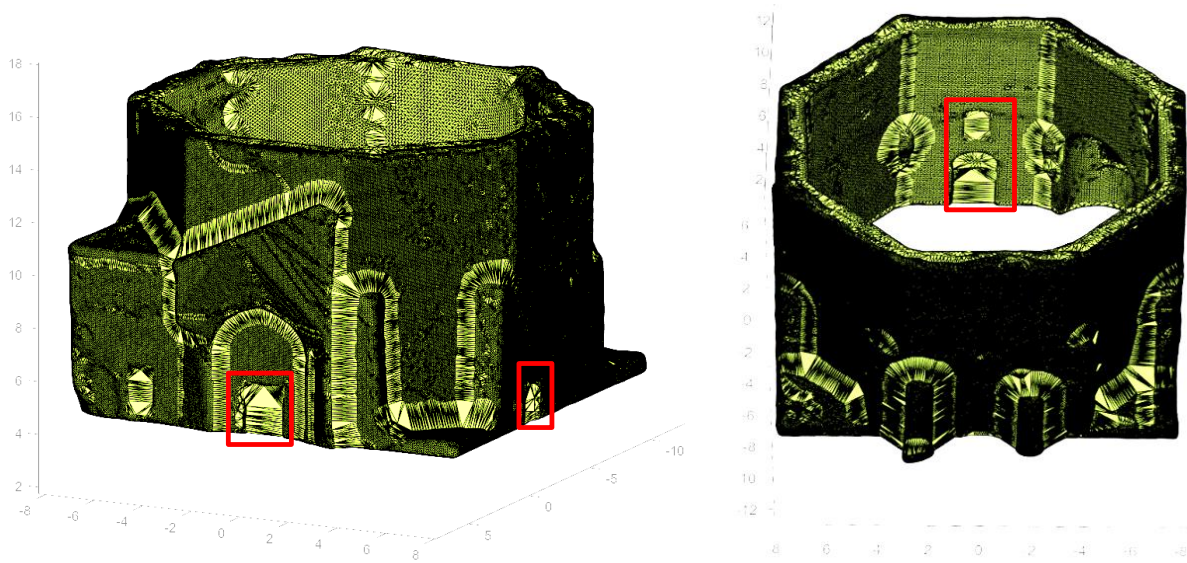


*Figure 167: Attempt to transformation through alpha shape function, with an alpha radius of 0.8. All the doors and the niches have been close.*

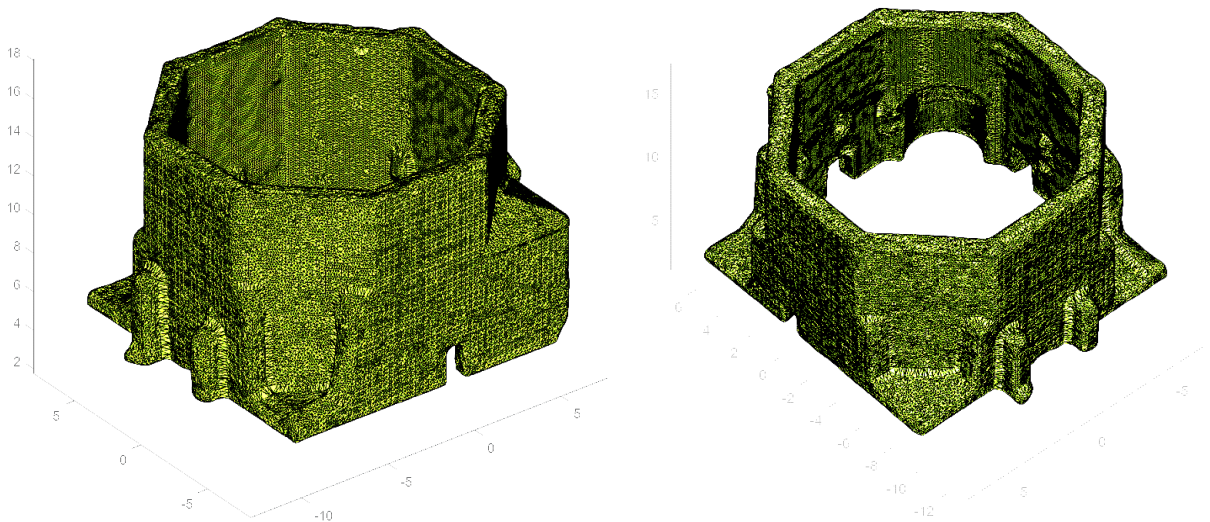


*Figure 168: The final model with an alpha radius of 0.28. All the doors are correctly defined and the final model perfectly follow the input data*

The next step has been the discretization of the space, in order to fill the space between the external mesh that compose the building through voxels. The final FE model is composed by 66018 voxels, with a dimension of 20 centimetres.

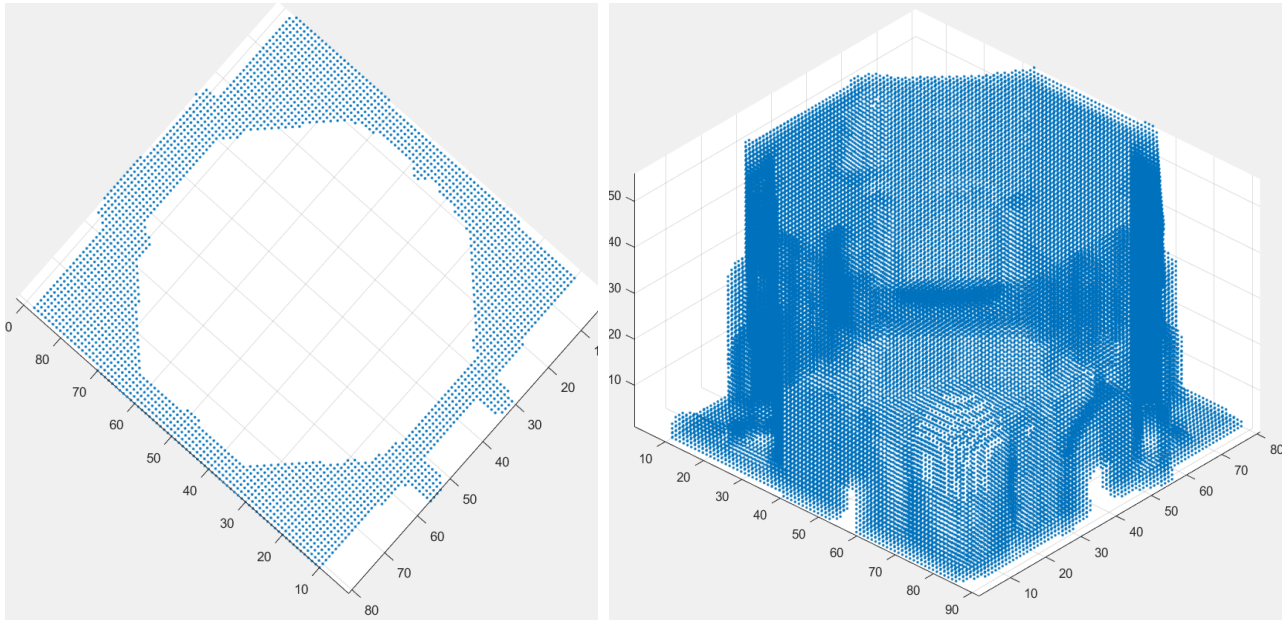


**Figure 169:** The three-dimensional model with the centres of each voxel. As shown in the figure with up view, the interior of the walls is correctly filled by voxels.

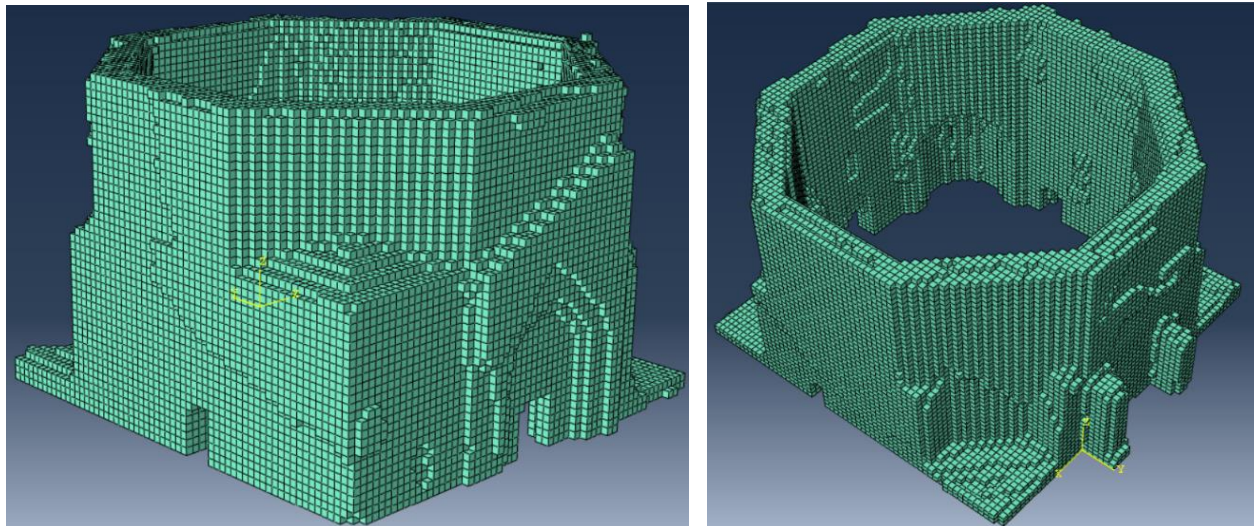


**Figure 170:** Three- dimensional voxel model: the output of Matlab code of HPC procedure

Furthermore, this method has been used also in order to transform the three-dimensional geometrical models, made by old data (par. 6.5.1) in a FE model. **Figure 171** shows the different steps for the transformation of the three-dimensional model in the first configuration of the Baptistery (**Figure 133**), and in **Figure 172** represents the transformation starting from the model shown in **Figure 136**. At last, in **Figure 173** the input FE models, suitable for the structural analyses, are shown.



**Figure 171:** Reconstruction of Baptistry with dome. From left to right, reading of point cloud dataset in Matlab code, Alpha shape with an alpha radius of 0.6, identification of the centres of voxels

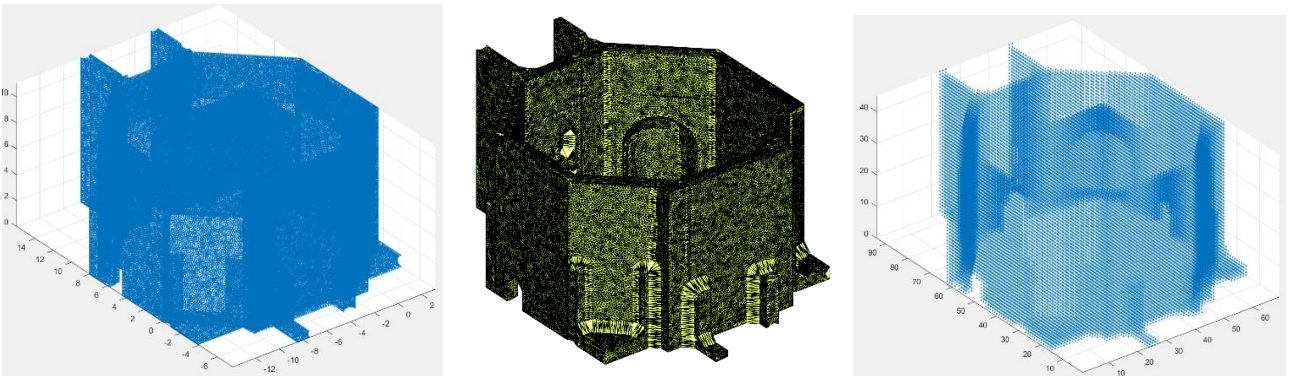


**Figure 172:** Geometric reconstruction of Baptistry. From left to right, reading of point cloud dataset in Matlab code, Alpha shape with an alpha radius of 0.6, identification of the centres of voxels

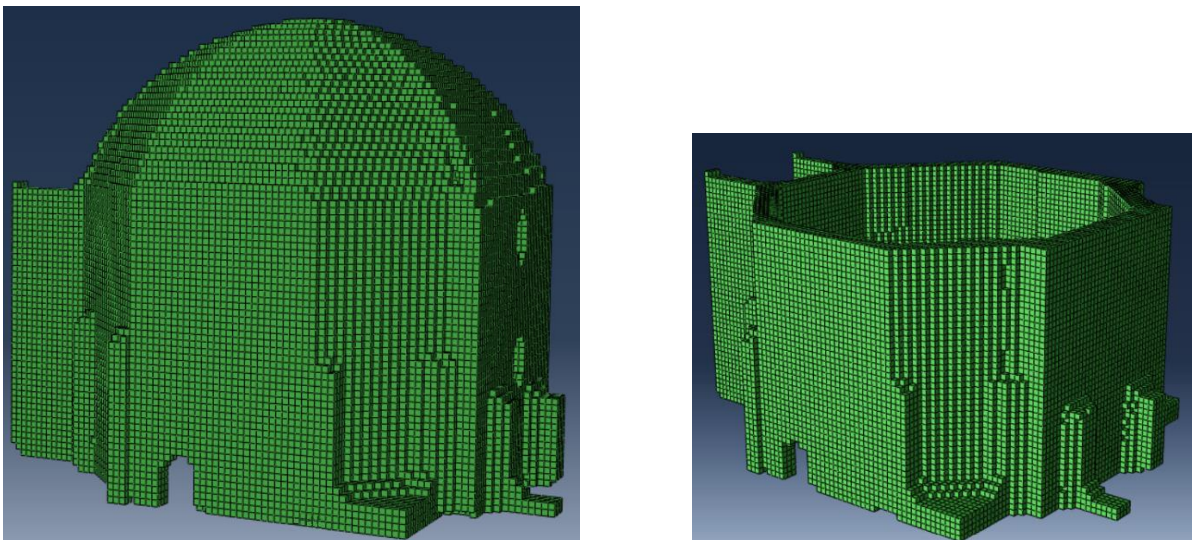


**Figure 173:** In the left, model composed by 59687 elements. In the right, model composed by 45901 elements

### 6.7.3 Automatic methods

In addition to the semi-automatic procedures just explained, two automatic methods have been applied in order to transform the initial point cloud into a FE model, suitable for the structural analysis. In both, the effort of the operator is minimum, because every phase is automated in the programming language.

The first one has been explained in par. 4.3.3, starting from the raw point cloud dataset, the code identified horizontal slices planes with a step of 30 centimetres and a thickness of 2 centimetres. In this way, considering that the initial point cloud is very noisy, there is not the risk that some parts of the perimetral point cloud dataset are missing, or are not well defined, because the planes with a chosen thickness are identified.

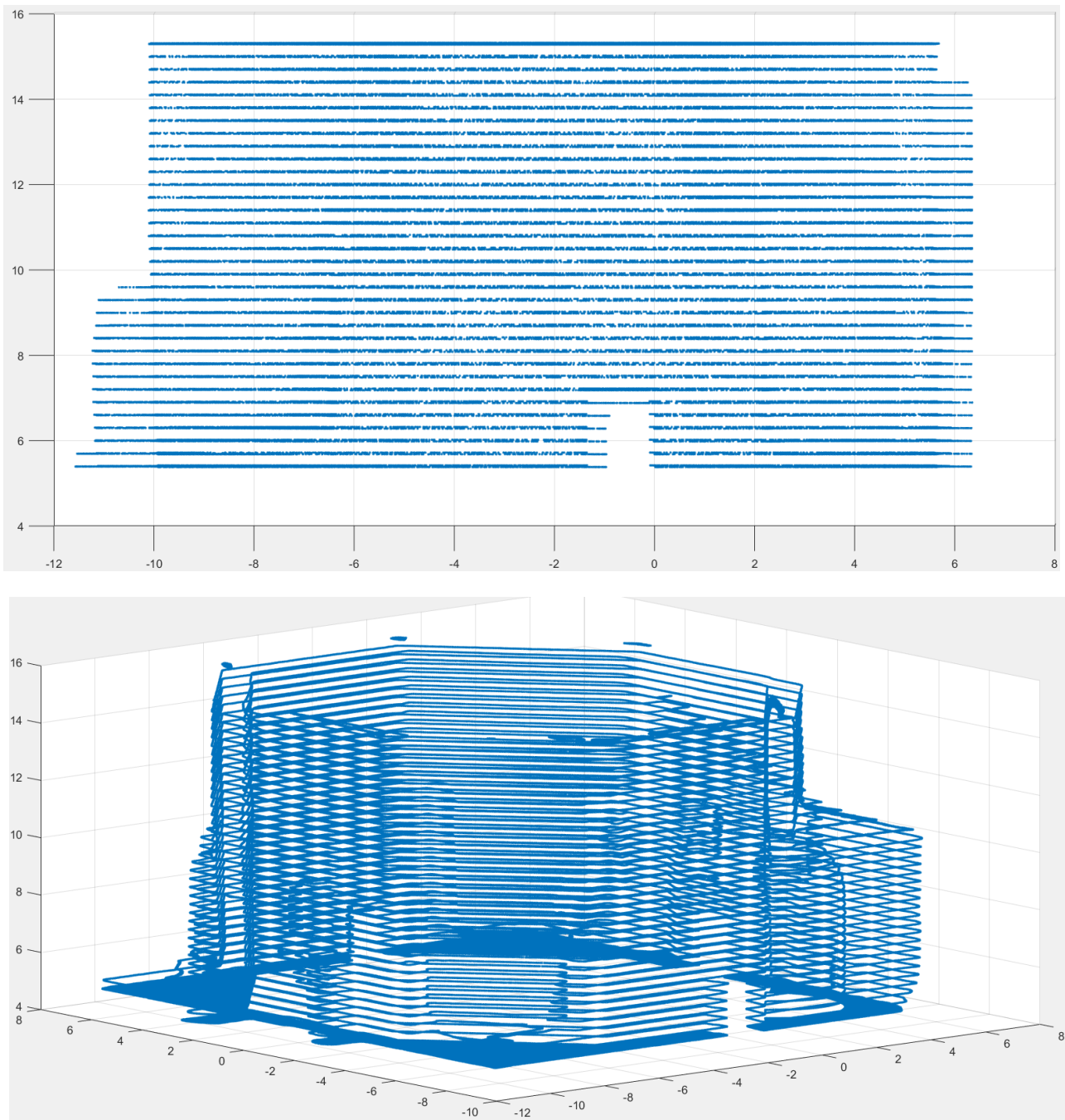


*Figure 174: The transformation from point cloud in the Matlab code. Despite they appear lines, the Baptistry has been transformed into horizontal planes, consisting of very dense points.*

The next step has been the transformation into voxel elements.

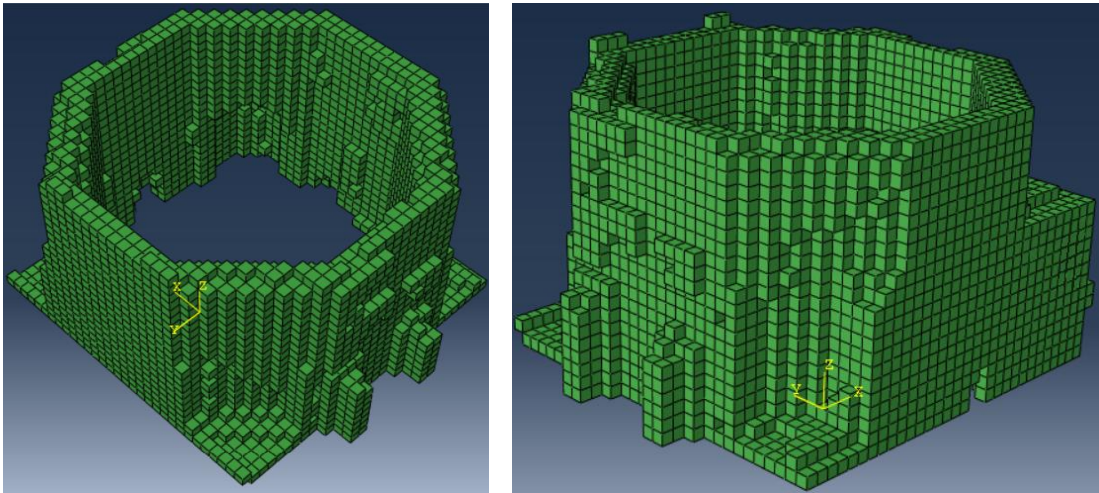


**Figure 175:** Voxel model with automatic procedure, generated in Matlab code, with a dimension of each voxel of 30 centimetres.

For the automatic method based on the discretization of the space (4.3.4), as input there is the raw point cloud. Through the discretization of the space, therefore, the point cloud dataset is transformed into elements with a shape and size chosen from the operator.

In this case, cubic elements have been used, in order to transform directly each element in a voxel, suitable for FE model. Both the procedures are totally automatic, but the limitation is that if we choose a little size for each element, the computing time is very high. For this reason, in order to optimize the processing time, cubic element with a size of 50 centimetres have been used.

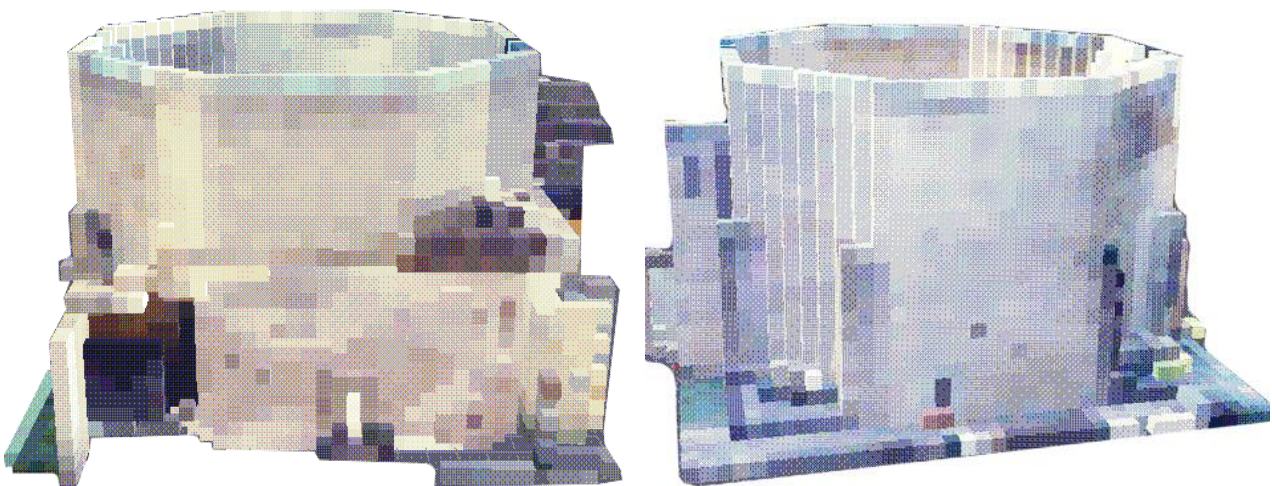


**Figure 176:** Voxel model with a size of 50 centimetres (Python code)

## 6.8 Results

Once obtained the voxel models with semi-automatic (Figure 170, Figure 171, Figure 172 and Figure 173) and automatic procedures (Figure 175 and Figure 176), the following remarks have been done:

- computational time;
- geometrical characteristics;
- results obtained from the structural analysis.

Furthermore, in order to assess the accuracy of the proposed models, in addition to the static analysis, a linear natural frequency analysis (eigenvalue analysis) is performed. As it is possible to see, several analysis and comparison data have been carried out, between semi-automatic and automatic procedures, the reconstructed models and numeric models, automatic procedures etc. All these analyses have been discussed in the following paragraphs.

### 6.8.1 Comparison between semi-automatic procedures

As shown in the Table 19, geometric characteristics are slightly different: this depends on the approximation of the Cloud2FEM procedure, in which (as previously explained) the dimension of each voxel is a cube with the high of the chosen step between the slices. For this reason, in this case specially in the oblique sides, a small part of volume is inevitably lost. On the contrary, for a littler dimension of each voxel, it would be necessary to reduce the step between each slice but this increases the total number of slices, and consequently the processing time.

Instead, in the HPC procedure the dimension of each voxel is smaller and this allows to have a better approximation of the real volume of the building.

In particular, in terms of computational time the HPC method is faster than the Cloud2FEM procedure because, once the input file is ready, all the HPC procedure is automatic. In fact, as seen previously, the programming code reads and transforms directly the input file into voxel model. Instead, for the Cloud2FEM procedure, the generation of the output file (voxel model) is longer because each slice have to be elaborate individually and transformate into images; so, the set of all the slices composing the dataset, and they are transformed into images. Then, each slice is transformed into an image and the input dataset for the programming code is the dataset of image (that is the number equal to the elaborated slices). Table 19 collects the geometric characteristics between two models, and in Table 20 the obtained results in terms of computed frequencies are shown. Figure 177 illustrates static linear analysis and Figure 178 the Mode Shape 1 and 2, where colours are associated to the magnitude.

Model	Mass (tons)	Volume (m <sup>3</sup> )	Voxel (n.)
Cloud2FEM	1272.76	572.89	32409
HPC	1201.25	606.01	66018

Table 19: Geometric characteristics between two models

Mode no	Model description	Frequency (HZ) Cloud2FEM	Frequency (HZ) HPC	Max displacement (Cloud2FEM)	Max displacement (HPC)
1	1 <sup>st</sup> bending mode (along X)	6.5086	6.8492	1.073	1.006
2	1 <sup>st</sup> bending mode (along Y)	7.3783	8.4455	1.099	1.063
3	axial mode	6.0082	6.9558	1.170	1.370
4	torsional mode	8.0909	8.9137	1.011	1.345

*Table 20: Natural frequencies' analysis: frequencies of the main mode shapes of the Baptistery. Comparison between the voxel-based models HPC and Cloud2FEM*

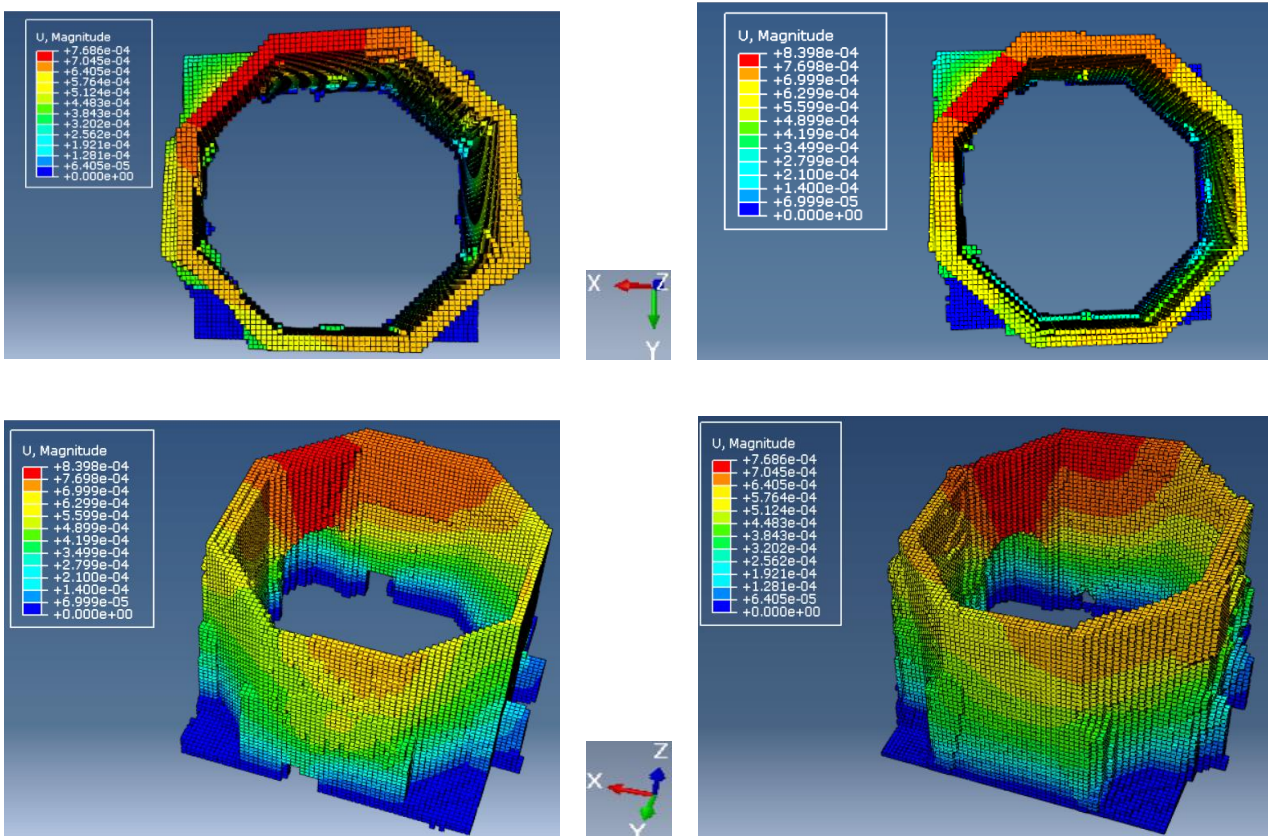


*Figure 177: Static analysis with results in terms of displacements. In the left, results of Cloud2FEM model; in the right, results of HPC model*

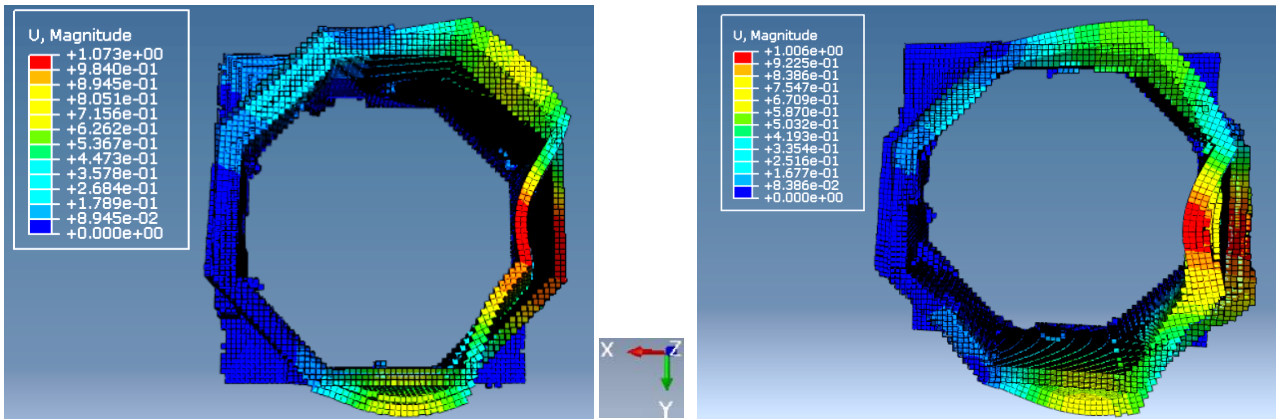


Figure 178: 1<sup>st</sup> bending mode along X, with displacements magnitude between Cloud2Fem model (left) and HPC model (right)

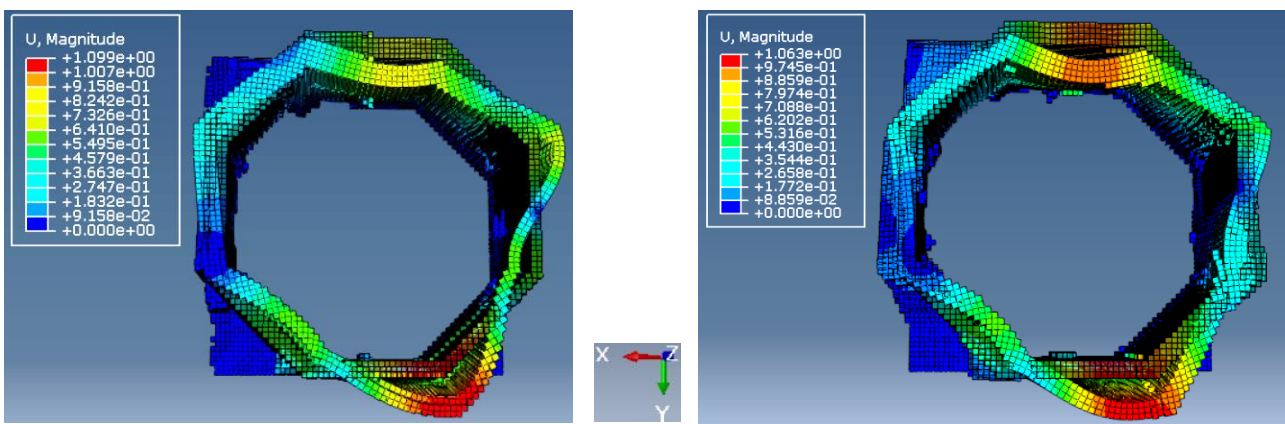


Figure 179: 1<sup>st</sup> bending mode along Y, with displacements magnitude between Cloud2FEM model (left) and HPC model (right)

## 6.8.2 Comparison between three-dimensional geometrical models

As seen previously (**Figure 173**), two voxel models have been created: the first one (model A) is the structure in its first configuration with the dome cover, and the second one (model B) created by the old data, but more recent (for more details, see par. 6.5.1). Through (Abaqus, Abaqus CAE/User's guide , v 6.14), static and dynamic analysis have been made, in order to evaluate the differences in terms of linear frequency and the natural mode shapes of vibration. As known, the mass of a structure influences its static and dynamic behaviour. By inspecting the **Table 21**, the geometric characteristics of the two models are very different, and this of course influences the static and dynamic behaviour. The comparison is done between the static analysis (**Figure 180**) and dynamic analysis (**Figure 181-Figure 184**) and the results are reported in **Table 22** (regarding the frequency) and **Table 23** (regarding the displacements). Furthermore, considering as reference the model with the dome, also the deviation (in percentage) in terms of frequency and displacement are reported.

Model	Height (m)	Volume (m <sup>3</sup> )	Mass (tons)	N. of voxel
3D Model A	17	942.61	1968.48	59687
3D Model B	10	717.20	1506.13	45901

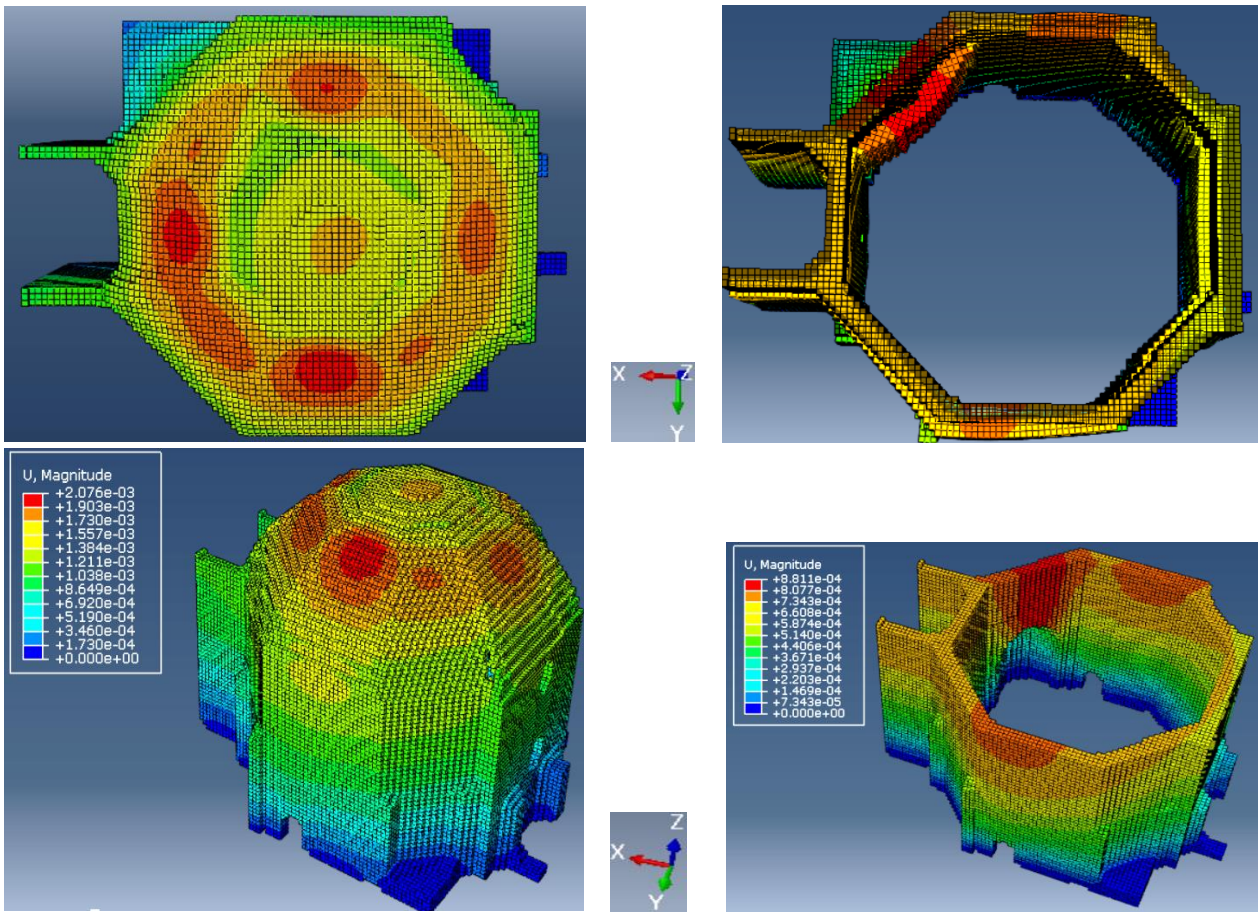
**Table 21:** Geometric characteristics, mass and number of voxel of two models

Mode No.	Mode description	Frequency (Hz) (A)	Frequency (Hz) (B)	Frequency (%)
1	1 <sup>st</sup> bending mode (along X)	6.8102	6.0595	11,023
2	1 <sup>st</sup> bending mode (along Y)	5.5512	7.5449	35,1%
3	axial mode	8.0375	6.1105	-23,97
4	torsional mode	8.9487	7.9466	-11,19

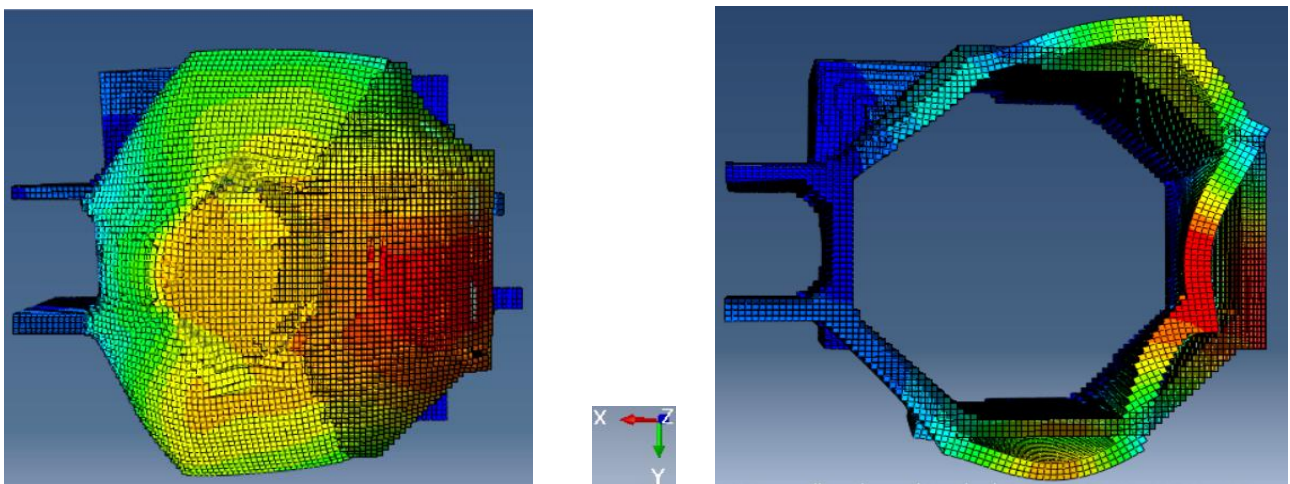
**Table 22:** Natural frequencies' analysis: frequencies of the main mode shapes of the Baptistery. Comparison between the voxel-based models A and B and deviation in percentage

Mode No.	Mode description	Max displacement (A)	Max displacement (B)	Displacement (%)
1	1 <sup>st</sup> bending mode (along X)	1.003	1.049	4,58
2	1 <sup>st</sup> bending mode (along Y)	1.002	1.086	8,38
3	axial mode	1.000	1.194	19,4
4	torsional mode	1.000	1.183	18,13

**Table 23:** Natural frequencies' analysis: displacements of the main mode shapes of the Baptistery. Comparison between the voxel-based models A and B and deviation in percentage



**Figure 180:** Static analysis with results in terms of displacements. In the left, results of 3D model A; in the right, results of 3D model B



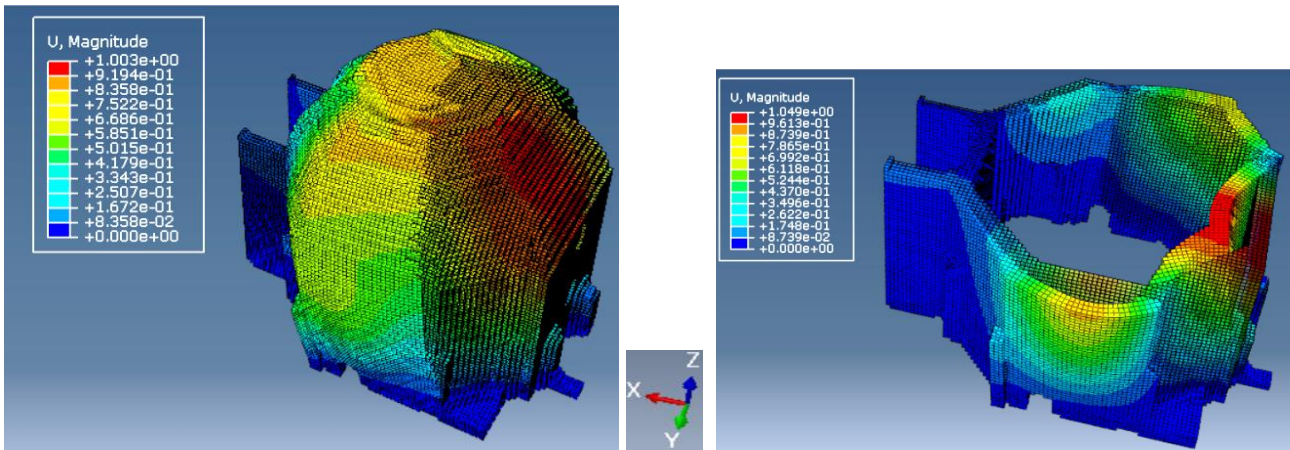


**Figure 181:** 1<sup>st</sup> bending mode (along X), with the overlap of deformed and undeformed shape, with displacement magnitude

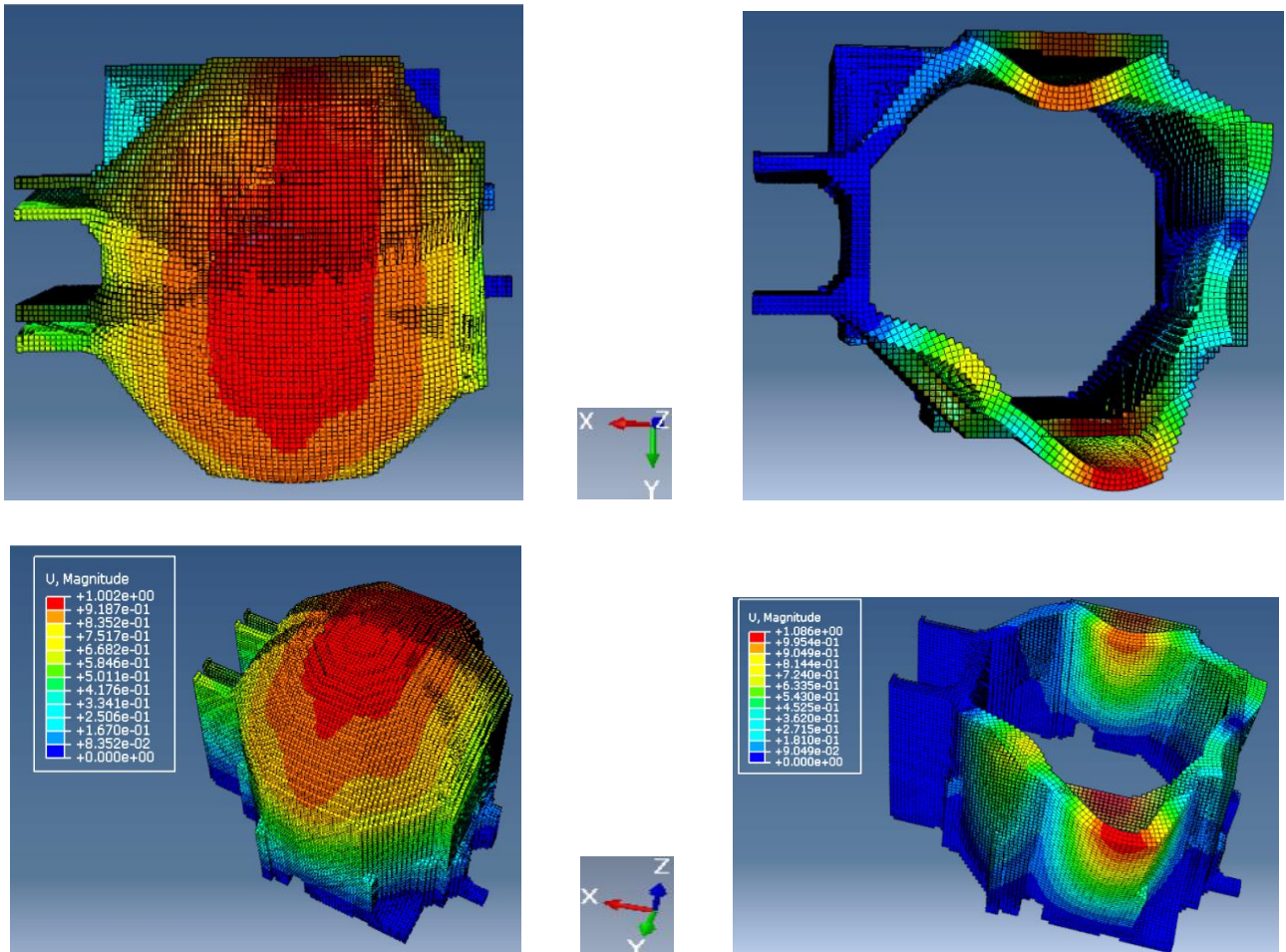


**Figure 182:** 1<sup>st</sup> bending mode (along Y), with the overlap of deformed and undeformed shape, with displacement magnitude

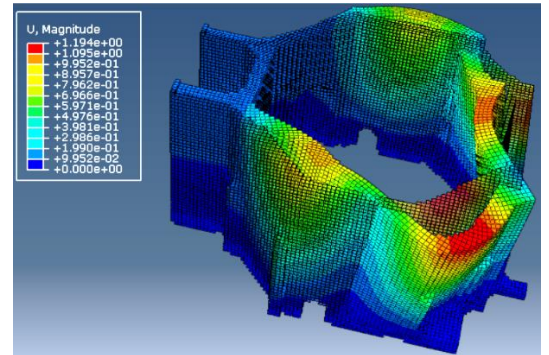
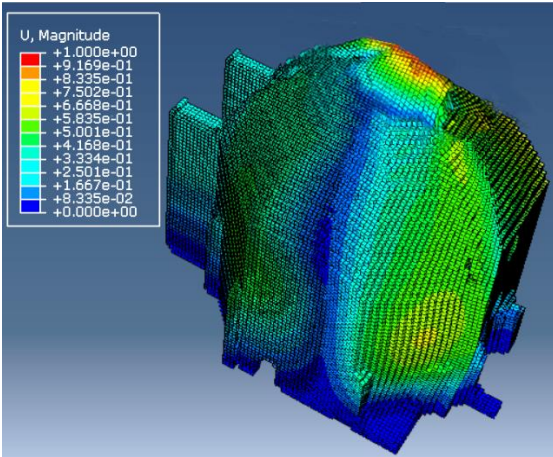
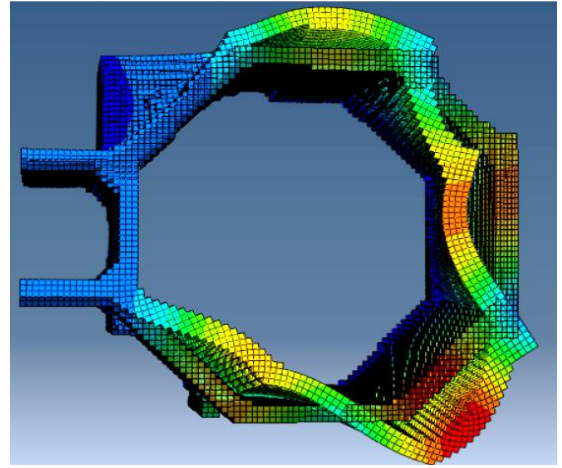
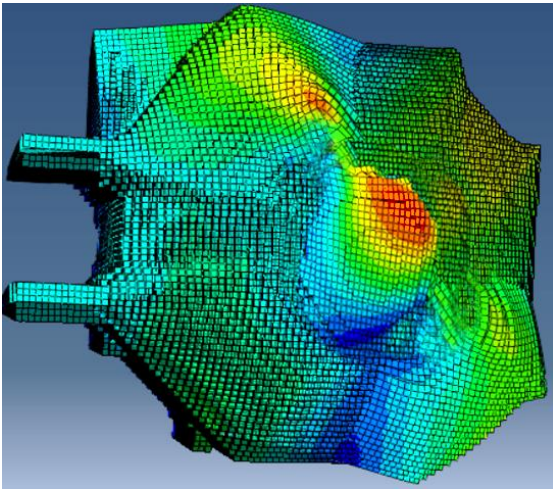
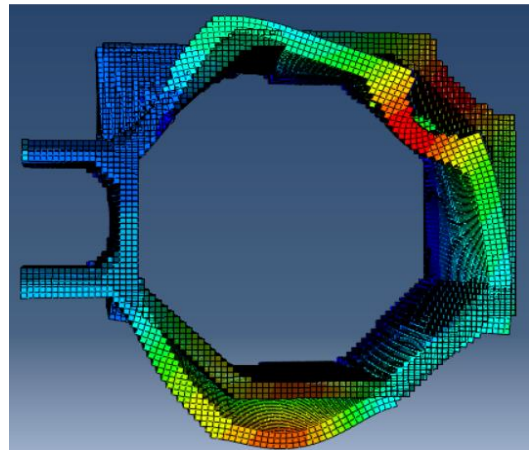
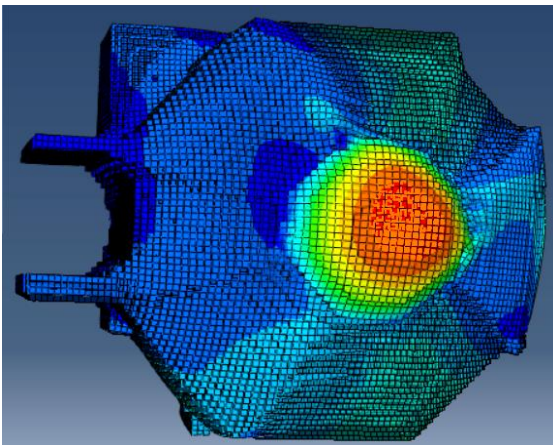


Figure 183: Axial mode, with the overlap of deformed and undeformed shape, with displacement magnitude



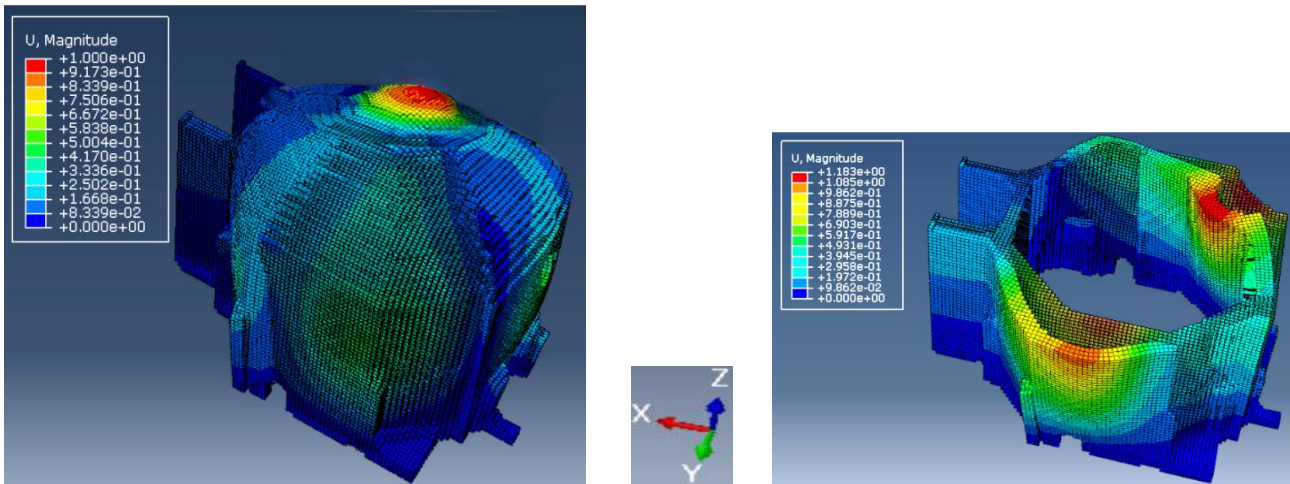


Figure 184: Torsional mode, with the overlap of deformed and undeformed shape, with displacement magnitude

### 6.8.3 Comparison between geometrical reconstruction and HPC model

Considering that the three-dimensional model (model B) seen in the Figure 136 and Figure 172 well represents the typical level of detail usually adopted for the modeling used in the structural analysis, it has been compared with the HPC model deriving from cloud, in order to analyse the difference in terms of displacements and frequency. Also in this case, the comparisons have been done in terms of displacements and frequencies for the first four mode shape, and the deviation in percentage, considering the HPC as reference. By observing the Table 24, the volume and the mass of the buildings are different, because in a geometric reconstruction it is not possible to follow perfectly the development of the walls in their height, as neither the perfect measurement of the height of the structure (as seen also in 6.5.2). In the Figure 185 and Figure 186, the structural analysis between the two models is reported; as shown, there is some geometrical difference as lateral support (left), in addition to those already mentioned. All these characteristics, have determined different results (Table 25,

Table 26), with a maximum displacement of about 4% along X, and 2% along Y.

Model	Volume (m <sup>3</sup> )	Mass (tons)	N. of voxel
HPC	606.01	1201.25	66018
B	717.20	1506.13	45901

Table 24: Comparison between geometric characteristics of two examined models

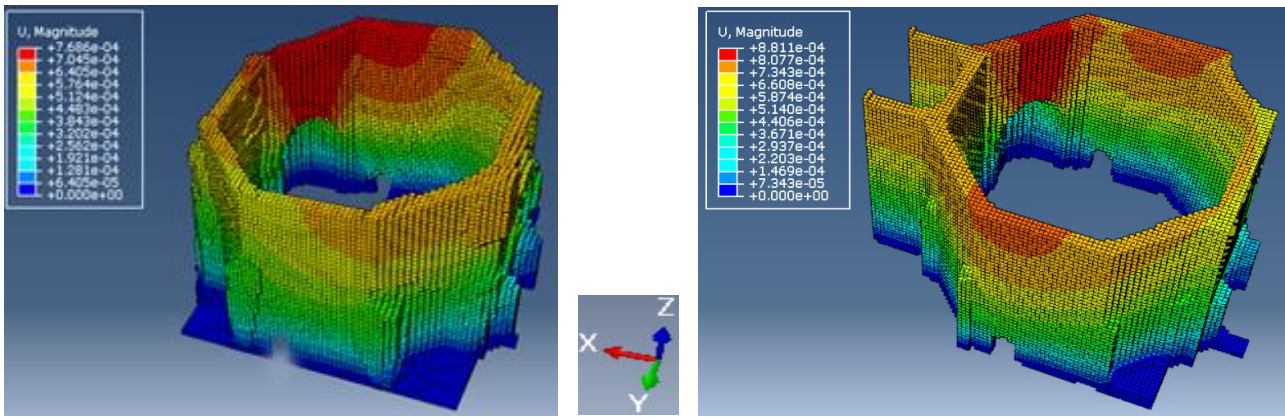


Figure 185: Static analysis between HPC model (left) and model B (right)

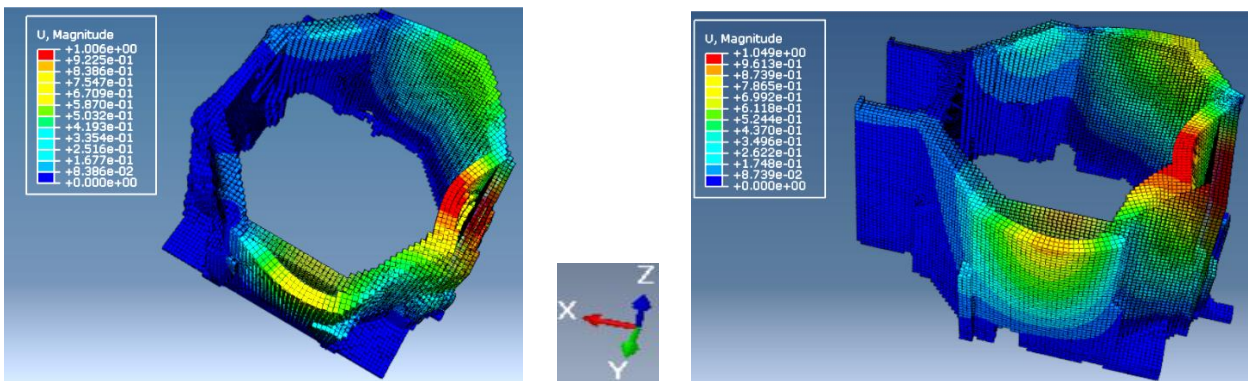


Figure 186: 1<sup>st</sup> bending mode (along X), with the overlap of deformed and undeformed shape, and displacement magnitude

Mode No.	Mode description	Frequency (Hz) (HPC)	Frequency (Hz) (B)	Frequency (%)
1	1 <sup>st</sup> bending mode (along X)	6.8492	6.0595	-11.52%
2	1 <sup>st</sup> bending mode (along Y)	8.4455	7.5449	-10.66%
3	axial mode	6.9558	6.1105	-12.15%
4	torsional mode	8.9137	7.9466	-10.84%

Table 25: Natural frequencies' analysis: frequency of the main mode shapes of the Baptistery. Comparison between the voxel-based models HPC and B and deviation in percentage

Mode No.	Mode description	Max displacement (HPC)	Max displacement (B)	Displacement (%)
1	1 <sup>st</sup> bending mode (along X)	1.006	1.049	4.27
2	1 <sup>st</sup> bending mode (along Y)	1.063	1.086	2.16
3	axial mode	1.370	1.194	-12.84
4	torsional mode	1.345	1.183	-12.04

*Table 26: Natural frequencies' analysis: frequency of the main mode shapes of the Baptistery. Comparison between the voxel-based models HPC and B and deviation in percentage*

#### 6.8.4 Comparison between HPC procedure and automatic methods

The last results derive from the automatic methods. The results of the two automatic procedures are practically the same: by considering the natural frequencies' analysis in the 1<sup>st</sup> bending mode, they diverge of about 5% along X, and 4% along Y, in terms of displacement. For this reason, only the values concerning the transformation from raw point cloud in a voxel model through Matlab code (Figure 174) have been reported, in terms of static and dynamic analysis.

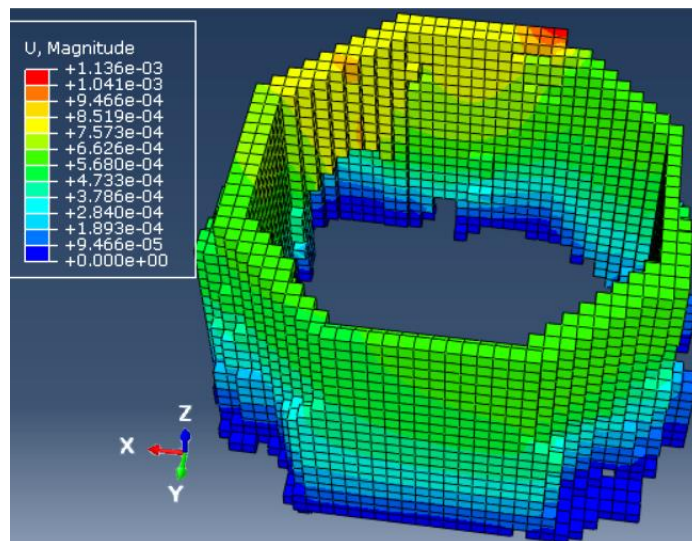


*Figure 187: Static analysis*

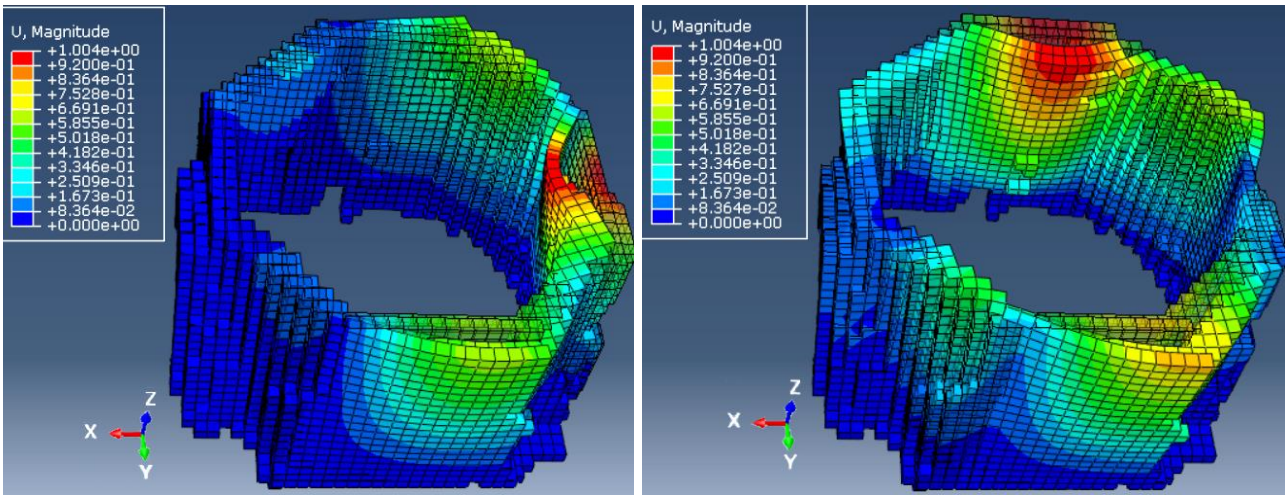


**Figure 188:** 1<sup>st</sup> bending mode with the overlap of deformed and undeformed shape, and displacement magnitude, along X (in the left) and along Y (in the right)

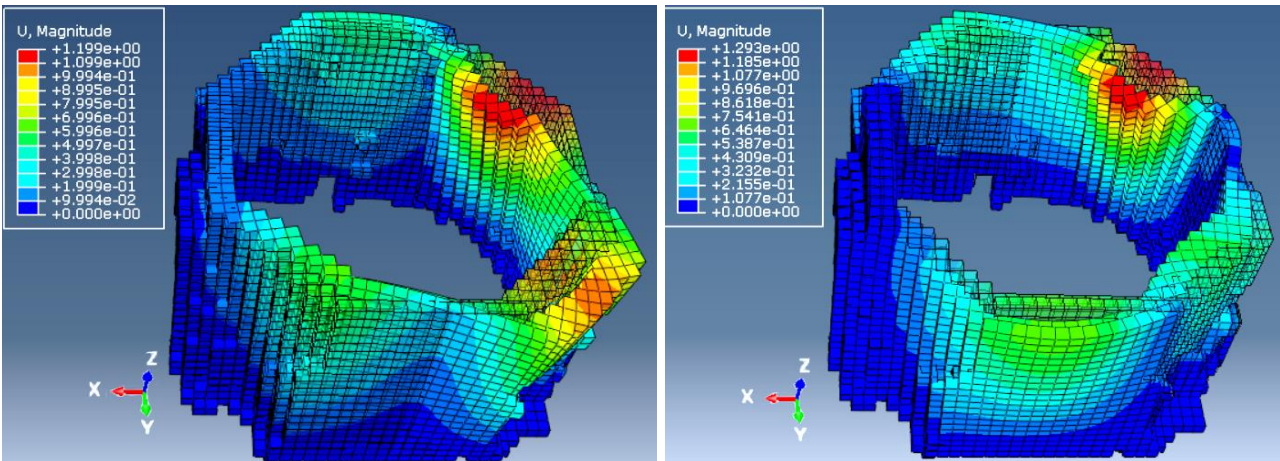


**Figure 189:** Axial mode (left) and torsional mode (right) with the overlap of deformed and undeformed shape, and displacement magnitude

In order to evaluate all the results, the structural analysis deriving from automatic method (identified as AM) and from the HPC procedure have been compared in terms of frequency and displacements, in addition to the geometric characteristic of the model. From **Table 27**, there is some small difference in terms of volume and mass by concerning the voxel model. Of course, this depends on the number of voxel, which are very different. By a greater number of voxel, a more accurate model is obtained because the approximation of the initial model is minimized. These differences, obviously have influenced the frequency and the displacements. From the comparison in terms of frequencies' (**Table 28**) and maximum displacements (**Table 29**), having as reference the HPC results, the deviation obtained has an error in percentage less than 3% along Y and less than 0.4% along X; instead, the maximum displacement is practically the same along the X direction (0.2%) and 5,55% along Y. These results validate both the procedures because, despite the codes starting from different input data, the results show very small differences.

Model	Volume (m <sup>3</sup> )	Mass (tons)	N. of voxel
HPC	606.01	1201.25	66018
AM	593.88	1247.14	5751

*Table 27: Comparison between geometric characteristics of two examined models*

Mode No.	Mode description	Frequency (Hz) (HPC)	Frequency (Hz) (AM)	Frequency (%)
1	1 <sup>st</sup> bending mode (along X)	6.8492	6.8763	0.396
2	1 <sup>st</sup> bending mode (along Y)	8.4455	8.2004	-2.90
3	axial mode	6.9558	6.1105	-12.15
4	torsional mode	8.9137	8.4984	-4.66

*Table 28: Natural frequencies' analysis: frequency of the main mode shapes of the Baptistery. Comparison between the voxel-based models HPC and AM and deviation in percentage*

Mode No.	Mode description	Max displacement (HPC)	Max displacement (AM)	Displacement (%)
1	1 <sup>st</sup> bending mode (along X)	1.006	1.004	-0.20
2	1 <sup>st</sup> bending mode (along Y)	1.063	1.004	-5.55
3	axial mode	1.370	1.199	-12.48
4	torsional mode	1.345	1.293	-3.86

*Table 29: Natural frequencies' analysis: frequency of the main mode shapes of the Baptistery. Comparison between the voxel-based models HPC and AM and deviation in percentage*

## 6.9 Considerations

A three-dimensional complete model of the Church of Pagans, and the Baptistery, in their internal part and external one, could be generated. The residual error deriving from external CRP have a maximum error less than a pixel; the internal TLS have an error with a maximum value of about 4 millimetres, instead from the topographical survey the medium value is 1,54 centimetres. Once merged all point cloud dataset and obtained the complete three-dimensional model for the exterior and the interior, the complex data offered different issues, analysis and studies. At first, the high number of data to process, which led to a slowdown of the computing processes; the second point was the overlap between different point dataset, derived from

different techniques, as for example the external walls of the baptistery with the dataset deriving from TLS and from CRP; the last point was the different density of dataset, as for example the external acquisition using TLS and CRP. These problems have been solved with cleaning data, spacing of points in order to obtain a more uniform point cloud dataset, and by deleting all that parts not belonging to the structure (vegetation, external elements...). A very complex and accurate polygonal model has been obtained. The comparison of the profiles to the old plans shows discrepancies, of little importance in the Church of Pagans, but more evident in the Baptistery and in the baptismal font. The baptismal font and the columns are the most characteristic parts of the Baptistery, and an accurate geometric reconstruction allowed to do different comparison with the actual numeric model (polygonal model), and overlaps with old data, showing discrepancies both in two-dimensional space that in three-dimensional space. Furthermore, to the columns it has possible to calculate the effective central core of inertia for all the sections that compose the element. From the historical analyses, two different reconstructions have been realized: the first one, with the initial configuration of the Baptistery with the dome cover, and the second one in a more recent configuration, very similar to the actual. The overlap between the second configuration and the polygonal model showed relevant discrepancies, because the geometric configuration cannot have the precision and the accuracy of the numeric model.

Also for this reason, among the different structural analyses carried out, also the comparison between the reconstructed model, and the model deriving from the point cloud dataset, in order to evaluate the different results. In order to proceed with the structural analysis, the polygonal model was further treated in different ways, with the final purpose to obtain a dataset suitable for the programming codes, by transforming the input data in a FE model, analysable in structural field. With four different methods, automatics and semi-automatics, a voxel model has been obtained. The output data is the same, because all the voxel models have the same physic characteristics, and a voxel is composed by corners where it is possible to define the loads bearing. The differences are in terms of computing time, geometrics characteristics, and number and dimensions of the voxels, from which depend the final results. Although this is not a research work in the structural field, several analyses (static and dynamic) have been carried out in order to evaluate the accuracy of the different methods. The comparison between the two semi-automatic procedures, shows some geometric differences, from which also the final results are slightly different. These geometric characteristics depends on the transformation of initial dataset, that in the HPC method follows closely the initial model, because the transformation from point cloud is directly done. Instead, despite both the procedures are semi-automatics, in the Cloud2FEM method there are more manual operations; in addition, the final resolution of each pixel (and then voxels) and the accuracy derive from the steps between the slices. However, if the step between the slices is very close, the manual procedure and the computational time extends considerably. Nevertheless, the final results in terms of static analysis, and the natural frequencies of the first four mode of shape, show little differences in terms of frequency and displacements, then the final models are both corrects. For the other structural analyses, the values deriving from HPC method have been considered as reference.

Another comparison has been carried out, between the geometric model in its first configuration with the dome cover, and the reconstructed model. Both the models have been transformed in a voxel model through the HPC procedure, and from the comparison of results it is possible to note how the structure in its first configuration had smaller values in terms of displacements, and variables values in terms of frequency along X and Y, in function of the its mass and its volume.

Concerning the automatic methods, from both a correct voxel model has been obtained, although with different approaches. The main limitation of these output models, are the computational efforts related to the number of voxels: voxels with larger size require a longer processing time. For this reason, it is advised to adapt the dimension of each voxel to the case study. In this case, voxels with a size of 50 centimetres have

been chosen, for a final model of less than five thousands of voxels. The values from both the models diverge of about 5% along X, and 4% along Y, in terms of displacement. For this reason, only the results deriving from a model have been reported, and compared with the results of HPC model, and the values are very satisfying. Considering the 1<sup>st</sup> bending mode along X and Y, there is a deviation of about 0,396% and 2,90% in terms of frequency, and of about 0,2% and 5,55% in terms of displacements.

## The San Luzi Bell Tower case of study

### 7.1 Introduction

In this chapter, the historical bell tower of the San Luzi church in Zuoz (Switzerland) has been analysed. This has been carried out during the period abroad spent in the University of Zurich, ETH. The bell tower showed high vibrations during the ringing of the bells. For this reason, a finite element model (FEM) of the bell tower is needed in order to come up with an appropriate solution. It has been created starting from the geometrical model, therefore the point cloud dataset has been used in order to obtain a FE model. The tower is more than 60 metres, and it is bound from three sides, in correspondence of the church (high about of 17 metres). The church with its tower has been measured by the University of Zurich, using a FARO Focus 3D S120 and the data acquisition for the geometrical model was planned, performed and the acquired data were processed. In order to be able to reliably register the 46 scans, total station measurements were performed additionally. With the total station, the coordinates of checkerboard targets used for the registration were determined. All these steps have been done by University of Zurich, in fact in this project the workflow started from the point cloud dataset merged and georeferenced. The analyses have been concentrated on the transformation of initial dataset, rather than the results of structural analysis. The main difficulties have been the transformation from initial point cloud into the polygonal model in which, because of the inside of the tower with very narrow spaces, it was very noisy.

Cloud2FEM procedure and HPC method have been used in order to obtain a final complete voxel model.

The first one was applied starting from the raw polygonal model, in the attempt to preserve all the internal elements. This presented some problems because the computational time of the operator was very long, and the final voxel model was characterized by more than 900 thousand of voxel. In spite of this high number, it had some problems, as the non-alignment of the vertex that compose the internal voxel of wood beams, deriving from a manual computational work by the operator.

The HPC method was applied starting from the final polygonal model, characterized by continuous surfaces, without holes and self-intersections of triangles. It has been spent quite some time in order to obtain a final polygonal model; as result, a correct voxel model composed by voxel of 25 centimetres has been obtained. Besides, a structural static and dynamic analysis has been carried out, assuming the characteristics of materials through the available photos. This has to be considered only as a first initial step, because the characteristics of the materials and the loads that weigh on the structure, are supposed.

### 7.2 Description

The San Luzi church is located in Zuoz (Switzerland) in the Upper Engadin. Its bell tower is about 60 meters high and is equipped with four bells. It is characterized by ten floor plan, as shown in the following figure. The internal spaces are very narrow, as it is possible to see from [Figure 191](#).

The historical bell tower of the San Luzi church shows high vibrations during the ringing of the bells. A finite element model (FEM) of the bell tower and the church is needed in order to come up with an appropriate solution. For the FEM, a geometrical model is necessary. Therefore, the goal of this project is to generate a precise FEM model, starting from the point cloud dataset. Workers in San Luzi noticed high tower vibrations when ringing the bells in 2003. One year later, measurements showed that the maximum vibration is 16 mm/s whereas the maximum acceptable value is only 3 mm/s. The two larger bells were then equipped with cranked yokes in order to distance the pendulum frequencies from the tower's natural frequency. The large

vibrations caused by the bells 1 and 2 could be removed successfully. Bell 3 (see Figure 1.2) still showed too high impacts during measurements in 2009 though. The pendulum frequency was lowered as well. But in 2011, it was found that this had negative instead of positive effects. In the following year, a 16-month monitoring was started, measuring accelerations of the bell tower, temperature, wind speed and wind direction. The fundamental frequency of the tower was determined and found to be varying following temperature and wind changes. The high vibrations caused by bell 3 cannot be removed through shifting the frequency because of limited technical possibilities. Solutions with a tuned mass damper are now considered. Therefore, a finite element model (FEM) of the bell tower is needed.



*Figure 190: San Luzi church with bell tower*

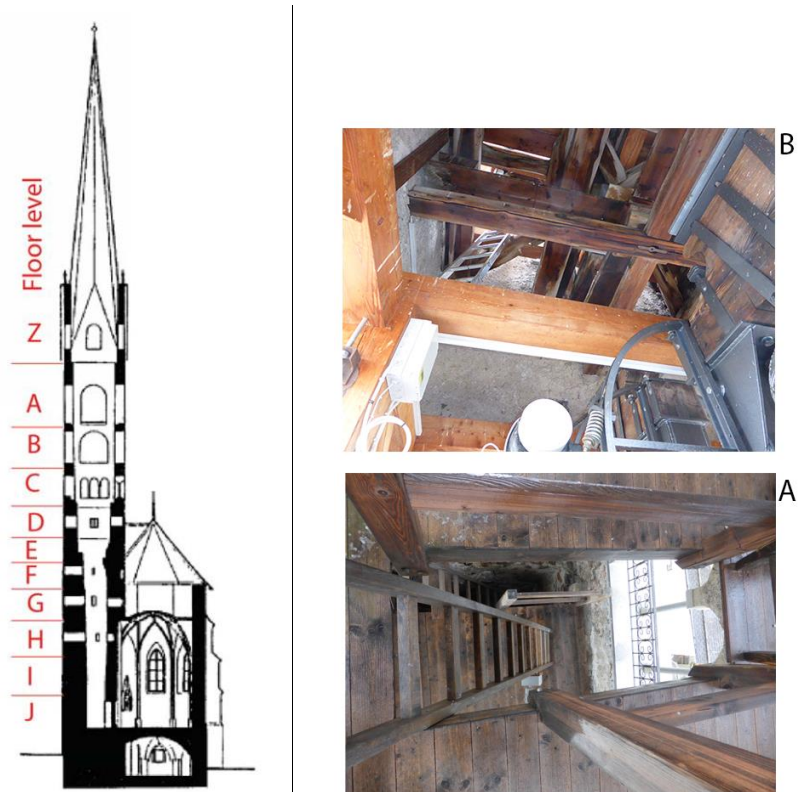


*Figure 191: Cross section of the tower bell with its floor plan (left); view of inside from A and B floors*



*Figure 192: From left, bell 1 view from lateral and downstairs, and bell 3 (see Figure 205)*

### 7.3 Measurement

The acquisition data have been done by the Institute of Geosensors and Engineering Geodesy (GEEG) of ETH Zurich, using two total stations and a laser scanner. The registration and the georeferencing of the scans, as well as the first cleaning of the points, are done in the FARO software SCENE. Laser scan targets (checkerboard targets) are placed inside and outside of the bell tower, the church and the crypt. A network and all checkerboard targets are surveyed by a total station. For the works inside the bell tower, the following safety precautions are taken:

- Risk of fall: When working at heights like on the bell tower, both humans and instruments have to be secured and prevented from falling. When working above level A (Figure 193, right image) climbing equipment is used.

- Bells: The bells are turned off during the measurements in the bell tower.

The network includes stations, tape targets, prisms, a far object and the cadastral points (see the Dorf network in Figure [Figure 57](#) and [Figure 196](#)). The total station measurements are carried out in two parts, the measurements outside and inside the bell tower. As many points as possible are installed visible both from inside and outside the tower (e.g. prism 1004, see [Figure 193](#) and [Figure 196](#)).

The bell tower, the church and the crypt are scanned with the FARO Focus 3D S120 such that at least 3 checkerboard targets are visible on each scan (see laser scanner location in [Figure 56](#)). After the registration, cleaning and georeferencing, a total point cloud composed by 24.883.887 million of points ([Figure 197](#)). Of these, more than 9 million concerns the bell tower and have been considered for the FE modeling.



**Figure 193:** Bell tower inside. Left: Looking from the A-floor to the Z floor. Middle: Prism number 1004. Right: Scan between the A and Z floor

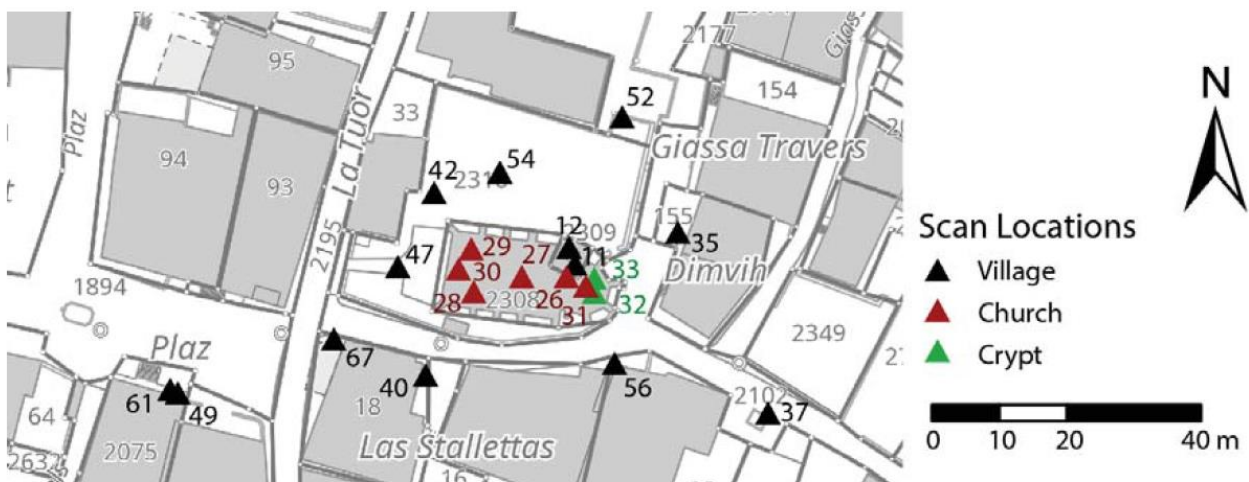


**Figure 194:** Laser scans position (inside the tower, only position 11 and 12 are given).

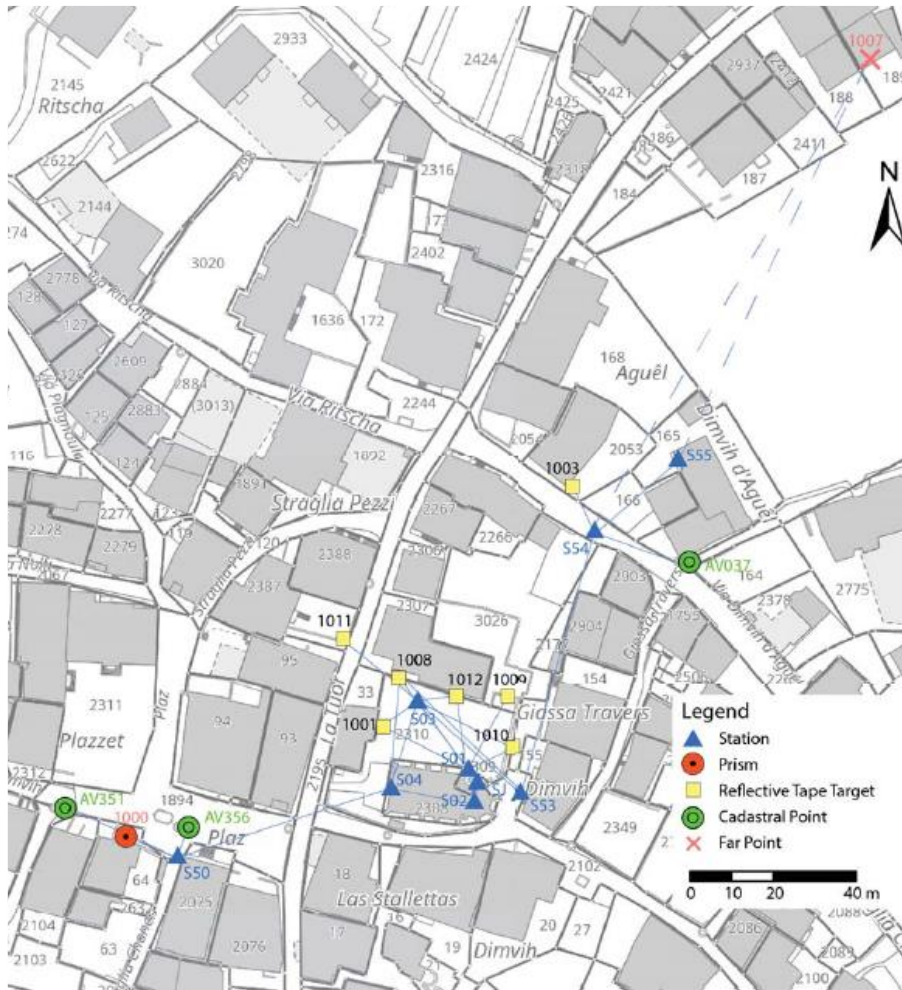


Figure 195: Network Dorf, all measurements of the ground

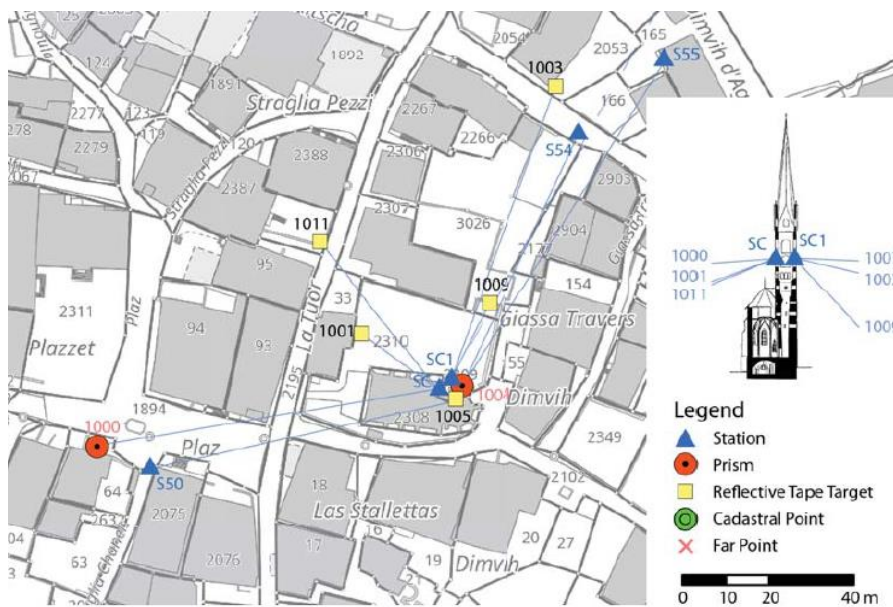
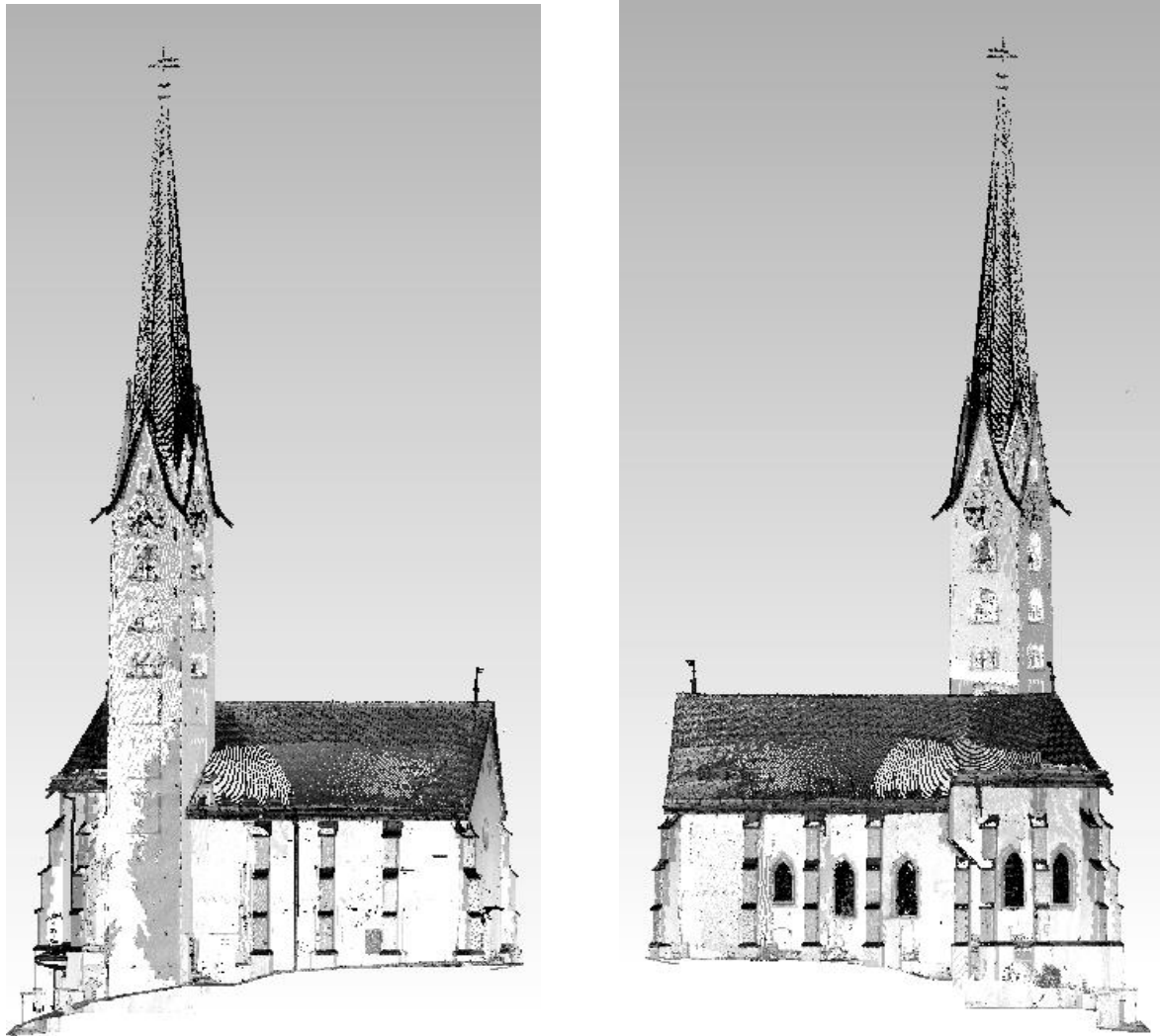


Figure 196: Network Dorf, measurements inside the bell tower of the C-floor on the map and on the side view of the tower.



*Figure 197: Point cloud dataset from North front (left) and South front (right)*

## 7.4 Bell tower: numerical model

Considering only the tower, the initial dataset was composed by more than 9 million of point. The point cloud is thinned out uniformly with a distance of 0.15 m, and with optimizing for uniformly distributed data. Furthermore, the roof has been deleted; in this way, a final dataset composed by 2.291.570 millions of points has been obtained. Since some parts of the building had significantly less data than the rest, meshes could not be generated there. Some of the parts without meshes were therefore reconstructed by fitting planes. The final model is a triangulated irregular network (TIN) with a few remaining holes that could not be reconstructed. The first polygonal model was composed by more than 2 million of triangles. The mesh generation was complete, but lots of holes were in the building, especially inside that is characterized by very narrow spaces, and (especially in the upper part) the thickness of the walls is larger than the width of the interior spaces.

As shown in [Figure 58](#), the polygonal model is very noisy. The blue parts represent the continuous surfaces, the yellow one are the cut or not-continuous surfaces; the green lines are the holes. For this reason, many hours were needed in order to obtain a continuous and correct model.

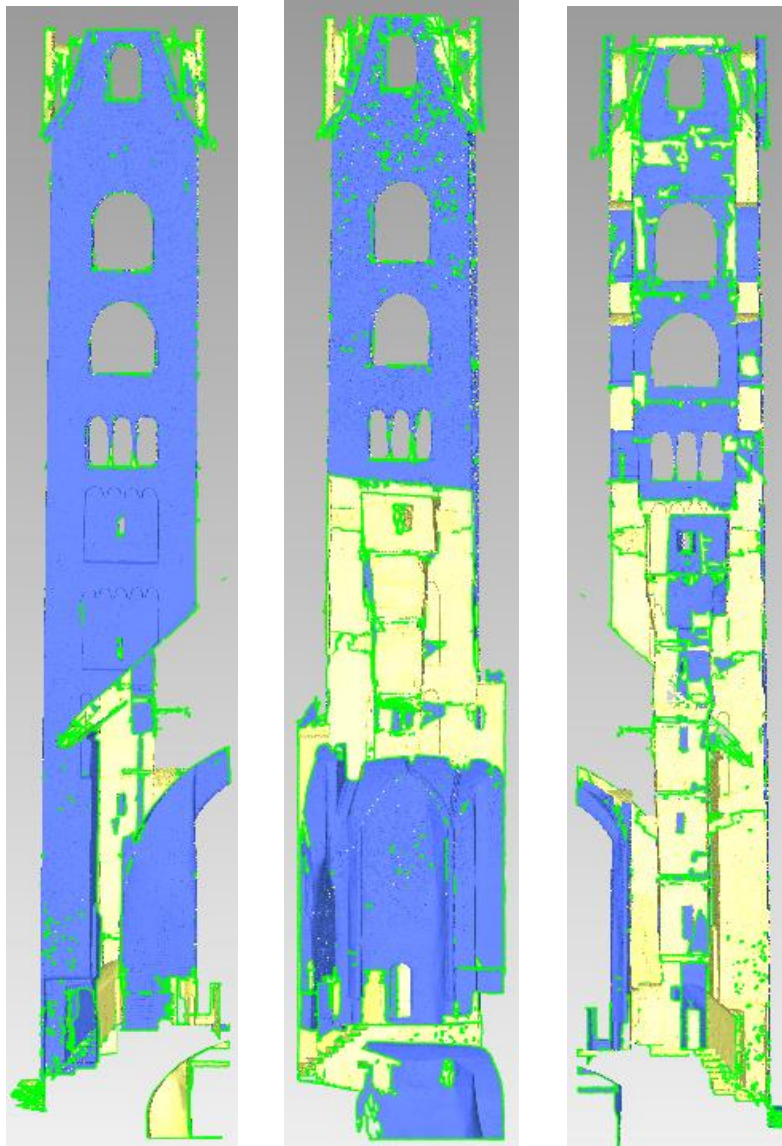


**Figure 198:** From left: polygonal initial model from West front, South- West front and West front. The green lines underline the not continuous surfaces (missing parts, cut elements etc...)

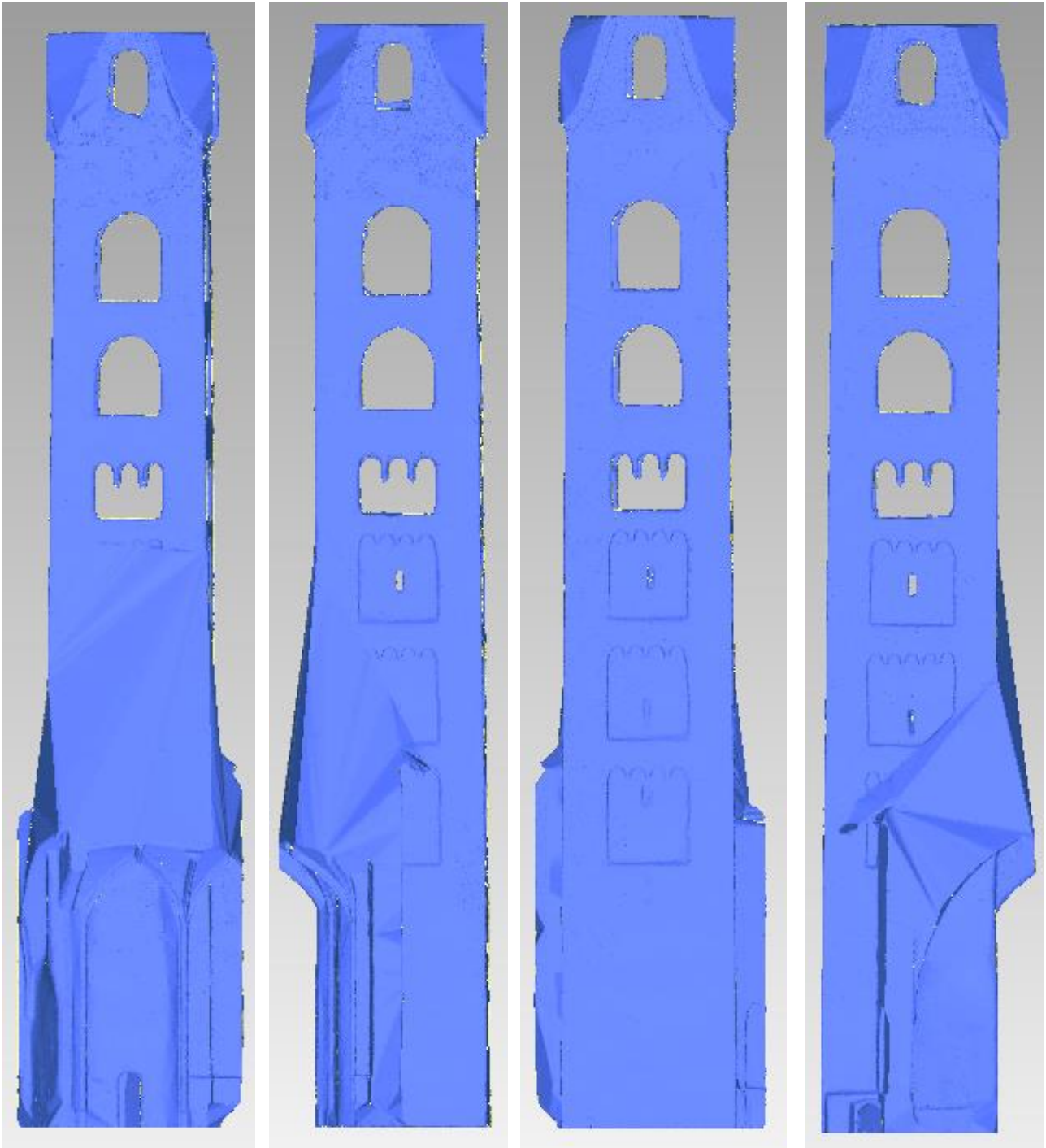


*Figure 199: Correct polygonal model of the external part. From Left: South West front, West front, North East front and South East front.*

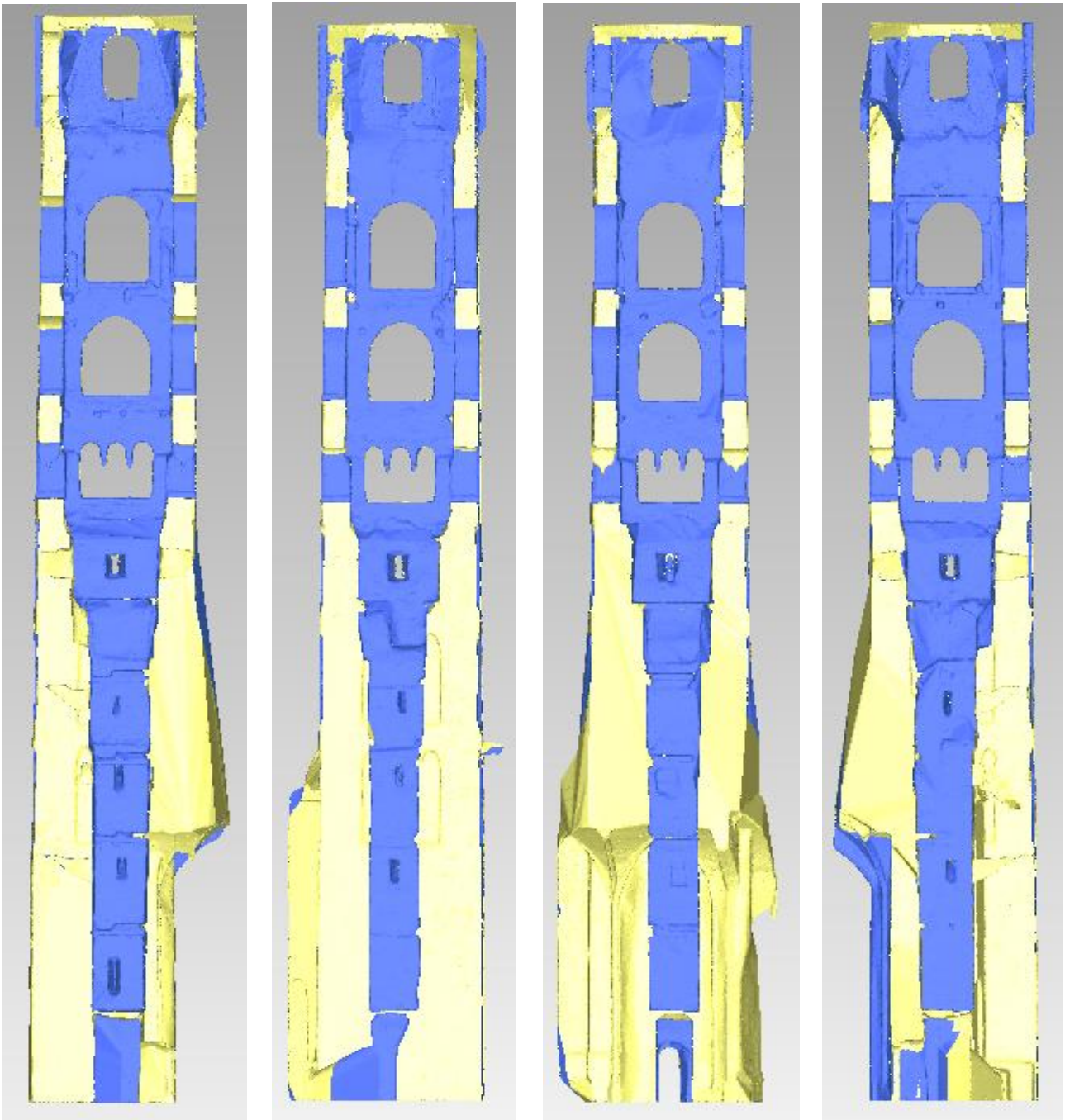


*Figure 200: Section from four fronts. It is possible to see that now the model is correct because the yellow part is only the thickness of the walls, the other surfaces are all in blue. Furthermore, there are not green lines that emphasized cuts and holes.*

## 7.5 Finite Element Model

Different approaches have been made for transforming the polygonal model into a FE model, in order to evaluate the better way in terms of computational time. In this case, in fact, a comparison in terms of accurate results cannot be done because there are not precise data regarding all the materials that compose the structure.

The tower bell is characterized by a very particular roof ([Figure 190](#)); therefore, all the floors are with wood beams, except that between G and H (see [Figure 191](#)) consisting of reinforced concrete. Also the stairs are in

wood (Figure 191), as well as the beams on which are fixed the four bells that characterize the tower (Figure 192). Despite the very accurate measurements, because of very tight spaces it was impossible to measure all these elements. For these reason, the FE analysis is approximate in terms of material properties, and therefor in terms of frequency.

### 7.5.1 Cloud2FEM procedure

At first, Cloud2FEM method was applied. For a better approximate the model, 32 vertical slices have been elaborated, starting from the initial polygonal model, with a step of 20 centimetres. The choose of vertical slices instead of the horizontal one, depends on the characteristics of the building. In fact, through the overlap between the polygonal initial model and vertical planes, with a step of 20 centimetres there is the intersection with all the elements that compose the tower. The main difficulty has been that, starting from the initial polygonal, the resultant slices were very noisy (Figure 201) and it was very difficult to process each slice. In fact, despite the experience of the operator with this procedure, for each slice it was necessary at least two hours.

After the elaboration of each slice, they have been transformed into image composing by pixels, with a resolution of 20 centimetres. The final voxel model was composed by 926.715 number of voxels. Despite this high number, the structural elements listed above, were not properly defined. The final result of the beams, for example, were elements constituted by voxels, with their vertex many unaligned. Of course, this was due on the high manual elaboration and even of interpretation, deriving from the input data very noisy (Figure 58).

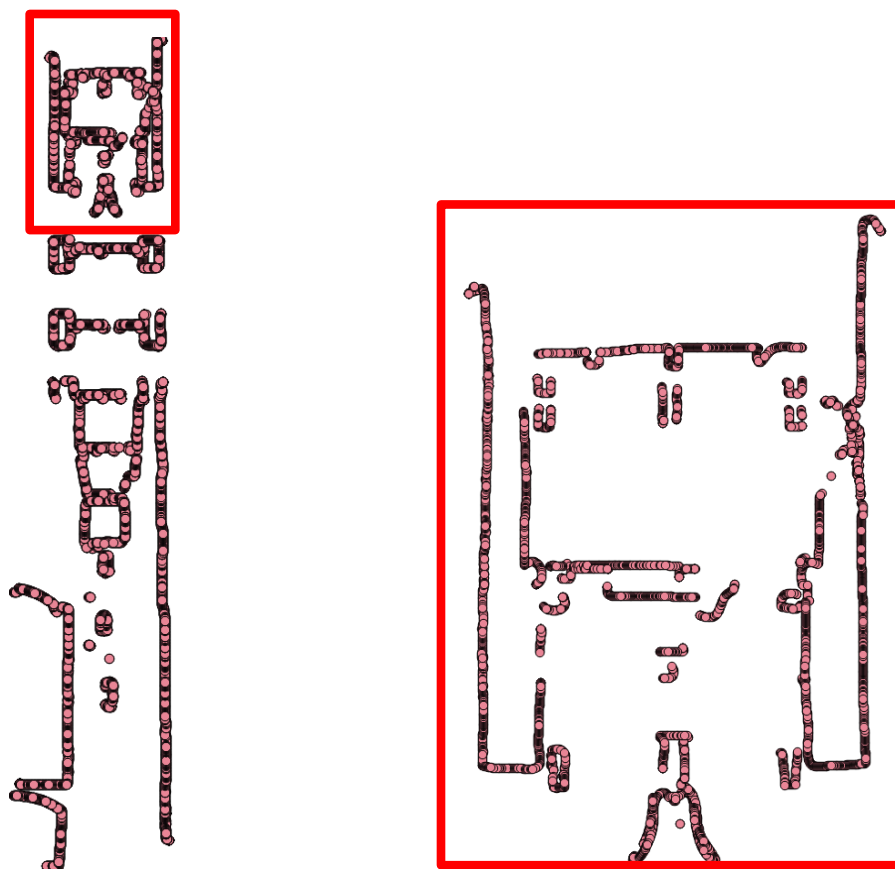
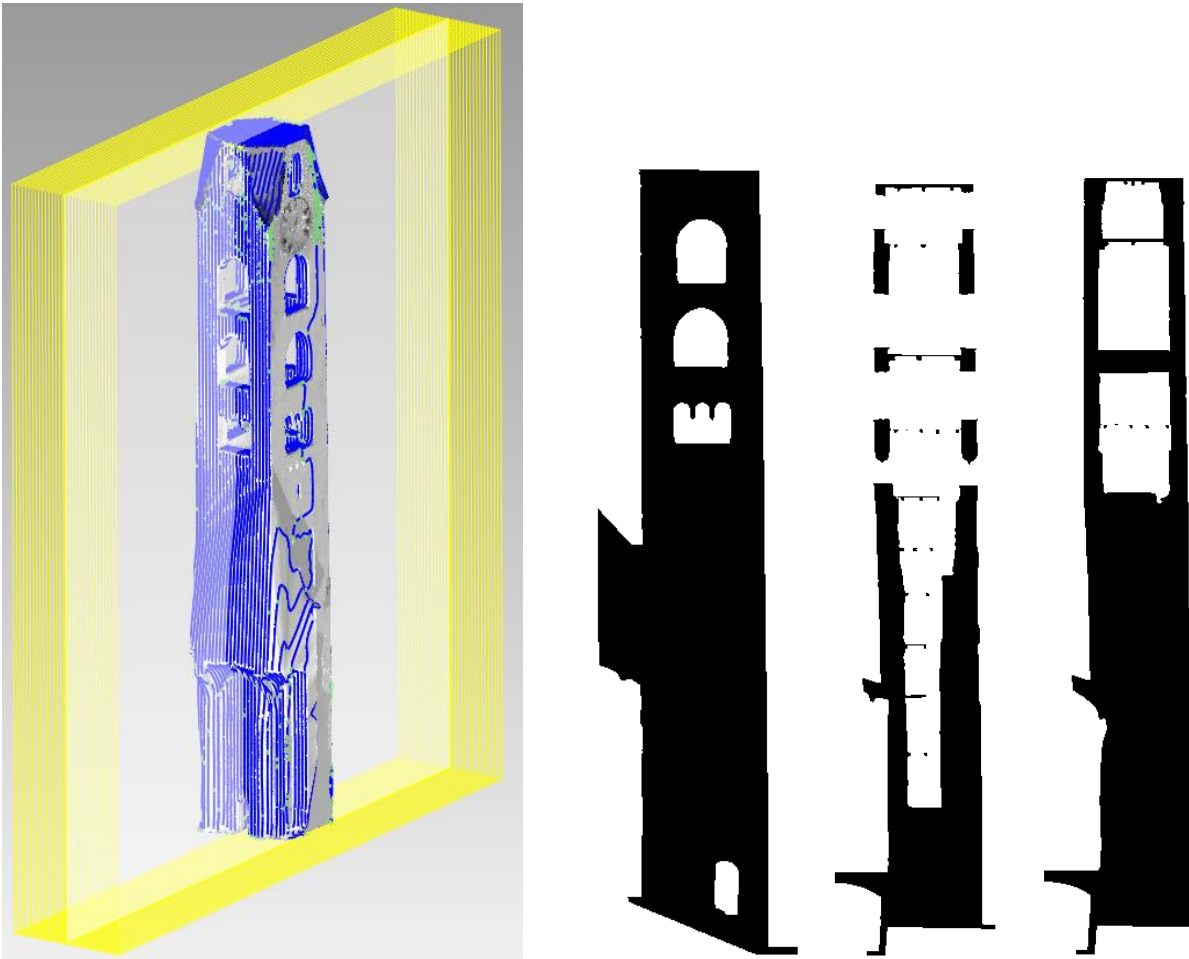


Figure 201: Initial slices before the elaboration. In the left, the zoom of the upper part is shown.



**Figure 202:** In the left, overlap between three-dimensional polygonal model and two-dimensional vertical planes, with a step of 20 centimetres. In the right, 6<sup>th</sup> slice, 20<sup>th</sup> slice and 28<sup>th</sup> slice, in which the white (255) is the empty part and the black part (1) is the structure. As shown, despite the structural elements (like beams and floors) are presents, they have a very poor quality.

### 7.5.2 HPC Procedure

After the test with Cloud2FEM approach, the initial polygonal model has been clean inside in order to improve the modeling and to reduce computational time, by removing of all structural elements as wood beams, and leaving (as seen in [Figure 200](#)) only the structural walls. This requested considerable time, because the initial polygonal model was very problematic. After this cleaning, the Matlab code has been applied. The first attempt failed, because considering that in some parts the walls are larger than the inside, the Alpha shape did not distinguish between external surface and internal one ([Figure 61](#)). With some precautions, as an offset of the external wall in the interspace, and an Alpha shape with an alpha radius of 0.2, a properly defined voxel model has been generated ([Figure 204](#)). The final voxel model has been characterized by 29997 number of voxels, with the dimension of each voxel of 25 centimetres.

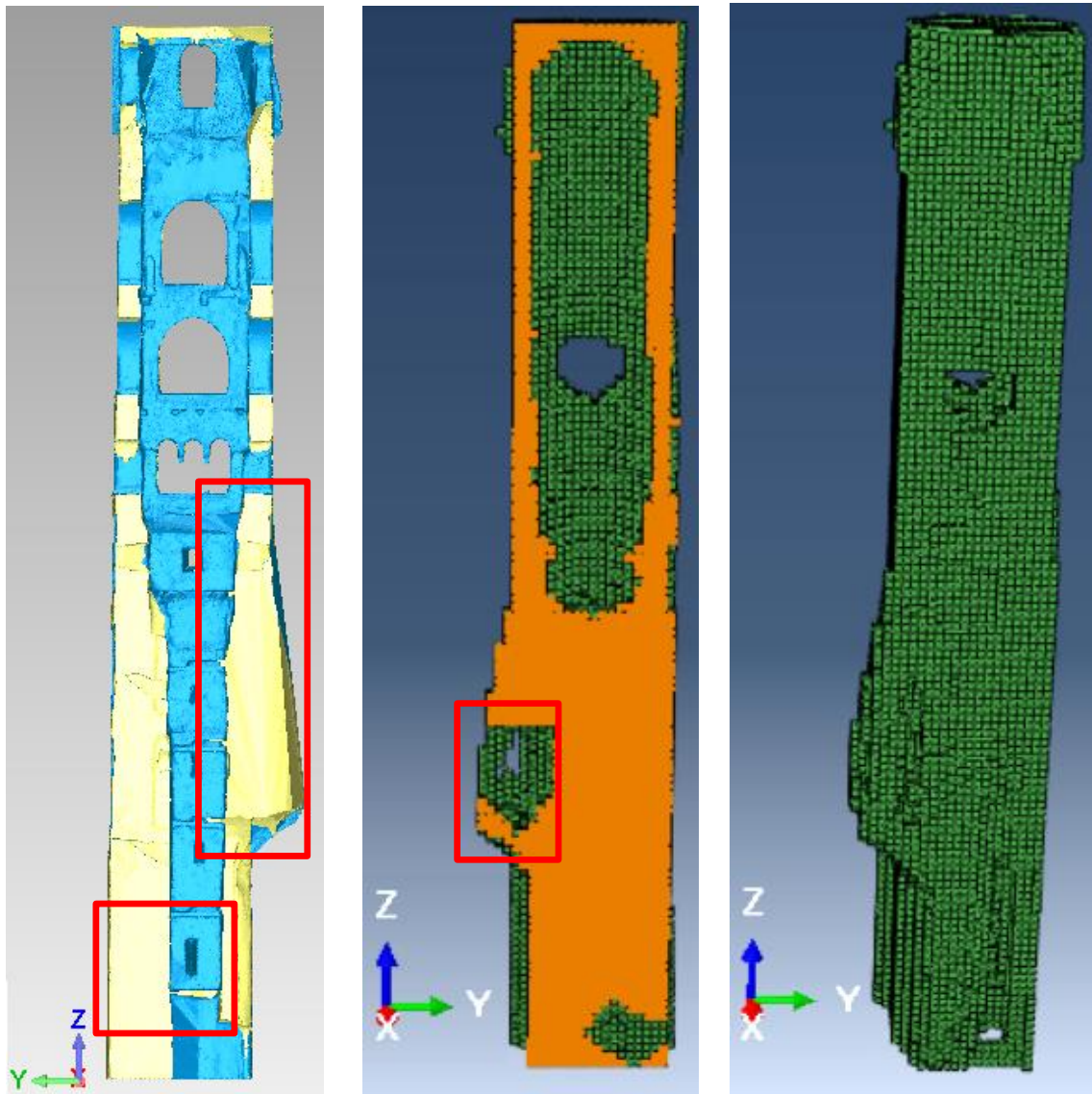


**Figure 203:** In the cross section (left) of polygonal model, two problematic part are underline in red, in which the interspace of the wall is larger than the inner space. Of course, alpha shape function cannot distinguish (and so close) the interspace, but it closed all the bottom part, as shown in the cross section (along Y) on the voxel model. By using of a high alpha radius (value=1), almost all the openings have been closed. Nevertheless, some internal parts (red) remain open. Furthermore, in the bottom part of the tower, all the inside space has been incorrectly closed, without considering the interspacing between the surfaces.

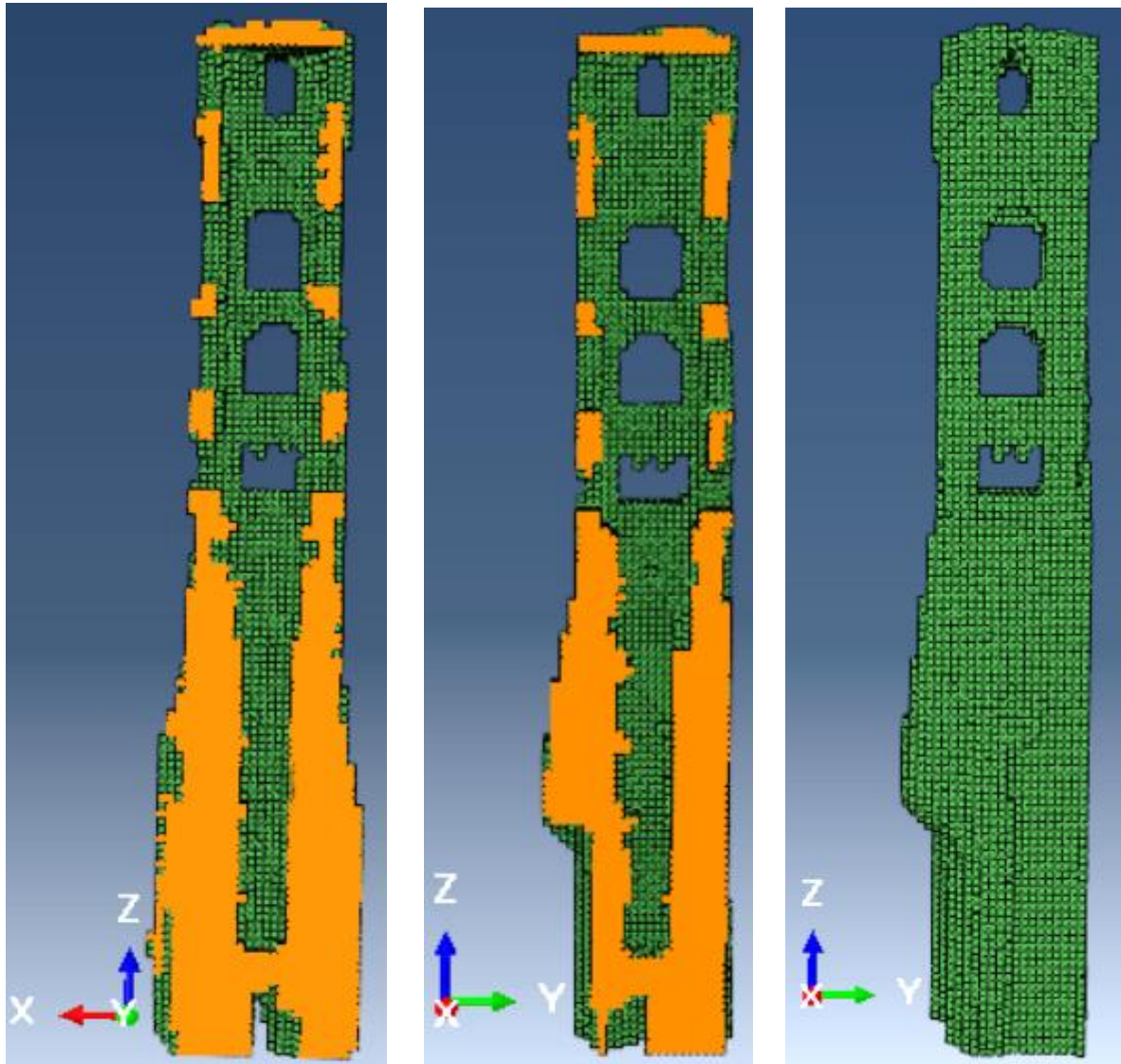
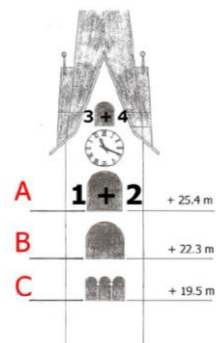


**Figure 204:** From left, cross section along X and Y, and final voxel model. The voxel model is defined with an alpha radius of 0.2. All the internal parts are well defined, in fact the interspaces between the internal surfaces and the external one are filled, and there are the windows.

Although there is not a survey or some indication about the materials that composing the tower, the structural analysis has been done, only in order to verify if the final voxel model is correct.

The only data available are the weights of the four bells, shown in the following table.



Bell	kg
1	1700
2	648
3	400
4	260

**Figure 205:** The location of bell 1 and 2,3 and 4 are indicated (left) and the reference of their correspondent weight (table in right)

The characteristics of chosen masonry have shown in the

**Table 30**; instead for the floors, a calculation of the own weight (with an hypothetical section) for each beam has been done, and then these values have been multiplied for the effective clear span of the floor. The final values have been applied where there are the supports of the beams, as concentrated forces on the masonry. Furthermore, the weight of the bells previously shown, have been applied as concentrated forces that rest on the masonry as the half of the forces equal and contraries. For example, in the zone 1-2, in addition to the weight of the beams

$$F_{\text{tot},12} = (17000+6480)/2 = 11740 \text{ N}$$

$$F_{12} = 5870 \text{ N}$$

a singular concentrated force F 12 for each bearing.

Type of masonry	$f_m$ (N/cm <sup>2</sup> )	$\tau_0$ (N/cm <sup>2</sup> )	E (N/mm <sup>2</sup> )	G (N/mm <sup>2</sup> )	w (kN/m <sup>3</sup> )
Masonry stones with good texture	192,6	4,15	1740	580	21

*Table 30: Reference values of the mechanical parameters*

For the weight of the roof, a resultant of own load and permanent loads have approximately considered. Built-in supports are insert in the ground, and translation along the direction of the Church next to the tower has been prevented. Of course, this is an approximation of the real structural analysis. In fact, it has to be considered only a first initial test, because the dimensions of beams are all supposed, and consequently the loads could be higher or lower (this depends on the chosen sections, if they are oversized or undersized). The results deriving from static and dynamic analysis in terms of natural frequencies' have been reported in

**Table 31.**

Mode no	Mode description	Max displacement	Frequency
1	1 <sup>st</sup> bending mode (along X)	1.006	1.5797
2	1 <sup>st</sup> bending mode (along Y)	1.003	1.3621
3	Axial mode	1.023	5.5365
4	Torsional mode	1.315	4.4618

**Table 31:** Natural frequencies' analysis: frequencies of the main mode shapes of the bell tower

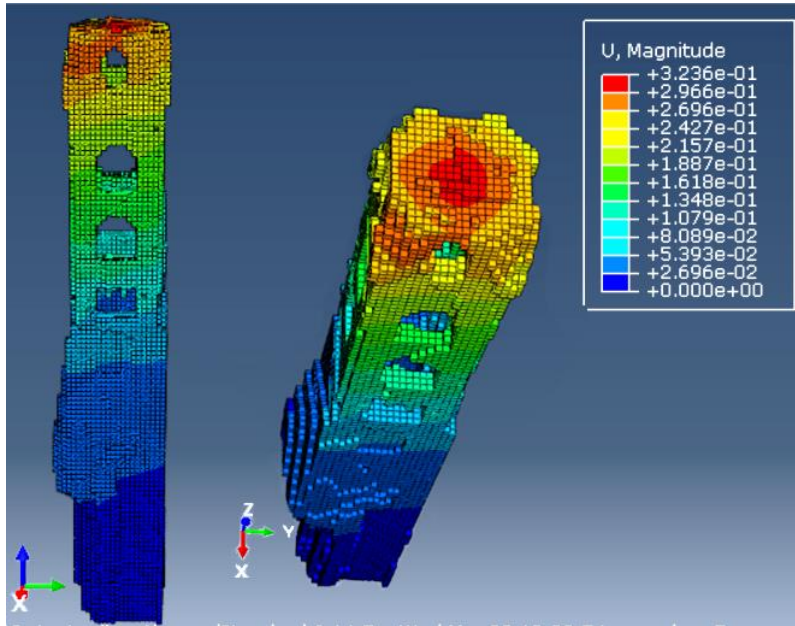


Figure 206: Static analysis

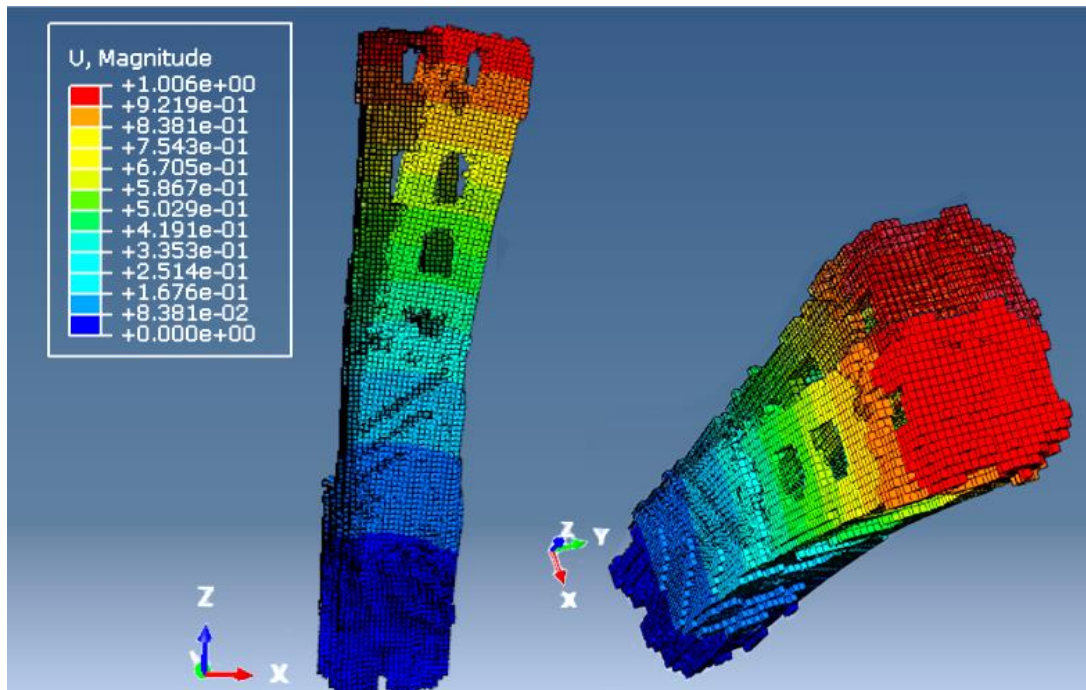


Figure 207: 1<sup>st</sup> bending mode (along X)

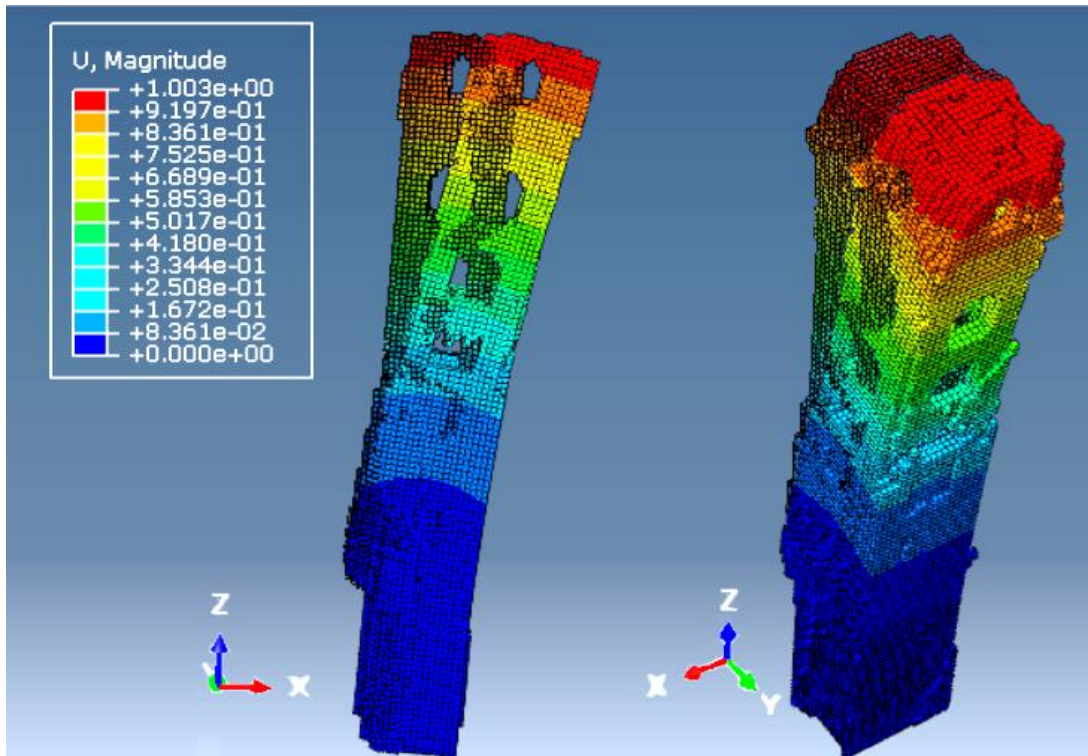


Figure 208: 1<sup>st</sup> bending mode (along Y)

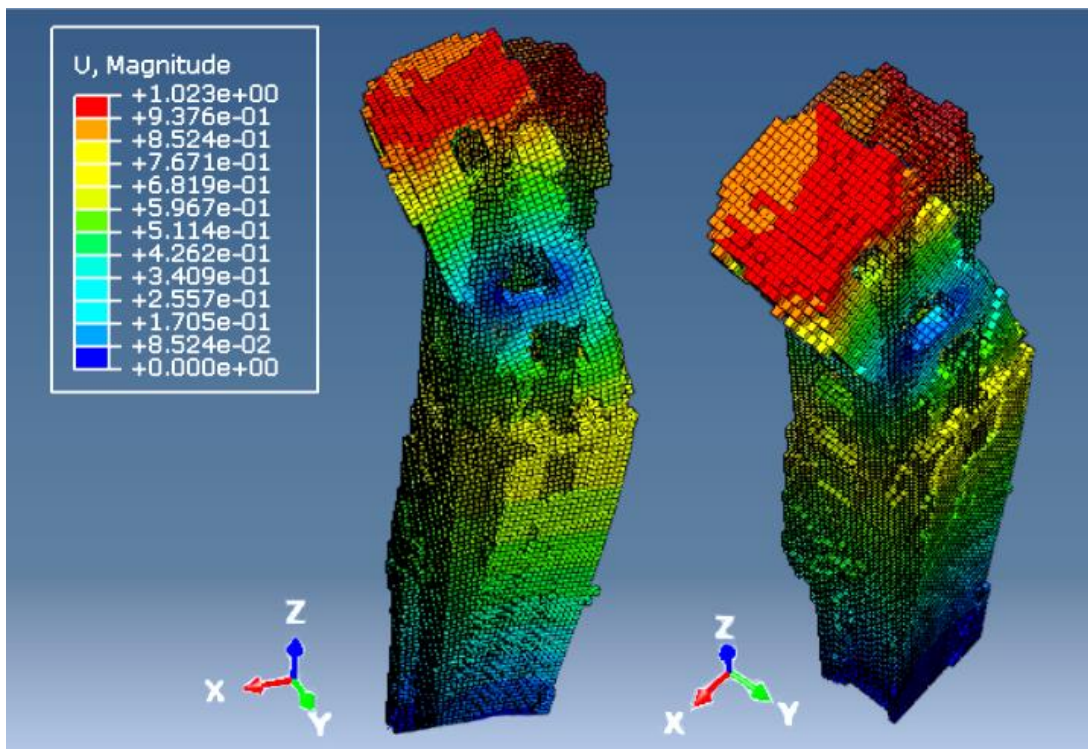


Figure 209: Axial mode

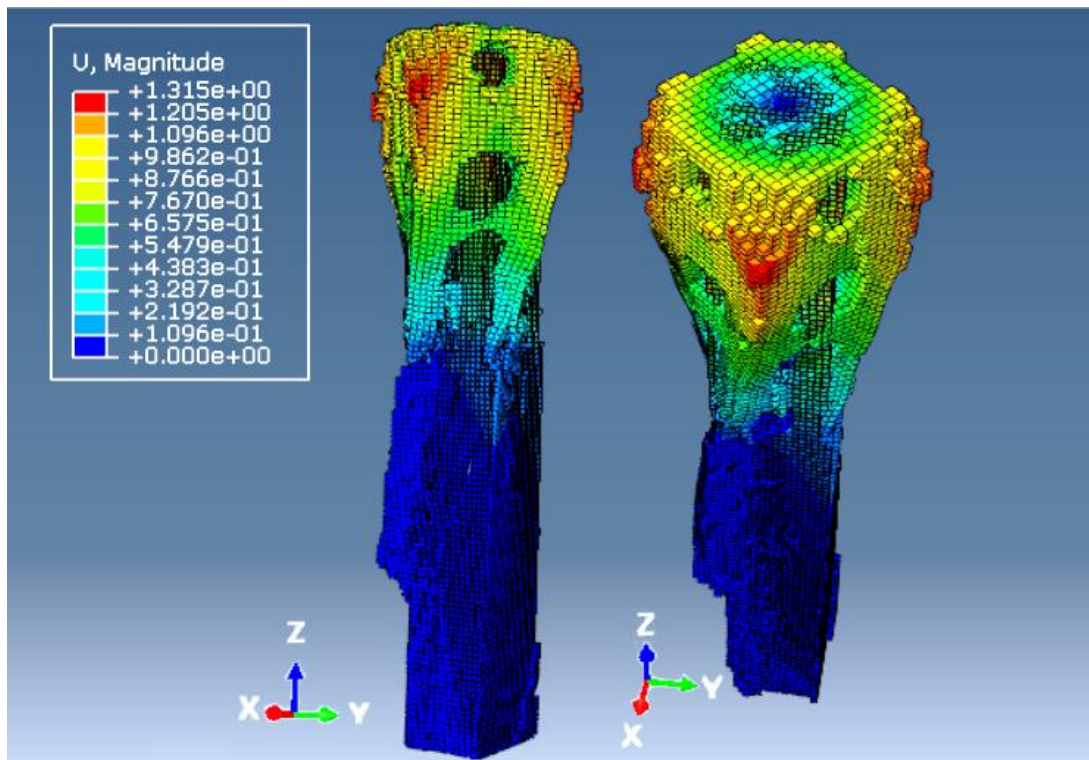


Figure 210: Torsional mode

## 7.6 Considerations

Starting from the generation of polygonal model, the 3D model of the bell tower has been generated. This is a very particular case study because of different elements. First, there is not an outside and inside record of every surface. For example, the roof of the church and of the bell tower could only be scanned from outside and not from the inside. This leads to a problem with the normals of the surfaces and therefore it is difficult to connect the roof correctly with the rest of the tower. A second problem is that the software used (in this case, Geomagic Wrap 2014) sometimes does not recognize correctly which side of a surface is the inside and which is the outside. It is not possible to flip normal of specific areas only. This leads to errors in the model, where some parts are not connected properly. A third problem are the missing parts. Some areas of the church were not scanned and could not be reconstructed easily by fitting planes. There are three different reasons why some parts in the TIN are missing. The first one is that too few scans were made during the data acquisition due to a lack of time. The second reason is that not all parts of the building were accessible or visible (inside of the roofs not accessible, parts of church roof not visible). The third point is that mainly the bell tower's roof was only visible in a very flat angle, which leads to a poor signal reflection. Combined with the large scanning distance, the roof has a quite low point density compared with the rest of the building. In fact, on the bell tower roof the point cloud is less dense because of the incident angle and the large distance of more than 120 m. Through further scans, missing parts can be completed. Especially for completing the roof other instruments could be introduced. A laser scanner with a longer range or photogrammetric measurements could be tested to complete the model. It has been possible to bridge the gaps manually, and this allowed to obtain a correct polygonal model, deleting the roof for transforming it in a horizontal surface. Both polygonal models, the raw one and the correct one, have been used in order to obtain a FE model, with semi-automatic procedures. Both voxel models do not fully correspond to reality, because there are approximations as the internal elements. For this reason, as a future study, it would be useful to obtain a

combined FE model, consisting of voxel and shell or beam elements. In this way, the computational time would be optimized, for three reasons. First of all, there would be no need to make a further calculation of the loads applied as a concentrated load (then, multiplying the effort for the clear span) and it would guarantee save in terms of computational process. The second point is that, if the loads are applied directly as distributed forces and not as concentrated one, the final results of the structural analysis are more correct and precise than those with concentrated forces, because they would respond perfectly to reality. Finally, the time spent on modeling of additional elements, would be time saved for the calculation of the transformation from distributed loads in concentrated forces, and this would ensure a model perfectly corresponding to the reality.

## Conclusions and further outlook

The three-dimensional models, deriving from point cloud dataset and directly transformed into FE models, allow to have accurate results for structural analyses, without approximations or loss of important elements. In general, three-dimensional models (geometric or numerical) are used in different fields, as for example for documentation purposes, for supporting the restoration etc...

Some authors (Villarino, Riveiro, Gonzalez-Aguilera, & Sanchez-Aparicio, 2014) recently pointed out the limits for transforming the initial point cloud, directly in a FE model, despite several studies were performed.

In this context, the present work represents an attempt to gather all available input data, in order to transform the initial point cloud into a FE model, suitable for structural analyses, by avoiding to loss important data. The aim is, furthermore, the obtaining of a complete model, and not an oversimplified one.

In order to transform the initial point cloud into a Finite Element model, available for structural analysis, different methods have been studied. The distinction has been made, depending on whether the contribution of the operator is or minimal or necessary. In the first case, two methods have been grouped in the automatic procedures; in the second case, two other procedures have been identified as semi-automatics.

All the four proposed methods always guarantee the generation of a filled model, ready to use for structural analyses, and for producing an input data for FE modeling.

In order to validate and show the capabilities of the proposed techniques, different case studies are presented and discussed.

The study of the first approach, the Cloud2FEM procedure, was applied to a very damaged case study, with some parts collapsed. The concept to create horizontal sections, overlapped to the polygonal model, allowed that the operator could control every element; in this way, all that non continuous or damaged parts were not lost.

For the second case study, the complex of Aquileia, consist of Basilica, Baptistery, Church of Pagans, a complete analysis has been made because, in contrast to the other two buildings, the study started from the acquisition data, and it offered lots of analyses and comparisons. Concerning the structural analyses, the first procedure (Cloud2FEM) has been applied, and starting from this, the aim was to optimize as more as possible the computational time, and to reduce the manually operations by the operator. For this reason, the other three procedures identified are more fast, without compromising results. All the four proposed methods always guarantee the generation of a filled model ready to use for structural analysis purpose to produce data input for FE modeling.

The third and last case study has been the San Luzi bell tower, in which the two semi-automatic procedures have been applied, and a comparison in terms of computational time has been carried out.

In general, the current research permitted to relate the point cloud input data, into a detailed FE model, by connecting, then, the Geomatics with the Structural Engineering. Regardless of the procedures identified and developed, the whole process can be summarized as follows.

The input data (regardless of the used technique of measurement for the acquisition) has to be cleaned and uniform, in order to obtain a more homogeneous point cloud dataset. Then, the dataset will be transformed into a polygonal model (for the two automatic procedures), correcting the possible errors. Finally, the output of the Geomatics, will be the input for the programming code. Through the four different methods, automatics and semi-automatics, a voxel model has been obtained. The output data is the same in its internal structure, because all the voxel models have the same physic characteristics, and a voxel is composed by corners where it is possible to define the loads bearing. The differences are in terms of computing time, geometrics characteristics, and number and dimensions of the voxels, from which depend the final results.

So, in the present work:

- the development of the programming code in order to obtain a final voxel model have been possible;
- the definition of geometric modeling has been carried out, for a comparison with the numerical modeling, in term of loss of level of detail;
- an historical reconstruction, carried out through the old data, has been made, and comparison with real (actual) model have been possible;
- the FE models deriving from Geomatics acquisitions were obtained, and compared in terms of displacements and frequency.

Others key aspects and contributions of the current research were:

- integration data of different instruments, in order to obtain a complete dataset, suitable for several analyses;
- the issues related to dataset with different characteristics (in terms of density);
- the transformation of a very complex dataset (in terms of points and triangles) in a model, through the reduction and sampling of elements without the loss of important parts;
- the comparison of photogrammetric elaborations, carried out with different software;
- static considerations and comparison between geometric and numerical modeling.

It would be interesting, transforming the programming codes, to automate all four procedures identified, in order to reduce the computational time by the operator. A limitation has been encountered in voxel models deriving from automatic procedures, related to the computational efforts in relation to the number of voxels: voxels with larger size require a longer processing time. Despite the final structural analyses are correct, this will be the subject for future researches, in order to solve the issues related to the dimension of voxels.

These processes are very general and will be useful to generate FE models not only for cultural heritage, but also in other fields. Further development should concentrate on the defining limit of the level of detail of a polygonal model, beyond which the values deriving from the structural analysis will be compromised.

Voxel-based FE models are characterized by several thousands of degrees-of-freedom and therefore computational cost for conducting response history analyses is often high. As future development, it would be very interesting to integrate the Voxel-based FE model generation in programming code, where model order reduction can be easily applied (Milani & Lourenco, 2012). Reduced order FE models, which are less computational demanding, can be profitably used for material parameter calibration and response history analyses.

An interesting topic, concerns the integration of data deriving from different geomatics instruments and techniques, in order to choose the best part of each dataset. In this way, it could be possible the merging only the best and well defined part from each point cloud.

The data collected can be used in future to calibrate the numerical models. The present work constituted the starting point; future work will be dedicated to develop some of these issues and ideas.



## Acknowledgements

Firstly, I wish to thank Prof. Gabriele Bitelli and Prof. Luca Vittuari for the support and all the opportunities that they offered me during these years.

Furthermore, I am grateful to Francesca Franci and Margherita Cecilia Spreafico for all the support, especially in the last period.

My colleague Alessandro Lambertini supported the initial phase of my research with advices and his knowledge about Python code.

I would like to express my sincere thanks to Prof. Andreas Wieser, and all his group of research, for all the advices and the wonderful period that I spent with them in Zurich.

In particular, discussion about modeling and FE analysis with Eugenio Serantoni supported and inspired my research.



## References

- Abaqus. (v 6.14). Abaqus CAE/User's guide .
- Africani, P., Bitelli, G., Lambertini, A., Minghetti, A., & Paselli, E. (2013). Integration of LIDAR data into a municipal GIS to study solar radiation. *Int. Arch. Photogramm. Remote Sens. Spat. Inf. Sci., XL-1/W1*, 1-6.
- Almac, U., & Pekmezci, I. (2016). Numerical Analysis of Historic Structural Elements Using 3D Point Cloud Data. *The Open Construction and Building Technology Journal*. DOI: 10.2174/1874836801610010233 .
- Alsadik, B., Gerke, M., & Vosselman, G. (2014). Visibility analysis of point cloud in close range Photogrammetry. *International Society for Photogrammetry and Remote Sensing*. DOI: 10.5194/isprsannals-II-5-9-2014.
- Anderson. (1994). *Linear, static finite element analysis*. Michigan: Ann Arbor.
- Arias, P, Armesto, J., Lorenzo, H., & Ordóñez, C. (2006). Digital photogrammetry, gpr and finite elements in heritage documentation: geometry and structural damages,. *ISPRS Commission V Symposium 'Image Engineering and Vision Metrology', IAPRS Volume XXXVI, Part 5*. Dresden.
- Armesto, J., Roca-Pardinas, J., Lorenzo, H., & Arias, P. (2010). Modelling masonry arches shape using terrestrial laser scanning data and nonparametric methods. *Eng. Struct.*, 32,, 607–615.
- Atamturktur. (2006). Structural Assessment of Guastavino Domes . *M.S. Thesis* . The Pennsylvania State University.
- Atamturktur. (2009). Verification and Validation under Uncertainty Applied to Finite Element Models of Historic Masonry Monuments. *Proceedings of the IMAC-XXVII*. Orlando, Florida USA: Society for Experimental Mechanics Inc.
- Attene, M. (2014). Direct repair of self-intersecting meshes. *Graphical Models* . DOI:10.1016/j.gmod.2014.09.002.
- Attene, M., Campen, M., & Kobbelt, L. (2013). Polygon Mesh Repairing: An Application Perspective,. *ACM Comput. Surv.*, 45 (p. 1-33). doi:10.1145/2431211.2431214.
- Barazzetti, L., Banfi, F., Brumana, R., Gusmeroli, G., Oreni, D., Previtali, M., . . . Schiantarelli, G. (2015 a). BIM From Laser Clouds and Finite Element Analysis: Combining Structural Analysis and Geometric Complexity. *Int. Arch. Photogramm. Remote Sens. Spatial Inf. Sci., XL-5, W4* , 345-350.
- Barazzetti, L., Banfi, F., Brumana, R., Oreni, D., Previtali, M., & and Roncoroni, F. (2015). HBIM and augmented information: towards a wider user community of image and range-based reconstructions. *The International Archives of the Photogrammetry, Remote Sensing and Spatial Information Sciences*,, 35-42.

- Barrile, V., Bilotta, G., D'Amore, E., Marando, R., Meduri, G., & Trovato, S. (2015). Structural Analysis of Cultural Heritage assisted by 3D Photogrammetry Conference. *8th International Conference on Environmental and Geological Science and Engineering*. Salerno, Italy.
- Bathe, J.-K. (1996). *Finite Element Procedures*. Upper Saddle River, New Jersey: Prentice Hall.
- Baumann, M., & Hadorn, P. (2015). Geometrical Modeling of a Historic Bell Tower, San Luzi, Zuoz. *Report of master thesis*. ETH, Zurich, Switzerland.
- Bertoli, G. (1739). *Le antichità d'Aquileja profane e sacre: per la maggior parte inora inedite raccolte, diseguate ed illustrate*. Venice.
- Besl, P., & McKay, N. (1992). Method for registration of 3-D shapes. *Proc. SPIE.*, (p. 586–606).
- Bitelli, G., Dubbini, M., & Zanutta, A. (2004). Terrestrial Laser Scanning and digital photogrammetry techniques to monitor landslide bodies. *Int Arch Photogramm Remote Sens Spat Inf Sci* 35, (p. 246-251).
- Bitelli, G., Girelli, V., Marziali, M., & Zanutta, A. (2007). *Use of historical images for the documentation and the metrical study of cultural heritage by means of digital photogrammetric techniques*. Athens, Greece: Proceedings of CIPA, XXI Symposium,.
- Boehler, W., Heinz, G., & Marbs, A. (2002). The potential of non-contact close range laser scanners for cultural heritage recording. *Int. Arch. Photogramm. Remote Sens.*, 34, 430–436.
- Böhler, W., & Marbs, A. (2002). 3D Scanning Instruments. *Proceedings of CIPA WG6 Scanning for Cultural Heritage Recording*. Corfu, Greece.
- Boothby, T., & Atamturktur, S. (2007). A Guide for the Finite Element Analysis of historic load-bearing masonry structures. *10th North American Masonry Conference*. St. Louis, Missouri, USA.
- Borri, & Maria, D. (2009). Eurocode 8 and italian code. A comparison about safety levels and classification of interventions on masonry existing buildings, . *Eurocode 8 Perspectives from the Italian Standpoint Workshop* (p. 237-246). E. Cosenza .
- Borri, A., & Grazini, A. (2006). Diagnostic analysis of the lesions and stability of Michelangelo's David. *Journal of Cultural Heritage*, 7(4) (p. 273-285). DOI: 10.1016/j.culher.2006.06.004.
- Borri, A., Falletti, F., Fastellini, G., Grassi, S., Grazini, A., & Marchetti, L. (2005). *La stabilità delle grandi statue: il David di Michelangelo (italian)*. Roma.
- Brandt. (2012). *Battisteri oltre la pianta-Gli alzati di nove battiseri in Italia*.
- Brandt, O. (2009). Il battistero cromaziano. *Atti della XL Settimana di Studi Aquileiesi*, 323-375.
- Bridson, R. (2007). Fast Poisson disk sampling in arbitrary dimensions. *ACM SIGGRAPH Sketches*, 22.
- Calib3V. (s.d.). Software for calibration of full frame camera. *IUAV, University of Venice, Laboratory of Photogrammetry Circe*.

- Callieri, M., Cignoni, P., Ganovelli, F., Impoco, G., Montani, C., Pingi, P., . . . Scopigno, R. (2004). Visualization and 3D data processing in David restoration. *IEEE Computer Graphics and Applications*, 24 (2)· March 2004 (p. 16-21). doi: 10.1109/MCG.2004.12740.
- Cannella, M. (2015). Digital Unwrapping and visualization of complex architectural. 8-14.
- Casolo, S., & Sanjust, C. (2009). Seismic analysis and strengthening design of a masonry monument by a rigid body spring model: The Maniace Castle of Syracuse. 31. *Eng. Struct.*, 1447–1459.
- Castellazzi, D’Altri, Bitelli, Selvaggi, & Lambertini. (2015). From Laser Scanning to Finite Element Analysis of Complex Buildings by Using a Semi-Automatic Procedure. *Sensors*, 15, 18360-18380.
- Castellazzi, D’Altri, Miranda, D., Ubertini, Bitelli, Lambertini, Selvaggi, Tralli. (2016). A mesh generation method for historical monumental buildings: an innovative approach. *ECCOMAS Congress 2016-VII European Congress on Computational Methods in Applied Sciences and Engineering* , (p. 1-8). Crete Island.
- Castellazzi, G., D’Altri, A., De Miranda, S., Ubertini, F., Bitelli, G., Lambertini, A., Selvaggi, I., Tralli, A. M. (2016). Automated voxel model from point clouds for structural analysis of cultural heritage (p. 191-197). Prague: doi:10.5194/isprsarchives-XLI-B5-191, 2016.
- Cattari, S., Degli Abbati, S., Ferretti, D., Lagomarsino, S., Ottonelli, D., & Tralli, A. (2014). Damage assessment of fortresses after the 2012 Emilia earthquake (Italy). *Bull. Earthq. Eng.*,12, (p. 2333–2365).
- Cecchi, A., Milani, G., & Tralli, A. (2007). A Reissner–Mindlin limit analysis model for out-of-plane loaded running bond masonry walls. *International Journal of Solids and Structures*, (p. 1438-1460).
- Chen, J. (2008). Architectural Modeling from Sparsely Scanned Range Data. *Int. J. Comput. Vis.*, 78,, 223–236.
- Chen, Y., & Medioni, G. (1991). Object modeling by registration of multiple range images. *IEEE International Conference on Robotics and Automation*, 3,, (p. 2724–2729).
- Chiabrando, F., Sammartano, G., & Spanò, A. (2016). Historical buildings models and their handling via 3d survey: from points clouds to user-oriented hbim. *The International Archives of the Photogrammetry, Remote Sensing and Spatial Information Sciences*, (p. Vol. XLI-B5). Prague, Czech Republic: ISPRS.
- Chiarugi, A., Fanelli, A., & Giuseppetti, G. (1993). Diagnosis and strengthening of the Brunelleschi Dome. *IABSE Symposium*. IABSE, Zürich.
- Chopra, A. (1995). *Dynamics of Structures*, 3rd ed. NJ, USA: Prentice Hall: Upper Saddle River.
- Cignoni, P., Callieri, M., Corsini, M., Dellepiane, M., Ganovelli, F., & Ranzuglia, G. (2008). MeshLab: An open-source mesh processing tool. . *ERCIM* .
- Circ. 09, 6. (2009). Istruzione per l'applicazione delle nuove norme tecniche per le costruzioni di cui al decreto ministeriale 14 Gennaio 2008 (Instructions for the application of the new technical norms on constructions). Ministero delle Infrastrutture e dei Trasporti.

- Clark, M., McCann, D., & Forde, M. (2003). *Application of infrared thermography to the non-destructive testing of concrete and masonry bridges*. *NDT & E Int.* 36 .
- CloudCompare. (s.d.). Cloud Compare, software open source, version 2.6.1.
- Clough, R. W. (1960). The finite element method in plane stress analysis. *Second ASCE Conference on Electronic Computation*, (p. 345-378). Pittsburgh, PA.
- Corsini, M., Cignoni, P., & Scopigno, R. (2012). Efficient and flexible sampling with blue noise properties of triangular meshes. *IEEE Trans. Vis. Comput. Graph.*, 914–924.
- Corti, G., Costagliola, P., Bonini, M., & Landucci, F. (2014). Modelling the failure mechanisms of Michelangelo's David through small-scale centrifuge experiments, . *Journal of Cultural Heritage*. DOI: 10.1016/j.culher.2014.03.001.
- Creazza, G., Matteazzi, R., Saetta, A., & Vitaliani, R. (2002). Analyses of Masonry Vaults: A Macro Approach Based on Three-Dimensional Damage Model. *Journal of Structural Engineering*, Vol. 128, No. 5, (p. 646–654).
- Croci, G. (1995). The Colosseum: safety evaluation and preliminary criteria of intervention. *Structural Analysis of Historical Constructions*. Barcelona, Spain.
- Croci, G., & Viscovik, A. (1995). Causes of failures of Colosseum over the centuries and evaluation of the safety levels. *Public assembly structures. From antiquity to the present. IASS-Mimar Sinan University,,* (p. 29-52). Istanbul, Turkey.
- De Canio, G. (2012). Marble devices for the Base isolation of the two Bronzes of Riace. *The 15th World Conference on Earthquake Engineering* . Lisboa, Portugal.
- Dore, C., Murphy, M., McCarthy, S., Brechin, F., Casidy, C., & Dirix, E. (2015). Structural Simulations and Conservation Analysis-Historic Building Information Model (HBIM). *The International Archives of the Photogrammetry, Remote Sensing and Spatial Information Sciences*. Avila, Spain .
- Dorninger, P., & Pfeifer, N. (2008). A Comprehensive Automated 3D Approach for Building Extraction, Reconstruction, and Regularization from Airborne Laser Scanning Point Clouds. *Sensors*, 8, 7323–7343.
- Eastman, C., Teicholz, P., Sacks, R., & Liston, K. (2008). *BIM Handbook. A guide to Building Information Modeling for Owners, Managers, Designers, Engineers, and Contractors*., Hoboken, New Jersey: John Wiley & Sons,.
- Ebeida, M. S., Mitchell, S. A., & Patney A., D. A. (2013). A Simple Algorithm for Maximal Poisson-Disk Sampling in High Dimensions,. *EUROGRAPHICS 2012*. P. Cignoni, T. Ertl (Guest Editors), Volume 31 (2012), Number 2.
- eCognitionDeveloper. (s.d.). *eCognition Developer 8*. Definiens AG, Trappentreustr. 1, D-80339 München, Germany.
- Edelsbrunner, H. (1995). Smooth surfaces for multi-scale shape representation. *Foundations of software technology and theoretical computer science*, (p. 391-412). Bangalore.

- Edelsbrunner, H., & Mücke, E. P. (1994). Three-dimensional alpha shapes. *ACM Transactions on Graphics (TOG)*, 13(1), (p. 43-72).
- Edelsbrunner, H., Kirkpatrick, D., & Seidel, R. (1983). On the shape of a set of points in the plane. *IEEE Trans. Inf. Theory*, 29, (p. 551-559).
- Eurocode6. (2005 c). Design of masonry structures - Part 1-1: General rules for reinforced and unreinforced masonry structures. *CEN – EN 1996-1*.
- Eurocode8. (2005 a). Design of structures for earthquake resistance, Part 1: General rules, seismic action and rules for buildings. *CEN-EN 1998-1*.
- Eurocode8. (2005 b). Design of structures for earthquake resistance, Part 3: Strengthening and repair of buildings. *CEN – EN 1998-3*.
- FARO. (s.d.). Laser Scanner Focus 3D. Available online: [www.faro.com/en-us/products/3d-surveying/](http://www.faro.com/en-us/products/3d-surveying/).
- Fastellini, G., Grassi, S., Marrucci, M., & Radicioni, F. (2005). Michelangelo's David: historical images for the preservation of a masterpiece. *CIPA 2005 XX International Symposium*. Torino, Italy.
- Forcellini, D., Facchini, L., Betti, M., Morandini, C., Clyde, D., & Segas, P. (2015). Seismic protection systems for artifacts: a base isolation proposal for Michelangelo's David. *14th World Conference on Seismic Isolation, Energy Dissipation and Active Vibration Control of Structures*. San Diego, USA.
- Fritsch, D., Khosravani, A. M., Cefalu, A., & Wenzel, K. (2011). Multi-sensors and multiray reconstruction for digital preservation. *Photogrammetric week'11*, 305-323.
- Fritsch, Khosravani, A., Cefalu, A., & Wenzel, K. (2011). Multi-sensors and Multiray Reconstruction for Digital Preservation. *Photogrammetric Week '11* (p. 305-323). Wichmann, Berlin/Offenbach: D. Fritsch.
- Furukawa Y., C. B. (2010). Towards internet-scale multi-view stereo. *Computer Vision and Pattern Recognition*, 1434-1441.
- Galasco, A., Lagomarsino, S., Penna, A., & Resemini, S. (2004). Non-linear seismic analysis of masonry structures. *13th World Conference on Earthquake Engineering Vancouver, B.C., No843*. Vancouver, Canada.
- Garcia, F., & Ottersten, B. (2014). CPU-Based Real-Time Surface and Solid Voxelization for Incomplete Point Cloud. DOI: 10.1109/ICPR.2014.475.
- Geomagic. (2014). Geomagic Wrap. 3DSystem.
- Girelli, V., Tini, M., Zanutta, A. (2005). *Traditional and unconventional photogrammetric techniques formetrical documentation of cultural heritage: the example of the "Rolandino dei Passaggeri" Tomb (St. Domenico Square) survey in Bologna*. Torino, Italy: S. Dequal (Ed.), Proceedings of CIPA, XX Symposium, September 26–01 October, 2005.
- Granada Agreement. (1985). *Convention for the Protection of the Architectural Heritage of Europe, Council of Europe*.
- GrassGIS. (7.2). *OS Geo Project*.

- Grimm, C. (1988). *Masonry Cracks: A Review of the literature*.
- Gruen, A., Remondino, F., & Zhang, L. (2002). Reconstruction of the Great Buddha of Bamiyan, Afganistan. *International Archives of Photogrammetry and Remote Sensing* , 363-368.
- Grussenmeyer, P., Alby, E., Landes, T., Koehl, M., Guillemin, S., Hullo, J.-F., Smigiel, A. (2012). Recording approach of heritage sites based on merging point clouds from high resolution photogrammetry an terrestrial laser scanning. *International archives of the Photogrammetry, Remote Sensing and Spatial Information Sciences*, 553-558.
- Guarnieri, A., Milan, N., & Vettore, A. (2013). Monitoring of Complex Structure for Structural Control Using Terrestrial Laser Scanning (TLS) And Photogrammetry. *Int. J. Archit. Herit.*, 7, 54–67.
- Guarnieri, A., Pirotti, F., Pontin, M., & Vettore, A. (2006). Combined three-dimensional surveying techniques for structural analysis applications. . *In Proceedings of the 3rd IAG Symposium on Geodesy for Geotechnical and Structural Engineering and 12th FIG Symposium on Deformation Measurements*. Baden, Austria.
- Hackel, T., Wegner, D., & Schindler, K. (2016 b). Contour Detection in Unstructured 3D Point Clouds. *Conference: 2016 IEEE Conference on Computer Vision*, DOI: 10.1109/CVPR.2016.178.
- Hackel, T., Wegner, J., & Schindler, K. (2016 a). Fast semantic segmentation of 3d point clouds with strongly varying density. *ISPRS Annals - ISPRS Congress*. Prague.
- Hinks, T., Carr, H., Truong-Hong, L., & Laefer, D. (2013). Point Cloud Data Conversion into Solid Models via Point-Based Voxelization. *J. Surv. Eng.*, 139, , 72-83.
- Hutchinson, T., & Chen, Z. (2006). Improved image analysis for evaluating concrete damage. *J. Comput. Civil Eng.* 20 (3), 210-216.
- ICOMOS. (1964). International charter for the conservation and restoration of monuments and sites . *Second International Congress of Architects and Technicians of Historic*.
- ICOMOS. (1996). Charter on the protection and management of underwater cultural heritage.
- ICOMOS. (2003). *Recommendations for the analysis, conservation and structural restoration of architectural heritage*. International Scientific Committee for Analysis and Restoration of Structures of Architectural Heritage.
- ISO standard, 2.-1. (2010). Building information modelling - Information delivery manual - Part 1: Methodology and format.
- Kacyra, B. (2009). CyArk 500–3D Documentation of 500 Important Cultural Heritage Sites. *Photogrammetric Week '9* (p. 315-320). Whichmann Verlag, Heidelberg: D. Fritsch.
- Kersten, P., Hinrichsen, N., Lindstaedt, M., Weber, C., Schreyer, K., & Tschirschwitz, F. (2014). Architectural Historical 4D Documentation of the Old-Segeberg Town House by Photogrammetry, Terrestrial Laser Scanning and Historical Analysis. *5th International Conference, EuroMed 2014*, (p. 35-46). Limassol, Cyprus.

- Koponen, S., Toratti, T., & Kanerva, P. (1991). Modelling elastic and shrinkage properties of wood based on cell structure. . *Wood Sci. Technol.*, 25–32.
- Kraus, K. (2007). *Photogrammetry, Geometry from Images and Laser Scans*; . Berlin, Germany.
- Lança, P., Lourenço, P., & Ghiassi, B. (2015). Structural assessment of a masonry vault in Portugal . *Structures and Buildings*. DOI: 10.1680/stbu.14.00093.
- Lanckoronski, K. G. (1906). *Der Dom Von Aquileia*. Wien: Verlag Von Gerlach & Wieding.
- Lourenço. (1995 b). An orthotropic continuum model for the analysis of masonry structures. *Delft university of technology*. Delft, the Netherlands.
- Lourenço. (2009). Finite element modelling of deformation characteristics of historical stone masonry shear walls,. *Engineering Structures* .
- Lourenço, P. (1996). Computational strategies for masonry structures. *Ph.D. Dissertation*. Delft, Netherlands: Delft University of Technoogy.
- Lubowiecka, I., Armesto, J., Arias, P., & Lorenzo, H. (2009). Historic bridge modelling using laser scanning, ground penetrating radar and finite element methods in the context of structural dynamics. *Eng. Struct.*, 31,, 2667–2676.
- Macchi, G., Ruggeri, M., Eusebio, M., & Moncecchi, M. (1993). Structural assessment of the leaning tower of Pisa. *Structural preservation of the architectural heritage* (p. 401-408). Zürich, Switzerland: IABSE.
- Malecki, A., Potdevin, G., Biernath, T., Ettl, E. K., Lasser, W. T., J., M., . . . Pfeiffer, F. (2014). X-ray tensor tomography. *EPL (Europhysics Letters)* 105(3):38002. DOI: 10.1209/0295-5075/105.
- Martinez, J., Soria-Medina, A., Arias, P., & Buffara-Antunes, A. (2012). Automatic processing of terrestrial laser scanning data of building facades. *Autom. Constr.*, 22, (p. 298-305).
- Martínez, S., Santiago, J. O., & Gil, M. L. (2015). Geometric documentation of historical pavements using automated digital photogrammetry and high-density reconstruction algorithms. *Journal of Archaeological Science*, 1-11.
- Matlab. (R2016a). TheMathWorks. Inc.
- Meli, R., & Sánchez-Ramírez, A. (1995). Structural aspects of the rehabilitation of the Mexico City Cathedral. *Structural analysis of historical constructions*, (p. 123–140). CIMNE, Barcelona, Spain.
- Meshlab. (2014). *Open source Mesh Processing Tools*.
- Milani, E., Milani, G., & Tralli, A. (2008). Limit analysis of masonry vaults by means of curved shell finite elements and homogenization. *International Journal of Solids and Structures*, 45 (20), (p. 5258-5288).
- Milani, G., & Lourenco, P. (2012). 3D non-linear behavior of masonry arch bridges. *Computers & Structures*. DOI: 10.1016/j.compstruc.2012.07.008.

- Milani, G., Lourenço, P., & Tralli, A. (2006 a). Homogenised limit analysis of masonry walls. Part I: Failure Surfaces. *Computers and Structures*, (p. 166-180).
- Milani, G., Lourenço, P., & Tralli, A. (2006 b). Homogenised limit analysis of masonry walls. Part II: Structural Examples. *Computers and Structures*.
- Milani, G., Lourenço, P., & Tralli, A. (2007). 3D homogenized limit analysis of masonry buildings under horizontal loads. *Engineering Structures*, (p. 3134– 3148).
- Mola, F., & Vitaliani, R. (1995). Analysis, diagnosis and preservation of ancient monuments: the St. Mark's Basilica in Venice. *Structural analysis of historical constructions*, (p. 166–188). CIMNE, Barcelona, Spain.
- Moreira, A., & Santos, M. (2007). Concave Hull: A k-Nearest Neighbours Approach for The Computation of the Region Occupied By A Set of Points. *Proceedings of the 2nd International Conference on Computer Graphics Theory and Applications* , (p. 61-68). Barcelona, Spain .
- Ngo, D., & Scordelis, A. (1964). Finite element analysis of reinforced concrete beam. . *J Am Concr Inst* 64:152.
- NTC. (2008). Norme Tecniche per le Costruzioni,. *D.M. 14/01/08*.
- Núñez, M., & Pozuelo, F. (2009). Evolution of the architectural and heritage representation, 91. *Landsc. Urban Plan.*, 105–112.
- Oñate, E., Hanganu, A., Barbat, A., Oller, S., Vitaliani, R., . . . Scotta, R. (1996). Structural Analysis and durability Assessment of Historical Construction Using a finite element Damage Model. *Publication CIMNE n. 73, U.P.C. de Catalunya*. Barcelona, Spain .
- Oreni, D., Brumana, R., Della Torre, S., Banfi, F., Barazzetti, L., & Previtali, M. (2014). Survey turned into HBIM: the restoration and the work involved concerning the Basilica di Collemaggio after the earthquake (L'Aquila. *ISPRS Ann. Photogramm. Remote Sensing Spatial Inf.* , (p. 267-273).
- Orlando, A. (2014.). Estense Fortress at San Felice Sul Panaro: Modelling and Seismic Assessment. Master Thesis, University of Genoa, .
- Ozkul, T. A., & Kuribayashi, E. (2007). Structural characteristics of Hagia Sophia: A finite element formulation for static analysis. *Building and Environment*, 42, (p. 1212–1218).
- Papa, E. (2001). Damage and failure models. Computational modelling of masonry brickwork and blockwork structures. (p. 1-26). Stirling, Scotland: Saxe-Coburg Publications.
- Patias, P., Grussenmeyer, P., & Hanke, K. (2008). *Application in Cultural Heritage DOcumentation* . International Society for Photogrammetry and Remote Sensing ISPRS.
- Peña, F., Lourenco, P., Mendes, N., & Oliveira, D. V. (2010). Numerical models for the seismic assessment of an old masonry tower. *Engineering Structures* (p. 1466-1478). DOI: 10.1016/j.engstruct.2010.01.027.
- Pesci A., C. G. (2011). Laser scanning the Garisenda and Asinelli towers in Bologna (Italy): detailed deformation patterns of two ancient leaning buildings. *J. of Cultural Heritage*, 117-127.

- Photoscan. (2013). Agisoft LLC. *Agisoft Photoscan User Manual: Professional Edition*.
- Pieraccini, M., Dei, D., Betti, M., Bartoli, G., Tucci, G., & Guardini, N. (2014). Dynamic identification of historic masonry towers through an expeditious and no-contact approach: Application to the “Torre del Mangia” in Siena (Italy). *Journal of Cultural Heritage*. 2014; 15(3), 275-82.
- Python 2.7.13, D. (2016).
- Quan. (2010). Image-Based Modeling. *Springer Science Business Media*.
- Quattrini, R., Malinverni, E. S., Clini, P., Nespeca, R., & Orlietti, E. (2015). From TLS to HBIM. High quality semantically-aware 3D modelling of complex architecture. *The International Archives of the Photogrammetry, Remote Sensing and Spatial Information Sciences, Volume XL-5/W4, 2015 3D Virtual Reconstruction and Visualization Volume XL-5/W4, 2015*. Avila, Spain: Volume XL-5/W4, 2015 3D Virtual Reconstruction and Visualization of Complex Architectures.
- Remondino, & Lambers. (2008). *Optical 3D measurement techniques in archaeology: Recent developments and applications*.
- Rhinoceros. (5.0). Robert McNeel & Associates.
- Riveiro, B., Solla, M., De Arteaga, I., Arias, P., & Morer, P. (2013). A novel approach to evaluate masonry arch stability on the basis of limit analysis theory and non-destructive geometric characterization. *Automation in Construction*. 2013; 31(0):140-8.
- Roca, P. (2001). Studies on the structure of Gothic Cathedrals. In: *Lourenço PB, Roca P (eds) Historical constructions. University of Guimaraes*. Guimaraes.
- Roca, P. (2005). Considerations on the significance of history for the structural analysis of ancient constructions. *Structural Analysis of Historical Constructions* (p. 63-73). Modena, Lourenço & Roca (eds).
- Roca, P., Cervera, M., Gariup, G., & Pela', L. (2010). Structural analysis of masonry historical constructions. Classical and advanced approaches. *Arch. Comput. Methods Eng.* , 299–325.
- Romão, X., Paupério, E., Guedes, J., & Costa, A. (2006). Authoring and multimedia technologies for management and presentation of information on heritage constructions. *Structural Analysis of Historical Construction* .
- Ruizhongtai, C., Hao, Q., & Mo, K. (2016). PointNet: Deep Learning on Point Sets for 3D Classification and Segmentation.
- Saadeghvaziri, M. A., & Mehta, S. (1993). An analytical model for URM Structures. *6th North American Masonry conference*, (p. 409-418). Philadelphia, Pennsylvania.
- Sanchez-Aparicio, L. J., Riveiro, B., Gonzalez-Aguilera, & Ramos, L. F. (2014). The combination of geomatic approaches and operational modal analysis to improve calibration of finite element models: A case of study in Saint Torcato Church (Guimarães, Portugal). *Construction and Building Materials, Vol. 70* (p. 118-129). <http://dx.doi.org/10.1016/j.conbuildmat.2014.07.106>.

- Sánchez-Aparicio, L. J., Villarino, A., García-Gago, G., & González-Aguilera, D. (2015). Non-contact photogrammetric methodology to evaluate the structural health of historical constructions . *The International Archives of the Photogrammetry, Remote Sensing and Spatial Information Sciences, Volume XL-5/W4*. Avila, Spain : doi:10.5194/isprsarchives-XL-5-W4-331-2015.
- Scognamiglio, L., Margheriti, L., Mele, F., Tinti, E., Bono, A., & de Gori, P. (2012). The 2012 Pianura Padana Emiliana seismic sequence: locations, moment tensors and magnitudes. *Annals Geophys.*
- Scopigno, R., Cignoni, P., Callieri, M., & Ponchio, F. (2003). Using optically scanned 3D data in the restoration of Michelangelo's David. *Proceedings of SPIE - The International Society for Optical Engineering 5146*. DOI: 10.1117/12.499921.
- Serantoni, E., & Wieser, A. (2016). TLS-based deformation monitoring of snow structures. *Proc DVW TLS Seminar*.
- Serantoni, E., Selvaggi, I., & Wieser, A. (2017). Areal deformation analysis of a visco-plastic structure. *Ingenieurvermessung 2017 (submitted)*. Graz, Austria.
- Shan, J., & Toth, C. (2008). Topographic laser ranging and scanning: principles and processing. Boca Raton: CRC press.
- Sorace, S., & Terenzi, G. (2015). Seismic performance assessment and base-isolated floor protection of statues exhibited in museum halls . *Bull Earthquake Eng.* , (p. 1873-1892).
- Spangher, A. (2016). Contribution of geomatic models to structural engineering;. *PhD Thesis* . University of Udine.
- Strunden, J., Ehlers, T., Brehm, D., & Nettesheim, M. (2015). Spatial and temporal variations in rockfall determined from TLS measurements in a deglaciaded valley, Switzerland. *J Geophys Res F Earth Surf* 120 (p. 1251–1273). doi: 10.1002/2014JF003274.
- Sun, Z., & Cao, Y. K. (2015). Data processing workflows from low-cost digital survey to various applications: three case studies of Chinese historic architecture. *The International Archives of the Photogrammetry, Remote Sensing and Spatial Information Sciences, XL-5, W7*, (p. 409-416).
- Szolomicki, J. (2015). Application of 3D Laser Scanning to Computer Model of Historic Buildings,. *Proceedings of the World Congress on Engineering and Computer Science, Vol II WCECS 2015*. San Francisco, USA.
- Taliercio, A., & Binda, L. (2007). The Basilica of San Vitale in Ravenna: Investigation on the current structural faults and their mid-term evolution. *Journal of Cultural Heritage* 8, (p. 99-118).
- Taubin, G. (1995). Curve and surface smoothing without shrinkage. *Proceedings of the Fifth International Conference of Computer Vision*. Cambridge, USA: IEEE Computer Society Washington, DC.
- Tavano. (1972). Aquileia cristiana. Antichità Altoadriatiche.
- Tavano. (1996). Aquileia e Grado. Storia arte e cultura. LINT.
- The Athens Charter for the Restoration of Historic Monuments. (1931). *First International Congress of Architects and Technicians of Historic Monuments*.

- Truong-Hong, L., & Laefer, D. (2013). Validating Computational Models from Laser Scanning Data for Historic Facades. *J. Test. Eval.*, 41, , 481–496.
- Truong-Hong, L., & Laefer, D. (2014). Octree-based, automatic building facade generation from LiDAR data., 53, . *Comput.-Aided Des.*, 46–61.
- Tschirschwitz, F., Mechelke, K., Jansch, H., & Kersten, T. P. (2016). Monitoring and Deformation Analysis of Groynes Using TIs at the River Elbe. *ISPRS-International Archives of the Photogrammetry, Remote Sensing and Spatial Information Sciences*, (p. 917-924).
- UNESCO. (1945, November 16). Constitution of the United Nations Educational, Scientific and Cultural Organisation.
- UNESCO. (1954, May 14). Convention for the Protection of Cultural Property in the Event of Armed Conflict with Regulations for the Execution of the Convention. *UNESCO*.
- UNESCO. (1972). *Photogrammetry applied to the survey of historic monuments, of sites and to archaeology*. UNESCO editions.
- Vatan , M., Selbesoğlu, M. O., & Bayram , B. (2009, December 2-4). The use of 3D Laser Scanning Technology. *XIII Scientific Technical Conference*, p. 656-669.
- Vercher, J., Gil, E., Mas, A., & Lerma, C. (2013). Diagnosis/Intervention criteria in damaged slabs by severe corrosion of prestressed joists. *Journal of Performance of Constructed Facilities*.
- Villarino, A., Riveiro, B., Gonzalez-Aguilera, D., & Sanchez-Aparicio, L. (2014). The Integration of Geotechnologies in the Evaluation of a Wine Cellar Structure through the Finite Element Method . *Remote Sensing* (p. 11107-11126). doi:10.3390/rs61111107 .
- Vosselman, G., & Maas, H. G. (2010). *Airbone and Terrestrial Laser Scanning*. CRC Press. .
- Wang, H., Huang, Z., Li, L., & Chen, Y. (2014). Three-dimensional modeling and simulation of asphalt concrete mixtures based on X-ray CT microstructure images. *Journal of Traffic and Transportation Engineering (English Edition)* , (p. 55-61).
- Wu, C. (2011). VisualSFM: A visual structure from motion system. <http://ccwu.me/vsfm/doc.html>.
- Zienkiewicz, O., & Taylor, R. (1991). *The finite element method*. . New York: McGraw Hill .
- Zogg, H. M., & Ingensand, H. (2008). Terrestrial laser scanning for deformation monitoring-load tests on the Felsenau Viaduct (CH). *The International Archives of the Photogrammetry, Remote Sensing and Spatial Information Sciences*, 37, (p. 555-561).
- Zvietcovich, F., Castaneda, B., & Perucchio, R. (2015). 3D solid model updating of complex ancient monumental structures based on local geometrical meshes. *Digit. Appl. Archaeol. Cult. Herit.*, 2, 12-27.